Synthesis of an 8-membered oxygen-containing benzo-fused heterocycle using flow technologies

by

Bernice Mercia Currie

Submitted in fulfilment of the requirements for the degree

Magister Scientiae

in the

Faculty of Natural and Agricultural Sciences

at the

University of Pretoria

UNIVERSITEIT VAN PRETORIA
UNIVERSITY OF PRETORIA
YUNIBESITHI YA PRETORIA

January 2024

Supervisor: Prof Darren L. Riley

Co-supervisor: Dr Jenny-Lee Panayides

Declaration

I, Bernice Mercia Currie, declare that the dissertation, which I hereby submit for the Degree Magister Scientiae Chemistry at the University of Pretoria, is my own work and has not previously been submitted by me for a degree at this or any other tertiary institution.

Signed:  Date: 2024/01/24

Acknowledgements

Grace upon grace (John 1:16)

First and foremost, I would like to thank my supervisor Prof. Darren L. Riley for accepting me to join his research group and for his continuous support and providing me with the opportunity to complete my MSc degree. Thank you for encouraging me to grow as a researcher, without your guidance and mentoring this dissertation would have never been possible.

I would also like to thank my co-supervisor, Dr Jenny-Lee Panayides for her invaluable guidance, expertise, and patience throughout this research project. Thank you for the valuable discussions and feedback on my work. I was fortunate to have two exceptional supervisors by my side throughout this project.

I would like to acknowledge the funding provided by the Council for Scientific and Industrial Research and the facilities and resources from the Chemistry Department at the University of Pretoria.

I am also grateful for Dr Madelein Wooding for MS help and discussions, and Dr Mamoalosi Selepe for NMR help.

I would also like to thank Dr Nicole Neyt for her contributions on this project and suggestions. You have established the foundation of this project and I was very grateful to have continued working on it.

I would like to thank Michelle Janse van Rensburg for her help with DoE for certain stages and for motivating me throughout this project. I am so grateful for sharing an office with you and discussing all the happiness and sadness over a coffee. Thank you for always being there.

I would also like to express my appreciation to the Riley research team; Lerato Dibokwane, Lorinda Van Wyk, Zen Johnston, Wessel Bonnet and Anya Botes. It was a pleasure getting to know all of you and working with you and sharing knowledge and passion for chemistry. I am thankful for the support, help and friendships that was built.

I would also then like to thank other postgraduates at the University of Pretoria for their support and contributions including Estefan van Vuuren for help with the RCM stage, Reinard Klopper for motivation during writeup, Wiehan Rudolph for isolation techniques and consultations, Serena Joubert and Babatunde Awe for always listening and motivating me. It was wonderful having so many people outside the research group caring and providing support and advice.

Thank you to all my friends and family for your encouragement and support especially; Welmari and Jacques Volschenk for motivation and putting up with me, Linda Prinsloo for always being there when I need to chat, Pamela Page for being a true friend in times of need, and all my cousins for caring. Thank you for being my rock, shoulder to cry on and making me laugh in times when I needed it the most.

Lastly but not the least, I would like to thank my parents Stanley and Zelda Currie for their encouragement, sacrifices, support and endless love. I wouldn't have come this far without you. Thank you for always being a call away. Thank you for having faith in my potential and for celebrating this important milestone in my life with me.

Also, a very special thank you to my grandmother Christine Currie for caring, checking up and providing me with food, I would've starved if it wasn't for ouma. But thank you ouma for all the support, motivational messages and weekend escapes when times were tough. Thank you for continuously believing in me and comforting me when I was overwhelmed.

To my late grandfather Peter Currie - I am forever thankful for the encouragement and endless love you have given me. I hope I have and will always make you proud. Thank you for believing in me and motivating me to pursue postgraduate studies.

And lastly to my Life Group and church community - I am deeply grateful and blessed for your words of wisdom and prayers as they have brought me comfort and peace during challenging times.

“It always seems impossible until it's done.”

- ***Nelson Mandela***

Abstract

Flow chemistry has become an appealing alternative synthetic technology globally over the last few decades finding application in both academic and industrial laboratories driven largely by the fact that it commonly provides higher selectivity, yield and purity compared to batch chemistry that has become time-consuming, ineffective, and challenging to scale up. This dissertation describes the application and development of a flow process towards the synthesis of an 8-membered oxygen-containing benzo-fused heterocycle. The synthesis consisted of six stages that included two allylation steps, a Claisen rearrangement, an alcohol protection, an aldehyde reduction and a ring-closing metathesis step. The target molecule, (*Z*)-7-isopropoxy-8-methoxy-3,6-dihydro-1*H*-benzo[*c*]oxocine **25,** was selected with an interest in developing an improved approach to accessing the scaffold for future structure-activity relationship screening and demonstrating that modern process technologies like flow can also be used routinely to perform fundamental research in a more sustainable and responsible manner. In summary, all six steps were successfully translated into flow and improved yields were shown with the use of greener solvents and operating at unconventionally high temperature and pressures especially when considering the Claisen rearrangement step. Design of experiment was also used in the last two stages which included i) the second allylation which required a strong base such as sodium hydride and was used as a slurry pumping through peristaltic pumps, and ii) the final ring closing metathesis stage in which two ruthenium-based catalysts were investigated with the use of a greener solvent. It was found that the flow approach yielded an overall percentage yield of 37.7 % in 105 minutes, compared to the batch approach that yielded an overall percentage yield of 0.77 % in 154 hours.

Abbreviations

Abbreviation	Definition
ACN	acetonitrile
ADMEP	acyclic diene metathesis polymerization
BPR	back pressure regulator
CapEx	capital expenditure
DBU	1,8-Diazabicyclo[5.4.0]Undec-7-ene
DCM	dichloromethane
DIBAL	diisobutylaluminium hydride
DMAP	4-(dimethylamino)pyridine
DMC	dimethyl carbonate
DMF	N,N-dimethylformamide
$DMSO_2$	dimethyl sulfone
DoE	design of experiments
FEP	fluorinated ethylene propylene
FTIR	fourier transform infrared
GII	Grubbs catalyst 2nd generation
HG II	Hoveyda-Grubbs second generation catalyst
HPLC	high pressure liquid chromatography
HRMS	high-resolution mass spectrometry
LC-MS	liquid chromatography-mass spectrometry
$LiAlH_4$	lithium aluminium hydride
LiHMDS	lithium bis(trimethylsilyl)amide
MW	microwave
NHC	nitrogen-containing-heterocyclic carbene
OpEx	operating expenditure

OVAT	one-variable-at-a-time
PDMS	polydimethylsiloxane
PEEK	polyetheretherketon
PFA	perfluoroalkoxy alkanes
PTFE	polytetrafluoroethylene
PTFE	polytetrafluoroethylene
qNMR	quantitative nuclear magnetic resonance
RCM	ring closing metathesis
Red-Al	sodium bis(2-methoxyethoxy)aluminium hydride
Rf	retention factor
ROM	ring opening metathesis
ROMP	ring opening metathesis polymerization
THF	tetrahydrofuran
TLC	thin layer chromatography
Tres	residence time
UV	ultraviolet

Table of Contents

Chapter 1. Introduction and literature review

This chapter provides an overview of flow chemistry, starting from the fundamental principles behind the technology, with some examples of different phase systems. It also discusses the advantages and limitations associated with implementing flow systems and concludes with discussing the use of advanced optimization techniques in the form of Design of Experiment.

1.1. Introduction to flow chemistry

For centuries, the round bottom flask and test tubes have been the most crucial pieces of equipment in chemistry laboratories. They are adaptable and practical for managing small-scale reactions. When considering the effects on the environment and the economy, batch chemistry has become time-consuming, ineffective, and challenging to scale up. Flow chemistry has become an appealing alternative globally over the last few decades finding application in both academic and industrial laboratories driven largely by the fact that it commonly provides higher selectivity, yield and purity.[1] With the intention of accelerating drug discovery and improving efficiency by utilizing smaller reactors, Mark Gilligan and Richard Gray started designing the Syrris flow systems in 1940, followed by the design of other flow reactors and components to facilitate greener and more sustainable synthesis.[2]

Flow chemistry can be defined as a continuous process of pumping chemical reagents through a system of small volume interconnected channels and microreactors where they converge and mix under desired reaction conditions in a highly controlled environment to produce material continuously.[3] A flow system consists of the following fundamental parts: inlet pumps used to continually pump and distribute reagents and solvents into the system; microreactors where the reaction occurs under the preferred temperature, a back pressure regulator to ensure consistent pressure within the system followed by a collection reservoir for the product.[4] Flow synthetic routes are preferred over batch chemistry when operating at unconventionally high temperature and pressure as smaller reaction volumes of flow systems allow the reaction to occur faster in a safer manner with minimal risks which is not the case for batch reactions.[5] In this section the key parameters and components of flow systems will be summarized.

1.1.1 Key Components:

Since flow chemistry is fundamentally different from batch processing in many ways, it is important to comprehend the key parameters and essential components before applying the technology. In batch processes, reaction time denotes the whole amount of time required to carry out the reaction from inception to quenching or working up.[4] In contrast, flow chemistry is more adaptable as it depends on the ratio of the reactants, concentration, and flow rate. Additionally, we do not use the term reaction time but rather use residence time, T_{res} (Equation 1), which is determined by the volume of the reactor in relation to the overall flow rate of the system.

Equation 1: Calculation of residence time

$$T_{res}(min) = \frac{\text{Reactor volume (mL)}}{\text{Total flow rate (mL.min}^{-1})}$$

While traditional batch chemistry makes use of flasks or vessels, flow chemistry uses various components and reactor units as highlighted in Figure 1. In order to setup a reaction in flow, a reagent and solvent delivery system along with pumps to feed the fluids into the system, are required. The fluids are allowed to mix using an appropriate mixing unit before the reaction occurs in the appropriate reactor unit under the preset cooling, heating, irradiating, and electrochemical conditions at the calculated residence time. Because the reactor unit is linked to a quenching unit, the residence time is controlled. Before product collection, a pressure regulator is inserted to maintain constant pressure regimes and ensure a pressurized system.[6,7] An in-line workup and purification unit could be used prior to product collection to benefit linking reactions. Flow components can be combined and assembled interchangeably depending on the reaction required. The fundamental flow components and reactors are displayed in Table 1 and discussed in the following section.

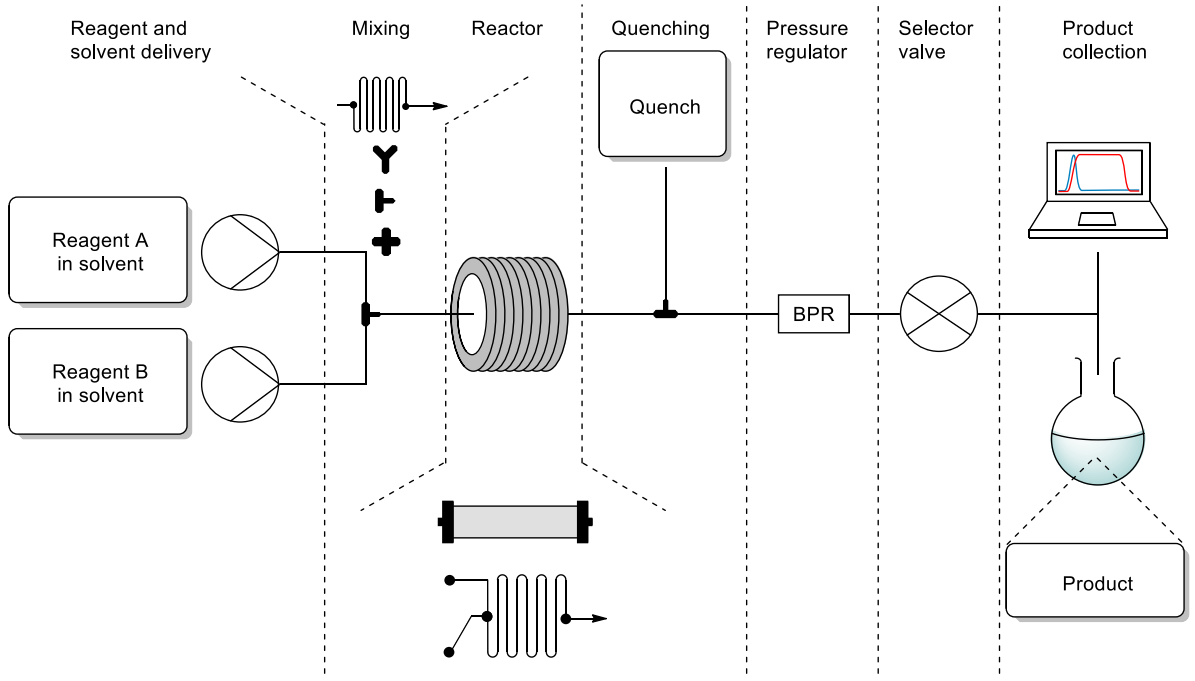

Figure 1: Example flow setup scheme employing various flow components

Table 1: Fundamental flow components with flow symbols and examples from the laboratory

Component	Flow scheme symbol	Example
HPLC pump	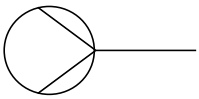	
Peristaltic pump	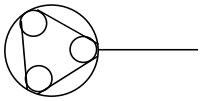	
Selector valve	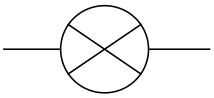	
Injection loop	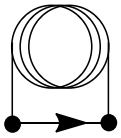	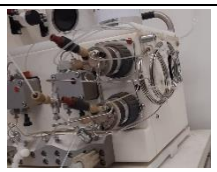
Coil reactor	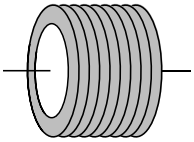	
Packed-bed reactor (column reactor)	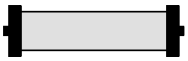	
Mixing chip	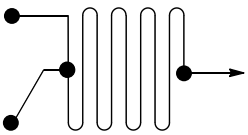	
Static mixer	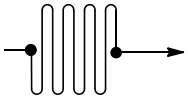	
T-piece mixer		
Back pressure regulator (BPR)	BPR	

1.1.1.1 Connecting units

Flow systems are normally pressurized sealed systems, and the units are linked together with a variety of tubing, adaptors, nuts, and ferrules which are similar or identical to the ones commonly used in HPLC systems. The type of tubing and its size is determined by the chemical compatibility and system pressure required. For pressure systems below 30 bar it is recommended to use perfluorinated polymer tubing such as FEP, PFA, PTFE, and PEEK. However, when considering systems requiring high pressures or temperatures, more durable materials such as specific alloys or stainless-steel reactors are preferred.[6]

1.1.1.2 Reagent and solvent delivery systems

Flow reactors require precise fluid control, to regulate the residence time and ensure efficient mixing, which can be achieved by either hydrodynamic flow or electrokinetic flow.[6] Hydrodynamic pumping also known as pressure driven flow is where a pressure difference or positive pressure is applied to the system's input and is linked to the flow dynamics in peristaltic, HPLC and syringe pumps. A general limitation of hydrodynamic pumping is that as the channel diameter decreases, capillary resistance increases, thus higher pressures are required to pump the solution.[8] Additionally, the hydrodynamic flow velocity profile (Figure 2), has a parabolic shape due to faster flow rates near the center of the channel and slower flow rate near the channel sides. This occurs as the fluid in contact with the channel sides experiences more friction than the fluid in the center of the channel, overall, this results in the diffusion of the flow plug.[4,6]

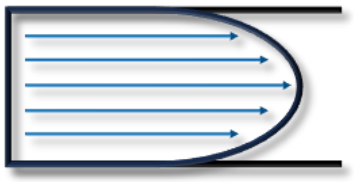

Figure 2: Hydrodynamic flow velocity profile (adapted from Riva 2009)[4]

Hydrodynamic flow can either be laminar or turbulent depending on the flow rate, viscosity, channel dimensions and the Reynolds number.[4,6] Laminar flow is the orderly, organized, and layered movement, whereas turbulent flow is irregular and chaotic. A dimensionless mass transfer coefficient, known as the Reynolds number (Equation 2) can be used to classify the hydrodynamic flow movement as laminar, transient or turbulent. Laminar flow results from R_e < 2300, and turbulent flow results from Re > 4000.[9] In between these values transitional flow occurs, which is characterized by laminar type flow dominating near the centre of the pipe and turbulent flow at the inner surface of the pipe where friction is higher.[6] In typical

microfluidic devices where the internal diameter of channels is in the range of 0.1 to 5 mm laminar and transitional flow dominates with turbulent flow being rarely achieved. [9]

Equation 2: Reynolds equation

$$R_e = \frac{Q\, D_H}{\upsilon\, A}$$

Where:

Q : flowrate of the fluid
D_H : inner diameter of tube
υ : viscosity of the fluid
A : cross-sectional area of channel

On the other hand, electrokinetic flow also known as electroosmotic flow describes the application of a potential difference across the reactor's ends. The initial effect of this flow is the migration of ions in solution towards an oppositely charged electrode followed by the double layer that develops on channels with charged surfaces.[4] In this instance a negative charge is developed on the surface of glass or silica due to partial ionization at neutral to basic pH. A double layer is then formed close to the surface by positive species in the solution. Thus, the migration of ions in the solution will be towards partial negative surface groups on the charged surfaces.[4] The linear relationship between the applied voltage and the velocity of electroosmotic flow allows for precise fluid control. In contrast to the parabolic shape of hydrodynamic flow, the velocity profile is essentially flat across the channel as shown in Figure 3. This allows for more precise residence times and flow patterns and considerably lowers dispersion.[4,6] This flow dynamic is related to nanofluidic and microfluidic devices including lab-on-a-chip applications.

Figure 3: Electroosmotic flow velocity profile (adapted from Riva 2009)[4]

Unfortunately, the use of electrokinetic flow is constrained to using polar solvents like methanol, water, acetonitrile, dimethylformamide, and tetrahydrofuran and reactor materials such as silicon and glass at neutral to basic pH, treated with polydimethylsiloxane (PDMS).[4,6] Practically speaking, hydrodynamic pumping is more frequently used as it is operationally simpler, involving the introduction of the reagent/s or pushing solvent into the system directly using pumps which are connected to reagent reservoirs or sample injection loops. The approach can be applied to most substances and solvents, with the further incorporation of

injection loops to allow the sample to be directly injected into the system in an analogous fashion to HPLC sample loading when performing a moisture sensitive reaction.[6]

1.1.1.3 Pumps

The pumps used for the delivery and pumping of reagents and substrates are dependent on the application and reaction conditions required. There are several methods for the distribution of liquids, gasses, homo- and heterogeneous solutions through the flow system. The following subsection will describe the commonly used pumping units.

a. HPLC pumps

HPLC pumps are normally utilized for liquid delivery where higher pressures are required as they employ piston pumps with check valves to ensure a forward flow of the solution. Pumping issues might arise with the use of volatile solvents such as dichloromethane, diethyl ether, and chloroform. This can be avoided by pre-pressurization of the liquid, or by degassing the system.[6] Due to the ceramic heads' tendency to cause chemical reactivity and degradation, HPLC pumps are incompatible with strong lithium bases such as lithium bis(trimethylsilyl)amide (LiHMDS) and *n*-Butyllithium (*n*-BuLi), hence sample loop injectors are advised for these substrates.[10]

b. Peristaltic pumps

Peristaltic pumps are capable of pumping well-suspended slurries, salts, and some viscous liquids at extremely fast rates. The solution of a peristaltic pump is pushed through the flexible tubing by the force of a central rotor.[6] The material of the tubing is dependent on the substrate and solvent employed. If the wrong tube is used with an incompatible solvent, the system and tubing may be harmed. Peristaltic pumps are suggested for highly reactive and moisture-sensitive reactions like Grignard or organolithium reactions.[5] The drawbacks of peristaltic pumps include inconsistent pumping which may affect the residence time of the reaction, and pressure limitations due to the general maximum operating pressure of ~10 bar for the tubing.

c. Syringe pumps

Syringe pumps are employed for precise pumping at lower flow rates. Syringe pumps continuously inject a pre-determined volume of liquid at a pre-determined flow rate into the system. However, the utility of syringe pumps are limited at high pressures and fast flow rates.[6]

As syringe pumps and peristaltic pumps cannot handle high pressures, HPLC pumps are used for systems requiring high pressure. At low flow rates, syringe pumps offer precision pumping while HPLC and peristaltic pumps produce inconsistent results. Furthermore, unlike HPLC pumps' check valves which are affected by tiny particles, air bubbles and variations in the liquid phase, peristaltic pumps are capable of pumping slurries and multi-phasic solutions. Additionally, in the case of peristaltic pumps the reaction matrix is only in direct contact with the tubing, whereas HPLC pumps and syringe pumps have the matrix in direct contact with the system pumps. If blocking were to occur by precipitation, the entire system must be cleaned. As a result, one needs to carefully select the pump used based on several variables including the solvent, solution homogeneity, system pressure and flow rate.

1.1.2 Flow reactor units

Flow reactors can be categorized into three sections: microreactors, meso reactors and large-scale reactors. These reactors differ in their channel size, shape, scale, flow behavior, fabrication techniques and application.[4] Large scale reactors are designed for industrial-scale production with channel diameters ranging from 10 mm to 1 cm and material production capacities of up to a ton per annum.[10] Due to their large diameter size and fast flow rates, they operate under turbulent flow movement. Meso reactors fall between large scale and micro scale reactions as they can handle moderate quantities of reactants. Since their diameters range from millimeters to centimeters, they operate under turbulent and laminar flow movement. To improve overall throughput, meso reactors can also be a combination of several microreactors to increase the total volume.[10]

Microreactors have typical channel diameters of 10 to 1000 µm, are frequently used on laboratory scale and they are available in a wide number of shapes and materials. The physical, and chemical properties of the material used for construction and the delivery of reagent and solvent into the system are taken into consideration when choosing a microreactor.[4] Microreactors can be manufactured out of glass, quartz, metals, ceramic, silicon, stainless steel, and/or polymers.[1] The advantages of using microreactors are precise control, fast kinetics and mixing with minimal dispersion.[8] Practically, as microreactors can be expensive scaling by numbering-up can be limiting due to the associated cost. To limit this one can employ the use of a single pumping unit to which several microreactor units are connected in parallel, unfortunately this introduces engineering challenges as it can prove difficult to ensure that flow rates remain consistent across all units.[10]

1.1.2.1 Microreactor units

Since microreactors, as previously mentioned, have smaller channel diameters, their flow behavior operates primarily in the laminar to translational regime,[4] in contrast turbulent flow which affords rapid mixing is rarely achievable without the use of in-line static mixing elements. Microreactors can also operate under "plug flow" or "segmented flow" flow patterns. Plug flow is preferred because it reduces mixing in the direction of fluid flow, each "plug" is perfectly mixed in the microfluidic channel's radial direction, and each "plug" reacts independently from the "plug" ahead or behind it.[10] Since there is precise control over reaction kinetics, steady state can be reached as the reactant concentration is constant in time at each point in the reactor. Additionally, some microreactors use "segmented flow" which refers to a flow pattern in which slugs are generated and separated by biphasic systems or gas segments. As a result, steady state cannot be reached in "segmented flow" as there is dispersion at the beginning and ending tails.[4,6,10] Microreactors can be further classified into:

a. Mixing chips

Mixing chips are classified as the best mixing and heat transfer microreactors due to a high surface-to-volume ratio. Mixing chips operate under turbulent flow generated by the integration of mixing turrets in microchannels generally ranging from 50 to 1000 µm. They are commonly manufactured from borosilicate glass, silicon, stainless steel or ceramic. Recently, photochemical transformations and catalysts immobilization on channel walls have been integrated with the manufacturing of mixing chips. Drawbacks associated with mixing chips include low throughput due to pressure limits, the tendency to block and clog due to small channels, and high costs associated with the manufacture of specialized chips.[6,10]

b. Microscale coil reactors

Coil reactors are used as a less expensive alternative to mixing chips. They have inner diameters ranging from 0.2 to 1.6 mm and can operate under laminar or transitional flow.[10] The flow behavior is dependent on the flow rate, Reynolds number and design of the coil. Coils are normally manufactured from inert fluoropolymers (PTFE, FEP and PFA), stainless steel, Hastelloy[1] or copper.[6] Coils are selected based upon the application of the reaction, temperature, and pressure. While stainless steel is chosen for high-temperature and high-

[1] Hastelloy can withstand high temperature and corrosion as is manufactured from corrosion-resistant nickel alloy and contain molybdenum and chromium

pressure reactions, FEP coils are recommended for UV/vis irradiation, and for substrates that are corrosive, Hastelloy coils are advised.[6] The temperature of coils can easily be adjusted by a temperature-controlled reactor unit, or by placing the coil in a heating or cooling bath. Transparent coils can also be used with photochemical processes by placing the coil either around or within a light source.[6,10]

c. Packed bed reactors

Packed bed reactors (columns), also known as packed tubular reactors, involve the use of a column housing solid supported reagents such as heterogeneous catalysts or insoluble reagents. They typically have diameters ranging of 1 mm to 2 cm (usually larger than mixing chips) and are made from borosilicate glass, stainless steel, or polymeric materials with resealable end pieces and a filter frit.[6,10] The volume of material within the column is determined using the weight of the solid reagent and the density of the solvent. The efficiency of the column depends on the particle size of the solid reagent, as larger particles have lower surface-to-volume ratios that cause channels to form within the column. Whereas tightly packed columns and small particles have much higher surface-to-volume ratios and smaller channels, which can lead to high pressures and system obstructions. Columns provide the advantage of heterogeneous catalyst separation, but they also carry a risk of leaching of metals (particularly when handling corrosive reagents) and deactivation of the column reagent/catalyst over time.[6]

1.1.3 Pressure regulating systems

BPR are employed to control and maintain the pressure within the sealed flow system. When working with gas releasing processes, BPR's are essential to prevent liquid-gas slugs, which may cause an increase in the total volume and affect the residence time.[10] Additionally, they provide a safer alternative when operating at temperatures above the solvent's boiling point and performing reactions at elevated pressures.[6] Most systems employ one of three types of BPR: spring loaded, adjustable, or electronic.

1.1.3.1 Spring-loaded back pressure regulator

Spring loaded BPR's are small cartridge-type devices and can only operate at a predetermined pressure value. As seen in Figure 4, they function by opening a flow passage when the fluid flow rate is higher than the threshold pressure and the fluid pushes against the spring-loaded plunger. One disadvantage is that the pressure cannot in general be adjusted in-line, instead a different unit must be used depending on the required pressure.

Some spring loaded BPR's can be adjusted by opening the cartridge and adjusting the spring tension manually, however there is a small pressure range.[6]

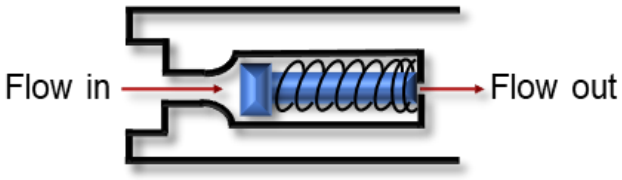

Figure 4: Spring loaded back pressure regulator (adapted from Plutschack and co-workers) [6]

1.1.3.2 Adjustable back pressure regulator

Adjustable back pressure regulators provide fast response times as the pressure can be adjusted without interrupting the flow process, and they have the advantage of having a large pressure range. As seen in Figure 5, adjustable BPR's function by using a reference pressure via mechanical forces to push against a diaphragm to adjust the flow passage. They are easy to use and provide manual control over the system, but the disadvantages include limited precision and monitoring of pressure as the conditions might change frequently.[6]

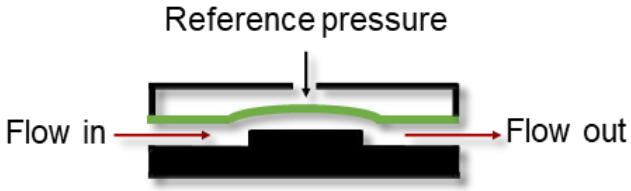

Figure 5: Adjustable back pressure regulator (adapted from Plutschack and co-workers) [6]

1.1.3.3 Electronic back pressure regulator

Electronic BPR's are used with automated systems and operate using pressure sensors that are integrated in the system, connecting to a dashboard that adjusts the pressure and monitors the reaction. Electronic BPR's provide remote monitoring in automation and high accuracy in maintaining the system pressure, however they are expensive and are dependent on power sources.[11]

1.1.4 Multiphasic Systems

Flow systems can be used to carry out several reactions with various phases. The flow movement, delivery systems, pumps, and microreactors are dependent on the phase of the

reagents and substates.[6] The flow regimes and reactor specifications for each multiphasic system are different and will be covered here.

1.1.4.1 Liquid−liquid systems

Biphasic liquid-liquid systems operate using laminar flow and segmented flow when two immiscible liquids are combined. At low flow rates, laminar flow is achieved, whereas rapid mixing in microchips can result in segmented flow. Some reactors contain in-line obstacles to the flow, such as stainless-steel beads, which promote chaotic mixing and improved mass transfer. The main benefit of liquid-liquid systems is the improvement in mixing between the two phases while maintaining a stable fluid distribution. However, scaling out is a drawback as high flow rates require large amounts of materials.[4,6] An example of a liquid-liquid system is the Wittig reaction using dichloromethane and water as seen in Scheme 1.This reaction is also conducted with a phase transfer catalyst to increase the solvents' interfacial area, and ultrasonic bath can also be employed.[4]

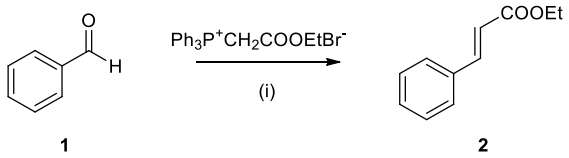

1 2

Scheme 1: Wittig reaction (i) Base, DCM/H_2O

1.1.4.2 Solid−liquid systems

Solid-liquid systems consist of a packed-bed reactor housing a solid supported reagent or catalyst and a liquid phase. They are useful for heterogeneous catalysts, solid supported polymers, scavengers, and insoluble reagents. At lower flow rates, they operate in plug flow but at higher flow rates they display turbulent or slug flow. Since the entire column or channel is packed with solid material, particle movement might be constrained, resulting in lower flow rates than required. These systems have the advantage of enhanced heat distribution and close phase contact, but they also have the drawbacks of dispersion, being time-consuming, and having a limit on the quantity of solid reagent that the column can hold.[4,6] The protection of aldehyde and ketones with dithiol, as shown in Scheme 2, was demonstrated as an example of a solid-liquid system employing a column packed with an acidic supported catalyst, Amberlyst-15.[4]

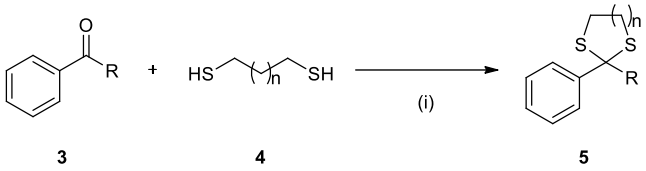

3 4 5

Scheme 2: Protection with dithiol using Amberlyst-15 in column (i) R= H, Me, n= 1,2, ACN

1.1.4.3 Gas−liquid systems

Gas-liquid reactions are highly advantageous in flow as they offer a safe environment for performing reactions using hazardous gasses such as hydrogen, carbon monoxide, chlorine and fluorine. They operate under slug and annular flow regimes by pressing the liquid against the coil reactor's surface wall while the gas passes through the middle as demonstrated with a tube-in-tube reactor. The use of gaseous reagents has benefits because it is more cost-effective, improves interfacial mixing, safety and provides control over gas pressure.[4,6] As an example, the synthesis of amides through carbonylative coupling, as shown in Scheme 3, used aryl halides, benzylamine and palladium-phosphine catalyst have been demonstrated using this approach.[4]

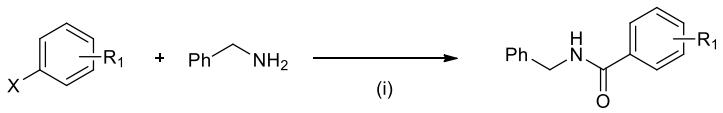

6 7 8

Scheme 3: Carbonylative coupling (i) CO (g), Pd-phosphine, 80 °C, X= Br, I

1.1.4.4 Gas−liquid−solid systems

Gas−liquid−solid systems are incredibly useful in flow for hydrogenation reactions. The H-Cube by ThalesNano is an example of an instrument in which the solution is mixed with gaseous hydrogen and passes through a cartridge (CatCart) packed with a heterogeneous catalyst. The benefit of conducting hydrogenations in flow is high interfacial area, which improves mass transfer. However, due to cartridge capacity, upscaling might be a challenge and catalyst leaching might also be a concern.[4,6] The reduction of imines to amines shown in Scheme 4 is an example of a hydrogenation reaction using a 10 % Pd/C cartridge.[4]

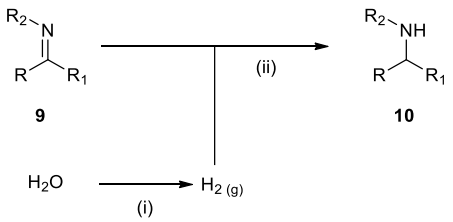

9 10

Scheme 4: Catalytic reduction (i) electrolysis, (ii) 10 % Pd/C reactor cartridge

1.2 Advantages of flow chemistry

Flow technology has emerged as a disruptive/leapfrogging technology in academia and the pharmaceutical manufacturing sector as it provides several key advantages over batch-mode synthesis. This section will discuss the advantages of using flow reactors for performing reactions, as well as their contribution to environmentally friendly and sustainable synthesis.

1.2.1 Advantages of reactor design

1.2.1.1 Large surface area-to-volume ratio

In batch-mode, unexpected exothermic runaway reactions can happen on larger scale as temperatures are managed using a cooling bath or jacket which due to the nature of their design cannot ensure uniform temperature control. Since flow reactors are designed with small channel diameters, their surface area-to-volume ratio is much larger than batch reactors, making temperature control orders of magnitude better.[10] With heat being evenly distributed, flow offers the advantage of quickly heating and cooling, making it a safer containment option as exotherms are avoided or reduced by using smaller volume tubes instead of large volume batch reaction vessels.[12,13] Mass transfer is also improved with efficient mixing occurring by using mixing devices or higher flow rates.[13] Furthermore, because of the large surface area-to-volume ratio for the narrow tubes used in flow reactors, coiled reactors provide improved efficiency for photochemical and microwave induced reactions as they provide enhanced irradiation.[12,14]

1.2.1.2 Control over reaction parameters

The precise control that flow reactors offer over reaction parameters such as residence time, concentration, flow rate and temperature generally lends itself to improved selectivity, reproducibility, purity and yield.[15] When unstable or short-lived reactive intermediates are considered, flow offers the benefit of reaction optimization within an isolated system.[3] Additionally, it aids in the prediction of a steady-state concentration profile and determining the timing of when steady state is reached.[16]

1.2.1.3 Increased pressure

Traditional batch processing has temperature limitations linked to the boiling point of the solvent system employed; however, flow reactors can operate at higher temperatures by using back-pressure regulators to elevate the solvents boiling point. Flow processes can

therefore be performed at temperatures above the boiling point of the solvents, allowing for the use of low boiling and more environmentally friendly solvents like acetone and methanol. As a result, flow enables the use of a wider range of solvents and temperatures for the acceleration and optimization of certain processes that are not possible in batch.[12,13] Additionally, supercritical fluids can also be used, with the advantage of allowing the reaction to be monitored and performed on a smaller scale as opposed to the batch method of stopping the reaction when using an autoclave.[14]

1.2.1.4 Simple control of hazardous reagents or unstable intermediates

Highly reactive reagents and intermediates can be difficult to handle in batch, while flow has the advantage of employing hazardous and highly reactive intermediates that were created in situ as part of the synthesis towards the product.[13] Unstable intermediates can be easily managed in flow since they are protected from exposure and decomposition.[13] Additionally, flow provides the safe and controlled use of hazardous reagents like phosgene, lithium diisopropylamide, diazo compounds and organic azides and gasses such as carbon monoxide, hydrogen gas and oxygen gas.[13–15] The benefit of flow is that it only requires a small amounts of highly reactive intermediates to react in the flow stream, as there is uniform heat distribution and mass transfer.[12] Therefore, its beneficial and safer to perform hazardous reactions in flow, since there is no transfer or workup of hazardous solutions as they can be synthesized, processed and quenched inside the microreactor.[14]

1.2.2 Advantages related to the continuous nature of the process

1.2.2.1 Simple scaling up

There are two ways to perform larger scale reactions in batch: either performing the reaction in numerous batches or employing larger reaction containers. As the volume of batch reactors do not scale linearly, one is quicky faced with mass and heat transfer challenges linked to changes in mixing.[14] In flow there are three methods:

- scaling out, which refers to running the process in reactors with longer flow paths with the same residence time;
- numbering up, which uses multiple reactors in parallel; and
- scaling up, which refers to using reactors with larger channel diameters.[5]

The benefit of using flow technology is that the scale-up is largely direct allowing rapid upscaling without the aforementioned difficulties experienced in batch-mode.[14]

1.2.2.2 Telescoping

Flow provides the benefit of telescoping multiple reactions, where single-step flow processes are combined into multi-step sequential sequences which can be performed without separation, isolation and purification between steps.[10] Telescoping is beneficial because it reduces the time needed for intermediate workup procedures like quenching, washing, separating, extracting and drying.[12] Inaccuracies, yield loss and handling of highly reactive intermediates are reduced, and in-line analytical equipment can also be included to monitor reaction performance.[10,12] Thus, telescoping provides an increase in reaction efficiency and yield, while operating on a safe platform, and being more environmentally friendly through the elimination of unnecessary intermediate separation/isolation/purification steps.[10]

1.2.2.3 In-line monitoring and purification

Since batch procedures consist of more workup steps than reaction steps, flow provides the benefit of in-line purification to improve process yields while being more time-efficient. Solid supported reagents, scavengers or performing liquid-liquid extractions in-line are examples of purification techniques used under flow conditions. In-line monitoring can be employed to provide real time information on the progress of a reaction, by following steady state conditions and conversion with the use of FT-IR, UV or Raman spectroscopy.[10] Therefore, flow can allow the in-line monitoring and purification of the reaction matrix, which is beneficial as optimization conditions can be achieved sooner, while removing off-line workup procedures and reducing the possibility of errors and yield loss.[10,17]

1.2.2.4 Investment

Flow technology makes economical use of space as smaller equipment is utilized compared to large batch reactors. The upfront capital cost of purchasing flow equipment may be expensive when considering large-scale production, but it would be offset by increased throughput, increased operational efficiency, reduced energy consumption and reduced waste generation due to telescoping of steps.[15] Flow technology offers lower operating expenditure (OpEx) and capital expenditure (CapEx) as the costs linked to facility operation, for example manpower, utilities, floor space, etc and working capital for example in-process inventory and waste disposal are significantly reduced.[18,19]

1.2.2.5 Chemical sustainability

To reduce or eliminate the generation of hazardous substances and provide a sustainable synthesis, chemists consider the twelve principles of green chemistry and green engineering when designing their synthetic approach.[15] In Figure 6, the green factors relevant to flow chemistry are shown in blue. In addition, flow chemists also consider the principles of green engineering like maximizing efficiency and minimizing excess when designing processes that are more environmentally sustainable.

According to traditional green chemistry principles, it is recommended to maintain a temperature close to that of the surroundings to avoid energy-intensive cooling and heating cycles.[15] Despite often performing reactions at high temperatures using flow equipment which demand more energy, the use of insulation, small reactor volumes and improved heat transfer are found to still use less energy overall compared to long batch processes for equivalent reactions and material processed.[14]

Recycling catalysts and solvents can also be a sustainable flow approach. Since the catalyst remains stationary in a column, the design enables easy separation as the reaction mixture only passes through the packed column. In contrast batch processes require separation and filtration of the catalyst from the reaction mixture. As such, this leads to less environmental exposure when the catalyst is recycled in flow, and equivalent catalyst systems are observed to have a longer lifespan through recycles.[14] Flow also enables solvent recycling when working with a single solvent or a biphasic system, and solvent-free conditions are feasible when using liquid reagents or combination liquid and solid reagent systems.[14,17]

Flow generally provides a reduced economical footprint when considering the space-time yield, which is the amount of product generated per unit time and unit volume.[15] Therefore, flow has a significant impact on developing more sustainable processes when considering the benefits like enhanced mass and heat transfer, reduced workup procedures, solvent and catalyst recycling, reduced energy consumption, high selectivity, and maximization of yields.[3]

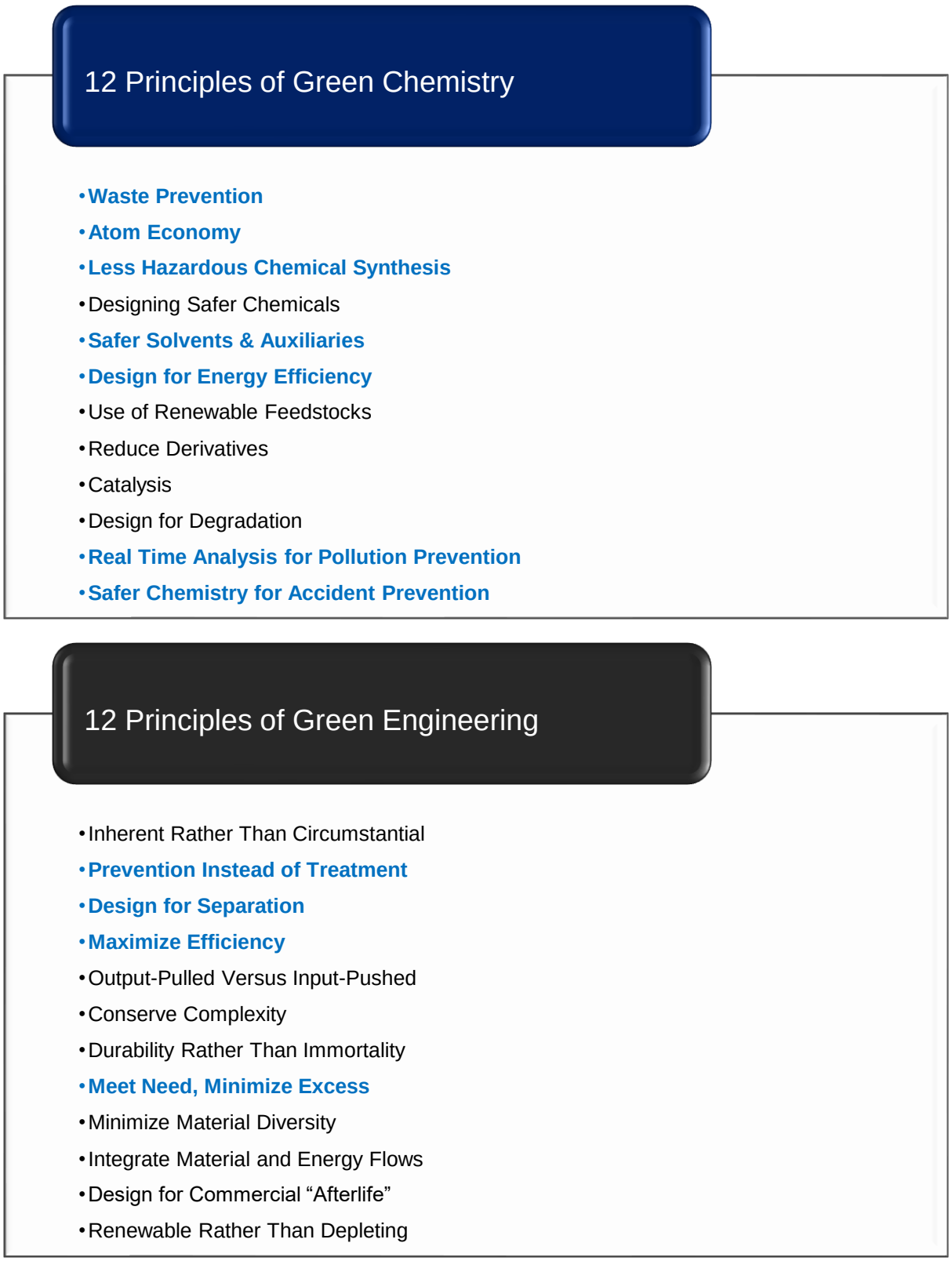

Figure 6: The twelve green chemistry and engineering principles with the impact of continuous processing displayed in blue are reproduced from Dallinger and co-workers.[15]

1.3 Limitations of flow chemistry

Although flow chemistry represents a very adaptable and practical method for conducting chemical reactions, there are a few drawbacks to consider. The choice of solvent when considering multi-step synthesis can be difficult because it should solubilize the starting reagents, products and by-products that are formed. The solvent chosen should also simplify or eliminate workup and purification, and when telescoping different reaction steps a single solvent system is preferred (as it is more easily recycled reducing solvent consumption and the need for energetically unfavorable evaporations and solvent swopping is avoided).[17]

Flow systems are highly susceptible to clogging and fouling in the presence of solids due to the small dimensions of the individual flow components.[7] Fouling can occur because of the accumulation of solid product on the channel surface, decomposition, corrosion, crystallization or precipitation of products or by-products.[6] Solids can be managed when they are suspensions through the use of peristaltic pumps, but the results are often not as reproducible as when dealing with homogeneous systems.[6] Solids and suspensions can also be managed by using ultrasonication, piezoelectricity or with the inclusion of a solubilizing stream, but this of course adds complexity to the process.[6,12]

Setup times on flow reactors can be longer due to the requirement to thoroughly inspect each connection between channels and reactor components before starting a reaction to prevent leaks, pressure fluctuations and exposure to hazardous reagents at elevated temperatures.[6] Furthermore, a learning curve exists for the scientist/operator as they need some comprehension of reaction kinetics, fluid dynamics, flow parameters and compatibility of flow systems in terms of pressure, temperature, concentration and solvent selection.[10,20]

Flow reactors and associated components are also relatively expensive; although there are recent examples of more economically feasible in-house 3D printed reactors and the production costs are coming down as use becomes more widespread and manufacturers increase production output.[6] A further restriction when considering scale-up, is the limit to the amount of reactors that can be used concurrently when taking reactor cost, tailing and dispersion into consideration if a numbering up approach is adopted.[14] That being said, the technology is essentially directly scalable and the use of appropriate dimensional scaling techniques in conjunction with numbering up (if required) still offers distinct advantage over dimensional upscaling under batch mode. Finally, the process of developing a flow method can be time consuming, which could pose a constraint when adhering to tight process development deadlines, however, once a general method is developed it can often be rapidly adapted for routine operation.[12]

1.4 Optimization approaches

Process development for pharmaceutical targets can be challenging, from preliminary test reactions through establishing an efficient manufacturing process for large-scale production. It is timely endeavor and it is challenging to adequately explore available reaction space without resorting to the use of modelling approaches. As a result, software driven mathematical modelling can be employed for reaction screening and optimization and will be discussed, with the approaches used in the research project for screening and optimization of selected steps described in detail.

1.4.1 One variable at a time (OVAT)

Conventional optimization methods typically include a trial-and-error method that involves adjusting one variable at a time (OVAT). Normally the variable of interest will be systematically changed while the other variables are kept constant.[21] Variables can include solvent, temperature, concentration, catalyst and reaction time.[22] This is a one-dimensional approach that takes time and can be considered a poor strategy as it omits the interaction between two or more variables and may overlook critical interactions and parameters.[21] As shown in Figure 7, it can increase the number of reactions with increasing variables, and it also represents a limited region of the experimental domain. This is because the parameter space only considers two variables. Therefore, if two or more variables are interacting a OVAT approach may restrict researchers from identifying the “true” optimal conditions.[22] In Figure 7, the star represents the optimal discovery point, but it is not at the most desired output as OVAT depends heavily on the starting point selected.[23]

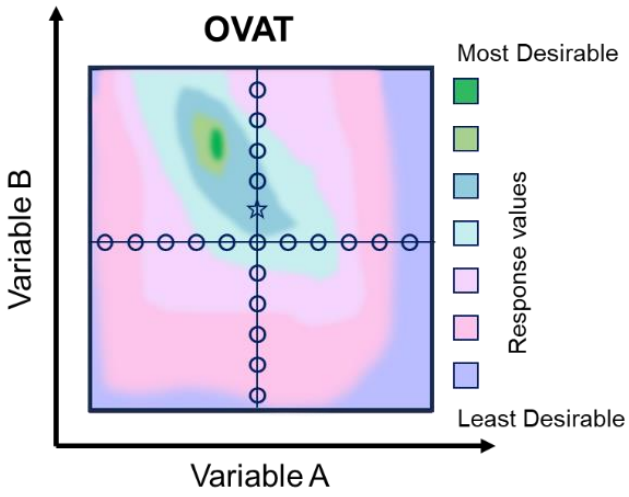

Figure 7: Visual example of OVAT method

1.4.2 Design of Experiment (DoE)

The second method, a statistical approach, allows for the simultaneous change of multiple variables to screen a reaction space.[22] DoE is often defined as a systematic approach for reaction optimization that allows a smaller number of experiments to determine the optimum results by considering a variety of reaction parameters and interactions.[24] DoE is beneficial in process development as the experiments are planned under the best conditions for improved results such as yield, purity, and selectivity.[24] Additionally, it helps to improve existing experiments by altering reaction conditions to employ green-solvents or lower reagent use. DoE can identify how various parameters and variables interact and influence the outcome of the reaction.[25] An illustration of DoE can be seen in Figure 8, where an optimal result was obtained after screening the reaction space using five experiments. In contrast to the OVAT approach, where 21 experiments were carried out and the optimum conditions were misidentified.[21]

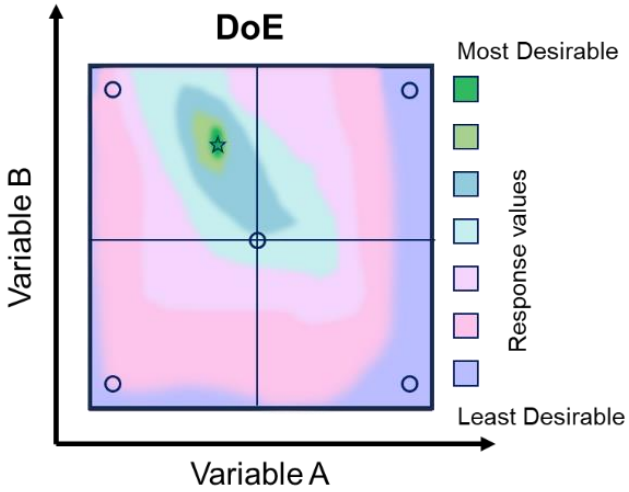

Figure 8: Visual example of DoE method

1.4.3 General overview of DoE

A DoE approach considers three primary factors: independent variables, experimental domain, and responses when designing a detailed set of experiments with specified conditions. The independent variables are those that can be manipulated and controlled during the experiment and have an impact on the experimental results. There are two main categories of independent variables: continuous variables, which may be varied over a wide range of values, such as concentration and temperature, and discrete variables, which describe qualitative variables such as equipment, solvent, reagents and catalyst.[24]

Experimental domain describes the process of investigating an experimental procedure by determining upper and lower bounds on continuous variables or specifying discrete variables such as the type of solvents. The experimental domain will include all combinations of the experimental variables. Lastly, the response is the measured outcome of the results. The response usually includes the yield, purification, cost of production or reaction time required for higher conversions.[24] DoE can be employed at three different points in the development of a reaction: early in process where optimal conditions are not yet known; when exploring robustness to determine reaction boundaries; and when optimizing conditions for small improvements like reducing the financial impact of reagent costs or when conducting a sustainability assessment.[23] Figure 9 illustrates a systematic flow chart that can be used to adapt a DoE study at any stage.

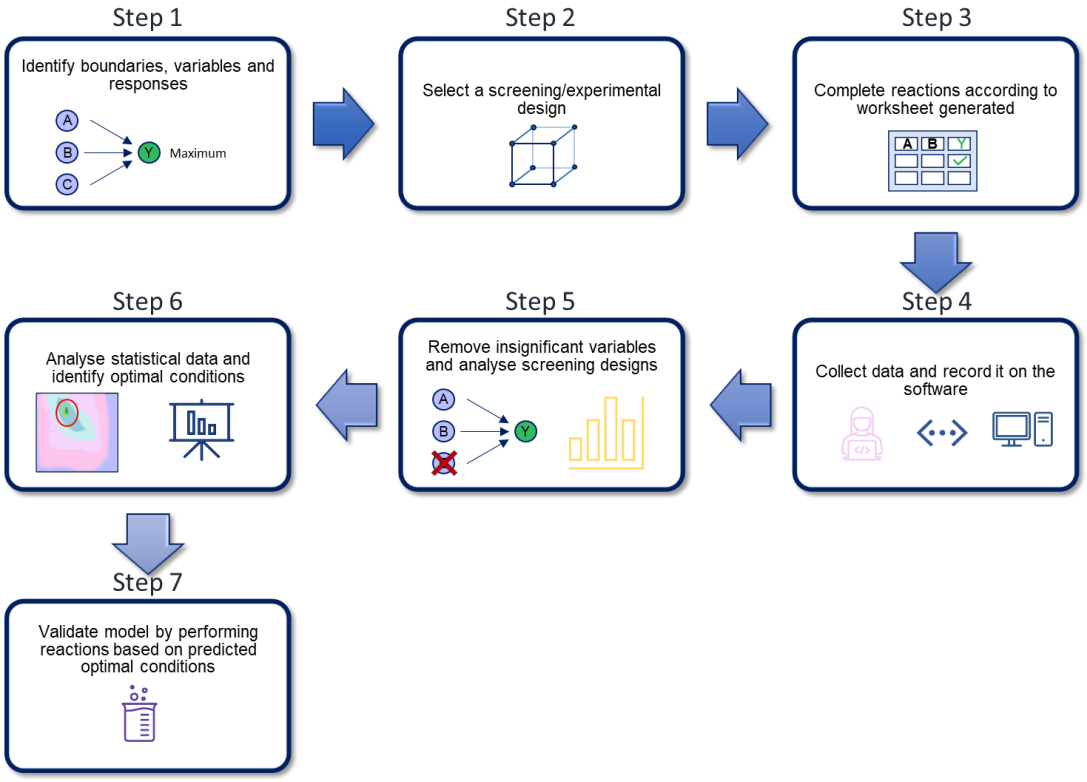

Figure 9: Flow chart to approach a DoE screening and optimization

1.4.4 General sequence of events in DoE to optimize a process

Step 1: Initially, a screening space is created, identifying the boundaries, variables, and responses. By conducting preliminary experiments, using existing knowledge, or working under experimental limitations like temperature and pressure limits based on solvent boiling point and reagent solubility, one can determine reaction boundaries. Prioritizing variables is an important step as the more variables used, the more reactions, material and time will be

required. Lastly, measured responses must be identified with the various techniques requiring isolation, and LCMS, qNMR or similar conversion measurements. To ensure accuracy and reproducibility, relevant results must be obtained.[21,23]

Step 2: After a screening space has been established, an experimental design is selected with the number of experiments required based on the desired outcome, number of variables and resources available.[23]

Step 3: The DoE software generates a worksheet with all the details and conditions of the reactions to be conducted. Once this is in hand, the reactions are conducted experimentally, and the required data is collected.

Step 4: After recording the data, the software analyzes each response individually. To develop a first-order linear model that can assess the significance of each variable, a quantitative relationship is established between the input variables and their interactions on the target responses using linear regression.[21]

Step 5: The insignificant variables are removed, allowing for an effective and thorough study of the remaining variables. In a second DoE optimization design, a more comprehensive response surface is used as screening designs are employed to eliminate the irrelevant variables and factors and place focus on the more relevant ones.[23]

Step 6: A mathematical model is generated based upon key statistical metrics, which generates histograms plots, 2D contour plots, and a 3D response surface for model visualization, along with a few other statistical representations like model validity, reproducibility and R-squared terms. The software predicts the reaction conditions where the best results can be achieved, this is commonly known as the “sweet spot plot”.

Step 7: The model is validated with additional experiments to compare the predicted response with the experimental response.[21,23]

1.4.5 Screening and optimization designs

When planning a multivariable screening experiment, it is important to choose the screening design that will statistically show the significant and insignificant variables.[21] Understanding how experimental variables directly affect each other and how they interact will provide valuable information regarding the outcome.[26] The DoE software provides experimental conditions under which each variable is examined at fixed levels after a screening design

was selected.[21,27] Typically, a full factorial design is recommended, and the number of experiments are calculated by:

$$N^K + m$$

Where:

N : number of levels per factor m : number of center points

k : number of factors investigated

It is evident that as the number of variables rises, the number of experiment's do as well. The center-points are crucial because they are used to demonstrate the curvature in the responses between the variable boundaries and are repeated to validate the reproducibility of the model.[27] The center point experiments are duplicate of triplicate experiments conducted to detect if there is any non-linearity in a response. To display significant and insignificant variables, the responses are used in combination with other responses to compute average response and multi-factor interaction effects. Figure 10 illustrates how linear regression can be used to statistically determine the impact of each variable by constructing a trendline, where the further from the diagonal line the data points are, the larger the influence of that variable.[23]

After the irrelevant variables have been eliminated, the significant variables can be studied with various optimization designs dependent on the application. The most popular approach is the central composite design as illustrated in Figure 11. With a decent curvature estimation for response maximization, they are easily made orthogonal and rotatable and operate by maintaining the central values of all variables aside from the variable under investigation.[21]

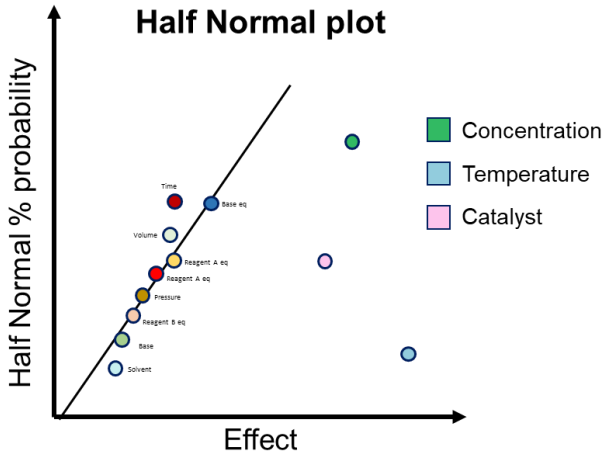

Figure 10: Half normal plot showing the influence of various variables adapted from Weissman and co-workers.[23]

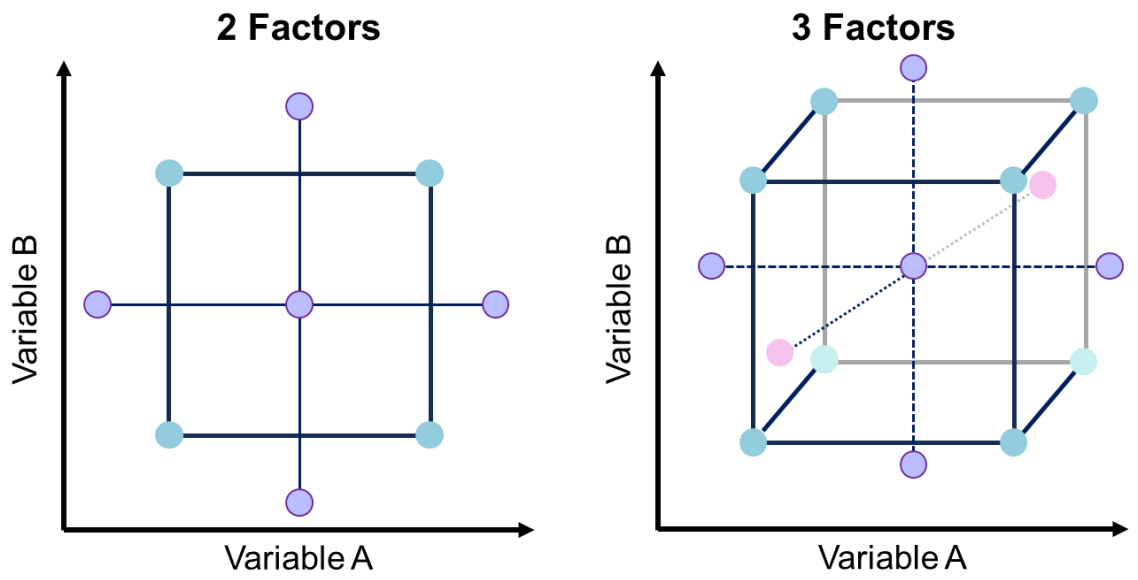

Figure 11: Visual representation of 2-factor and 3 factor optimization design of central composite, adapted from Williamson and co-workers.[21]

1.4.6 Drawbacks of DoE

Although DoE is a powerful tool for optimization, and its use in the development of pharmaceutical processes has grown, there are some limitations to statistical tools[25]. One major drawback is that it uses a lot of resources because reactions take time, material and labor to complete. Also, because there are so many variables and interactions within the complexity of many pharmaceutical drugs, creating worksheets can be difficult, especially with little information available about the compound and potential negative side-reactions. Lack of knowledge about the compound can also lead to safety concerns, as DoE may lead to exploration of potentially dangerous and unstable conditions. The final disadvantage is data analysis, as specialized statistical software and statistical knowledge are required to avoid the misinterpretation of results which can lead to incorrect conclusions and waste of resources.[21–23,28]

Chapter 2. Introduction to benzo-fused heterocycles

A brief description of benzo-fused heterocycles, the target of this dissertation, will be provided in this chapter with a focus on the key reaction steps.

2.1. Introduction to benzo-fused heterocycles

Benzo fused heterocycles are a class of compounds consisting of benzene rings fused with heterocyclic rings that contain at least one atom of nitrogen, oxygen, or sulfur. Due to their natural abundance and biological activities, oxygen-containing heterocycles have historically provided a substantial contribution to drug discovery and synthetic applications.[29] Oxygen-containing heterocycles are classified based on their:

1. saturation level,
2. abundance,
3. aromaticity, and the
4. positions of the oxygen atoms

Examples of oxygen-containing heterocyclic pharmaceutical compounds include Taxol **11** which is used for cancer treatment (first reported in 1971),[30] Digoxin **12** which is used to treat heart failure and atrial fibrillation (approved in the late 1990's), [31] and Lovastatin **13** which is used as cholesterol lowering medication (isolated in the 1980's).[32]

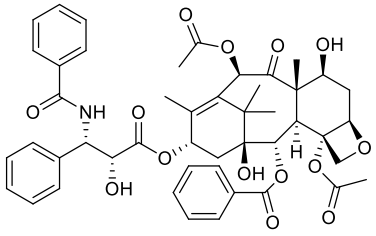

11

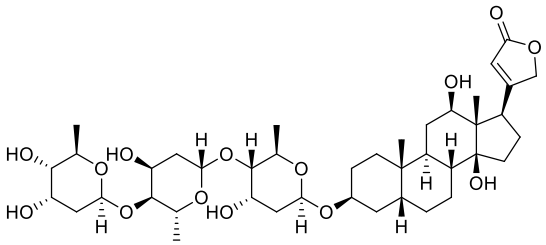

12

Figure 12: Taxol **11** and Digoxin **12** chemical structures

Examples of 5-,6-,7- and 8-membered oxygen-containing heterocycles containing the oxygen atom in the one-position are commonly reported in literature as these heterocycles are frequently used as antibiotics and antimicrobial agents in pharmaceutical applications.[33] An example of a naturally occurring benzo-fused compound with oxygen in the one-position is Cnidioside **14**, which possesses cytotoxic and antimicrobial activities and can be found in the plant *Ruta graveolens*.[34]A Lobatamide C analogue **15**, which was synthesized with a large lactone ring and was evaluated for V-ATPAse inhibition, is an example of a pharmaceutical template with the oxygen in the one-position.[34]

13 14

Figure 13: Lovastatin **13** and Cnidioside **14** chemical structures

Compounds with the oxygen atom in the two-position are more uncommon since these compounds mostly occur in higher oxidized forms.[34] These compounds are also beneficial as pharmaceutical templates. For instance, Drypemolundein A **16**, which was isolated from the stem bark of the plant *Drypetes molunduana*, has demonstrated anti-inflammatory and analgesic properties.[35] It was noted that ring-closing metathesis (RCM) was a common step often employed in the synthesis processes of benzo-fused heterocycles. van Otterlo and co-workers employed ruthenium-mediated metathesis with second-generation Grubbs II catalyst, focusing on RCM and alkene isomerization for the synthesis of 5-,6-, 7- and 8-membered oxygen-containing heterocycles.[34]

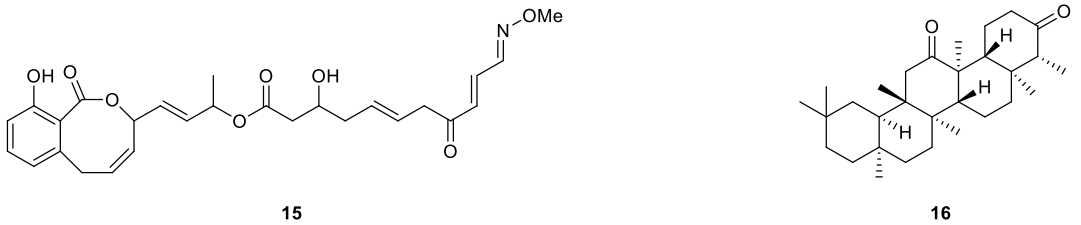

15 16

Figure 14: Lobatamide C analogue **15** and Drypemolundein A **16** chemical structures

2.2 Target molecule for current research

This section discusses the synthesis of the target molecule, (*Z*)-7-isopropoxy-8-methoxy-3,6-dihydro-1*H*-benzo[*c*]oxocine **25**, an 8-membered oxygen-containing benzo-fused heterocycle. The target molecule was selected as we were interested in developing an improved approach to accessing the scaffold for future structure-activity relationship screening and to demonstrate that modern process technologies like flow can also be used routinely to perform fundamental research in a more sustainable and responsible manner. A batch synthetic route to this pharmaceutical template had been previously investigated and published by van Otterlo and co-workers,[34] however, the synthesis for the 8-membered ring had not yet been demonstrated under flow conditions.

The overarching aim of this project was to evaluate the use of flow technologies for the optimization and synthesis of the target 8-membered oxygen-containing benzo-fused heterocycle. The synthetic scheme was previously validated by the Riley group at University of Pretoria based on the publication by van Otterlo and co-workers (Scheme 5).[34] In our groups hands it was found that the first allylation (Step 1), iso-propyl protection (Step 3) and second allylation (Step 5) were time consuming and took 20 hours at 60 °C to produce the desired products in low yields. Furthermore, these three steps and the Claisen rearrangement (Step 2) were conducted in dimethylformamide, which is considered a hazardous solvent and is challenging and energetically demanding to remove in post reaction processing.

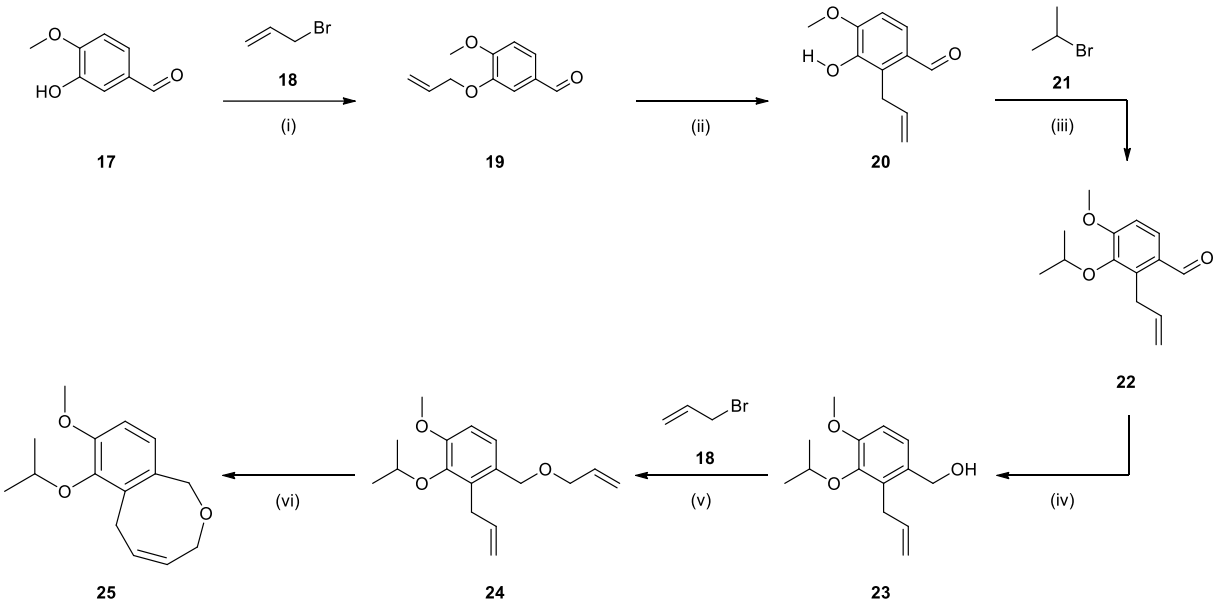

Scheme 5: Riley group results: (i) K_2CO_3, 60 °C, 20 hours, DMF (33 %); (ii) 150 °C, DMF, 64 hours (27%); (iii) K_2CO_3, 60 °C, 18 hours, DMF (27 %); (iv) Red-Al (65 % in toluene), 15 – 20 °C, 3 hours, DCM (93 %); (v) K_2CO_3, 160 °C, 20 hours, DMF (27 %); (vi) Grubbs II catalyst (5 mol %), 60 °C, 1 hour, toluene (52 %). Van Otterlo and co-worker results: (i) K_2CO_3, 60 °C, 20 hours, DMF (99 %); (ii) 150-160 °C, DMF, 64 hours; (iii) K_2CO_3, 60 °C, 18 hours, DMF (75 % over 2 steps); (iv) $LiAlH_4$, 0 °C, 12 hours THF, N_2 (86 %); (v) NaH, reflux, 20 hours, THF, N_2 (77%); (vi) Grubbs II catalyst (5 mol %), 60 °C, 2 hours, toluene (52 %). [34,36]

The Claisen rearrangement and RCM steps are both key steps in the synthesis of (*Z*)-7-isopropoxy-8-methoxy-3,6-dihydro-1*H*-benzo[*c*]oxocine **25**. Both these steps produce low yields in batch due to their reaction mechanism and reaction requirements. The following section will cover the background information and mechanism for these two steps.

2.2.1 Introduction to Claisen rearrangement

The Claisen rearrangement is a chemical rearrangement method that is frequently employed in organic synthesis, particularly in the study of aromatic bond structures, molecular rearrangement and the synthesis of natural products, flavors, and fragrances.[37,38] Rainer Ludwig Claisen made the initial discovery in 1912, but the mechanism was not put forth until the 1960's. When allyl vinyl ethers are heated into homoallyl carbonyl compounds, they undergo the Claisen rearrangement, which is a [3,3]-sigmatropic rearrangement, and produces a γ,δ-unsaturated carbonyl.[37,39] Additionally, it is also a unimolecular process meaning the rearrangement occurs within the molecule and no additional molecules are involved.[39] Some structural characteristics, such as a C=C-O-CH_2CH=CH_2 chain with the C=C-O group belonging to an aromatic ring or open chain, are necessary for the rearrangement and delocalization of electrons to occur.

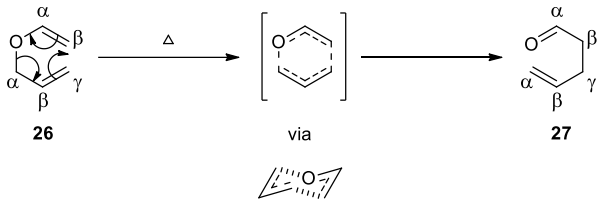

Scheme 6: General mechanism for the Claisen rearrangement

The general mechanism shown in Scheme 6 involves a rearrangement into the ortho-position as the allyl group's γ-carbon atom encounters the nucleus' ortho-carbon.[38] As a result, the carbon-oxygen bond was broken, and the allyl group was attached to the aromatic ring at the same time. As the allyl group binds to the nucleus via the γ-carbon atom, the electrons from the broken carbon-oxygen bond will go towards the oxygen. Resonance energy in the intermediate step lowers the energy required to break the carbon-oxygen bond, hence lowering the activation energy needed for the reaction.[38] The intermediate ortho-dienone then undergoes inversion of the allylic group producing the desired product. Asymmetry from the double bond is transferred, according to stereochemical studies, not only by cyclic delocalization but also through a structure that resembles a chair with three-dimensional geometry.[39]

Claisen rearrangements are typically conducted under atmospheric pressures while refluxing for several hours at high temperatures (100 – 350 °C).[37] Due to the high temperatures required for refluxing, employing photochemical, thermal activation, or microwave-assisted heating techniques can help shorten the required reaction time.

The term “microwave (MW) irradiation” refers to electromagnetic radiation with frequencies between 0.3 and 300 GHz. The ability of the solvent or reagent to absorb microwave energy and transform it into heat is necessary for MW enhanced chemistry.[40] When compared to conventional heating, MW heating provides advantages such as penetrative radiation, material selectivity, non-contact heating that prevents overheating, and rapid heating or cooling resulting in higher yields in less time. The disadvantages of MW heating include a shallow penetration depth when scaling up and a few safety issues including the flammability of organic solvents and the lack of systems with proper pressure and temperature control.[40,41] The reaction vessels employed are manufactured from microwave-transparent materials like Teflon, quartz and borosilicate glass.[40]

Ley and co-workers demonstrated MW-assisted heating for the Claisen rearrangement of allyl ether **28** in the synthesis of the natural product Carpanone. The reaction was conducted at temperature of 220 °C in a doped toluene-ionic biphasic system using 1-ethyl-3-methyl-1*H*-imidazoliumhexafluorophosphate **29**. It was found that performing a single irradiation for 45 minutes resulted in a lower yield of 86 % compared to performing three successive irradiations of 15 minutes each to obtain 97 % yield.[42]

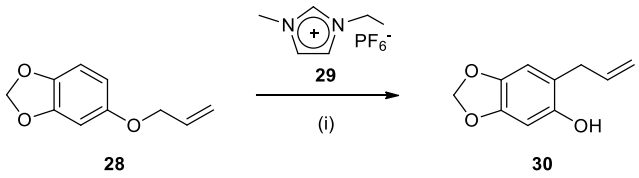

Scheme 7: MW, 220 °C, 3 × 15 minutes, toluene (97 %)

The use of MW irradiation for the Claisen rearrangement of allyl vinyl ether **31** to an aldehyde was also reported by Normann and Buchwald. It was found that 80 % of the product **32** was produced in dimethylformamide after 5 minutes at temperature of 250 °C. In contrast, a higher yield of 90 % was obtained with conventional heating at a temperature of 120 °C, however the reaction took 24 hours to complete.[40]

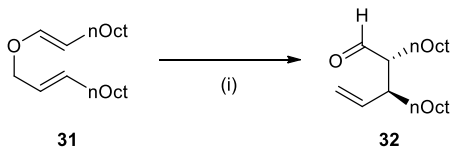

Scheme 8: MW, 250 °C, 5 minutes, DMF (80 %)

2.2.2 Introduction into ring closing metathesis

Olefin metathesis is a term that can be used to describe reactions that produce carbon-carbon bonds, which are crucial steps in the synthesis of many pharmaceutical targets. Ring-closing metathesis (RCM), ring opening metathesis (ROM), ring opening metathesis polymerization (ROMP) and acyclic diene metathesis polymerization (ADMEP) are a few examples of olefin metathesis reactions.[33] The word “metathesis’ is derived from Greek words “meta” for change and “thesis” for position,[43,44] or transposition.[45] RCM can be explained as the recombining of two carbenes to create a cyclic structure, i.e. the production of a carbon-carbon double bond from two alkene bonds with the help of a transitional metal catalyst.[33] In the project reported herein we envisaged employing the use of RCM as a key step in the preparation of the 8-membered oxygen containing ring in the benzo-fused heterocycle targeted.

In the 1950’s, molybdenum on alumina catalysts were used for transitional metal-catalyzed reactions.[46] Unfortunately, the catalyst’s sensitivity to air and moisture as well as the side-reactions produced by oxygen functional groups limited the catalyst’s use in organic synthesis.[46] Due to its great selectivity and molecular mechanisms, which had the potential to lead to advancements for medicinal applications, olefin metathesis in organic synthesis and homogeneous catalysis quickly attracted more interest.[45] It was found that ruthenium catalysts showed promising results, in contrast to tantalum, molybdenum, and titanium catalysts, which were incompatible with alkenes containing oxygen functional groups. Finally, Yves Chauvin, Robert H. Grubbs and Richard R. Schrock made a breakthrough culminating in them being awarded the Nobel prize in Chemistry in 2005 for their contribution to the “development of the metathesis method in organic synthesis”.[43]

Following this, ruthenium catalysts became widely utilized in organic and polymer chemistry because of their high reactivity and functional group tolerance.[47] Grubbs published the first generation “Grubbs I” catalysts **33** in 1995, and mechanistic analyses revealed that the ruthenium complex displayed reactivity because of phosphine dissociation, which led to the formation of a 14-electron Ru-complex. However, it also demonstrated that the dissociative step is reversible, which causes the catalyst in solution to be highly unstable.[47] A bulky, electron rich nitrogen-containing-heterocyclic carbene (NHC) ligand was used in place of one phosphine ligand (PCy_3) to overcome the reversibility issue. The NHC ligand has increased reactivity and stability due to its nucleophilic and electrophilic capabilities, which makes it a stronger sigma-donating ligand. Given the name the Grubbs second generation

"Grubbs II" catalyst **34**, this catalyst is widely accessible and used more frequently for cross-metathesis reactions.[33,43]

Gavin Madeley provided a detailed explanation of the enhancements made possible by Grubbs II catalysts as opposed to Grubbs I catalyst.[33] He claimed that by substituting one of the PCy_3 ligands with the NHC ligand, the electron density was pushed towards the metal center and the Ru-P bonds were weakened, making bonding more facile and stable. The inclusion of the bulky NHC ligand, which stabilized the 14-electron intermediate and reduced PCy_3 re-association to the metal, was another advantage.[33]

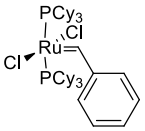

33

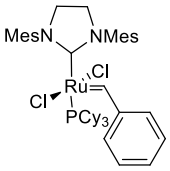

34

Figure 15: First generation Grubbs catalysts **33** and Grubbs second generation catalyst **34**

Despite the catalyst's excellent functional group tolerance and good application there was still potential for improvement with the Grubbs II catalyst in terms of air stability and catalytic lifespan. Hoveyda and co-workers created the Hoveyda-Grubbs catalyst **35** by substituting a PCy_3 ligand with a bidentate benzylidene ether ligand.[48,49] Furthermore, to create a phosphine-free Hoveyda-Grubbs second generation catalyst **36**, the PCy_3 ligand in the Grubbs II catalyst was also modified by substituting the PCy_3 ligand with a bidentate benzylidene ether. Improvements were reported in the catalyst's thermal stability, oxygen and moisture tolerance, and they afforded high reactivity towards electron-deficient substrates such as fluorinated and acrylonitrile olefins.[48] This catalyst also demonstrated the ability to be recycled and immobilized.[48,49] Because of the large isopropyl group's steric hindrance and electron donation towards the metal center, the catalyst initializes slower than the Grubbs II catalyst.[48]

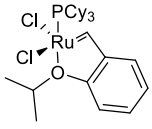

35

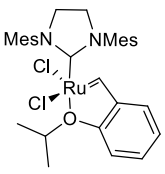

36

Figure 16: Hoveyda-Grubbs catalyst I **35** and Hoveyda-Grubbs second generation catalyst **36**

To prevent catalyst deactivation by contact with oxygen or moisture, it has been suggested that olefin metathesis be carried out in aprotic, dry, degassed organic solvents under an inert atmosphere.[49] The ring-closing metathesis of larger molecules is constrained by the increase in catalysts loadings that result in unwanted olefin isomerization and decomposition, thus the solvent systems must be assessed considering the molecule's complexity.[47]

Examining the catalytic mechanism (Figure 17) in further detail will help to completely comprehend the catalyst's role in the reaction. The mechanism for olefin metathesis was first proposed by Yves Chauvin and Jean-Louis Hérisson in 1971. The ring closing metathesis starts with a [2+2] cycloaddition (step a) with an activated metal carbene complex and the olefin starting material to create a metallic cycloalkene intermediate (step b).[46] Cycloreversion then results in the release of ethene gas (step c) with the ruthenium carbene now residing at the terminal position of the olefin. This ruthenium carbene then undergoes an intramolecular [2+2] cycloaddition (step d) with the terminal alkene. This new intermediate then undergoes a cycloreversion splitting (step e) into the regenerated metal catalyst and the new cyclized alkene. It has been found that the development of ethene gas as a by-product increases the disorder of the system making the reaction at this stage irreversible.[33] Additionally, it was noted that carbonyl olefination is affected by stoichiometric amount of the metal complex, whereas olefin metathesis is affected by catalytic quantities of the metal.[46]

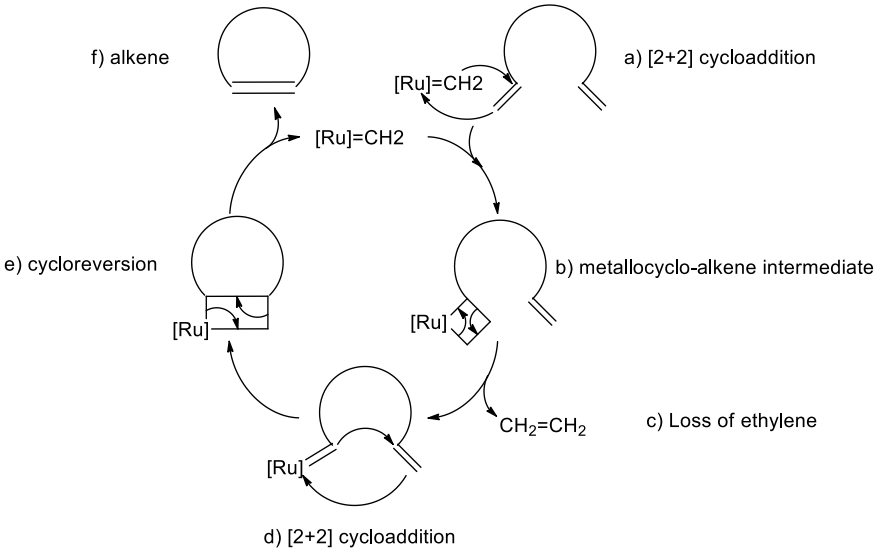

Figure 17: Catalytic cycle for ruthenium ring closing metathesis reactions

2.2.3 Proposed project plan: aims and objectives

The focus of this project was to evaluate and improve the synthesis of the target benzo-fused heterocycle under batch and flow conditions in the context of yields, environmental impact and greenness of reagents and solvents. The proposed flow approach involved six stages as shown in Scheme 9. The overarching synthetic aim was proposed to be achieved through the following objectives:

1. The first stage (first allylation) was envisioned by employing a packed-bed column with potassium carbonate and reacting it with isovanillin **17** and allyl bromide **18**.
2. The second stage (Claisen rearrangement) was envisioned by employing a stainless-steel coil reactor for heating beyond the solvents boiling point.
3. The third stage (protection of alcohol group) was envisioned by employing a packed-bed column with potassium carbonate and reacting it with **20** and 2-bromopropane **21**.
4. The fourth stage (aldehyde reduction) was envisioned by employing a packed-bed column with polymer-supported sodium borohydride or a borohydride solution
5. The fifth stage (second allylation) was envisioned by employing a packed-bed column with potassium carbonate or sodium hydride and reacting it with **23** and allyl bromide **18**.
6. The last stage (RCM) was envisioned by employing a mixing chip with a ruthenium-based catalyst to afford the desired product **25**.

Another objective is the replacement of dimethylformamide with a greener solvent.

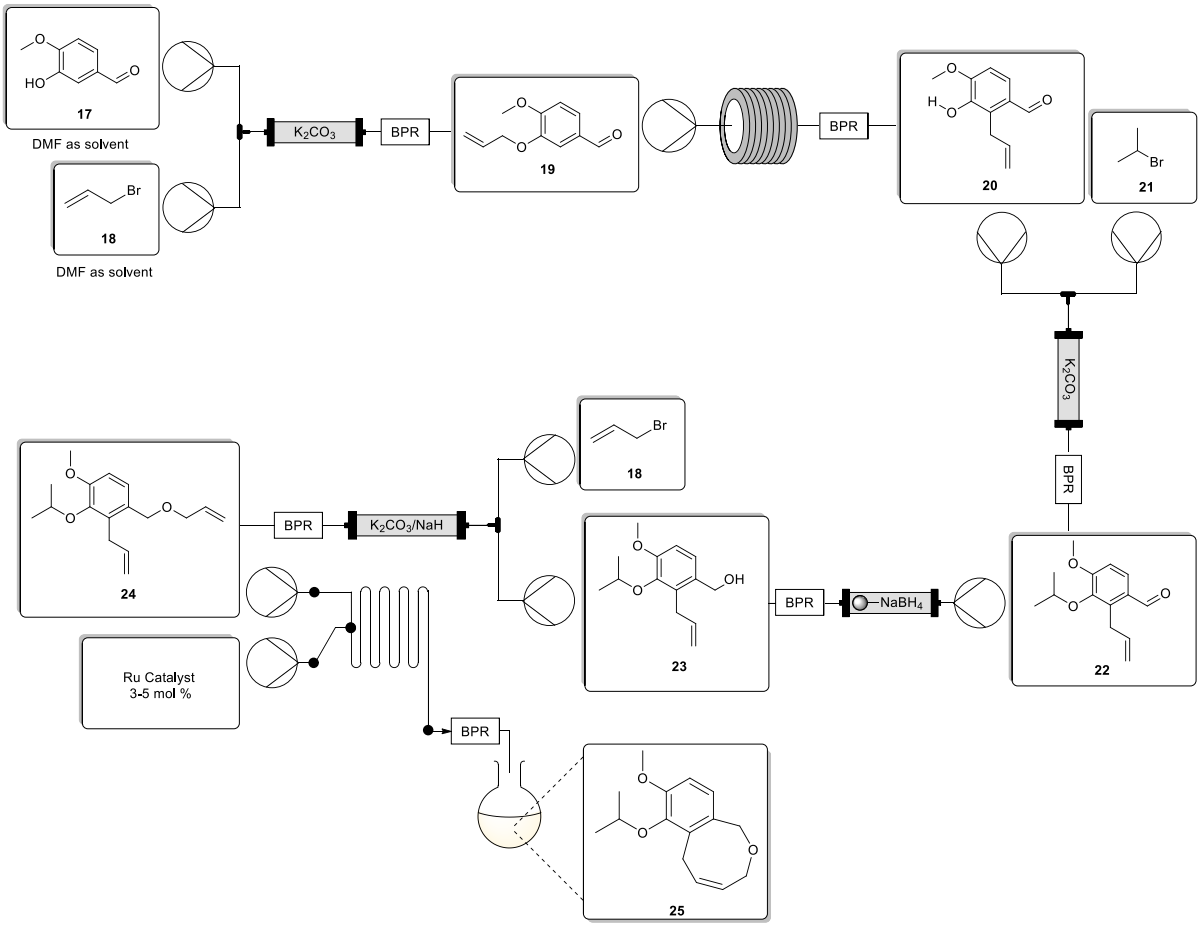

Scheme 9: Proposed flow approach for the synthesis of **25**

Chapter 3. Flow methodology development for (*Z*)-7-isopropoxy-8-methoxy-3,6-dihydro-1*H*-benzo[*c*]oxocine

This chapter provides detailed results and discussions for each synthetic step towards the target benzo-fused heterocycle under batch and flow conditions.

3.1. Allylation of Isovanillin

The first stage of the planned synthetic route includes the allylation of 3-hydroxy-4-methoxybenzaldehyde (isovanillin) **17**. Mechanistically, the phenolic alcohol group of isovanillin **17** is deprotonated by treatment with base to form a phenolate anion intermediate which then acts as a nucleophile undergoing S_N2 reaction with an allyl halide to produce the allylated product **19** (Scheme 10). Allylation reactions are useful in organic synthesis providing a means of installing new carbon-carbon bonds. The resulting allyl functional group commonly occurs in many bioactive species of pharmaceutical importance and can act as a handle for accessing different functional groups.

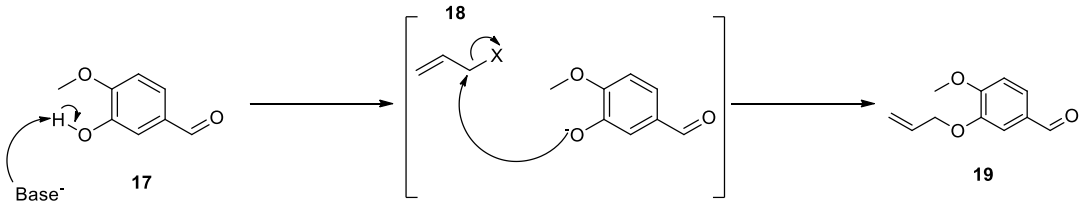

Scheme 10: General mechanism of allylation of isovanillin **17** via deprotonation and S_N2 reaction

3.1.1 Previously reported flow-based allylations

Cortes-Bordia and co-workers have demonstrated an autonomous self-optimising synthesis of the natural product Carpanone employing flow techniques.[50] The synthetic approach started with the allylation of commercially available sesamol **37**. Based on investigations under batch conditions they initially envisioned using potassium carbonate as the base with allyl bromide **18** in acetone as this provided the allylated product **39** in >80 % yield. This, however, proved unsuitable for flow translation as both the potassium carbonate and the by-product potassium bromide are insoluble in acetone resulting in reactor blockages. They considered using an Omnifit™ glass column packed with potassium carbonate or Amberlyst A26. This approach, however, led to several concerns as the use of the immobilized base required human intervention and in-line regeneration, and as a result automation would not be easily achieved. They found that replacing the base with potassium hydroxide and the alkylating agent with allyl iodide **38** afforded a homogeneous solution when the reaction was performed in aqueous methanol.

Unfortunately, preliminary batch reactions failed to give the expected product in good yield, this failure was proposed to be due to poor mixing, however, they felt this could be overcome under flow conditions. The flow setup employed consisted of two HPLC pumps connected upstream of a stock solution of sesamol **37** (0.40 M) and potassium hydroxide (0.60 M) in

methanol/water (95/5) and a second stock solution of allyl iodide **38** (0.80 M) in methanol/water (95/5) (Scheme 11).

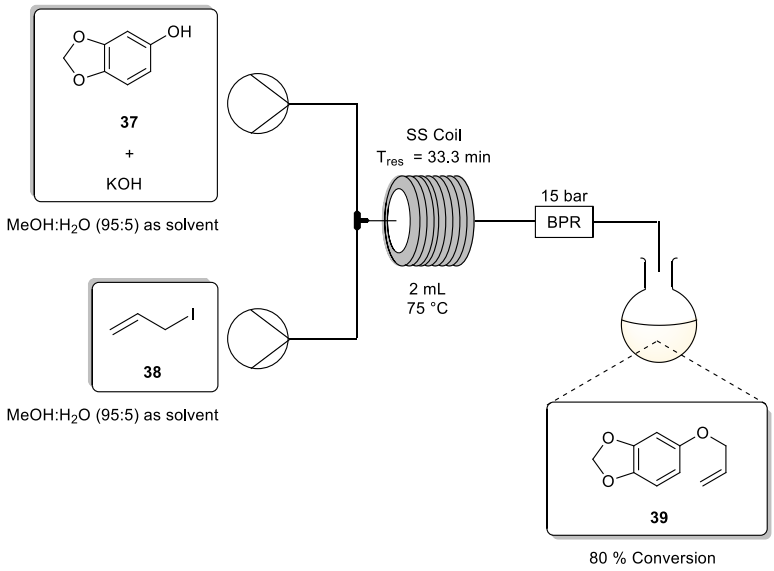

Scheme 11: Flow synthesis for the allylation of sesamol **37**

The two stock solutions were then combined at a stainless-steel T-piece mixer and thereafter heated in a stainless-steel coil reactor (2 mL) placed on a heating plate. The pressure was controlled using an electronic back pressure regulator. The product was monitored with an in-line UV detector and collected using a programmable fractional collector. Optimization reactions were performed considering three variables (temperature, stoichiometry, and residence time) and proceeded in a fully autonomous manner controlled by MATLAB. The optimal conditions were reached after 11 experiments at a temperature of 75 °C and 33.3 minutes residence time using 1.83 equivalents of allyl iodide **38** to obtain 80 % conversion of product **39** based on HPLC analysis.

Kirschning and Oltmanns then studied the use of sodium phenolates **40** with allyl bromide **18** without using a phase-transfer catalyst in a variety of phenolic ortho-allylation experiments employing flow technologies (Scheme 12).[51] The flow system utilized two HPLC pumps, one for allyl bromide **18** (1.00 M) in benzene and the other for a sodium phenolate **40** (0.10 M) in water. Before entering an induction headed steel packed-bed reactor, the two stock solutions were combined at a T-piece mixer. The system pressure was maintained at 110-160 bar and an improved yield was observed with the addition of a base to the sodium phenolates. The ideal temperature ranged from 110 to 130 °C, with a residence time of 11.33 minutes affording yields higher than 61 %, depending on the ability of the substituent groups to donate or withdraw electron density.

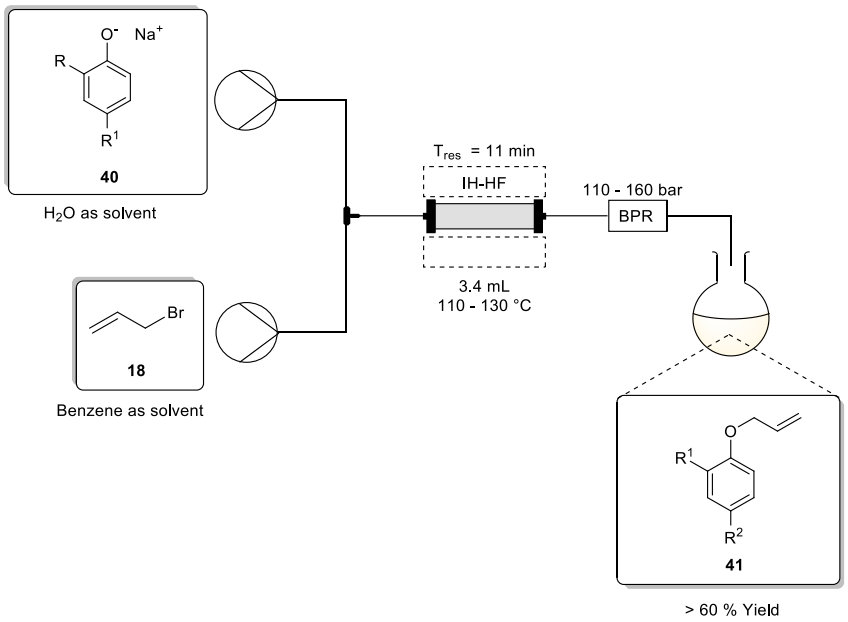

Scheme 12: Flow preparation of O-allylation of phenols **41** using sodium phenolates **40**

Finally, Riley and co-workers used the allylation of isovanillin **17** as an example reaction to demonstrate the operation of a dashboard developed for automation of flow reactors.[52] Two HPLC pumps were connected downstream of stock solutions of **17** (0.50 M) in dimethylformamide and allyl bromide **18** (0.68 M) in dimethylformamide (Scheme 13). The flow setup involved mixing of the two stock solutions at a T-piece mixer before entering a heated Omnifit™ packed-bed reactor housing potassium carbonate. Prior to collecting the desired product **19**, the reaction conversion was determined using an integrated at-line HPLC-UV analyser. A machine learning algorithm then communicated with the reactor suggesting the next set of conditions to screen. The reaction was optimised in an iterative fashion using this approach achieving an optimal output of 791 g dm^{-3} h^{-1} at a temperature of 77.3 °C after 4 minutes residence time when using 1.005 equivalents of allyl bromide **18**.

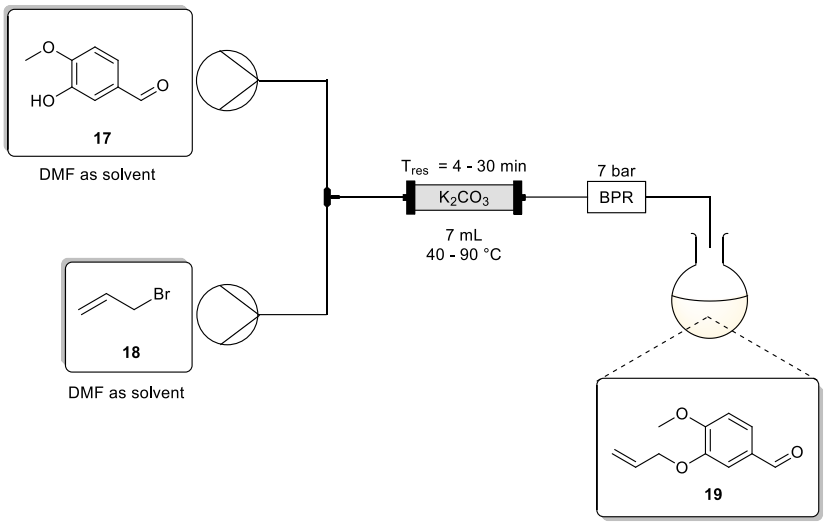

Scheme 13: Flow synthesis for the allylation of isovanillin **17** using allyl bromide **18** and potassium carbonate

3.1.2 Batch results for the allylation of isovanillin using potassium carbonate or DBU

The standard batch allylation conditions outlined by van Otterlo and co-workers were employed using allyl bromide **18** and potassium carbonate as a base in dimethylformamide (0.50 M).[34] The reaction was heated at 60 °C over 20 hours under an argon atmosphere (Scheme 14). The use of an argon was essential as dimethylformamide is hygroscopic, and we wished to avoid any potential hydrolysis of the allyl bromide **18**. As shown in Table 2, various reactions were carried out incorporating different solvents and bases. The long reaction time reported previously proved necessary as the overall yield increased with longer reaction times see entries 1, 2 and 3 where the yield was shown to increase from 82 % (20 h) to 98 % (64 h).

The use of dimethylformamide was deemed undesirable from an environmental and safety point-of-view as it is flagged as being a red solvent, in addition, its high boiling point means that its removal is time consuming and energetically unfavourable. We considered using toluene as a replacement, as the reaction did not actually require access to temperatures in excess of that afforded by toluene. Unfortunately, toluene proved to be less effective affording a poor yield of 2.1 % after 20 hours reaction time (entry 4). As expected, this improved with increasing reaction time ultimately affording 79 % yield after 64 hours. As dimethylformamide is a polar aprotic solvent, and toluene is a non-polar solvent we thought that there may be solvent effects at play. As such we next elected to screen acetonitrile as an alternative as it is a polar aprotic solvent but it is more easily removed due to a lower

boiling point. In addition, acetonitrile is better from a greenness point-of-view being designated as an amber solvent.

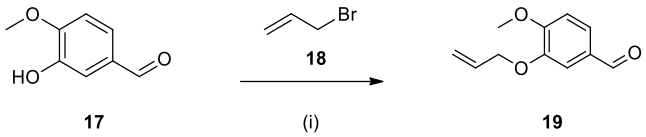

Scheme 14: Allylation of isovanillin **17** (i) K_2CO_3, 60 °C, DMF, 20 hours (82 %)

Table 2: Batch experiments for the allylation of isovanillin **17** using various bases in different solvents for 20 hours using 2.5 equivalents allyl bromide

Entry No	Reaction scale (g)	Solvent	Base	Yield (%)
1	10.05	DMF	K_2CO_3	82.0
2[a]	8.85	DMF	K_2CO_3	89.0
3[b]	**15.25**	**DMF**	**K_2CO_3**	**98.0**
4	5.04	Toluene	K_2CO_3	2.10
5[b]	2.00	Toluene	K_2CO_3	79.0
6	5.00	ACN	K_2CO_3	66.0
7[a]	10.00	ACN	K_2CO_3	88.0
8[c]	5.03	ACN	K_2CO_3	44.0
9	2.98	ACN	DBU	81.0

[a] 32 Hours, [b] 64 Hours, [c] 1.5 equivalents allyl bromide

Acetonitrile afforded better yields than toluene, however still fell short of those observed when using dimethylformamide with a reaction time of 32 hours being required to afford a comparable yield to that observed when using dimethylformamide after 20 hours (see entry 2 vs. 7). It was also deemed necessary to keep the stoichiometric excess of allyl bromide **18** used at 2.5 equivalents as the yield decreases substantial when this was reduced (see entry 6 vs. 8).

The final screen for this stage involved switching from a solid base to a liquid base. This change has the advantage for full automation of flow steps as immobilized columns would require repacking after a few reactions as noted by Riley and co-workers.[52] 1,8-Diazabicyclo[5.4.0]Undec-7-ene (DBU) was selected as an appropriate liquid base as it has a suitable pka of 24.34 in acetonitrile. DBU is a non-nucleophilic base that is a sterically hindered amidine and is used in organic synthesis as it is inexpensive and readily accessible.[53] After 20 hours of reaction time at standard allylation conditions, an 81 % yield

was achieved. The drawbacks of using DBU as a liquid base were its toxicity on an industrial scale and lengthy workup procedure as it requires liquid-liquid extraction as opposed to potassium carbonate, which just required filtration.

The product formation was confirmed by ^{1}H NMR spectroscopy. Figure 18 shows the ^{1}H NMR of isovanillin **17** together with the spectra for the alkylated products **19**, when prepared in acetonitrile and toluene respectively. Interestingly, when performed in toluene trace amounts of the thermally formed Claisen rearrangement product **20** are noted as evidence by a shift in the aldehyde proton from 9.70 ppm to 10.05 ppm, and the allyl CH_2 from 4.52 ppm to 5.07-4.89 ppm. This reaction was repeated, and similar results were obtained confirming that the allylation and Claisen rearrangement were both conceivable as a one-pot transformation but would ideally require extensive heating.

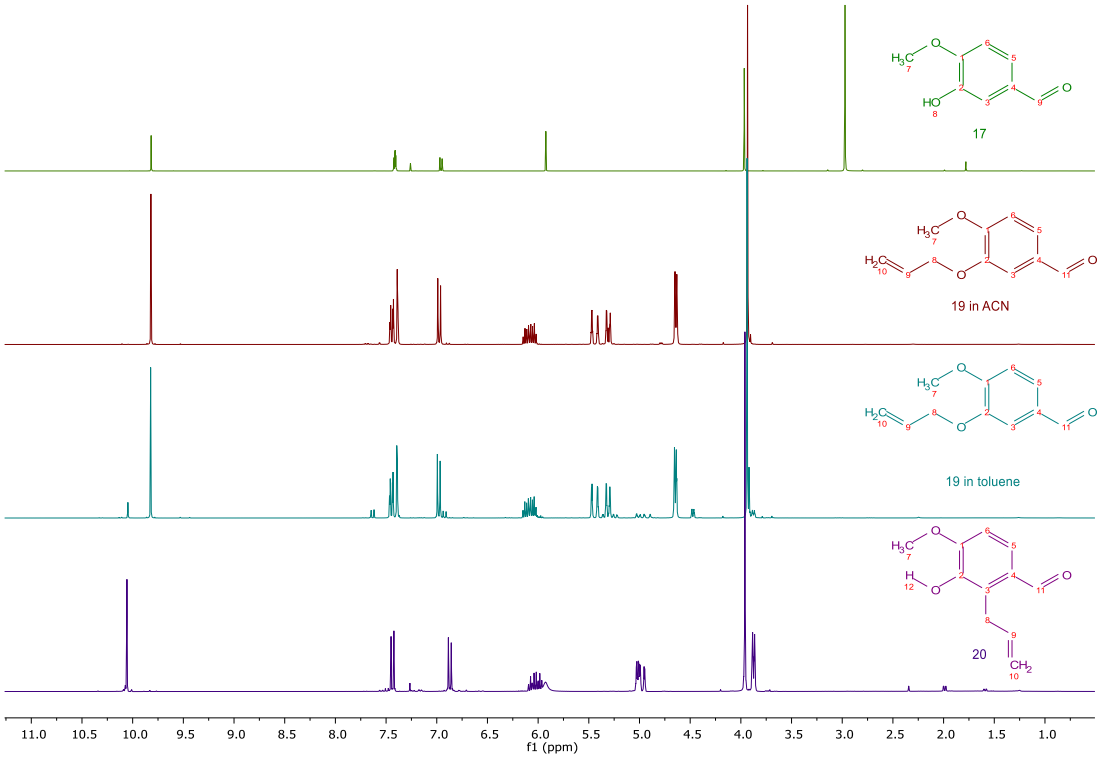

Figure 18: ^{1}H NMR spectra of isovanillin **17**, 3-(allyloxy)-4-methoxybenzaldehyde **19** in acetonitrile and toluene, 2-allyl-3-hydroxy-4-methoxybenzaldehyde **20**

3.1.3 Flow results for the allylation of isovanillin using potassium carbonate

Our team has previously looked at the allylation stage in-house using Amberlite IRA-400, triethylamine, and potassium carbonate as bases under flow conditions. The highest product conversion was obtained when using potassium carbonate as a base and dimethylformamide as a solvent. The flow setup consisted of using a single HPLC pump

connected to a stock solution of isovanillin **17** (1.0 equiv.) and allyl bromide **18** (2.0 equiv.) in dimethylformamide at a concentration of 0.33 M. The reaction was performed at a temperature of 80 °C and 45 minutes residence time to afford a 98 % isolated yield.

To further optimise the previously reported reaction conditions, several screens were performed. The flow setup consisted of a Uniqsis Binary Pump Module (BPM) containing two HPLC pumps. The pumps were connected downstream of the two stock solutions and thereafter combined at a T-piece mixer (Scheme 15). The flow stream then passed through a 10mm glass Omnifit™ packed bed reactor housing crushed potassium carbonate. Finally, the flow stream was passed through an 8 bar BPR and the product was collected and filtered through a pad of celite. The packed-bed reactor was heated to the desired temperature using a Uniqsis column jacket mounted on a heating block. The reactions were screened at 0.50 M concentration under which conditions all the reagents were readily soluble when using either acetonitrile or dimethylformamide.

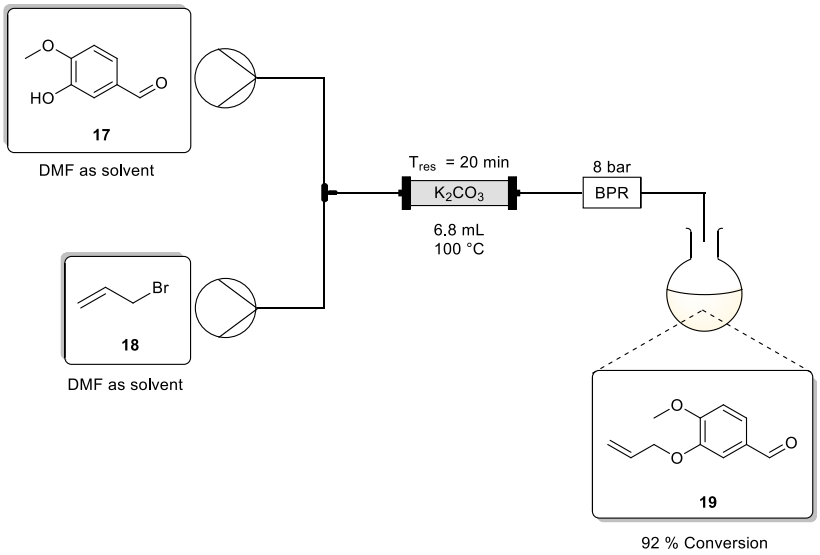

Scheme 15: Flow synthesis for the first allylation of isovanillin **17** using potassium carbonate

For flow optimization it was decided to start with acetonitrile as the solvent of choice as it is ecologically friendlier than dimethylformamide. Initially, the use of acetonitrile as a solvent in conjunction with a packed-bed reactor housing potassium carbonate was attempted (Table 3, entry 1). Unfortunately, the reaction aborted due to precipitation in the PTFE tubing after the column which appears to have been brought on by potassium carbonate leaching from the column. Following this, it was decided to exchange the potassium carbonate with DBU, and a modest yield of 67 % was realised after 30 minutes residence time (entry 2). In this instance as DBU is a liquid at ambient temperature the packed-bed reactor was exchanged for a 14 mL coil reactor heated to 80 °C. Unfortunately, the conversion was much lower than

the 81 % yield achieved under batch conditions. Inferring that there is an internal mixing problem, and the use of a mixing chip or static mixer could have been utilized to potentially improve the yield. Ultimately, however, although DBU afforded a homogeneous reaction matrix, we elected to not move forward with it as it is considered toxic, and its use require a lengthy workup.

Table 3: Flow experiments for the allylation of isovanillin **17** using two bases in different solvents at different residence times

Entry No	Reaction scale (g)	Solvent	Base	Allyl Bromide (equiv.)	Temperature (°C)	Residence time (min)	LC Conversion (%)
1[a]	0.50	ACN	K_2CO_3	2.5	80	30	0.0
2	0.25	ACN	DBU	2.5	80	30	67.0[b]
3	0.23	DMF	K_2CO_3	3.0	80	30	84.0 [b]
4	0.25	DMF	K_2CO_3	2.5	80	30	60.0
5	0.25	DMF	K_2CO_3	2.0	80	30	53.0
6	0.25	DMF	K_2CO_3	1.5	80	30	51.0
7	0.25	DMF	K_2CO_3	1.0	80	30	32.0
8	0.12	DMF	K_2CO_3	3.0	80	30	79.0
9	0.12	DMF	K_2CO_3	3.0	100	30	70.0
10	0.12	DMF	K_2CO_3	3.0	80	45	89.0
11	0.12	DMF	K_2CO_3	3.0	80	20	88.0
12	**0.12**	**DMF**	**K_2CO_3**	**3.0**	**100**	**20**	**92.0**
13	0.12	DMF	K_2CO_3	3.0	80	15	89.0

[a] Precipitation, reaction terminated, [b] Isolated yield

Since Riley and co-workers had previously performed the allylation using potassium carbonate as base and dimethylformamide as solvent, we chose to follow that route.[52] The concentration was increased to 0.50 M and the residence time was shortened to 30 minutes, using the setup shown in Scheme 15. This resulted in an isolated yield of 84 % (entry 3).The effect of the stoichiometric excess of allyl bromide **18** used was next examined by maintaining the temperature and residence time at 80 °C and 30 minutes, while lowering the allyl bromide equivalents (Table 3, entries 3-7). As anticipated, the product yield decreased steadily on moving from 3.0 to 1.0 equivalents. It is anticipated that the drop-off in yield is a mass transfer issue as the concentration of the allyl bromide stock solution was decreased but the residence time remained constant.

Additional optimization experiments were performed using stock solutions of isovanillin **17** (0.50 M) and allyl bromide **18** (1.50 M) both in dimethylformamide. As the temperature was increased and residence time was reduced, conversion increased (Table 3, Entries 8-13). Shorter residence times led to improved conversions, most likely due to improved mass transfer as the liquid phase became less laminar in nature. As expected, higher temperatures also seemed to improve performance, this could arguably be due to a combination of the resulting increase in molecular movement/energy more easily allowing the reagents to overcome the reaction activation energy barrier and increasing the mass transfer. Thus, ideal conditions were determined to be at temperature of 100 °C with a 20 minute residence time which afforded the desired product **19** in a 92 % conversion as determined by HPLC analysis using a standard curve. This translated to an 85 % isolated yield.

3.1.4 Batch results for the allylation of isovanillin using potassium hydroxide solution.

The use of the packed bed reactor as described above although efficient is not ideal as it requires manual intervention to change the base when spent and as such will create automation challenges and complicate reaction scale-up. As a result, it was decided to investigate the use of a basic solution of potassium hydroxide as recommended by Cortés-Borda and co-workers.[50] Since allyl iodide employed by Cortés-Borda and co-workers wasn't accessible at the time, we elected to screen the use of allyl bromide instead. Critically, it was noted in their publication that some precipitation occurred when using allyl bromide. As such, two reactions were initially screened under batch conditions to determine if flow translation was feasible. The reaction was carried out at a temperature of 70 °C using two different protic solvent systems (95 % methanol/water and 95 % ethanol/water). Concerningly, significant precipitation, arising from the formation of potassium bromide, occurred in both instances. Fortunately, this salt could be readily solubilised by increasing the ratio of water employed in the solvent mix. Thus, the quantity of water was increased from 5 to 30 % and the reaction was again screened using aqueous methanol and aqueous ethanol. In both instances good, comparable yields of 78 and 83 % respectively were obtained (Table 4). As the yields were arguably comparable, we decided to proceed with the use methanol for further optimization as it proved to be significantly more cost effective.

Table 4: Batch experiments for the allylation of isovanillin **17** using potassium hydroxide solution and two different solvents

Entry No	Reaction scale (g)	Solvent	Base	Yield (%)
1[a]	0.50	MeOH:H_2O (70:30)	KOH	78.0
2[b]	**0.50**	**EtOH:H_2O (70:30)**	**KOH**	**83.0**

[a] TLC Showed SM after 20 hours, [b] TLC showed limited starting material after 20 minutes

3.1.5 Flow results for the allylation of isovanillin using potassium hydroxide solution.

As the reaction produced moderate yields in batch without precipitation, it was decided to translate this step into flow using a similar setup to the one reported by Cortés-Borda and co-workers.[50] The flow setup (Scheme 16) was compromised of two HPLC pumps connected downstream to stock solutions of isovanillin **17** (0.50 M) with potassium hydroxide in methanol: water and allyl bromide **18** in methanol only. As allyl bromide and water are not miscible it is important to use only methanol for the second stock solution to ensure that a consistent concentration of the allyl bromide is introduced into the reactor. The two stock solutions were then combined at a T-piece mixer followed by a 0.5 mL static mixer for facilitating rapid mixing of the resulting biphasic matrix. This was followed by a 25 mL PTFE coil with an internal diameter of 1.5 mm that was mounted on a standalone Uniqsis heating block. It was chosen to employ the bigger diameter coil, instead of the normal 1.0 mm inner-diameter coil, to achieve faster flow rates and better mixing as initial test reactions showed no significant difference in conversion from using a smaller diameter coil. According to the article, an 80 % product conversion was obtained when reacting a stock solution of starting material at a concentration of 0.40 M with 1.83 equivalents of allyl bromide and 1.5 equivalents of potassium hydroxide. The optimal flow conditions were determined at a temperature of 75 °C and 33.3 minutes residence time. These flow conditions served as a guide for initial flow screening.

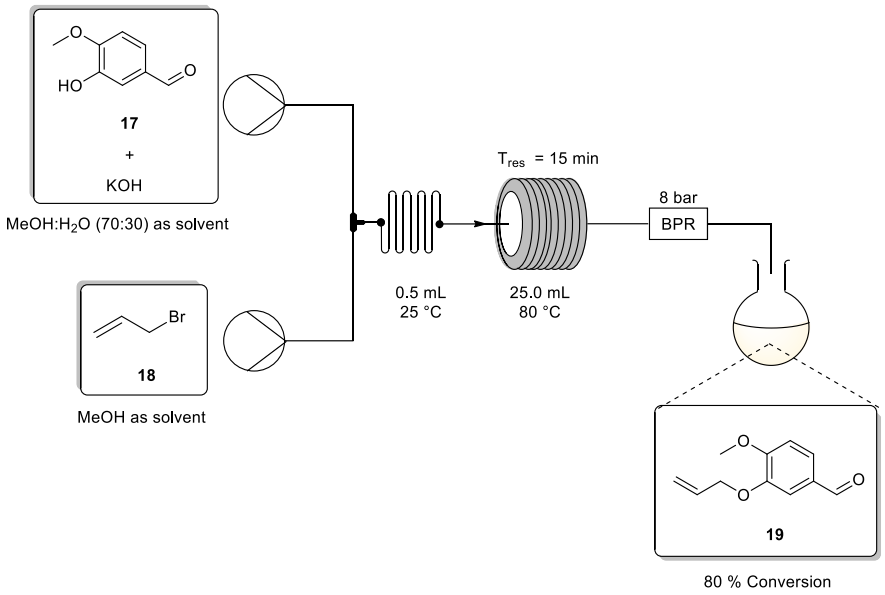

Scheme 16: Flow synthesis for the allylation of isovanillin **17** using potassium hydroxide solution

Initial reactions were performed using similar conditions to those reported by Cortés-Borda and co-workers using 1.80 equivalents of allyl bromide and 1.50 equivalents of potassium hydroxide with residence time of 15 minutes.[50] Under these conditions, a modest conversion of 68.0 % was realised (Table 5, entry 1). Thereafter, increasing the residence time to 22.5 minutes and the temperature to 85 °C afforded an increase in conversion to 75.5 % (Table 5, entry 2). It was then decided to increase the equivalents of allyl bromide to 2.0 and a similar conversion of 78.0 % was observed at 80 °C for both 15 minutes and 10 minutes residence time (entries 3 and 4). Additionally, it was found that increasing the temperature to 100 °C, had little effect on the observed conversion rate (entry 5). Overall, it was concluded that the reaction performed best with temperatures ranging between 80-85 °C coupled with a shorter residence time of 15 minutes. The shorter residence time is likely benefiting the reaction as the flow rate is higher, resulting in better mixing and mass transfer. Several additional screens led to the identification of optimal conditions employing the use of 1.80 equivalents potassium hydroxide and 2.00 equivalents allyl bromide at 80 °C with a 15 minutes residence time when using the 70:30 of methanol: water solvent mix (entries 6-11). On a 1.00-gram scale, a conversion of 92.9 % was observed which translated to an isolated yield of 88 % (entry 12).

Table 5: Flow experiments for the allylation of isovanillin **17** using potassium hydroxide solution in aqueous methanol

Entry No	KOH (equiv.)	Allyl Bromide (equiv.)	Temperature (°C)	Residence time (min)	LC Conversion (%)
1	1.50	1.8	75	15	68.0
2	1.50	1.8	85	22.50	75.5
3	1.50	2.0	80	15	78.0
4	1.50	2.0	80	10	78.4
5	1.50	2.0	100	10	76.5
6	1.80	2.0	75	15	76.9
7	**1.80**	**2.0**	**80**	**15**	**80.3**
8	1.80	2.0	85	15	79.3
9	1.80	2.0	90	15	77.3
10	1.85	2.0	80	15	78.1
11	1.85	2.1	80	15	80.1
12	**1.80**	**2.0**	**80**	**15**	**92.9** [a]

[a] 88 % Isolated yield. Reaction carried out on 1.0-gram scale

As batch results indicated a minor increase in the product yield when using aqueous ethanol, we next elected to evaluate if the optimal flow conditions identified would afford improved conversions when using 70:30 ethanol: water as the solvent system. In doing so the product conversion increased slightly from the 80.3 % (Table 5, Entry 7) observed in the methanol: water solvent mix to 83.6 % (Table 6, Entry 2). Additionally, although the product conversion appeared to decrease when the residence time was either increased or decreased, the range was very narrow 80.6 - 83.6 % and arguably one could consider that all three sets of conditions were performing comparably.

Table 6: Optimisation for the allylation of isovanillin **17** under flow conditions using potassium hydroxide solution in aqueous ethanol (70:30, EtOH: H_2O)

Entry No	KOH (equiv.)	Allyl Bromide (equiv.)	Temperature (°C)	Residence time (min)	LC Conversion (%)
1	1.80	2.0	80	20	80.6
2	**1.80**	**2.0**	**80**	**15**	**83.6**
3	1.80	2.0	80	10	81.9

In conclusion, the allylation stage was successfully translated and optimized under flow conditions. It may be carried out in one of two ways: either by utilizing a packed-bed reactor housing potassium carbonate, or by using a coil reactor with a potassium hydroxide solution. The batch reaction was conducted for over 20 hours, at a temperature of 60 °C using dimethylformamide affording an isolated yield of 82 %. In comparison, the flow translations showed improved product conversions in reduced time. The potassium carbonate route utilizing a packed-bed reactor yielded 92 % of desired product at optimized flow conditions of 20 minutes residence time at a temperature of 100 °C.

However, this approach suffered from limitations, these included, i) the use of a hazardous solvent (dimethylformamide), ii) challenges with automation and up-scaling linked to dispersion issues in the packed-bed reactor and iii) the need for manual intervention linked to repacking and replacing the packed-bed reactor when the base was spent. As a result, the reaction was modified by substituting dimethylformamide with greener protic solvents in the form of aqueous methanol or aqueous ethanol and replacing a packed bed reactor with a potassium hydroxide solution. When using aqueous methanol, optimal conditions afforded the desired product in an 88% isolated yield when using a 15-minute residence time at 80 °C and henceforth will be referred to as the optimized allylation reaction conditions.

3.1.6 Characterisation of the first allylation

The product formation was confirmed by isolation and subsequent inspection of both the proton and carbon NMR spectra of material produced under both the batch and flow processes at optimal reaction conditions. The change in signals from isovanillin **17** to 3-(allyloxy)-4-methoxybenzaldehyde **19** can be seen in the superimposed ^{1}H NMR proton spectra (Figure 19). A characteristic shift in position of the singlet methoxy signal from 3.97 ppm to 3.81 ppm is observed. The presence of the allyl group is evidenced by i) the CH_2 signal from **19**, that is upfield at 4.49 ppm (H_8) and represented by a doublet integrating for two protons, ii) the CH_2 on the alkene represented by a new doublet of doublets integrating for the two protons at 5.26 ppm and 5.39 ppm (H_{10}), and iii) the new signal visible at 6.02 ppm (H_9) due to the CH multiplet signal integrating for one proton.

Additionally, the ^{13}C NMR spectra (Figure 20) also confirmed the presence of the allyl group with the $CH{=}CH_2$ carbon signals at 132.36 ppm (C_9) and 118.21 ppm (C_{10}) respectively and the O-**CH_2**-CH signal at 69.40 ppm (C_8). The IR spectra showed the disappearance of the O-H stretch signal at 3184 cm^{-1} and the MS spectra showed a visible [M^{+}] signal at 193.1040 where the product requires a molar mass of 193.0865 g.mol^{-1}. The NMR, IR and MS results are comparable to those reported previously by van Otterlo and co-workers.[34]

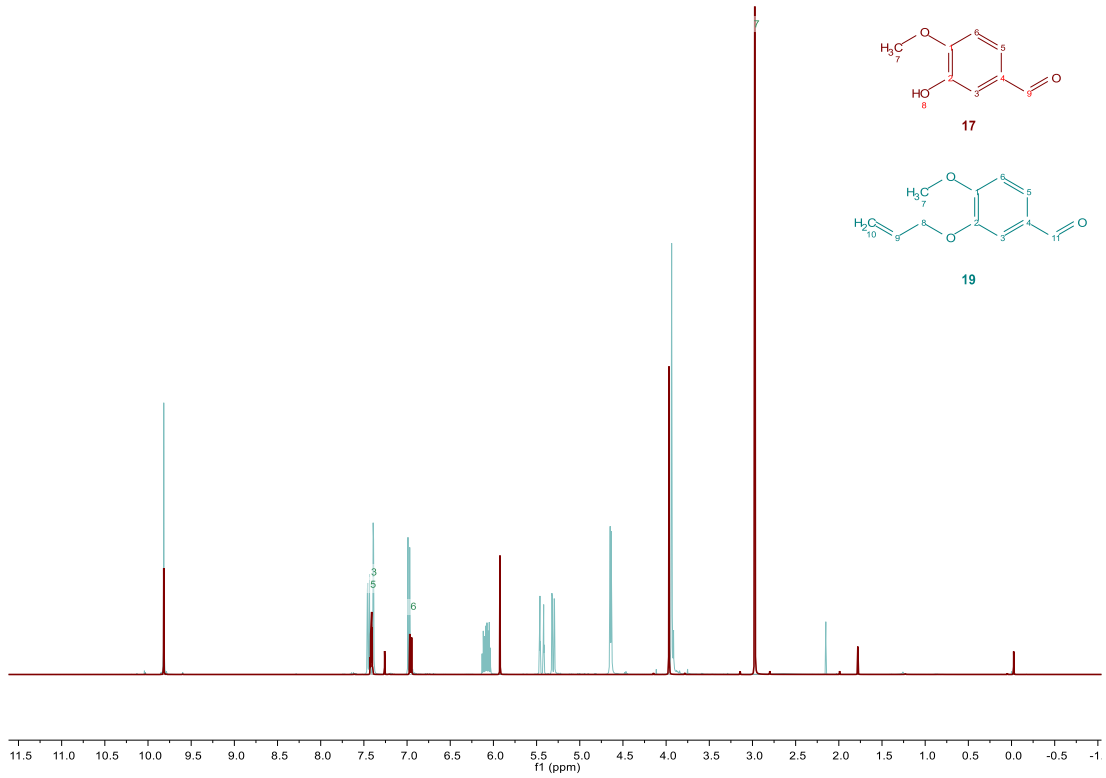

Figure 19: Superimposed ^{1}H NMR spectra of isovanillin **17** and 3-(allyloxy)-4-methoxybenzaldehyde **19**

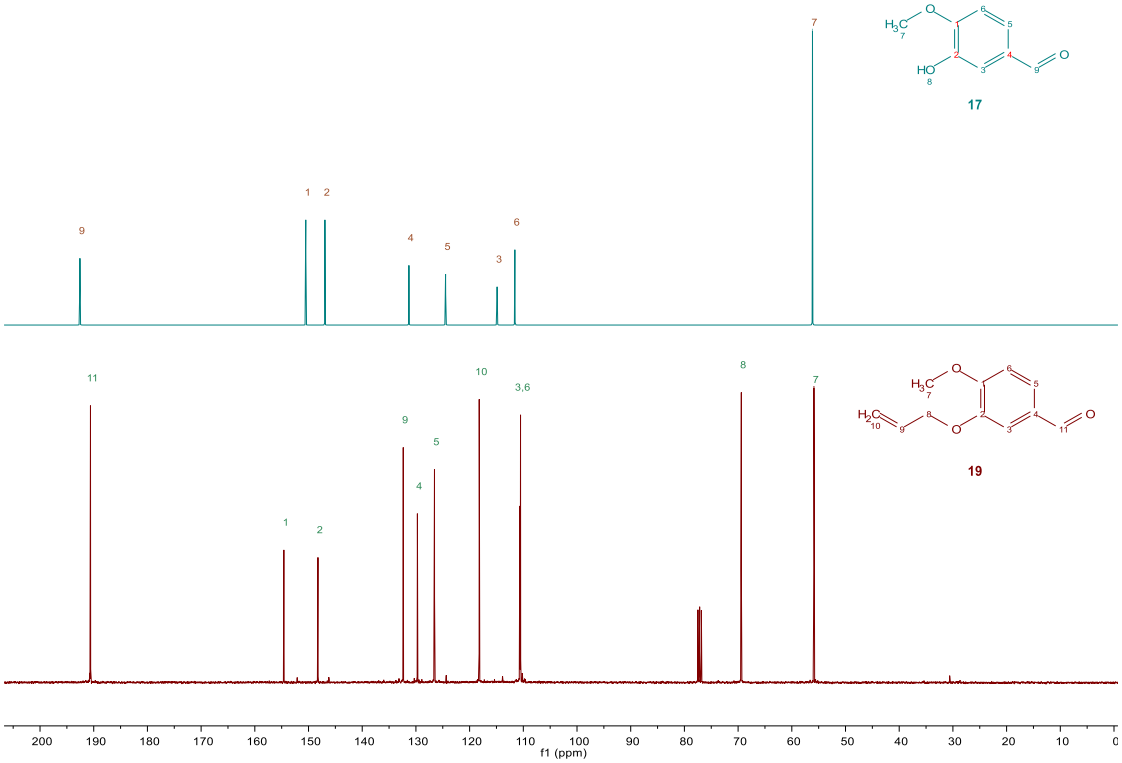

Figure 20: Stacked ^{13}C NMR spectra of isovanillin **17** and 3-(allyloxy)-4-methoxybenzaldehyde **19**

3.2 Claisen rearrangement

Stage 2 is the Claisen rearrangement which is a [3,3]-sigmatropic shift achieved through the heating of the allyl vinyl ethers to afford a γ,δ-unsaturated carbonyl systems.[37,39] In this case, a concerted shift in the pi-electrons results in the bond between the aromatic ring and allyl ether breaking while simultaneously re-attaching the allyl group on the adjacent carbon (Scheme 17). The intermediate dienone then undergoes a spontaneous re-aromatisation to afford **20**.

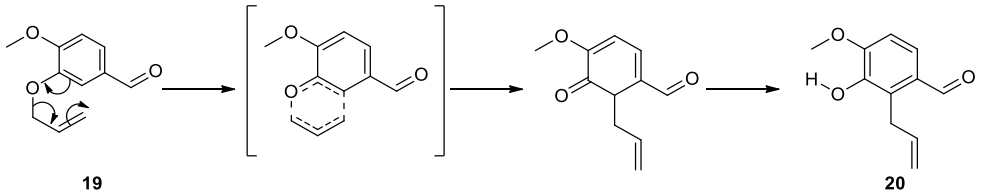

Scheme 17: General mechanism of the Claisen rearrangement **20**

Claisen rearrangements are performed under atmospheric pressures and refluxing at high temperatures ranging between 100-350 °C for several hours.[37] It has been found previously that solvents with higher boiling points generally show higher product conversions. Solvents commonly utilised included dimethylaniline (bp 193 °C), diethylaniline (bp 215 °C),[38] diphenyl ether (bp 258 °C),[54] xylene (bp 144 °C),[50] water (bp 100 °C), dimethylformamide (bp 153 °C), and toluene (bp 110.6 °C).[37,39,51] It was also discovered that polar solvents accelerate the reaction and high yields are often obtained when using solvents that undergo hydrogen bonding.

3.2.1 Previously reported flow based Claisen rearrangements

The Claisen rearrangement has been recognized by García-Lacuna and co-workers as an important step in the manufacture of the oral medication, Treprostinil, which is used for the treatment of cardiovascular diseases such as pulmonary arterial hypertension.[55] They discovered that decaline was the best solvent to solubilize the starting material, but methanol had to be introduced into the system after heating to dissolve the product and avoid precipitation. Two HPLC pumps were used in the flow setup (Scheme 18), one for the decalin solution **42** and the other for the methanol quench line. For the stainless-steel coil, a plug flow reactor was used, and an air oven was employed for heating. The highest conversion was observed at a 30-minute residence time and temperature of 250 °C. The product was collected in a flask, which after cooling to room temperature was separated. The decalin layer was washed with methanol and a brownish solid precipitate was obtained

from the combined methanol layers after evaporation *in vacuo*. Hexane was used to wash the brown solid to obtain a pale-yellow solid. After 9.5 hours and using 100 grams of starting material, a yield of 74.3g was obtained consisting of 91 % of the desired regioisomer **43**.

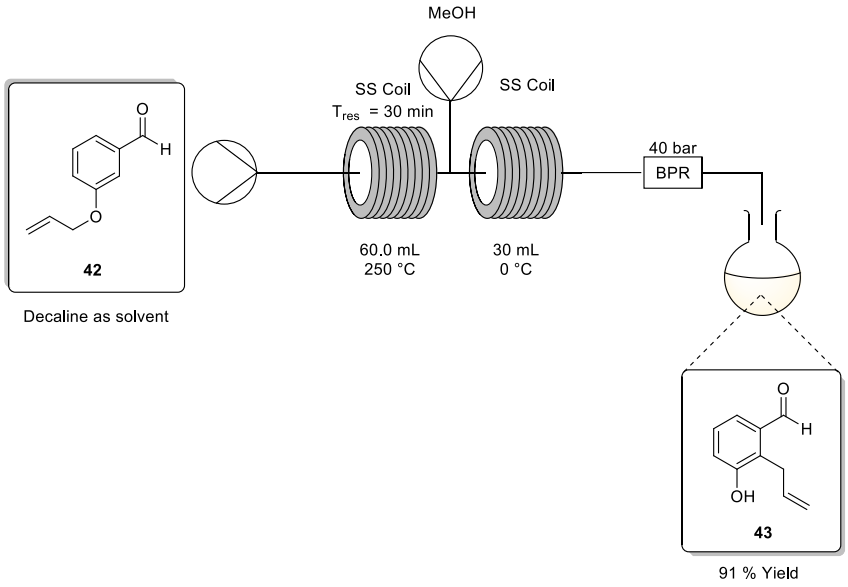

Scheme 18: Flow preparation of the Claisen rearrangement **43** using decaline as solvent

Cortes-Borda and co-workers have also demonstrated an autonomous flow procedure for the [3,3]-Claisen rearrangement of allyl sesamol **39** in the synthesis towards Carpanone**.**[50] Although higher boiling solvents are generally required for Claisen rearrangements, they discovered that acetone can be used with the added benefit that it is an environmentally friendly solvent. The flow setup (Scheme 19) was created using a single pump connected to a 5 mL stainless steel coil reactor. To avoid the vaporization of acetone, the system was pressurized to 70 bar with the use of an electronic BPR. Before product collection the results were analysed with an in-line benchtop NMR flow cell. Initial experiments at temperature of 222.4 °C and 27.6 minutes residence time, revealed a 100 % conversion as determined by NMR. The optimization space area for residence time and temperature were set to 2.5−50 minutes and 50−250 °C, respectfully. Optimized reaction conditions (250 °C and 150 seconds residence time) afforded a 74 % isolated yield at an output of 7.5 $g.h^{-1}$.

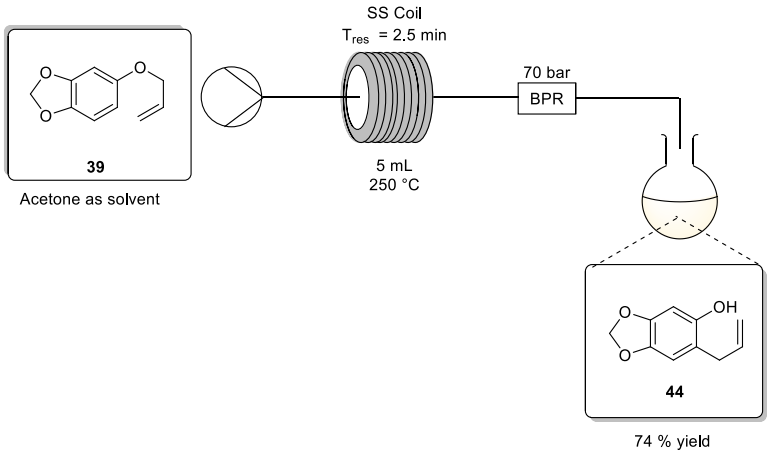

Scheme 19: Flow preparation of the Claisen rearrangement **44** from allyl sesamol **39** using acetone

Kirschning and Oltmanns developed a method for carrying out the Claisen rearrangement in water under flow conditions.[51] By investigating the rearrangement using various aromatic derivatives they found that electron rich allyl phenyl ethers such as methoxy groups produced higher yields in toluene while electron deficient allyl phenyl ethers produced higher yields in water. The flow setup employed consisted of two HPLC pumps linked to a 3.2 mL stainless-steel coil reactor (Scheme 20). The first pump introduced the phenyl ethers **41** into the flow system using an injection loop setup while the second introduced solvent. The stainless-steel coil reactor was heated in an enclosed uniform electric field created by an electromagnetic inductor. High-frequency operating conditions were employed, and the external temperature was maintained using an IR Pyrometer. The reaction was performed under high pressures and high temperatures with optimized conditions determined at selected residence times and a temperature of 265 °C for various derivative groups.

The group then followed this work with the development of a flow approach for telescoping the ortho-allylation and Claisen rearrangement for difluoriphenol **47** (Scheme 21). The flow setup used two HPLC pumps, one for the aqueous sodium phenolate solution **46** (0.098 M) in water and the other for allyl bromide **18** (1.00 M) in hexane. The solutions were mixed at a T-piece mixer, followed by inductively heating to 297 kHz in an oscillating electromagnetic high-frequency field at 150-160 bar.[51] The optimal conditions, afforded a 64 % yield of the desired product **47**, at a flow rate of 0.6 mL.min^{-1} and temperature of 110 °C for the ortho-allylation step and at 265 °C for the Claisen step. This study provided insight into using water as a flow solvent for Claisen reactions, however, high pressures are required, and scaling up can become challenging with using assisted inductive, high frequency heating.

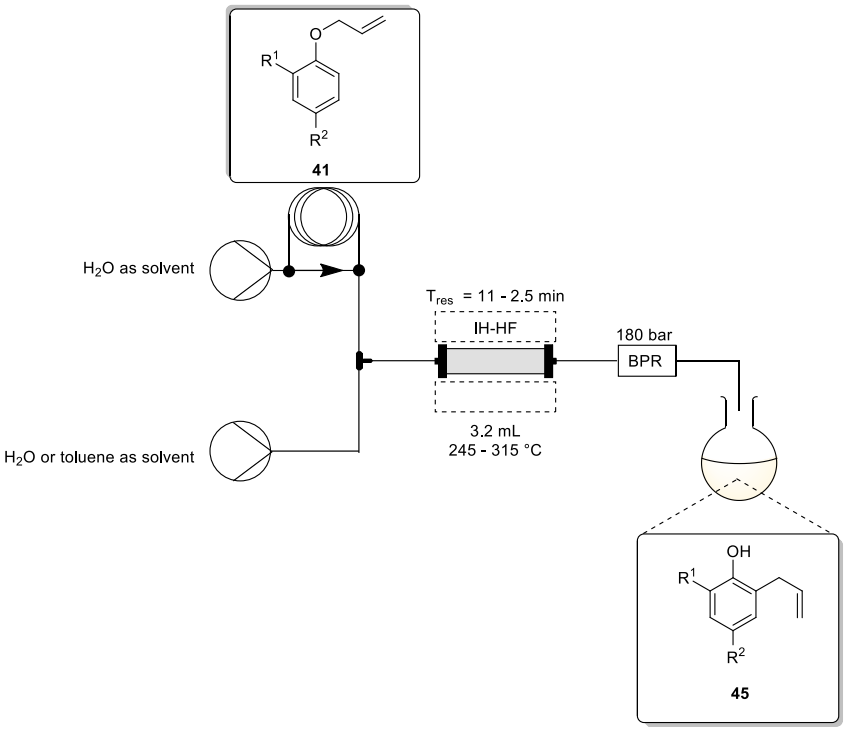

Scheme 20: Flow preparation of the Claisen rearrangement **45** of allyl phenyl ethers **41** using water

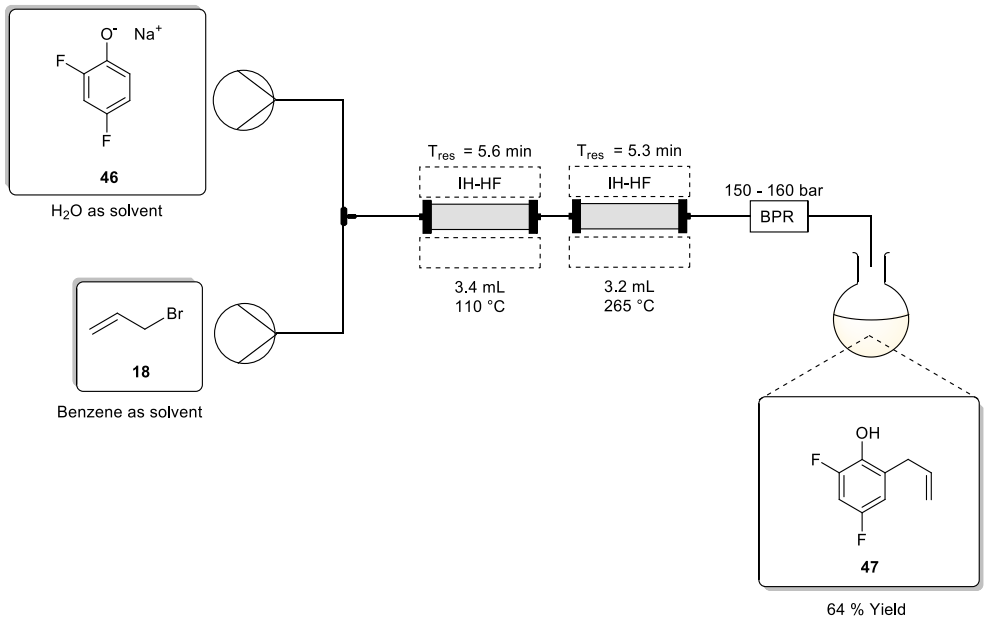

Scheme 21: Telescoped flow preparation for synthesis of Diflurophenol **47**

Kobayashi and co-workers investigated the influence of several parameters such as temperature, concentration, and solvent effects while studying the Claisen rearrangement of allyl phenyl ether **48** under flow conditions.[56] The flow setup employed consisted of one HPLC pump coupled in series to two stainless steel coils reactors (Scheme 22). One reactor was employed for heating of the solution while another was used for the cooling of the

reaction solution. They investigated the effects of solvent and temperature at 4 minutes residence time at a pressure of 100 bar and found that polar protic solvents, like 1-butanol provided the best yields at temperature of 280 °C. Further research revealed that longer carbon chains in primary alcohols also gave higher yields than secondary alcohols. Additionally, it was discovered that ethanol expands at higher temperatures leading to shorter residence times than expected. Lastly, they also performed the reaction without the use of a solvent, since both the reagent and product are oils at room temperature, and obtained 100 % conversion at 4 minutes residence time and a temperature of 280 °C.

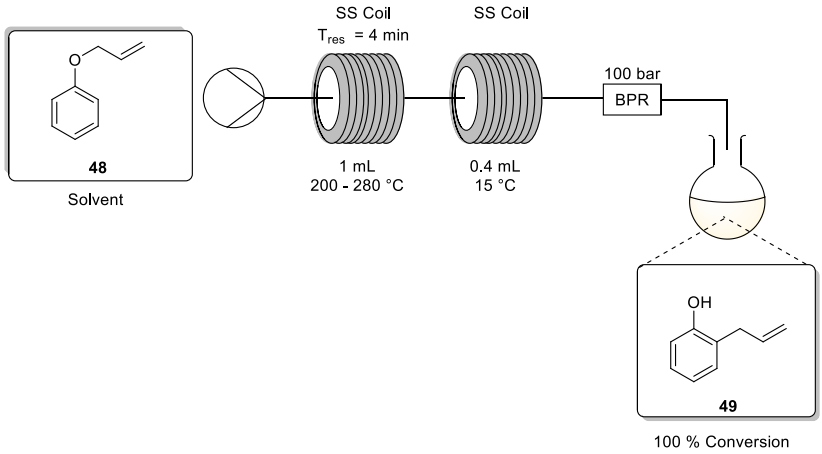

Scheme 22: Flow preparation for the Claisen rearrangement of allyl phenyl ether **48** to give 2-allyl phenol **49**

3.2.2 Batch result for the Claisen rearrangement

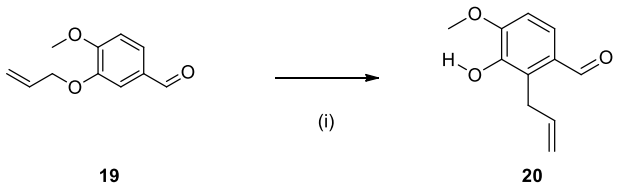

Scheme 23: Claisen rearrangement (i) 110 -120 °C, toluene (0.25 M), 72 hours (6.9 %)

This step was attempted in-house using dimethylformamide as a solvent, refluxing for 64 hours at 150-160 °C to obtain **20** in a low yield of 27 %. Critically, in dimethylformamide some decomposition and precipitation were observed visually after the 24 hour mark. Toluene was chosen as an alternative solvent to the dimethylformamide reported by van Otterlo, [34] despite having a lower boiling point, as its use afforded a simpler workup, and it is a greener solvent choice. Toluene's removal *in vacuo* also offers the possibility for solvent recycling, which is less challenging and energy intensive than when trying to recover and recycle dimethylformamide. In addition, dimethylformamide is carcinogenic and teratogenic,

hence it should ideally not be released into the environment. A batch reaction was carried out in a round-bottom flask on a 2.00-gram scale. The reaction was refluxed for 72 hours at temperature of 110-120 °C in toluene at a concentration of 0.25 M, resulting in a disappointing 6.9 % conversion. (Conversion was determined by q-NMR analysis using dimethyl sulfone as an internal standard). Despite this disappointing result, the reaction matrix was homogeneous and deemed suitable for flow translation.

3.2.3 Flow results for the Claisen Rearrangement

The Claisen rearrangement of **19** was previously evaluated in-house under flow using dimethylformamide as a solvent. It was noted that decomposition and precipitation occurred at longer residence times and higher temperatures (>220 °C), resulting in reactor blockage and fouling. In-house results showed that high product conversions could be achieved at residence times ranging from 45 to 60 minutes at a temperature of 240 °C. As noted earlier, it was decided to replace dimethylformamide with toluene, and test reactions were carried out using previously described conditions. The flow setup as seen in Scheme 24 was constructed using a Uniqsis Binary pump reactor system which is compatible with higher temperatures. A single HPLC pump was connected upstream to a stock solution of **19** in toluene and thereafter downstream to a heated 20 mL stainless steel coil, followed by a 2 mL stainless steel cooling coil at 0 °C. The latter ensured that the reaction mixture was rapidly cooled prior to passage through a 20 bar BPR and collection. Furthermore, it was essential to include the cooling coil to i) ensure that the reaction stopped rapidly on exiting the heating coil, this prevented additional conversion from occurring in the collection flask which would lead to inaccuracies in the conversions observed and ii) as a safety measure it prevented rapid uncontrolled gassing out upon exiting the reactor.

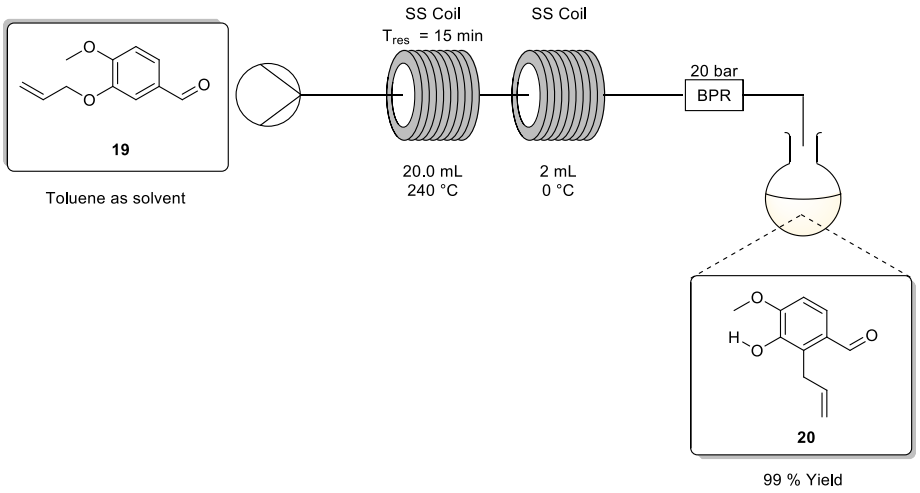

Scheme 24: Flow preparation for the Claisen rearrangement **20** using toluene

Flow experiments were carried out using a stock solution of **19** in toluene at various concentrations (Table 7). Immediately we observed near quantitative conversions (entries 1-4), regardless of the concentration, indicating the reaction is concentration independent. This was however not surprising as the process is a unimolecular rearrangement, but the experiments served to confirm that we could work up to 1.00 M concentration without any deleterious precipitation events. Furthermore, when the reaction was performed on a larger scale at concentrations of 0.50 M and 1.00 M, there was again no substantial variation in product yields (entries 5 and 6).

Table 7: Optimisation flow experiments for the Claisen rearrangement **20**

Entry No	Reaction scale (g)	Concentration [M]	Residence time (min)	Flow rate ($mL.min^{-1}$)	Yield (%)
1	2.00	0.25	45	0.44	96
2	2.00	0.50	45	0.44	98
3	2.00	0.75	45	0.44	95
4	2.00	1.00	45	0.44	94
5	10.62	0.50	45	0.44	100
6	10.00	1.00	45	0.44	99
7	2.00	0.50	30	0.67	99
8	0.38	1.00	45	0.44	93
9	0.38	1.00	30	0.67	96
10	0.38	1.00	20	1.00	100
11	**0.38**	**1.00**	**15**	**1.33**	**98**

Additional optimization experiments were conducted at a 30-minute residence time using a 0.50 M solution, yielding the desired product **20** in 99 % yield (entry 7). The residence time was also reduced while maintaining the temperature at 240 °C (entries 8-11). Based on entry 10, the ideal conditions for the Claisen rearrangement are attained after 15 minutes residence time with a temperature of 240 °C using a 20-bar BPR (entry 11). As a result of the shorter residence time, these conditions afforded a higher productivity and used less energy in comparison to previous in-house results which required a 45-minute residence time. As a result, the reaction may run for longer periods of time with less energy and solvent required, thus lowering the cost and carbon footprint related to the process.

3.2.4 Characterisation of the Claisen Rearrangement

The product formation was confirmed by isolation and subsequent inspection of both the proton and carbon NMR spectra of material produced under both batch and flow processes at optimal reaction conditions. Analysis of the ^{1}H NMR proton spectra (Figure 21) obtained using the batch approach showed limited conversion to **20**. In the case of the material produced under flow conditions, no residual starting material is observed. A small but characteristic shift in the aldehyde singlet signal from 9.83 to 10.06 ppm, integrating for one proton is observed (H_{11}). The rearrangement of the allyl group is evidenced by i) the CH_2 (H_8) signal that shifted from 4.50 ppm to 3.90 ppm, ii) the CH_2 (H_{10}) signal that shifted upfield from 5.35 ppm to 5.03 ppm as the carbon is attached to an less electronegative atom. Additionally, the broad alcohol signal (H_{12}) at 5.9 ppm confirms the presence of the phenolic proton.

Additionally, the ^{13}C NMR spectra (Figure 22) also confirmed the rearrangement of the allyl by i) the shift in C_3 downfield from 110.64 to 127.61 ppm, ii) the shift in C_8 upfield from 69.40 ppm to 28.44 ppm, iii) the shift in C_9 from 132.36 ppm to 143.88 ppm, and iv) the shift in C_{10} from 118.21 ppm to 115.37ppm. The IR spectra showed the appearance of the broad O-H stretch signal at 3354 cm^{-1}, and the MS spectra corresponded to the allylation MS spectra with the [M^{+}] signal at 193.1040 where the product requires a molar mass of 193.0865 $g.mol^{-1}$. The NMR, IR and MS results are comparable to those reported previously by van Otterlo and co-workers.[34]

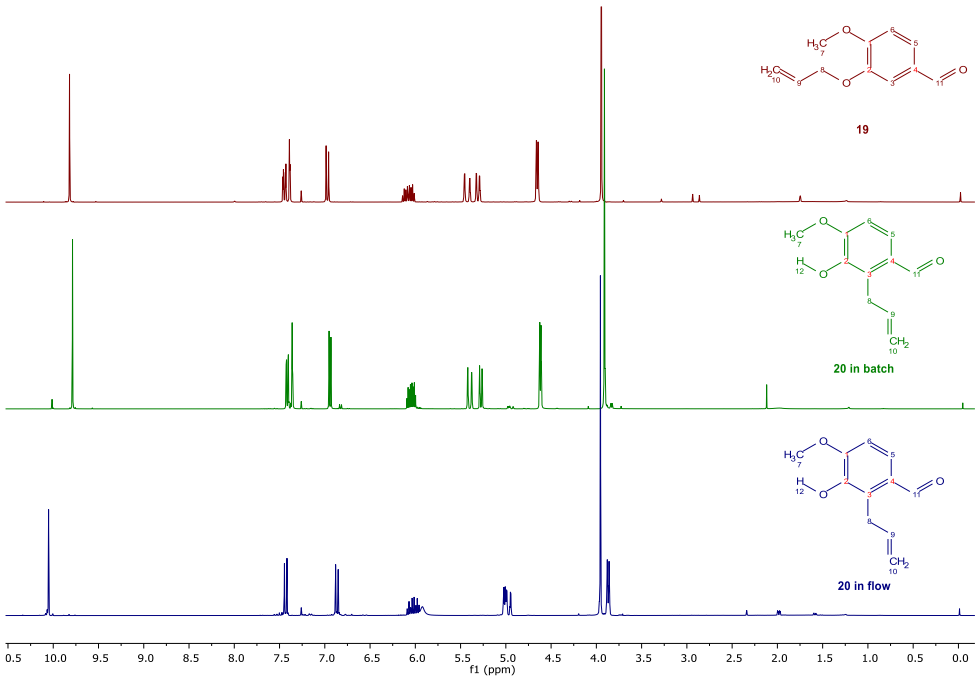

Figure 21: Stacked ^{1}H NMR spectra of 3-(allyloxy)-4-methoxybenzaldehyde **19**, batch and flow of 2-allyl-3-hydroxy-4-methoxybenzaldehyde **20**

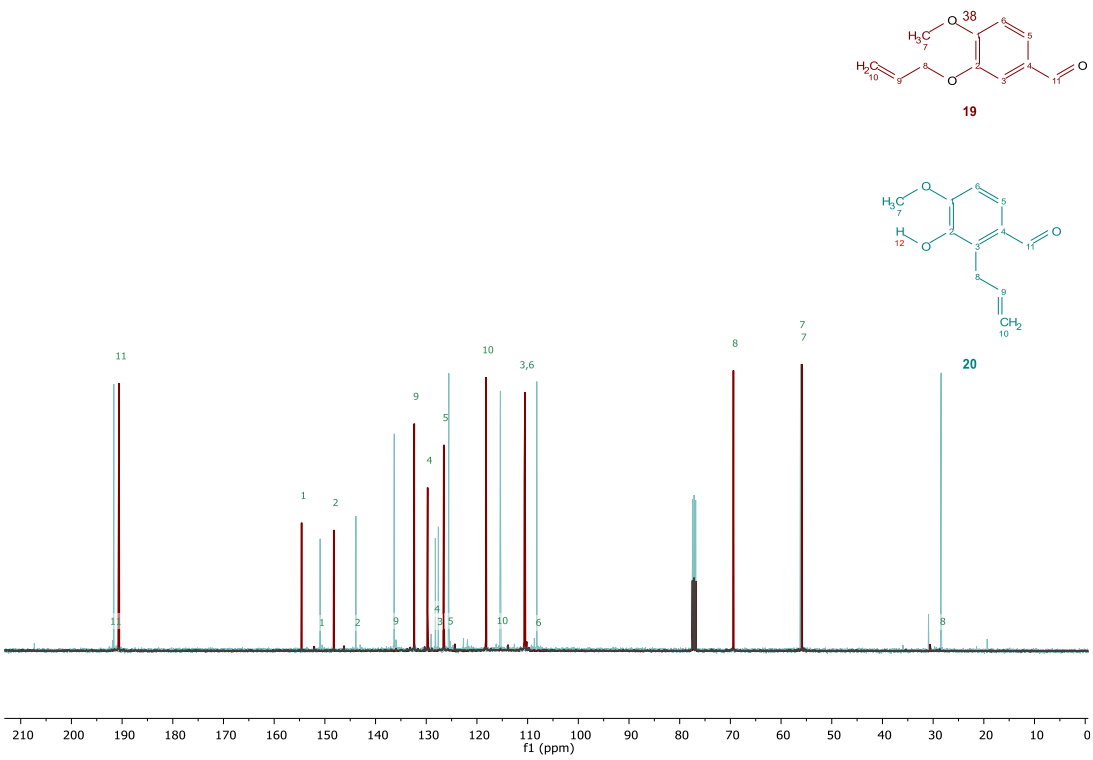

Figure 22: Superimposed ^{13}C NMR spectra of 3-(allyloxy)-4-methoxybenzaldehyde **19** and flow of 2-allyl-3-hydroxy-4-methoxybenzaldehyde **20**

3.3 Protection of the phenolic alcohol group

The third stage involves the use of a secondary alkyl halide and a base to protect the phenolic alcohol. The general mechanism is the same as the mechanism of the first stage with the deprotonation of the phenolic alcohol with a base to form a phenolate anion intermediate, that then effects the substitution, in this case with a secondary alkyl halide to provide the protected ether product **22**. The introduction of the bulky isopropyl group prevents the hydroxy group from interfering with subsequent synthetic stages as the ether is stable and unreactive.

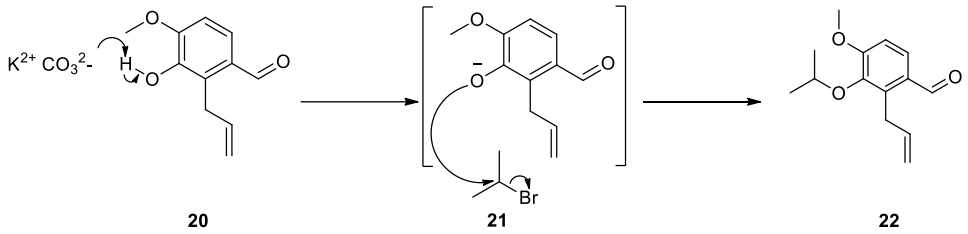

Scheme 25: General mechanism for the protection of the alcohol group

3.3.1 Batch results for the protection of phenolic alcohol group

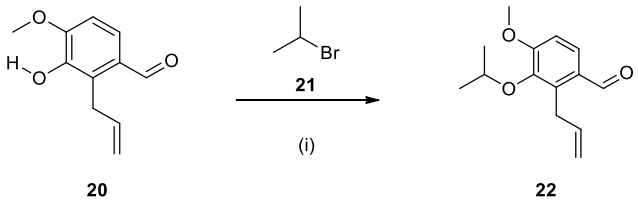

Scheme 26: Alcohol protection (i) K_2CO_3 (2.5 equiv.), 60 °C, DMF, 20 hours (78 %)

The batch procedure was based on reaction conditions by van Otterlo and co-workers using 2-bromopropane **21** and potassium carbonate.[34] The reaction was initially performed in dimethylformamide (0.50 M) over 20 hours under an argon atmosphere at temperature of 60 °C affording the desired product in 78 % yield (Table 8, entry 1). Additional screens were carried out to test reagent/product solubilities in different solvents for flow translation. Initially tetrahydrofuran was screened as it can be used to link the protection stage to the next allylation stage, unfortunately, a disappointingly low yield of 3.1 % was observed (entry 2). Alternatively, toluene was also evaluated as this would allow us to easily link the previous Claisen stage directly into the protection. Once again, we were left disappointed with a low yield of only 2.8 % observed. As a result, dimethylformamide at a 0.50 M concentration was selected for flow translation.

Table 8: Batch experiments of the protection of alcohol group in different solvents

Entry No	Reaction scale (g)	Concentration [M]	Solvent	Yield (%)
1	**9.00**	**0.50**	**DMF**	**78.0**
2	1.02	0.50	THF	3.10
3	1.03	0.50	Toluene	2.80

3.3.2 Flow results for the protection of the phenolic alcohol group

This step was investigated previously in-house, looking at various residence times and concentrations. Based upon these studies, preliminary reaction conditions involved performing the reaction at a concentration of 0.13 M in dimethylformamide using a packed-bed reactor housing potassium carbonate, with a 20-minute residence time at 80 °C to afford the product in 92 % yield. To verify the effectiveness of earlier reaction conditions, a few reactions were carried out at higher concentrations and increasing the equivalents of 2-bromopropane. The flow configuration was comprised of two HPLC pumps connected downstream to stock solutions of **20** and 2-bromopropane **21** both in dimethylformamide (Scheme 27). The solution was then mixed at a T-piece connector before passing through an Omnifit™ glass column packed bed reactor housing crushed potassium carbonate followed by an 8-bar BPR and finally product collection.

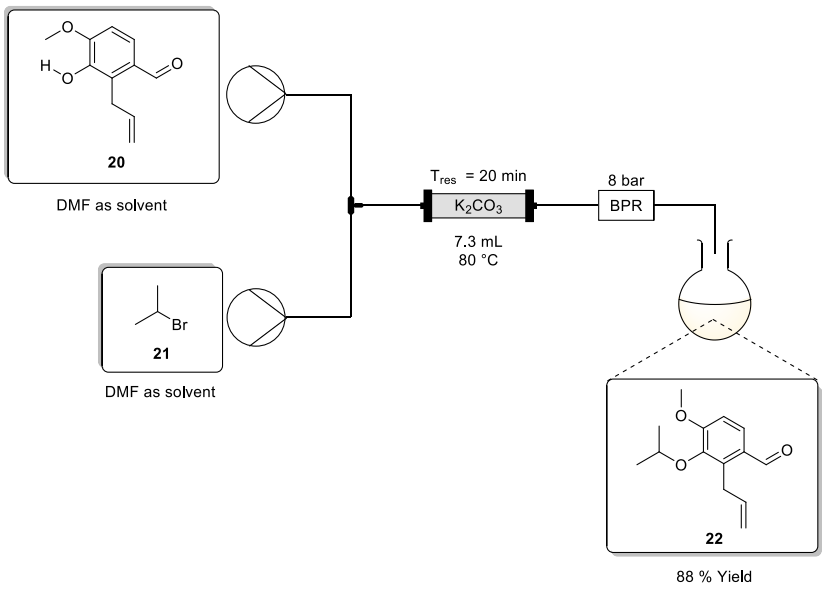

Scheme 27: Flow synthesis of the protection of **20** using potassium carbonate

The effect of concentration and the equivalents of 2-bromopropane was studied while maintaining the temperature at 80 °C and residence time at 20 minutes. When performed at 0.40 M in dimethylformamide using 2.5 equivalents of 2-bromopropane the desired product

was formed in high isolated yields of 86-88% (Table 9, entries 1 and 2). Interestingly, as noted in entry 3, as the concentration was increased slightly, the product yield decreased to 77% (entries 1 and 2 vs. 3). Furthermore, decreasing the equivalents of 2-bromopropane also resulted in a sharp drop-off in yield (entries 3-6). Although counterintuitive, increasing the concentration while retaining the residence time at 20 minutes may have negatively impacted the overall mass transfer occurring in the packed-bed reactor. We hypothesise that at lower concentrations the mass transfer is more efficient as there is less competition at the liquid-solid interface arising from the liquid phase reaction components. As the concentration of these components increases a saturation point is reached resulting in the mass transfer plateauing. Possible solutions to working at higher concentrations if required would be to work at lower flow rates (i.e. longer residence times), or alternatively to simply increase the volume of the packed-bed reactor while maintaining the flowrate.

Table 9: Flow experiments of the alcohol protection using potassium carbonate and different equivalents of 2-bromopropane

Entry No	Reaction scale (g)	Concentration [M]	2-bromo-propane (equiv.)	Residence time (min)	Yield (%)
1	4.34	0.40	2.5	20	86.0
2	**4.07**	**0.40**	**2.5**	**20**	**88.0**
3	0.25	0.50	2.5	20	77.0
4	0.25	0.50	2.0	20	68.0
5	0.25	0.50	1.5	20	64.0
6	0.25	0.50	1.0	20	60.0

As a result, the ideal conditions of this stage were determined to be a concentration of 0.40 M in dimethylformamide at temperature of 80 °C, 20 minutes residence time, using 2.5 equivalents of 2-bromopropane to obtain the product in 88 % yield after isolation. Due to time constraints, an attempt was not made to optimize this step employing a base solution. It would be recommended as potassium carbonate was previously replaced with potassium hydroxide in stage 1 using a bromine containing alkyl halide.

3.3.3 Characterisation of the protection of the phenolic alcohol group

Inspection of the ^{1}H NMR proton spectrum (Figure 23) revealed that the broad signal at 5.92 ppm representing the alcohol, had disappeared. The presence of the isopropyl group is shown by the appearance of two new signals up-field at 1.28 ppm and 1.26 ppm integrating

for a total of 6 protons corresponding to the CH_3 groups (H_{13} and H_{14}) together with the quartet of quartets at 4.5 ppm which represents the CH group (H_{12}). The ^{13}C NMR Spectra showed the isopropyl group through the presence of two superimposed signals visible at 22.53 ppm corresponding to the new two CH_3 bonds at carbon C_{13} and C_{14} and the signal at 77.49 ppm due to the CH carbon C_{12}. Additionally, the IR spectra also showed the disappearance of the broad O-H signal. The MS spectra showed a visible $[M+H]^+$ signal at 235.1351 where the product requires a molar mass of 235.29886 $g.mol^{-1}$. The NMR, IR and MS results are comparable to those reported previously by van Otterlo and co-workers.[34]

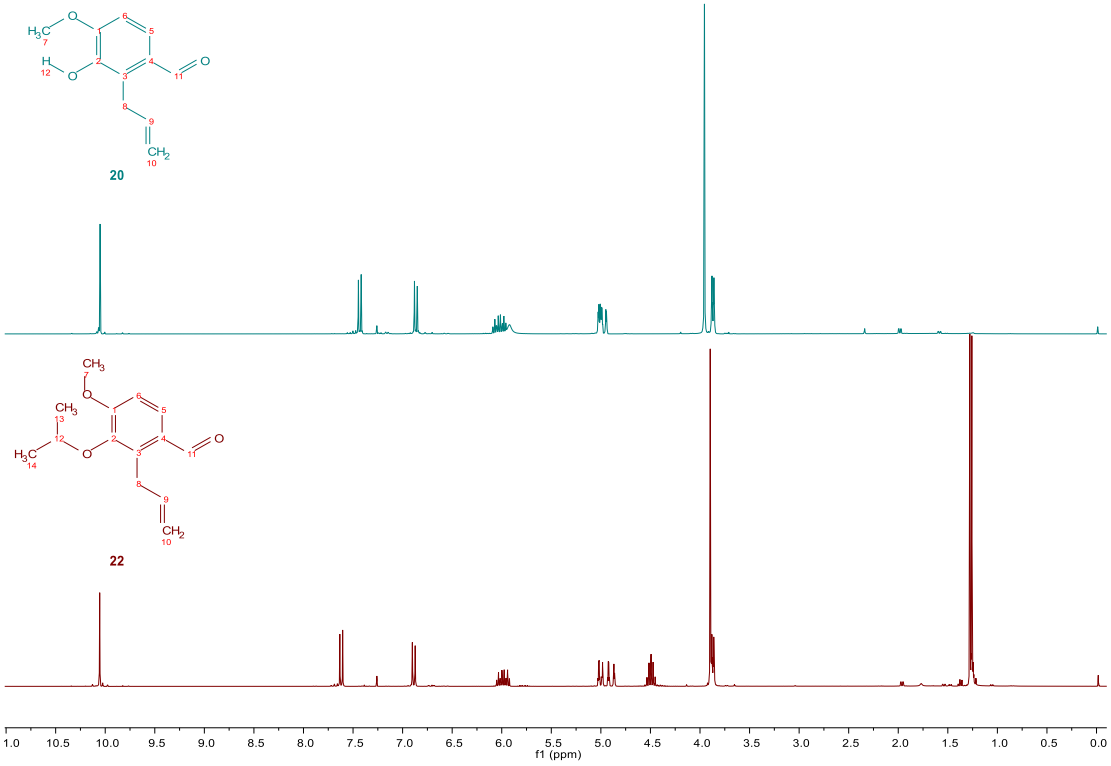

Figure 23: Stacked ^1H NMR spectra of 2-allyl-3-hydroxy-4-methoxybenzaldehyde **20**, and 2-allyl-3-isopropoxy-4-methoxybenzaldehyde **22**

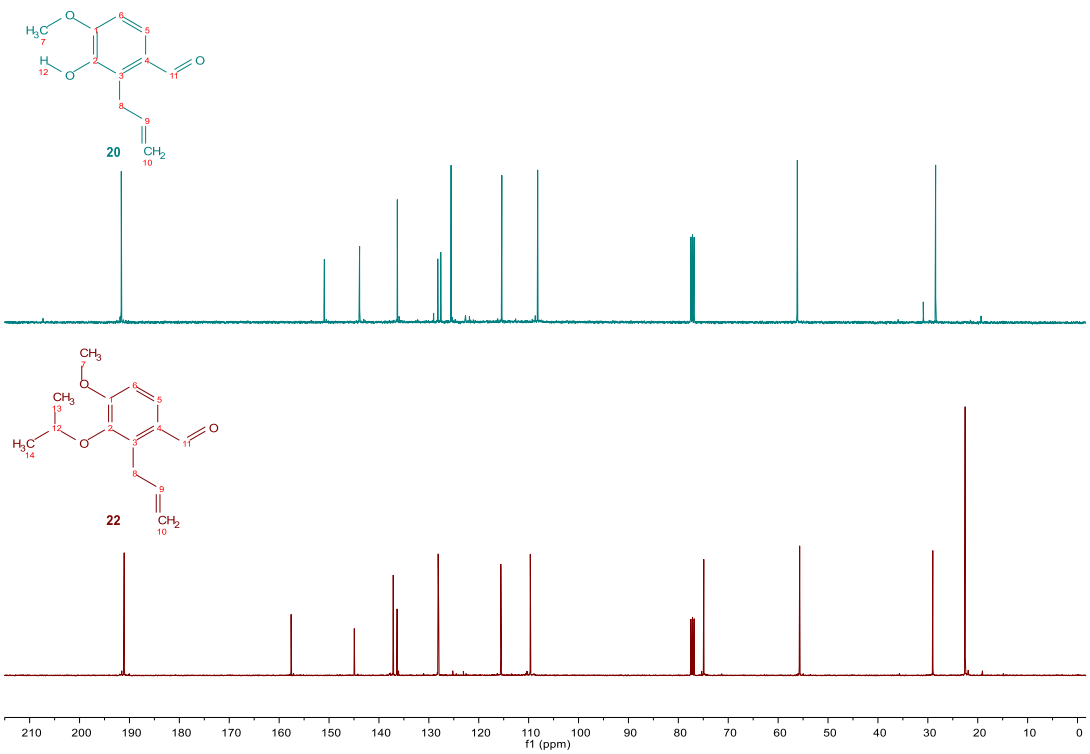

Figure 24: Stacked ^{13}C NMR spectra of 2-allyl-3-hydroxy-4-methoxybenzaldehyde **20**, and 2-allyl-3-isopropoxy-4-methoxybenzaldehyde **22**

3.4 Reduction of the aldehyde

The fourth stage is the reduction of the aromatic aldehyde group to afford a primary alcohol. The mechanism depicted in Scheme 28, proceeds via two steps consisting of a nucleophilic addition of a proton from a hydride ion source (sodium borohydride), followed protonation step in the presence of a protic solvent.

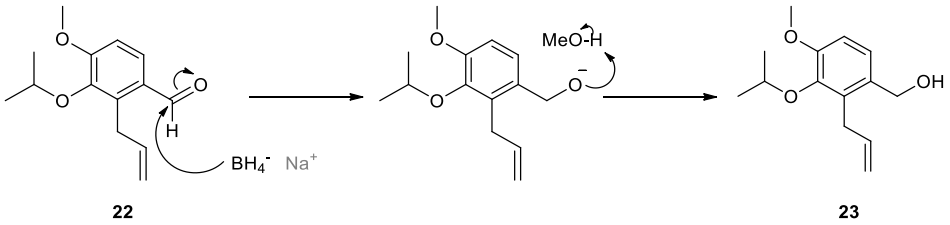

22 23

Scheme 28: General mechanism of the aldehyde reduction

Several solid- and liquid-phase hydride ion sources are commonly used as reductants. Sodium borohydride and sodium triacetoxyborohydride ($NaBH(OAc)_3$), are arguably two of the most commonly encountered but in both instances are insoluble in protic solvents, which are required mechanistically. In general, their use requires the presence of an aqueous co-solvent together with the protic solvent.[57] These reagents are also available in polymer-supported forms, which although expensive, can be readily employed under flow conditions.[58,59] Alternatively, there are also several reductants which are readily miscible in protic organic solvents, these including sodium bis(2-methoxyethoxy)aluminium hydride (Red-Al), lithium aluminium hydride ($LiAlH_4$), diisobutylaluminium hydride (DIBAL), and superhydride. These hydride sources are attractive as they afford homogeneous solutions, however, they are generally more hazardous to handle and critically often have tedious workup operations characterised by the formation of emulsions and metal salt by-products.[59]

3.4.1 Previously reported flow-based aldehyde reductions

Gilmore and co-workers were the first to report aldehyde reductions under flow conditions utilizing solid sodium borohydride rather than analogous polymer supported sodium borohydride.[60] They employed a packed-bed housing containing celite and sodium borohydride with tetrahydrofuran as a solvent. However, leaching, precipitation and pressure changes resulted in inconsistent results when screening benzaldehyde reductions. After investigating, they noticed that previously it was reported that polymer-supported borohydride reductions in an alcoholic solvent using lithium chloride enhanced reduction conversion. As a result, they hypothesized that addition of an alcoholic co-solvent and lithium chloride to their method would improve conversions. The flow system utilized one HPLC

pump connected downstream to an aldehyde stock solution in tetrahydrofuran (0.66 M), followed by a packed-bed reactor housing a celite/sodium borohydride/lithium chloride (1:1:0.76) mixture. They screened this approach using various aldehydes, ketones and amines and reported high product yields. Cinnamaldehyde **50** was used as a demonstration reaction (Scheme 29), affording the desired product **51** in 94 % yield at a 5.6-minute residence time and ambient temperature. They also reported in-flow reductive aminations using the celite/sodium borohydride/lithium chloride column.

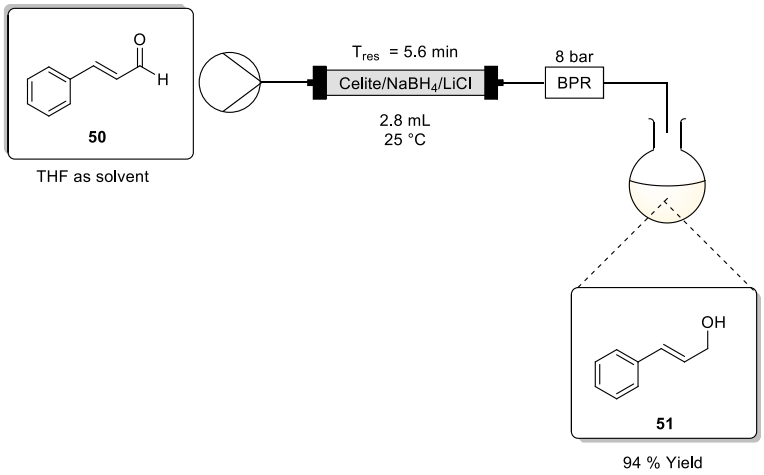

Scheme 29: Flow synthesis of aldehyde reduction of Cinnamaldehyde **50** using a packed column of celite/sodium borohydride/lithium chloride

Watts and co-workers performed the reduction of a nucleoside precursor using a sodium borohydride solution. [61] The reduction of an ester is a key step in the synthesis of Lamivudine, which is used for the treatment of HIV and chronic hepatitis. Three syringe pumps were employed as shown in Scheme 30 for stock solutions of the nucleoside precursor **52** in methanol (0.26 M), dipotassium hydrogen phosphate in water (0.65 M), and sodium borohydride in water (0.40 M). The sodium borohydride solution was prepared at a concentration of 0.39 M in water with 0.1 mL of a 25 % sodium hydroxide solution. The solution was allowed to mix in three microreactors before passing through an 8 bar BPR. They determined that full conversion was obtained after 3.3 minutes of residence time at a temperature of 20 °C affording the desired product **53** in an isolated yield of 94 %.

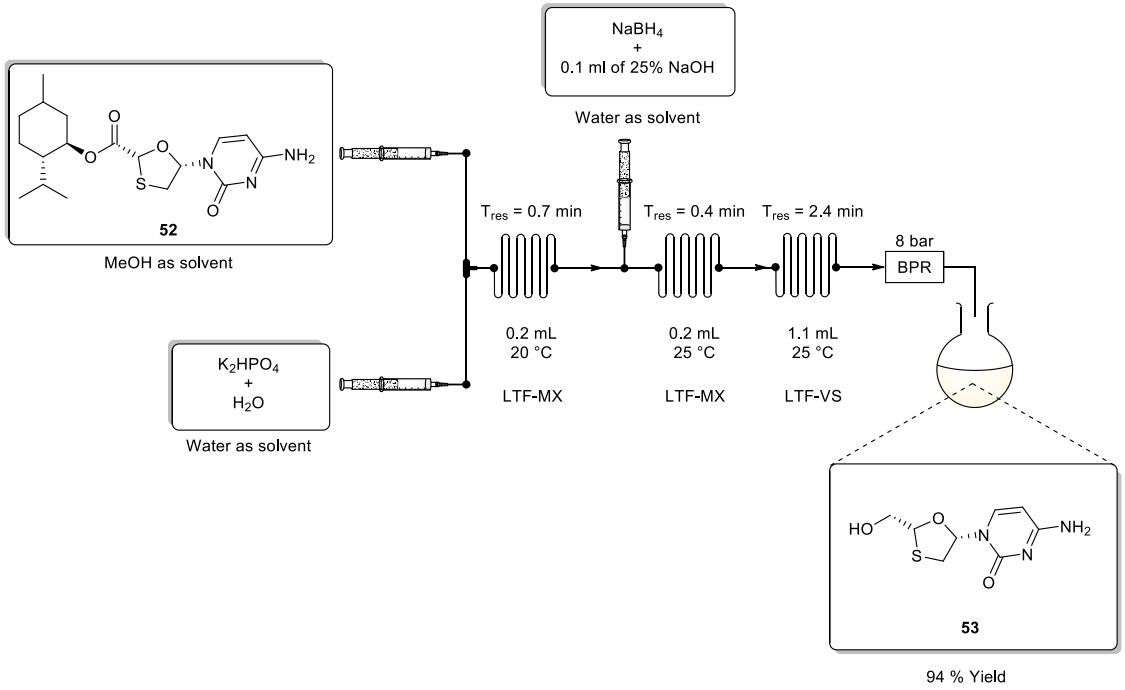

Scheme 30: Flow synthesis for aldehyde reduction of nucleoside **52** with basic sodium borohydride solution

3.4.2 Batch results for the reduction of the aldehyde

Previously, van Otterlo and co-workers performed the reduction step in tetrahydrofuran for 12 hours using lithium aluminium hydride at 0 °C to afford the product **23** in an isolated yield of 86 %.[34] This reaction was also investigated in-house using Red-Al (65 % toluene) in dichloromethane at a temperature of 15 – 20 °C affording a 93 % isolated yield. We elected to use toluene instead of a halogenated solvent in an effort to improve the safety and greenness of the reaction. The reaction was performed in a round-bottom flask under argon atmosphere over 20 hours using distilled toluene (0.15 M) at 0-20 °C to obtain **23** in 76 % yield (Table 10, entries 1 and 2).

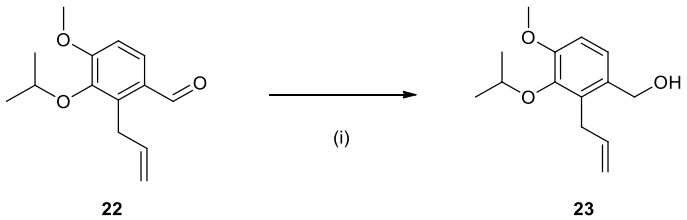

Scheme 31: Aldehyde reduction (i) Red-Al (60 % in toluene), 25 °C, toluene, 20 hours (76 %)

Although the use of Red-Al afforded the product in good yield additional reactions were screened using alternative reducing agents as Red-Al is not ideal for flow translation, primarily due to its high viscosity. Sodium borohydride and sodium acetoxyborohydride was

screened producing the desired product **23** in 62 and 59 % yields under comparable reaction conditions (Table 10, entries 3 and 4). Critically, some precipitation was observed, and it was therefore decided to test the approach by Watts and co-workers, using sodium borohydride in aqueous methanol. [61] After 20 hours, the product was isolated in a 47 % yield. Although lower yielding, we elected to translate this approach to flow as it did not suffer from the viscosity issues associated with Red-Al.

Table 10: Batch experiments of aldehyde reduction using various bases in different solvents

Entry No	Reaction scale (g)	Reducing agent	Solvent	Yield (%)
1	3.38	Red-Al (60 %)	Toluene	75.0
2	**4.50**	**Red-Al (60 %)**	**Toluene**	**76.0**
3	0.50	$NaBH_4$	EtOH	62.0
4	0.50	$NaBH(OAc)_3$	EtOH	59.0
5[a]	0.50	$NaBH_4$	MeOH:H_2O	47.0

[a] Added 0.1 mL 25 % sodium hydroxide

3.4.3 Flow results for the reduction of aldehyde using polymer supported sodium borohydride

This approach was previously demonstrated in-house using a packed-bed reactor housing polymer supported sodium borohydride. The reaction aldehyde **22** was dissolved in methanol and after a 50-minute residence time at ambient temperature the desired product **23** was obtained in an 85 % yield. The reaction was repeated, and an isolated yield of 83 % was obtained under the same conditions. The flow setup consisted of a single HPLC pump connected downstream of a stock solution of aldehyde **22** in methanol (0.20 M) followed by a glass Omnifit™ packed-bed reactor housing polymer supported sodium borohydride. The system pressure was maintained using an 8-bar back pressure regulator. Initial experiments showed that temperatures higher than 45 °C and/or residence times of less than 20 minutes resulted in a decrease in product conversion.

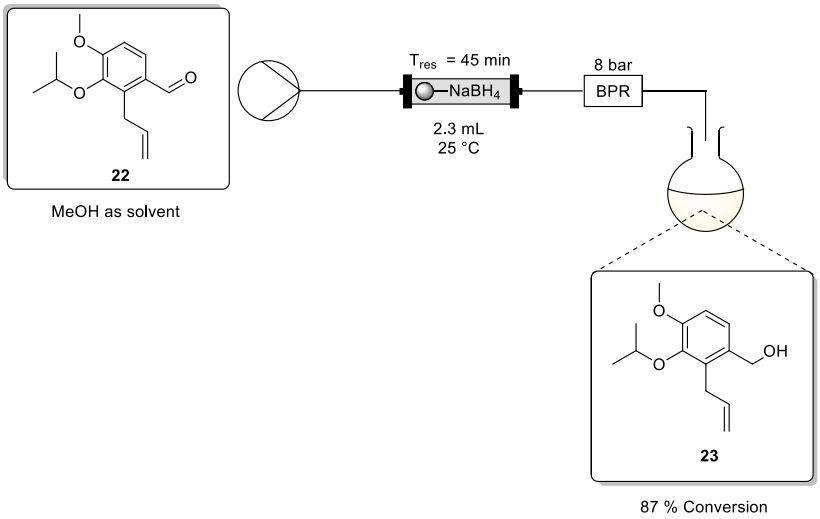

Scheme 32: Flow synthesis of the aldehyde reduction using polymer supported sodium borohydride

A preliminary experiment, as indicated in Table 12, entry 1, was carried out to assist in defining screening parameters for DoE screening. Employing a residence time of 25 minutes and a concentration of 0.20 M in methanol, the reaction afforded a 59.8 % conversion. A full-factorial DoE screening was chosen to test whether the result from utilizing a packed column is effective and reproducible. DoE screening reactions were carried out while maintaining the column temperature at room temperature and altering the concentration and residence time, as summarised in Table 11. The same flow setup shown in Scheme 32 was used. A total of 30 mL of product collected for each for HPLC analysis to determine product conversion using a standard calibrated curve. Two replicates were conducted at 45 minutes and 0.50 M concentration. The reaction scale was set at 0.15 g, with the column at room temperature, and methanol was used as the pushing solvent.

Table 11: Screening approach -Full Factorial Screening for aldehyde reduction

Screening approach-DoE Design-Full Factorial Screening					
Name	**Abbreviation**	**Units**	**Type**	**Use**	**Settings**
Concentration	Conc	M	Quantitative	Controlled	0.2-0.8
Residence time (minutes)	Res	Min	Quantitative	Controlled	30-20

The sodium borohydride polymer was replaced after every second experiment, and the replicates were carried out on a freshly packed column. The column's consistency was attempted to be maintained by packing the same mass of borohydride each time to a specified line marked on the column. Higher concentrations of the stock solution resulted in lower product conversion, as at 30 minutes residence time, and 0.20 M concentration yielded 69.5 % product, while 0.80 M yielded 44.9 % (Table 12, entry 2 vs. 3). Based on the

screen, the reaction achieved maximum conversion of 87.2 % after 45 minutes and concentration of 0.50 M.

Table 12: Flow experiments of the aldehyde reduction at different concentrations and residence times

Entry No	Reaction scale (g)	Concentration [M]	Solvent	Residence Time (min)	LC Conversion (%)
1	0.15	0.20	MeOH	25	59.8
2	0.15	0.20	MeOH	30	69.5
3	0.15	0.80	MeOH	30	44.9
4	0.15	0.20	MeOH	60	68.0
5	0.15	0.80	MeOH	60	63.4
6	0.15	0.50	MeOH	45	80.4
7[a]	**0.15**	**0.50**	**MeOH**	**45**	**87.2**

[a] 68 % Isolated yield on 0.15-gram scale

Unfortunately, the screening data indicated a poor and irreproducible model because its replicates were not within close enough proximity to one another. A few outliers were also detected but with only 7 experiments conducted, we felt there were not enough data points for a robust model. It did however provide us with an expected optimal area to be further explored (Figure 25). The optimal area can be explored at lower concentrations, however additional reactions would be required to determine the ideal residence time. Although, the polymer supported reagent offers the advantage of no additional workup and possible recycling, it also has limitations such as high costs, lower reactivity, non-reproducible results, and dispersion. As a result, we elected to not pursue this approach further instead opting to adapt the method reported by Watts and co-workers. [61]

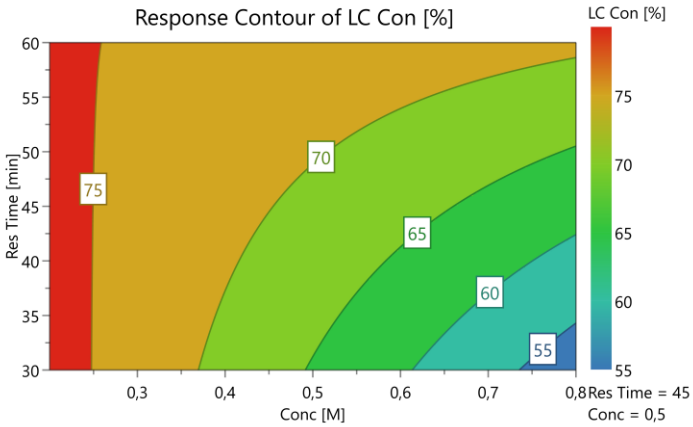

Figure 25: Representation of a 3-D contour plot for aldehyde reduction flow experiments using polymer supported sodium borohydride

3.4.4 Flow results for the reduction of aldehyde using sodium borohydride solution

An initial test reaction was carried out by adapting the method reported by Watts and co-workers. [61] Two HPLC pumps were connected downstream of stock solutions of **22** in methanol (0.22 M) and sodium borohydride in water with 0.1 mL of 25 % sodium hydroxide. The two streams were allowed to react in a 2.0 mL mixing chip at room temperature prior to passing through an 8-bar BPR (Scheme 33). Frustratingly, the HPLC pumps struggled to pump the sodium borohydride solution, resulting in a poor yield of only 10.7 %.

Table 13: Flow experiments of the aldehyde reduction using sodium borohydride in water with 0.1 mL of 25 % sodium hydroxide added

Entry No	Reaction scale (g)	Concentration [M]	Solvent	Temperature (°C)	Residence time (min)	Yield (%)
1	0.20	0.22	MeOH	RT	30	10.7

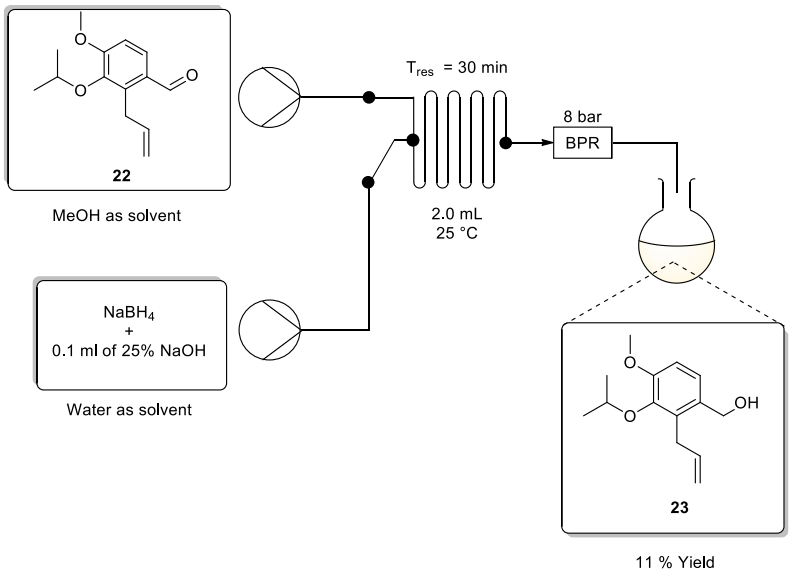

Scheme 33: Flow synthesis of the aldehyde reduction using sodium borohydride in water with 0.1 mL of 25 % sodium hydroxide added

After this setback, two additional batch reactions were carried out using an isopropanol: water and a methanol: water solvent mix respectively without the addition of sodium hydroxide. The reactions were performed at room temperature over 20 hours. Encouragingly, good yields were obtained in both instances with the aqueous isopropanol solvent mix performing best with an 87 % yield (Table 14). It was noted that the sodium hydroxide additive suggested by Watts and co-workers had little effect on the overall yield with comparable yields being obtained with and without it. Moving forward, we elected to

continue development using aqueous isopropanol as it afforded a higher overall yield and from a safety perspective did not suffer from the toxicity issues associated with methanol.

Table 14: Batch experiments of the aldehyde reduction for 20 hours

Entry No	Reaction scale (g)	Concentration [M]	Solvent	Ratio	Temperature (°C)	Yield (%)
1	0.250	0.25	IPA:H_2O	1:1	RT	87
2	**0.250**	**0.25**	**MeOH:H_2O**	**1:1**	**RT**	**74**

In translating to flow we elected to use two peristaltic pumps connected downstream of a stock solution of **22** in isopropyl alcohol, and an aqueous suspension of sodium borohydride. The peristaltic pumps were selected as they are capable of pumping fine suspensions/slurries. As seen in Scheme 34, a static mixer was used, along with a PTFE coil for heating and a 3 bar BPR. Before performing HPLC analysis, the product was quenched with saturated sodium bicarbonate and water. An initial reaction was carried out at concentration of 1.00 M, however the solution remained viscous, and only 83 % product conversion was achieved after 30 minutes residence time at 60 °C. This was already an improvement over the batch results obtained at room temperature for 24 hours.

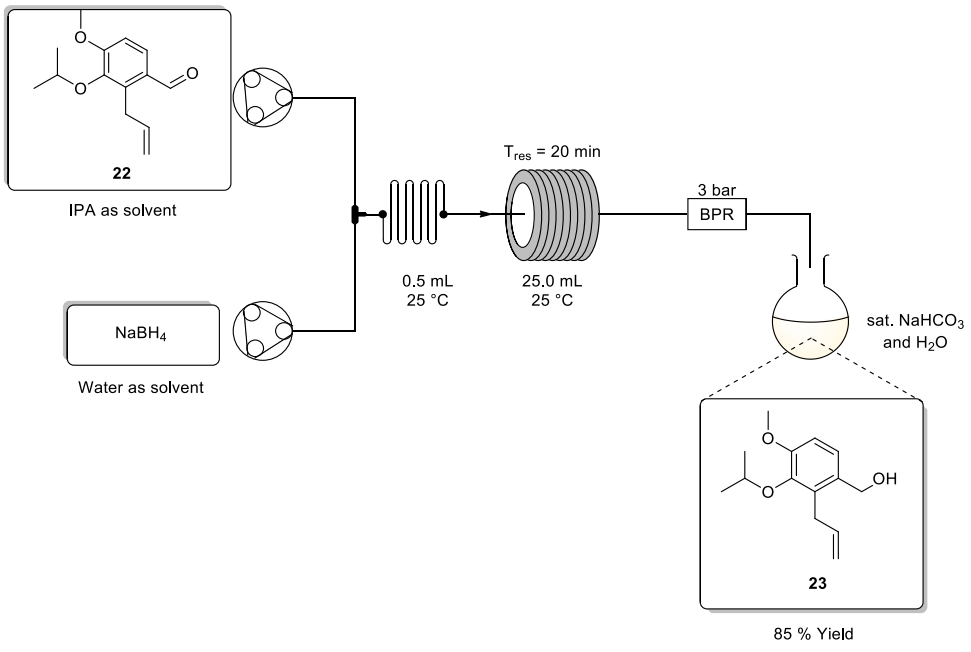

Scheme 34: Flow synthesis of aldehyde reduction using sodium borohydride in water

Further test reactions were carried out at a lower concentration of 0.25 M using a 20 mL coil with 1.0 mm inner diameter. Overall, higher product conversions were achieved with longer residence times, with a maximum conversion of 90 % achieved after 30 minutes (Table 15,

entry 4). Increasing the temperature to 80 °C (entry 5), afforded a decrease in product conversion to 84 %. We then decided to use a larger diameter coil (1.5 mm internal diameter) and determine if there was a substantial difference in conversion at a higher flow rate. In a similar fashion, product conversion again increased with increasing residence time (entries 6-8), with a maximum conversion of 93 % obtained with a 20-minute residence time at 30 °C.

Additionally, increasing the concentration to 0.50 M, reduced product conversion (entries 9-11), and increasing the temperature to 60 °C when performed at 0.5 M did not show any additional improvement (entry 11). Thus, the optimal conditions for the reduction step were identified as a temperature of 25 °C with a 20-minute residence time when using a 25 mL coil reactor with a 1.5 mm internal diameter while employing the use of peristaltic pumps. At the determined optimal conditions, a larger scale reaction of about 3 grams was performed (entry 12), and 88 % product conversion was achieved with an isolated yield of 85 %.

Table 15: Flow experiments for aldehyde reduction using sodium borohydride in water and isopropyl alcohol

Entry No	Reaction scale (g)	Concentration [M]	Residence time (min)	Coil Volume (mL)	Temperature (°C)	LC Conversion (%)
1[a]	0.15	1.00	30	20	60	83.0
2	0.15	0.25	15	20	60	80.0
3	0.15	0.25	20	20	60	88.0
4	0.15	0.25	30	20	60	90.0
5	0.15	0.25	30	20	80	84.0
6	0.15	0.25	5	25	30	79.0
7	0.15	0.25	10	25	30	82.0
8	**0.15**	**0.25**	**20**	**25**	**30**	**93.0**
9	0.15	0.50	20	25	30	84.0
10	0.15	0.50	30	25	30	83.0
11	0.15	0.50	20	25	60	79.0
12[b]	2.94	0.50	20	25	25	88.0

[a] Viscous sodium borohydride solution, [b] Isolated yield after workup 85 %, entries 1-5 conducted in a 1mm inner-diameter coil, entries 6-11 conducted in a 1.5 mm inner-diameter coil.

3.4.5 Characterisation of aldehyde reduction

Product formation was confirmed by inspection of proton and carbon NMR spectra, IR and MS. The stacked ^{1}H NMR spectra (Figure 26) confirms product formation by i) the disappearance of the singlet aldehyde signal (H_{11}) at 10.06 ppm, ii) the appearance of the broad alcohol signal (H_{15}) at 2.50 ppm, iii) the addition of the singlet CH_2 signal at 4.56 ppm, integrating for 2 protons, indicating a CH_2 signal formed (H_{11}), iv) the shift of H_5 upfield from 7.63 ppm to 7.06 ppm, v) the shift of H_6 upfield from 7.63 ppm to 6.73 ppm. Additionally, the ^{13}C NMR spectra (Figure 27) confirms product formation by i) the shift in the aromatic signals: C_4 from 128.14 ppm to 132.12 ppm and C_3 from 136.36 ppm to 132.41 ppm, ii) the significant shift in C_{11} from 191.06 ppm (CH=O) to 62.91 ppm (CH_2OH). The IR spectra also showed the appearance of a broad O-H stretch signal at 3380 cm^{-1}. The MS spectra also showed a visible [M-OH] signal at 219.1539 where the product requires a [M-OH] of 219.13795 $g.mol^{-1}$. The NMR, IR and MS results are comparable to those reported previously by Van Otterlo.[34]

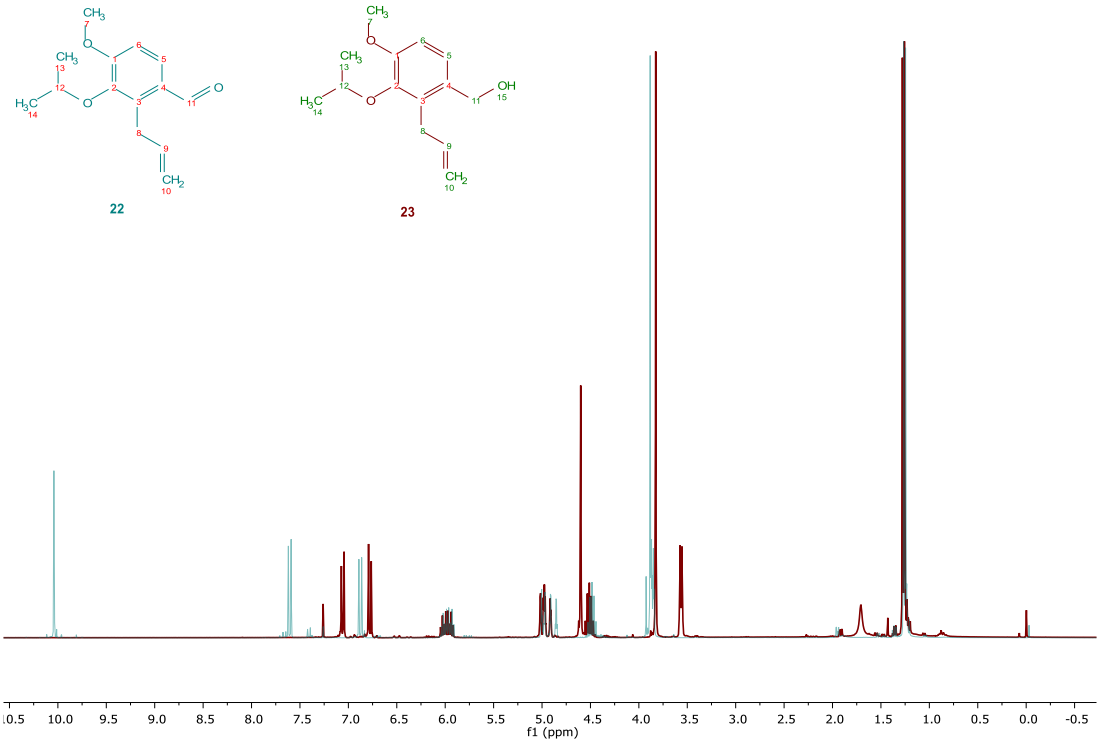

Figure 26: Superimposed ^{1}H NMR spectra of 2-allyl-3-isopropoxy-4-methoxybenzaldehyde **22** and (2-Allyl-3-isopropoxy-4-methoxyphenyl)methanol **23**

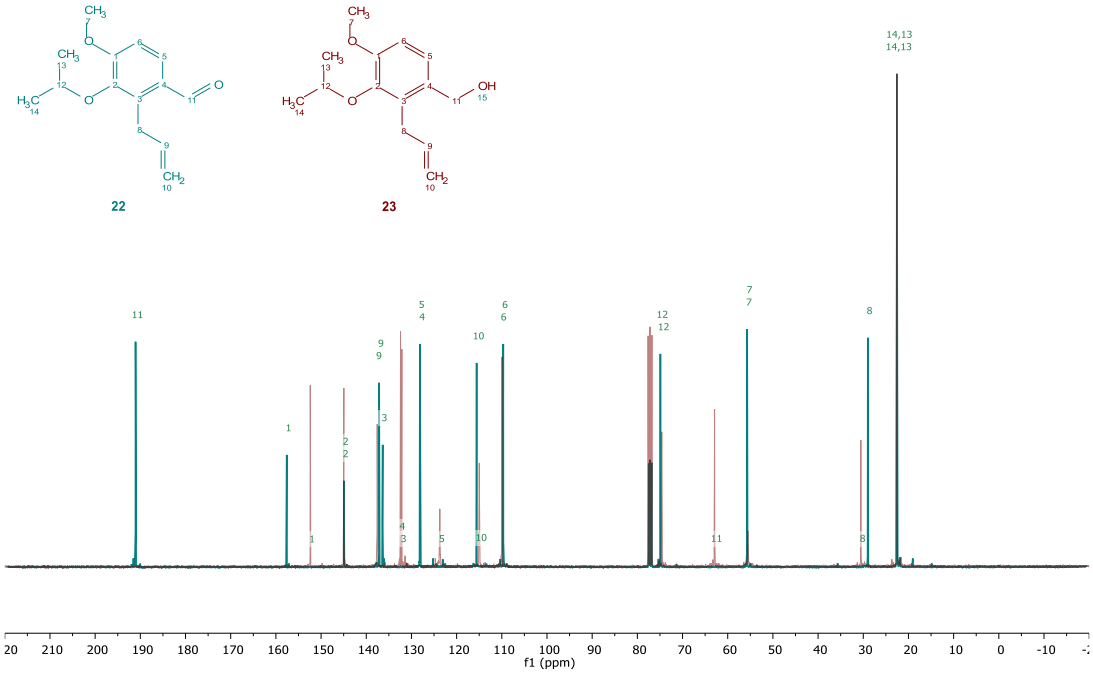

Figure 27: Superimposed ^{13}C NMR spectra of 2-allyl-3-isopropoxy-4-methoxybenzaldehyde **22** and (2-allyl-3-isopropoxy-4-methoxyphenyl)methanol **23**

3.5 Second Allylation

The fifth step in the synthesis is a second allylation utilizing a base and allyl halide. The general mechanism is demonstrated in Scheme 35 by which **23** undergoes deprotonation using sodium hydride to form a phenylmethanolate anion intermediate, acting as a nucleophile and attacking the allyl halide to produce the alkylated product **24**. As the benzylic alcohol is not as acidic as the phenolic proton from stage 1 the reaction requires a stronger base to affect the required deprotonation and typically the allylation of a benzylic alcohol tend to be more challenging

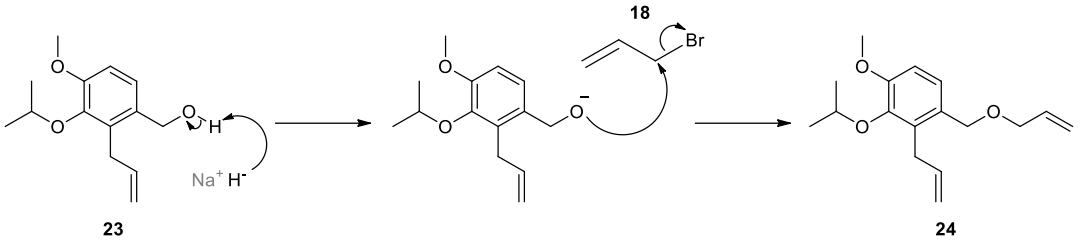

Scheme 35: General mechanism of the second allylation

3.5.1 Previously reported flow-based second allylations

Vapourtec™, a commercial flow reactor manufacturer, has a set of application notes of flow processes with detailed examples and experimental procedures as part of flow system demonstrations. A heterocyclic alkylation reaction was used as an example reaction to demonstrate the pumping of a sodium hydride dispersion slurry.[62] The flow system seen in Scheme 36 consisted of two peristatic pumps. One pump was used for a solution containing 1,2,3,4-tetrahydrocarbazole **54**, and 1-bromotetradecane **55** in tetrahydrofuran and dimethylformamide (3:1), while another pump was used for a continuously stirred suspension of sodium hydride (60 % dispersed in mineral oil) in anhydrous tetrahydrofuran under inert atmosphere. A 20 mL Vapourtec rapid mixing coil was used while maintaining the pressure at 7 bar using the third peristaltic pump as a BPR and product was collected in distilled water. After a few reactions, they determined optimal conditions at a temperature of 100 °C after 4 minutes to generate 13.0 g h^{-1} throughput with an isolated yield of 82 %. They noted a beige solid deposit forming on the reactor walls, which corresponded to the sodium bromide by-product, that was easily removed by washing the reactor with water. Furthermore, the HPLC chromatogram also revealed a mineral oil peak from the sodium hydride dispersion.

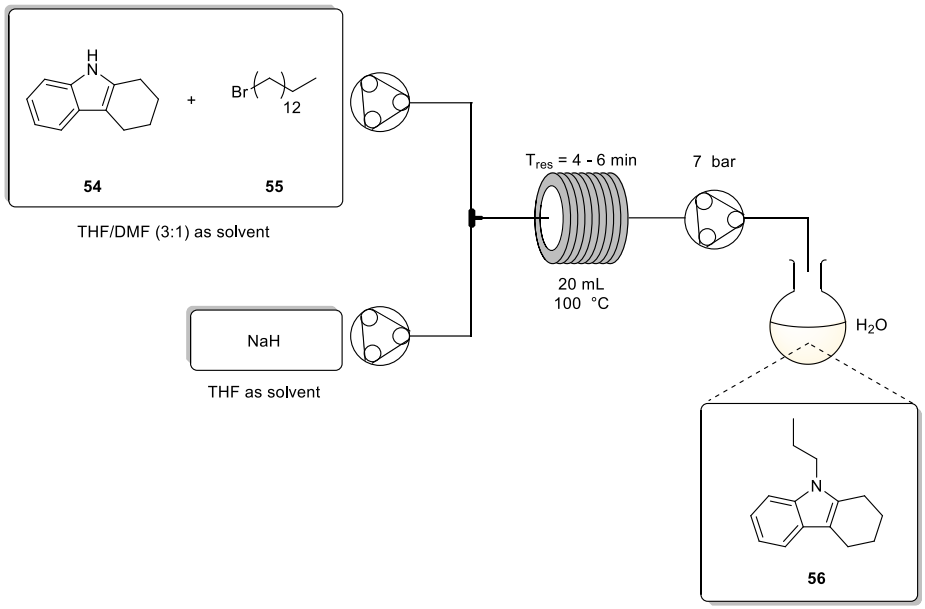

Scheme 36: Flow preparation of 1,2,3,4-tetrahydrocarbazole **56** using sodium hydride

3.5.2 Batch results for second allylation

Reaction conditions outlined by van Otterlo and co-workers were followed using allyl bromide **18** and sodium hydride as a base.[34] The reaction was carried out in a round-bottom flask under inert atmosphere, refluxing overnight in tetrahydrofuran. The reaction was quenched with 10 % sodium hydroxide and the solvent was removed *in vacuo* and extracted with dichloromethane and water for product isolation.

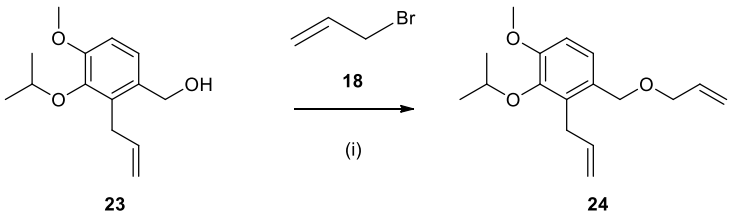

Scheme 37: Second Allylation (i) NaH, THF, 25 °C, 20 hours (80 %)

Initially, we investigated the possibility of using potassium carbonate because it was successful in the first allylation step. However, no product was formed with the ^{1}H NMR spectrum revealing no detectable product signals. This is not unexpected as the proton of the phenolic hydrogen in the first allylation was more acidic due to charge stabilization resulting from being directly bonded to the aromatic ring. This is not the case for the benzylic hydrogen, it is less reactive as it is a primary alcohol and thus requires a stronger base.

As a result, various reactions were carried out as detailed in Table 16 with the incorporation of different bases and solvents for testing flow compatibility and product conversion. Unfortunately, no product conversion was achieved after 20 hours utilizing triethylamine, sodium methoxide, potassium tert-butoxide, lithium diisopropylamide, and DBU. Interestingly, there was some product conversion at 80 °C using DMAP in both acetonitrile and DMSO as solvents. As expected, high product conversion was achieved at both room temperature and 60 °C using sodium hydride in tetrahydrofuran (0.20 M). A maximum product conversion of 85 % was achieved, importantly in this instance prior to reaction the sodium hydride in mineral dispersion was washed with hexane to remove the mineral oil. As the mineral oil is employed as a protective layer, washing the sodium hydride makes it more reactive by improving mass transfer, resulting in higher conversions.

Table 16: Batch experiments for the second allylation using different bases in selected solvents

Entry No	Reaction scale (g)	Solvent	Base	Base pka	Base equiv.	Product conversion	Yield %
1	0.25	DMF	K_2CO_3	10.3	5.0	No	-
2	0.25	DMSO	TEA	10.8	3.0	No	-
3[1]	0.25	ACN	TEA	10.8	3.0	No	-
4	0.25	MeOH	$NaOCH_3$	15-16	10.0	No	-
5	0.25	THF	KtBu	17.0	5.0	No	-
6	0.25	ACN	DBU	24.0	3.0	No	-
7	0.25	THF	LDA	35.7	5.0	No	-
8	0.25	ACN	DMAP	28.1	1.2	No	-
9[1]	0.25	ACN	DMAP	28.1	2.5	Yes	8.0
10[1]	0.25	DMSO	DMAP	28.1	2.5	Yes	27.0
11	1.29	THF	NaH [a]	35.0	5.0	Yes	41.0
12	0.15	THF	NaH [b]	35.0	5.0	Yes	80.0
13[2]	**1.70**	**THF**	**NaH [b]**	**35.0**	**2.5**	**Yes**	**85.0**

[1]Refluxed at 80 °C, [2] Heated to 60 °C, [a] Unwashed NaH (containing mineral oil) was used, [b] Washed NaH with hexane prior reaction

3.5.3 Characterisation of second allylation

From the stacked ^{1}H NMR spectra (Figure 28), product formation was confirmed by i) the disappearance of the broad alcohol signal (H_{15}) at 2.50 ppm, ii) the shift of the singlet signal (H_{11}) upfield from 4.55 ppm to 4.44 ppm, integrating for 2 protons, iii) the addition of the downfield signals (H_{15}) visible at 3.98-3.52 ppm, integrating for 2 protons, iv) the addition of the allyl group signals, CH=**CH_2** (H_{17}) signals at 5.18-5.30 ppm, integrating for 2 protons.

Additionally, the ^{13}C NMR spectra (Figure 29) also revealed the addition of the allyl group by i) the downfield shift from 62.91 ppm to 71.06 ppm that corresponded to the O-**CH_2** (C_{15}), ii) the new carbon signal visible at 134.97 ppm for the **CH**=CH_2 (C_{16}), and iii) the new carbon signal visible at 116.94 ppm corresponding to CH=**CH_2** (C_{17}). The IR spectra also showed the disappearance of the O-H stretch signal at 3380 cm^{-1}. The MS spectra also showed a visible $[M]^+$ signal at 276.1749 where the product requires a molar mass of 276.17254 $g.mol^{-1}$. The NMR, IR and MS results are comparable to those reported previously by van Otterlo and co-workers.[34]

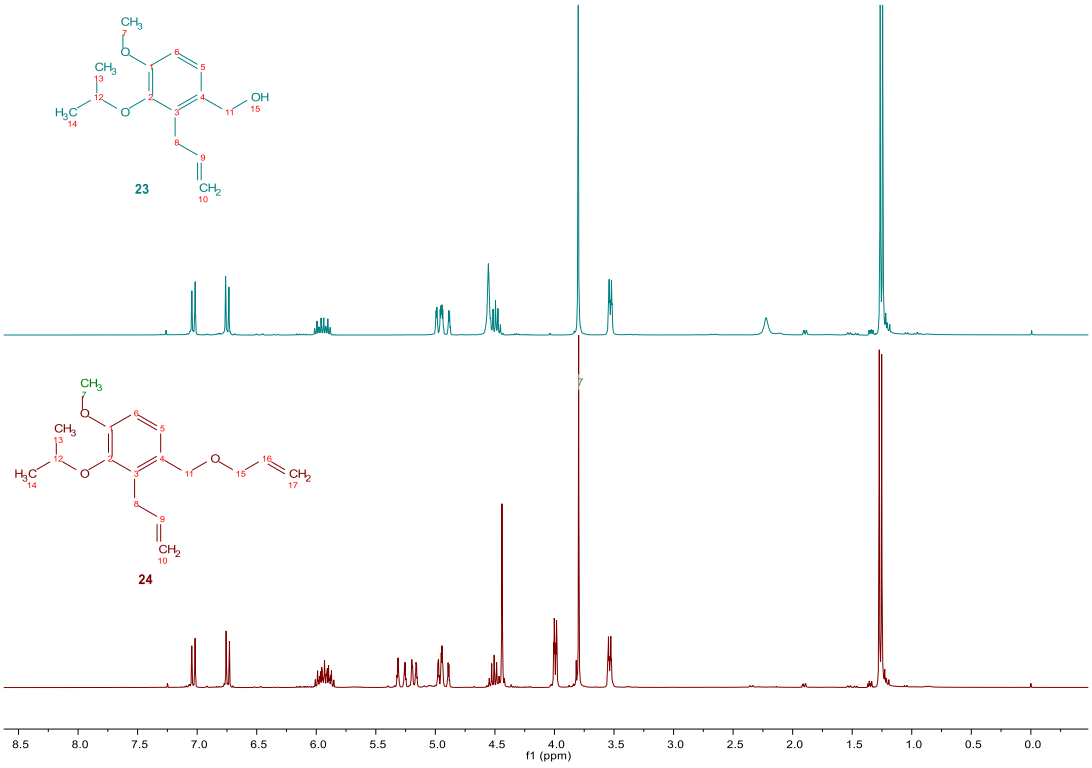

Figure 28: Stacked ^1H NMR spectra of (2-Allyl-3-isopropoxy-4-methoxyphenyl)methanol **23** and 2-allyl-1-((allyloxy)methyl)-3-isopropoxy-4-methoxybenzene **24**

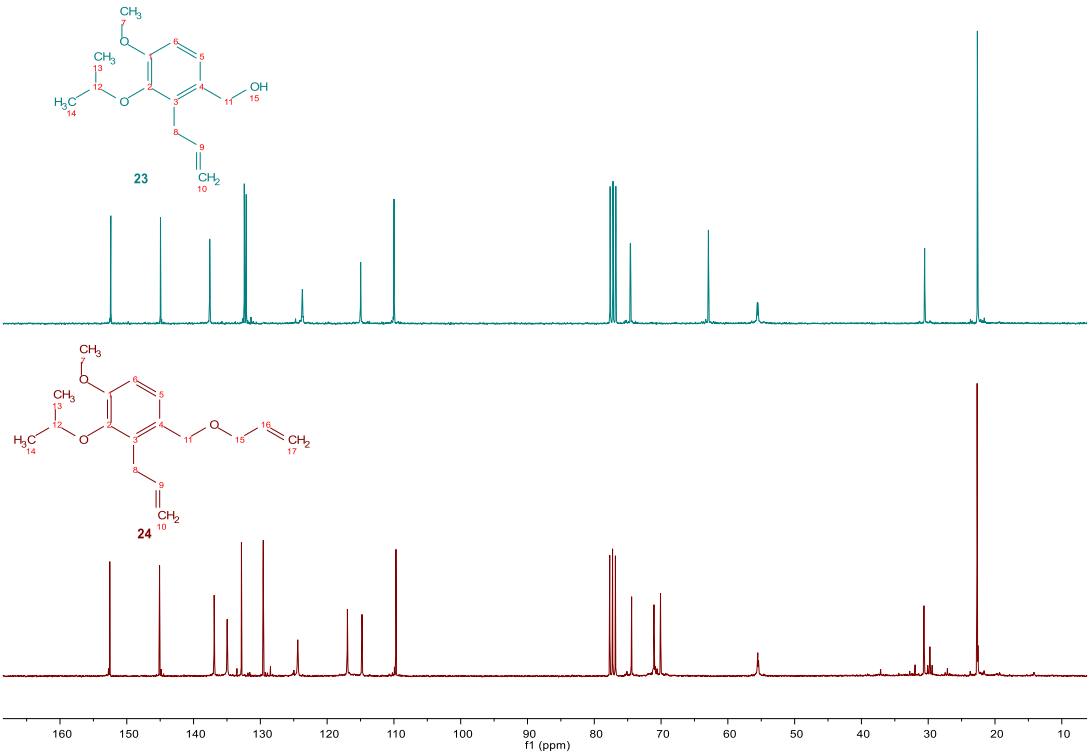

Figure 29: Stacked ^{13}C NMR spectra of (2-allyl-3-isopropoxy-4-methoxyphenyl)methanol **23** and 2-allyl-1-((allyloxy)methyl)-3-isopropoxy-4-methoxybenzene **24**

3.5.4 Flow results for second allylation using sodium hydride

The second allylation was previously attempted in-house using triethylamine under flow conditions, but no product was produced. DMAP or sodium hydride were initially planned to be used for flow translation since they produced moderate yields in batch. Initially, the use of a column packed with polymer supported DMAP dispersed on celite was screened at 80 °C, but no product was obtained after monitoring the reaction for a few reaction cycles, each with a 20-minute residence time. Secondly, a column packed with washed sodium hydride was attempted but was terminated because the sodium hydride produced a significant amount hydrogen gassing out in the BPR preventing the solvent and reagent from pumping through at a consistent residence time.

As a result, it was decided to employ the method detailed in the Vapourtec application note, which uses a sodium hydride slurry, as it represented a safer and more time efficient approach. To facilitate the pumping of the slurry we employed the use of peristaltic pumps as the pumping units, in addition a peristaltic pump was also used in place of a cartridge based BPR to regulate the system pressure. This was accomplished by manually setting the pressure to 7 bar. Mechanically, this works by pumping in the opposite direction at a specified flow rate to generate the appropriate back pressure. The system was kept inert by

purging with nitrogen gas using the reactor gas manifold, as well as employing the use of distilled tetrahydrofuran which was also kept inert.

The reaction was initially carried out using two peristaltic pumps: one for the stock solution of **23** (0.20 M) in tetrahydrofuran and a stirred sodium hydride slurry (0.50 M) suspended in tetrahydrofuran (Scheme 38). The two stock solutions were mixed at a T-piece mixer and the solution was allowed to deprotonate in a PTFE coil at various temperatures. Thereafter, a solution of allyl bromide was introduced at a second T-piece mixer using a standalone peristaltic pump. This was followed by a second heated coil reactor and finally a fourth peristaltic pump (which acted as the BPR) prior to collection.

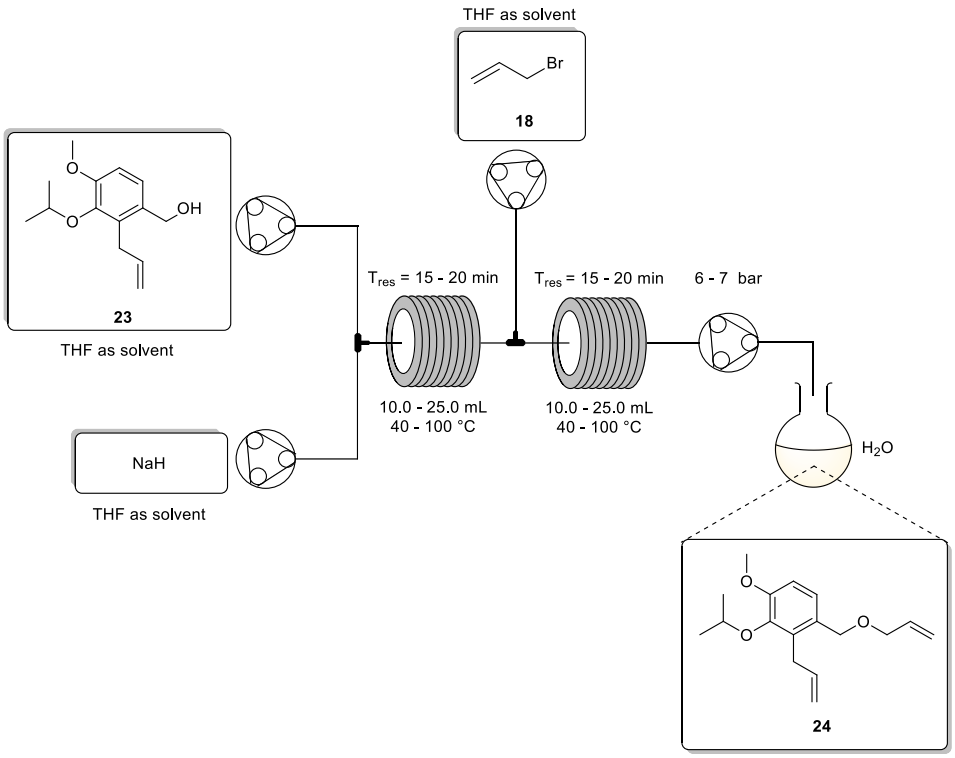

Scheme 38 : Flow synthesis of the second allylation using two peristaltic pumps with a standalone peristaltic pump for allyl bromide.

The first two entries used a coil with a 1.0 mm inner diameter, while the last entry made use of a 1.5 mm inner diameter coil (Table 17). From q-HNMR analysis, higher product conversion was achieved at a higher temperatures of 100 °C. The q-HNMR approached provided a method for calculating the product conversion of a product based on detectable signals using an internal calibrant ($DMSO_2$, 98 % purity). Thus, it can be hypothesized from these test reactions that an increased product conversion can be explored at higher temperatures. The low conversion, however, was at this stage hypothesised to be a result of a mixing issue inside the system.

Table 17: Flow experiments of the second allylation at various temperatures and residence times utilizing three peristaltic pumps at 0.20 M concentration using 2.5 equivalents of sodium hydride

Entry No	Reaction scale (g)	Temperature (°C)	Coil Volume (mL)	Residence time (min)	Flow rate ($mL.min^{-1}$)	q-NMR Conversion (%)
1 [a]	0.15	40	10	15	0.667	3.5
2 [a]	0.15	70	10	15	0.667	9.5
3 [b]	**1.12**	**100**	**25**	**20**	**1.25**	**13**

[a] Used 1.0 mm inner diameter coil, [b] Used 1.5 mm inner diameter coil

Since low yields were achieved with the previous setup using 2 pumps and a standalone pump, it was decided to prepare a solution combining **23** and allyl bromide **18** for one pump and utilizing a second pump for the sodium hydride slurry (Scheme 39). The flow streams were then combined at a T-piece mixer prior to passage through a 20 mL coil with a 1.0 mm internal diameter or a 52 mL coil with a 1.5 mL internal diameter. Finally, the flow stream exited the reactor via a peristaltic pump plumbed to operate as a BPR generating 6-7 bar backpressure.

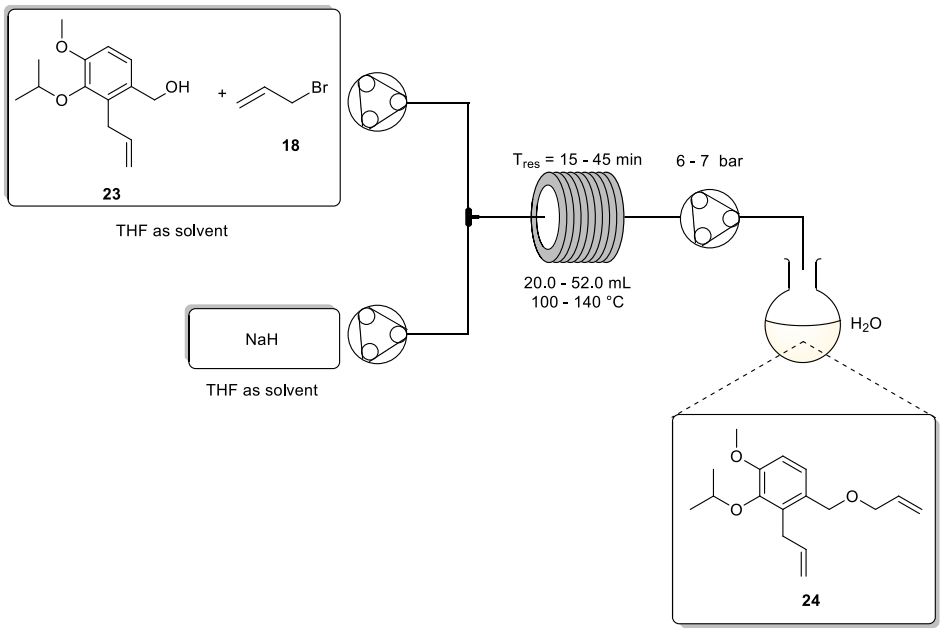

Scheme 39: Flow synthesis of second allylation using two peristaltic pumps

Earlier results suggested that higher conversions could be achieved at higher temperatures. As a result, several scenarios were screened at temperatures equal to or greater than 100 °C (Table 18) looking at the influence of increasing the equivalents of sodium hydride and/or changing the residence times. The setup employed the use of a 20 mL coil reactor (1.0 mm inner diameter). At a residence time of 45 minutes and temperature of 140 °C,

using 2.5 equivalents of sodium hydride a conversion of 21 % was achieved (Table 18, entry 1) increasing the excess of sodium hydride to 5.0 equivalents afforded an 18.5 % conversion (entry 2). It was discovered through q-NMR and ^{1}H NMR analysis that at higher temperatures of 140 °C there is an unknown by-product signal at 10.06 ppm in the aldehyde region that is not found in the starting material spectra as seen in Figure 30.

Table 18: Flow experiment for second allylation using two peristaltic pumps at various temperatures, residence times and sodium hydride equivalents at 0.20 M concentration

Entry No	Reaction scale (g)	NaH (equiv.)	Temperature (°C)	Residence time (min)	Flow rate (mL.min^{-1})	q-NMR Conversion (%0
1[a,1]	0.20	2.5	140	45	0.44	21
2[a,1]	0.15	5.0	140	45	0.44	18.5
3[1]	**0.15**	**2.5**	**100**	**15**	**1.33**	**28.5**
4[2]	0.15	2.5	100	15	3.47	3.5
5[2]	0.50	2.5	100	15	3.47	10.0
6[a,2]	0.15	2.5	120	15	3.47	20.5

[a] By-product signal observed on ^{1}H NMR spectra, [1] Used 1.0 mm inner diameter coil (25 mL), [2] Used 1.5 mm inner diameter coil (52 mL).

As a result, the temperature was decreased to 100 °C, yielding 28.5 % conversion at a 15-minute residence time. However, when the same residence time and temperature were used with a 52 mL coil with 1.5 mm bore tubing, the conversion decreased significantly to 3.5 % as seen for entry 4, and even increasing the reaction scale did not improve the conversion. Additionally at a higher temperature of 120 °C and the same residence time, the conversion improved to 20.5 %, however, the aforementioned by-product was again present. Furthermore, it was noted that as the coil diameter increases, the conversion decreased, potentially due to poorer mixing or increased dispersion. The increase in the coil volume and diameter size is not ideal for this reaction as the sodium hydride in the slurry tends to adhere to the inner surface area of the coil. As a result, the reaction solution passes over the sodium hydride that has become attached to the coil walls and prevents mixing and reacting with the solution. Thus, it was decided to employ a static mixer to improve the mixing and conversion in conjunction with a coil with a 1.0 mm inner diameter.

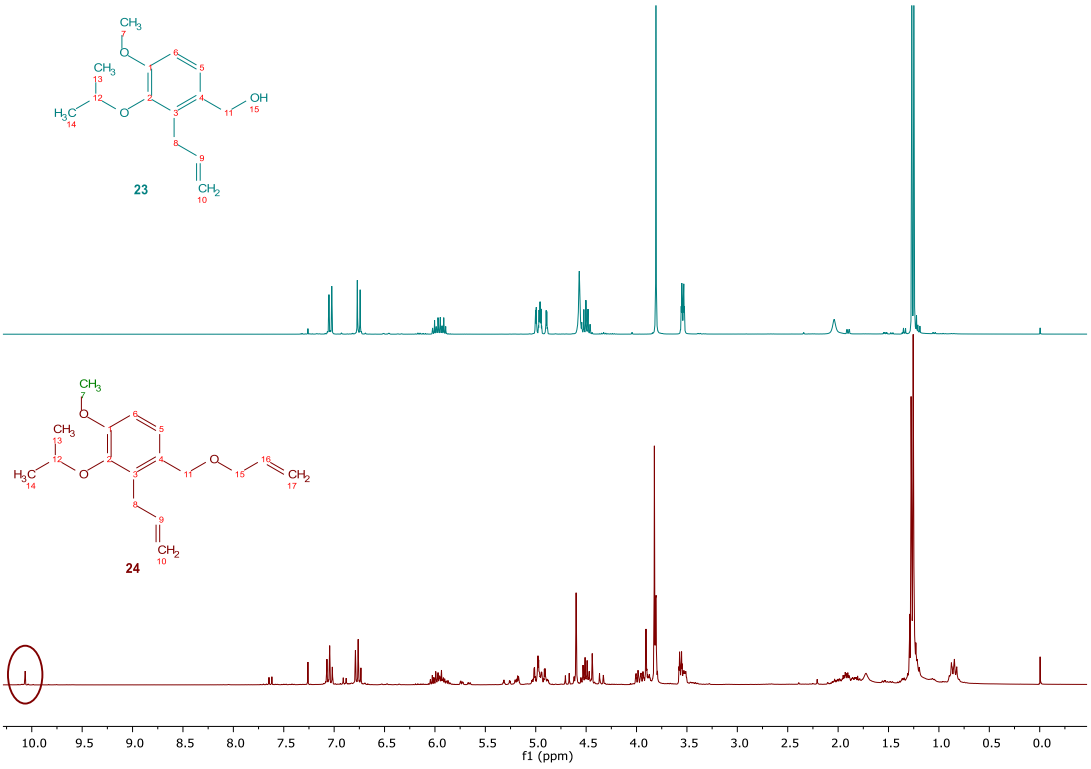

Figure 30: Stacked ^{1}H NMR spectra of (2-allyl-3-isopropoxy-4-methoxyphenyl)methanol **23** and 2-allyl-1-((allyloxy)methyl)-3-isopropoxy-4-methoxybenzene **24** to illustrate signal in aldehyde region

3.5.5 Flow results for the second allylation using sodium hydride employing a recycling approach.

After considering the outcomes of setups investigated up until this stage, it was decided to combine all the reagents into a single stock reservoir. This was deemed feasible as it was monitored that they do not react within the reservoir at ambient temperature. One peristatic pump was employed to pump the slurry with a second peristatic pump acting as the back pressure regulator. The flow stream was passed through a 0.5 mL static mixer connected in series to a 10 mL coil reactor (1.0 mm inner diameter) (Scheme 40). Thereafter, the solution passed through the second peristaltic pump (acting as a BPR) and finally a selector valve that can either direct the flow stream back to the reagent reservoir, or to a collection reservoir. In an attempt to improve the product conversion, we recycled the reaction solution prior to product collection.

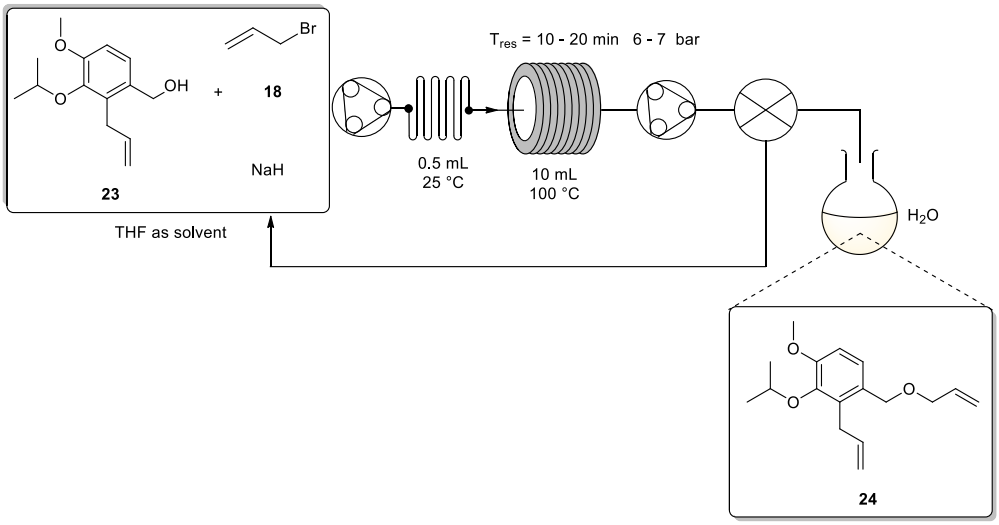

Scheme 40: Flow synthesis of second allylation recycling using a two-pump peristaltic system with a static mixer

It was noted earlier that a maximum product conversion was achieved at a temperature of 100 °C and 20 minutes residence time when using 2.5 equivalents of sodium hydride. Initially, the conditions were screened and the flow stream was subjected to recycling for 120 minutes (6-cycles) prior to collection (Table 19, entry 1). In this instance the product conversion increased marginally to 36 %. As this approach was time consuming, we chose to reduce the number of cycles to four and increase the equivalents of sodium hydride to 5.0 at the same residence time, in this case a 67 % product conversion was achieved (entry 2). The residence time was then reduced to 15 minutes and the reaction as cycled six times, affording a 68 % conversion (entry 3).

Table 19: Flow experiments for recycling of the second allylation using one peristaltic pump with a static mixer at different residence times at temperature of 100 °C using 20 mL coil at 0.20 M concentration

Entry No	Reaction scale (g)	NaH equiv.	Flow rate ($mL.min^{-1}$)	Residence time (min)	Cycles	NMR Conversion (%)
1	0.20	2.5	1.00	**20**	6	36.0
2	0.20	5.0	1.00	**20**	4	67.0
3	0.20	5.0	1.33	**15**	6	68.0

To further optimise this reaction a DoE was adopted screening several variables. A few preliminary reactions were carried out to determine the screening parameters. To be comprehensive, it was decided again to study the effect of using tubing with different internal diameters (1.0 mm vs. 1.5 mm) running two duplicate reactions with recycling and

determining the conversion from HPLC analysis using a standard curve. The reactions were carried out using the conditions detailed in Table 20, and it was shown through both HPLC and NMR analysis that the thickness of the coil does influence the reaction, as the smaller diameter coil showed 23 % more product conversion than the larger diameter coil.

Table 20: Flow experiments for recycling of the second allylation using one peristaltic pump with a static mixer testing two different diameter size coils at 0.20 M concentration using 5.0 equivalents of sodium hydride

Entry No	Reaction scale (g)	Temperature (°C)	Coil Volume (mL)	Residence time (min)	Flow rate ($mL.min^{-1}$)	LC Conversion (%)
1[1]	0.25	100	20	20	1.00	53.9
2[2]	0.25	100	25	20	1.25	30.9

[1] Used 1.5 mm tube, [2] Used 1.5 mm tube.

The flow setup for the DoE screening consisted of using a two-pump peristaltic system with one pump as the reagent inlet and one pump as the BPR (Scheme 41). A full-factorial screen was constructed with 2 replicates. The reaction was performed on a small scale of 255.00 mg and 18 experiments were carried out investigating the influence of several parameters shown in Table 21. While maintaining the concentration of the starting material and the temperature at 100 °C, a sodium hydride stoichiometric excess range of 2.5 to 7.5 equivalents and an allyl bromide stoichiometric excess range of 1.5 to 3.0 equivalents was selected. This was primarily driven by chemical intuition and our previous experience with the system. The residence time range employed was 10 to 20 minutes and the recycling range was from 3 to 9 recycles.

Table 21: Second allylation screening approach-DoE Design-Full Factorial Screening

Screening approach-DoE Design-Full Factorial Screening					
Name	**Abbreviation**	**Units**	**Type**	**Use**	**Settings**
Sodium hydride equivalents	NaH	mg	Quantitative	Controlled	2.5–7.5
Allyl Bromide equivalents	All	mL	Quantitative	Controlled	1.5–3.0
Residence time	Res	Min	Quantitative	Controlled	10-20
Cycling	Cyc	time	Quantitative	Controlled	3-9

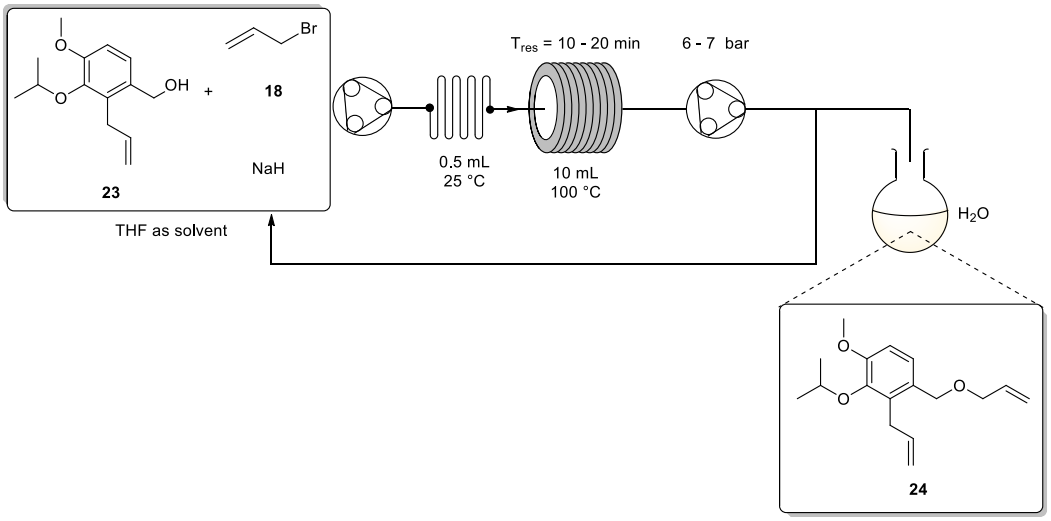

Scheme 41: Flow synthesis for recycling of the second allylation using one peristaltic pump and a static mixer with sodium hydride slurry.

The DoE screening results are summarised in Table 22, the product obtained was analysed by HPLC using a standard curve prepared from an isolated product. The HPLC sample was prepared by diluting the 30 mL collected product and completing a series of dilutions to obtain a concentration of 25 ppm and 32 ppm. Prior to sample preparation, no workup was performed. The conversion from HPLC analysis was captured and analysed using the MODDE 13 software package to determine where, under the ranges selected, the reaction optimum lies.

Table 22: DoE experiments for the recycling of second allylation

Entry No	NaH (equiv.)	Allyl Bromide (equiv.)	Residence time (min)	Flow rate ($mL.min^{-1}$)	Cycles	LC Conversion (%)
1	2.5	1.5	10	1.0	3	61.0
2	7.5	1.5	10	1.0	3	89.2
3	2.5	1.5	20	0.5	3	30.8
4	7.5	1.5	20	0.5	3	79.7
5	2.5	1.5	10	1.0	9	62.7
6	7.5	1.5	10	1.0	9	89.9
7	2.5	1.5	20	0.5	9	37.7
8	7.5	1.5	20	0.5	9	85.7
9	2.5	3.0	10	1.0	3	45.7
10	7.5	3.0	10	1.0	3	79.6
11[a]	2.5	3.0	20	0.5	3	39.5

12	7.5	3.0	20	0.5	3	82.3
13	2.5	3.0	10	1.0	9	59.0
14	7.5	3.0	10	1.0	9	84.0
15	2.5	3.0	20	0.5	9	30.4
16 [b]	**7.5**	**3.0**	**20**	**0.5**	**9**	**92.0**
17	5.0	2.3	15	0.7	6	71.7
18	5.0	2.3	15	0.7	6	65.9

[a] q-NMR revealed 49.66 % product conversion, [b] q-NMR revealed 99.09 % product conversion, 69 % Isolated Product

The replicate plot (Figure 31) depicts the difference between the experimental results achieved and the minimum and maximum value possible, as well as the two replicates reflected in blue. The replicate plot revealed that there is a significant difference between reactions using different equivalents of sodium hydride, as high product conversions were obtained for experiments using 7.5 equivalents of sodium hydride and very low product conversions were obtained for experiments using 2.5 equivalents of sodium hydride. The replicate plot also demonstrates that the experiments are within the minimum and maximum reaction parameters, and the replicates (entry 17 and entry 18) are quite near to one another, implying that the results are reproducible.

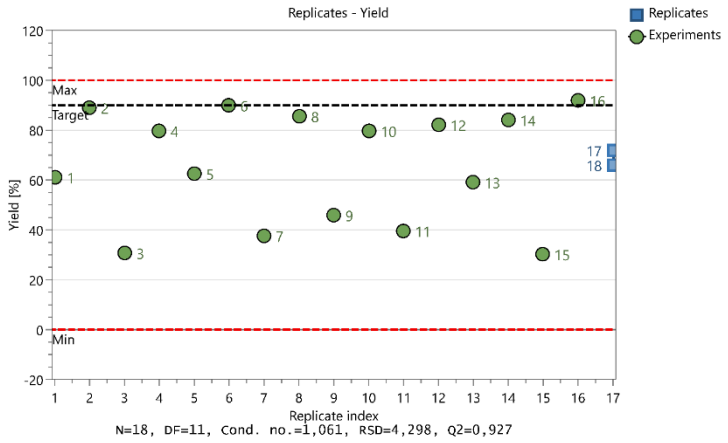

Figure 31: Representation of replicate plot that demonstrates the variation between results within the experimental limits

The histogram (Figure 32) depicts the shape of the response distribution; a normal distribution is preferred; otherwise, a positive or negative logarithmic transformation is required. The histogram derived from the results does not need to be modified according to the skewness test because more than 11 observations were made and a normal distribution was seen, indicating a good model estimate.

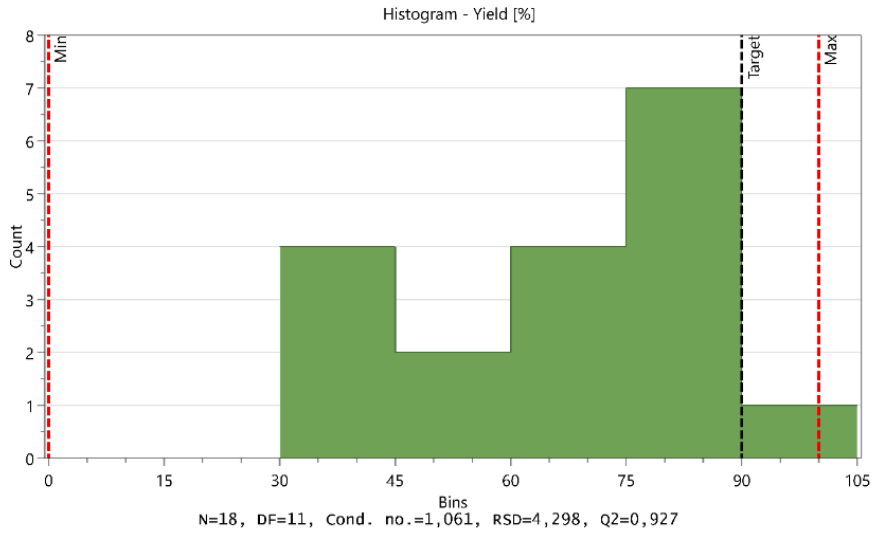

Figure 32: Representation of a histogram that displays a normal distribution curve

The coefficient plot (Figure 33) normally displays the importance and interaction between the elements in the model. The non-significant terms were removed to improve model's dependability and optimize the Q2 value, as these interactions do not contribute to the model quality.

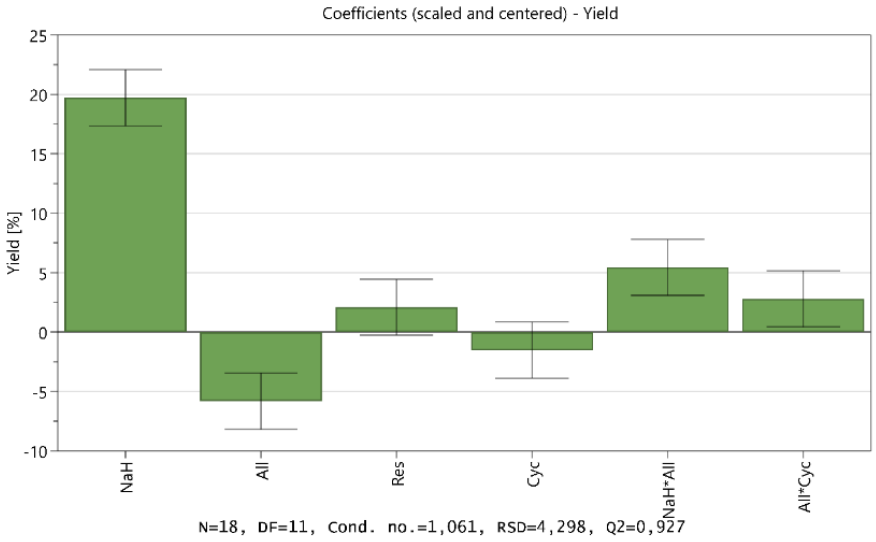

Figure 33: Representation of a coefficient plot illustrating important terms and their interactions

The non-significant terms were:

Term	The interaction between
NaH* Res	sodium hydride and residence times
NaH*Cyc	sodium hydride and cycling of reaction

All*Res	equivalents of allyl bromide and residence time
Res*Cyc	residence time and cycling.

The significant terms were kept since these factors and their interactions add to the model and are beneficial to the optimization of the reaction. The coefficient plot revealed that equivalents of sodium hydride and allyl bromide, residence time, cycling, the interaction between sodium hydride and allyl bromide, as well as the interaction between allyl bromide and cycling are significant terms. The equivalents of sodium hydride had the greatest effect on the yield. A square test was automatically carried out checking for square terms, no square terms were detected.

From the DoE data, a summary of fit plot was produced (Figure 34). This plot referred to the four parameters used to determine the model's quality, with 1 indicating a perfect model and 0 indicating a very poor model. The response has an R2 value of 0.974, indicating that the data fits within the regression model and that the model is significant for its purpose. The difference between Q2 and R2 should not be exceed by 20 % because Q2 is an estimate of future prediction precision. In this situation, the Q2 value is 0.927, which indicates a good model.

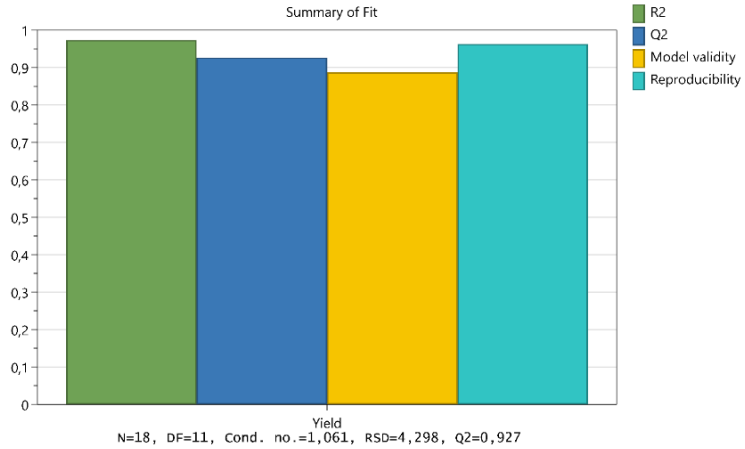

Figure 34: Representation of a summary of fit plot demonstrating the reliability and validity of the model

The model validity test is a diversity test that can detect statistically significant model problems such as outliers, transformation issues. the use of an incorrect model, or missing interactions. The model validity response was 0.887, indicating a good model and no model flaws were detected. The final parameter is the model's repeatability, which refers to the variation between replicates versus overall variability between outcomes. The value should be greater than 0.50, and the reproducibly in this situation was 0.963, indicating a good

model. Overall, the fit plot summarized that the model is quite good and reliable. The Observed vs Predicted plot (Figure 35) shows how close the results are to the line of best fit. The data indicated a good model with limited uncertainties as most of the points are close to the line of best fit and the R2 value is extremely close to 1.

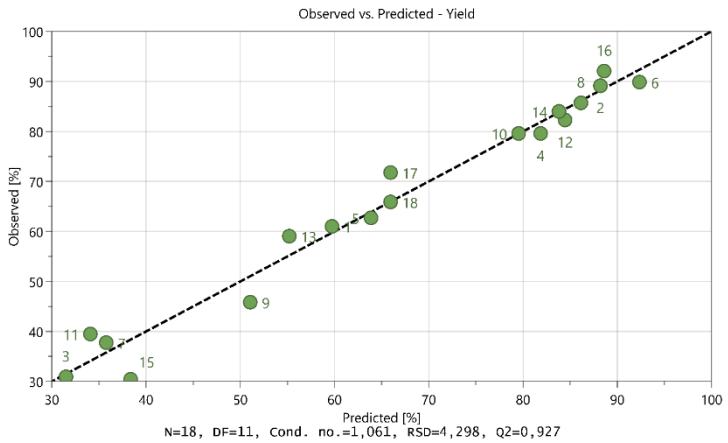

Figure 35: Representation of the observed vs. predicted plot for the results based on a line of best fit

Finally, the DoE data was transformed into contour plots with maximum product conversion shown by red zones (Figure 36). The flow conditions with the highest conversions were identified to be at 7.5 equivalents of sodium hydride, 1.5 equivalents of allyl bromide, 20 minutes residence time, and 3 cycles, as that is the only red region where a yield greater than 90 % can be expected. The reaction was likewise less successful with shorter residence times, longer cycles and utilizing less equivalents of sodium hydride, as seen by the lowest conversion in the contour plots. It is worth noting that all reactions that used 7.5 equivalents of sodium hydride had the higher conversions when compared to reactions that used 2.5 equivalents of sodium hydride under the same conditions. A maximum conversion of 92 % was achieved (Table 22, entry 16).

From this DOE experiment, it can be inferred that the peristaltic pumps were suitable and compatible for efficiently pumping highly reactive sodium hydride slurries. Repeatable results were obtained, and more research into the red region is required to identify the optimal conditions. DoE provides an indicator of reproducibility, precision, and selectivity. It can also easily detect errors, outliers and technique or method errors. The outcomes of this DoE process were near to expected values, and the difference between replicates was minor, indicating a good model with high reliability and reproducibility.

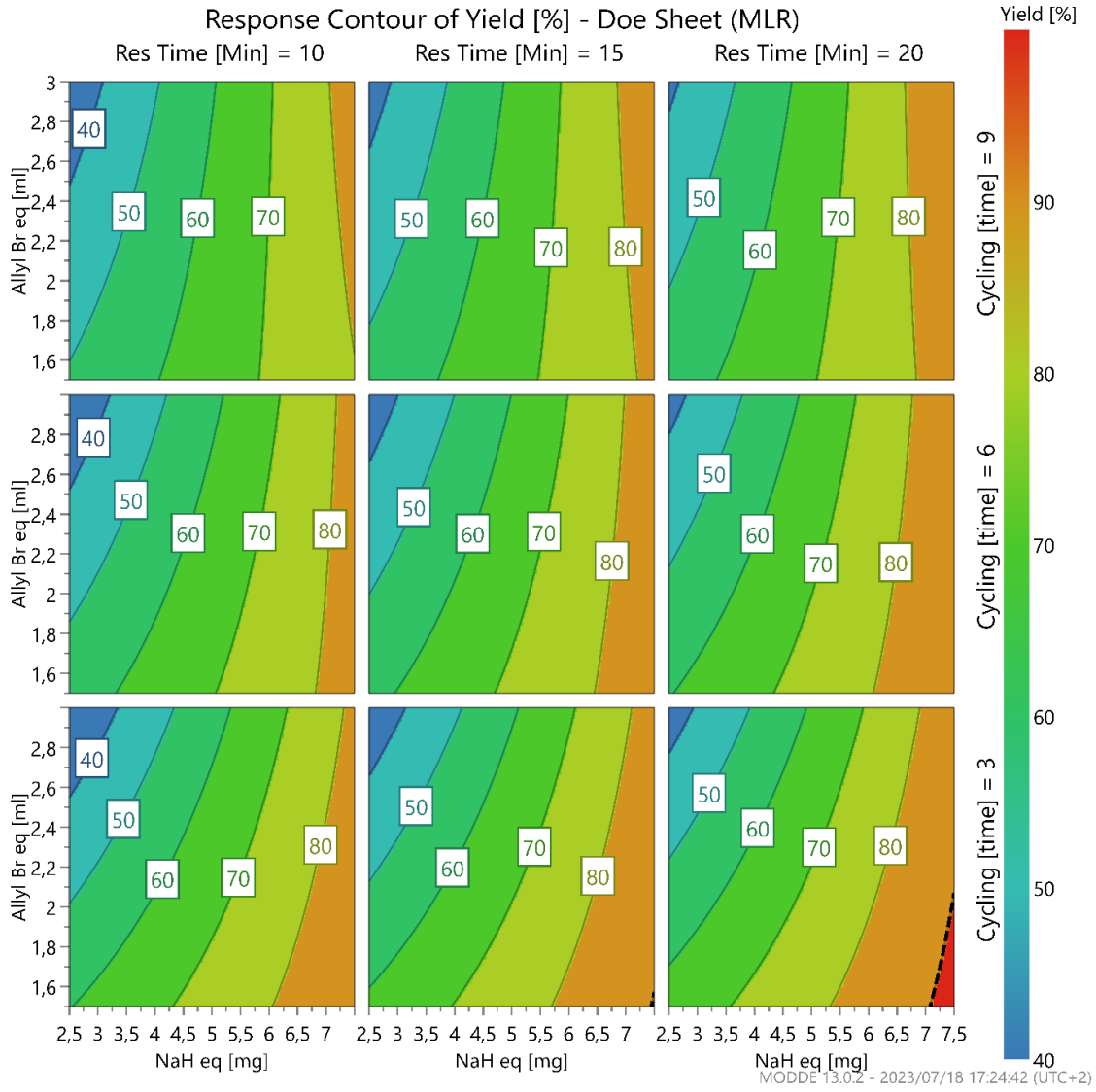

Figure 36: Representation of a 3-D contour plot illustrating the optimal area for achieving high product conversions

As previously stated, the results were obtained from HPLC analysis using a standard curve with known concentrations of 32 ppm and 25 ppm. The equation from the line of best fit was then used to determine the actual yield obtained by looking at the area under the curve and calculating the yield from the theoretical product mass expected. After workup, the HPLC data was compared to q-NMR data with the use of internal standard $DMSO_2$, and a small discrepancy was found. A peculiar peak was seen during the DoE experiments on the HPLC spectra, see Figure 37 at 2.1 minutes. The starting material peak appeared at 2.4 minutes and the product peak at 12.0 minutes using the chosen method.

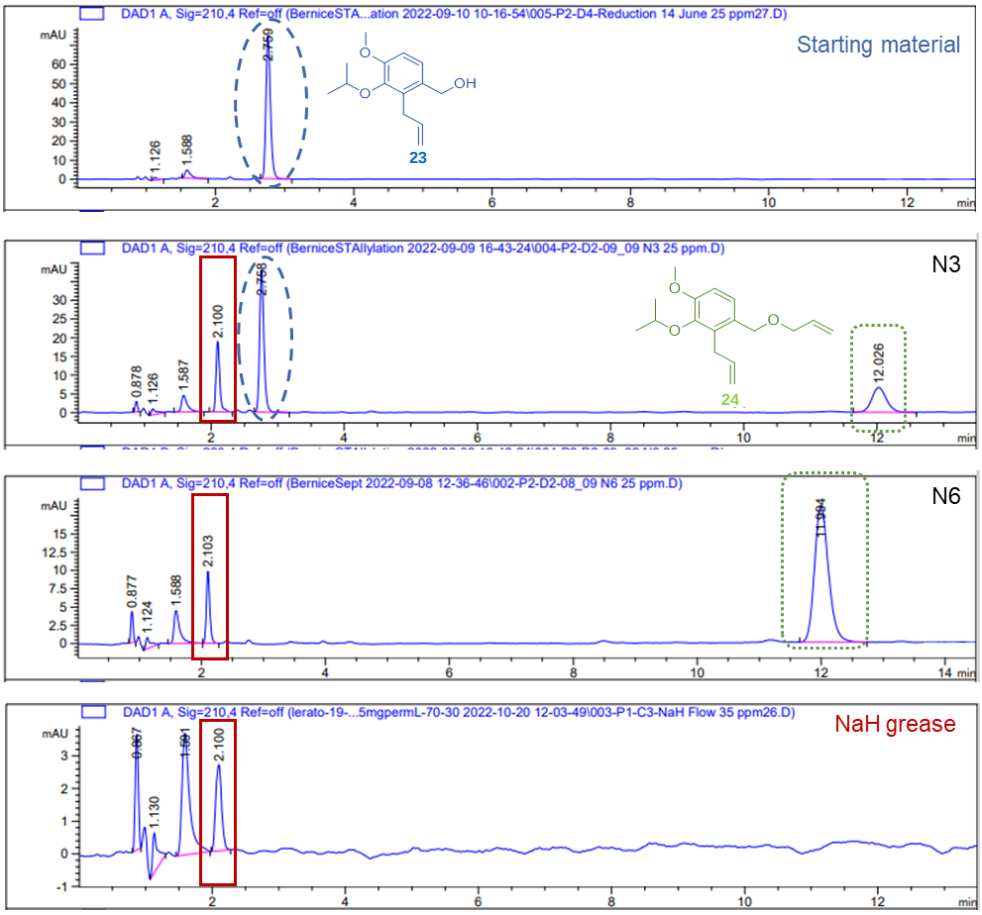

Figure 37: Sodium hydride grease is seen in the HPLC chromatogram. Assigning the peaks is done as follows: 2.103 minutes, unknown peak from grease from sodium hydride dispersed in mineral oil; 2.758 minutes, (2-allyl-3-isopropoxy-4-methoxyphenyl)methanol **23** ; 12.026 minutes; 2-allyl-1-((allyloxy)methyl)-3-isopropoxy-4-methoxybenzene **24**.

After running a blank flow experiment with only sodium hydride and allyl bromide in tetrahydrofuran, it was confirmed that the unknown peak was sodium hydride grease, as also observed by the authors of the Vapourtec's application note. As there is no grease seen in the product after workup, this is another reason why HPLC conversions are lower than q-NMR conversions. As the grease reduced product output and efficiency, this could provide a challenge on a larger scale.

3.6 Ring-Closing metathesis

The final step towards the 8-membered ring target molecule is a ring closing metathesis step. The mechanism, using ruthenium catalysts was previously described in the introduction and literature review chapter.

3.6.1 Previously reported flow-based ring closing metathesis

Ley and co-workers have demonstrated a ring-closing metathesis in the synthesis of Goniothalamin, a drug that has shown antiproliferative and cytotoxic effects on several tumour cell types.[63] For the ring closing step, they experimented with Grubbs first-generation, Hoveyda-Grubbs second generation and Grubbs second generation homogeneous catalysts. Since heterogeneous catalysts may result in issues like low catalytic efficiency, variable yields due to metal leaching and clogging of flow systems, homogeneous catalysts are preferred over packed immobilized catalysts. To assess catalyst selectivity, solvent selection, and concentration, batch processes were carried out. The batch approach consisted of either refluxing in dichloromethane at low concentrations which afforded good yields, or refluxing in toluene at higher concentrations that were proved ineffective.

The flow setup (Scheme 42) employed two HPLC pumps connected downstream of stock solutions of the starting material **57** and the ruthenium-based catalyst both in dry dichloromethane. The flow setup involved mixing the two stock solutions at a T-piece mixer before entering a 16 mL coil reactor heated to 100 °C. The pressure was maintained at 6.0 bar, and the product collected was passed through a plug of silica to remove the catalyst. They found low conversions were achieved for the Grubbs first generation catalyst at 100 °C after 16 minutes residence time. In contrast, maximum conversion was achieved using the thermally stable Grubbs second generation catalyst at 50 °C after 16 minutes residence time. However, due to the production of lactone by-products, they chose to perform this step-in batch for scaling up.

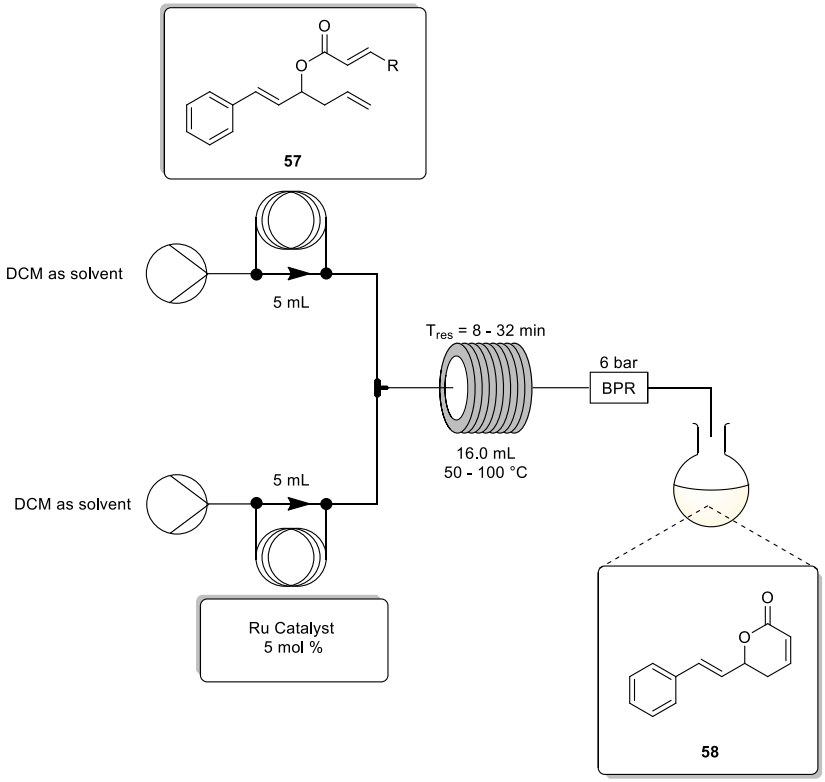

Scheme 42: Flow preparation of ring-closing metathesis of **58** using dichloromethane

Drop and co-workers reported an effective ring-closing metathesis method towards the synthesis of 2,5-dihydro-1H-pyrrole-3-carboxylates. [64] The flow setup (Scheme 43) employed a single HPLC pump with stock solution of several dienes and different homogeneous ruthenium catalysts dissolved in the chosen solvent, which was connected to a heating coil reactor. Initially a moderate yield was afforded after 30 minutes residence time at 90 °C by using 3 mol % of the ruthenium catalyst dissolved in dichloromethane. They envisioned using more environmentally friendly and greener solvents than dichloromethane. Prior research revealed that ethyl acetate and dimethyl carbonate (DMC) showed compatibility with RCM reactions. DMC was chosen because reactions in ethyl acetate produced lower product conversions than those in dichloromethane. It was found at 110 °C after 5 minutes and at temperature of 120 °C for 1 minute residence time, full conversion was attained. Additionally, they demonstrated a gram reaction at 120 °C for 37 minutes that produced a 91 % yield after isolation. They also contrasted the outcomes of a system using one pump to a system using 2 pumps as the ruthenium catalysts tends to decompose in the presence of an alkene substrate. It was found that no decomposition of the catalyst occurred as the outcomes were comparable.

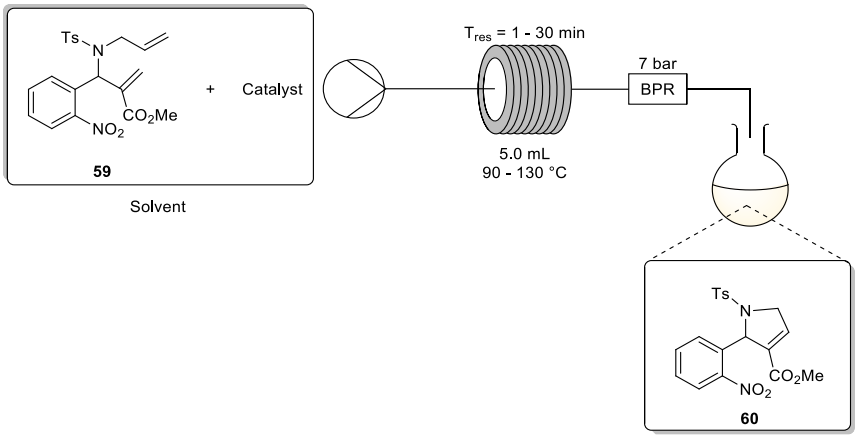

Scheme 43: Flow preparation of ring closing metathesis of **60**

Lastly, Toh and co-workers also investigated a ring-closing metathesis using a green solvent but including a soluble metal scavenger.[65] In this study, two homogeneous catalysts: Hoveyda−Grubbs second-generation catalyst and StickyCat PF_6 were used to compare the outcomes using a green solvent like ethyl acetate and a non-green solvent like dichloromethane. Similar yields were achieved using both solvents at low catalyst loading with a temperature of 30 °C for 3 hours. The Hoveyda−Grubbs second-generation catalyst at 0.3 mol % achieved higher yields at a temperature of 90 °C and 2.5 minutes residence time in ethyl acetate under flow conditions compared to using dichloromethane at the same conditions. However, under these conditions, minimal conversion variations were seen employing the StickyCat PF_6 catalyst in both solvents.

Additionally, they investigated effectiveness of SnatchCat, in removal of the ruthenium catalyst in both solvents. Prior to the addition of the scavenger, the ruthenium content for the Hoveyda−Grubbs second-generation catalyst was 21.3 ppm in dichloromethane and 855 ppm in ethyl acetate. After the introduction of SnatchCat the ruthenium content was 56.3 ppm in ethyl acetate. The ruthenium content in dichloromethane was independent of the amount of SnatchCat and the residence time implemented. However, the ruthenium content in ethyl acetate was reduced with a longer residence time and caused some precipitation, which could be eliminated with a short plug of silica gel.

They also carried out a large-scale flow synthesis involving a ring-closing metathesis to afford a Sildenafil analogue **63**. The flow setup (Scheme 44) consisted of employing two syringe pumps with stock solutions of a Sildenafil derivative **61** (72.84 g) in ethyl acetate and a ruthenium-based catalyst (0.6 mol %) in ethyl acetate. The stock solutions were sonicated to dissolve the catalyst while sealed under inert atmosphere. The flow setup involved the mixing of the two stock solutions at the T-piece mixer before entering coil reactor heated at

90 °C. After 5 minutes residence time, the scavenger was introduced to the solution at 2.64 mol % and was heated to a temperature of 90 °C for 5 minutes to produce 62 grams with a 94 % isolated yield after 24 hours.

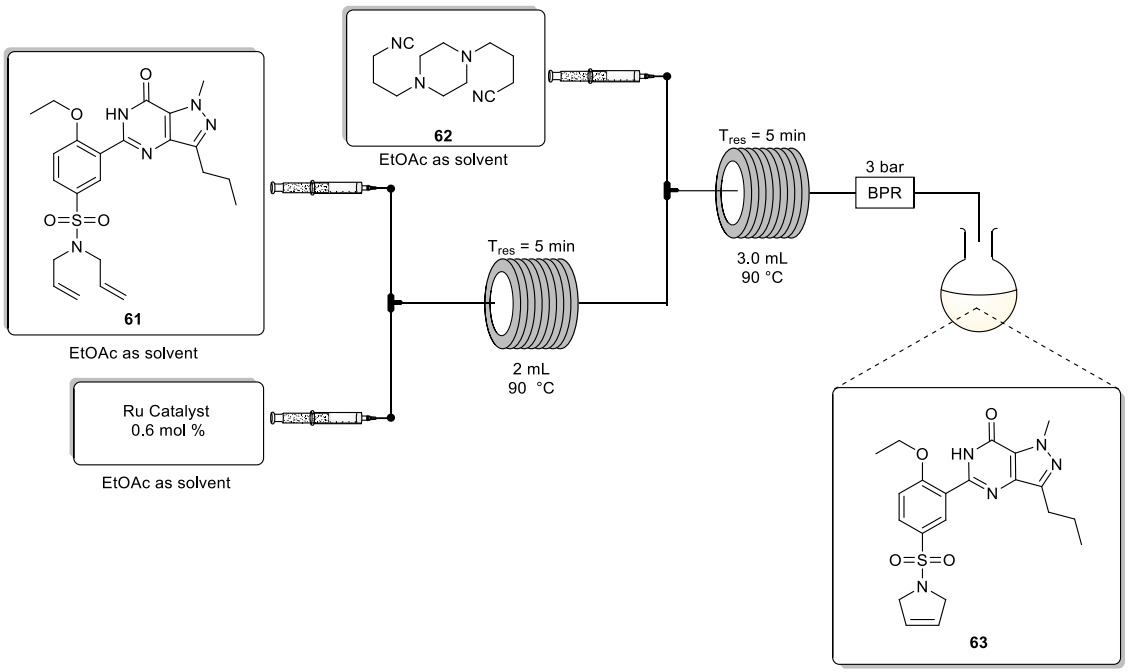

Scheme 44: Flow preparation of ring closing metathesis of a Sildenafil analogue **63**

3.6.2 Batch results for Ring-Closing metathesis

The final stage was reported by van Otterlo and co-workers employing the Grubbs II catalyst (5 mol %) in toluene at 60 °C for 2 hours under inert conditions to obtain a 52% yield of the desired product **25**.[34] It was discovered that this step had challenges as long reaction times were required while affording low yields and some catalyst decomposition. In our hand we were able to replicated the reaction in a 46% yield.

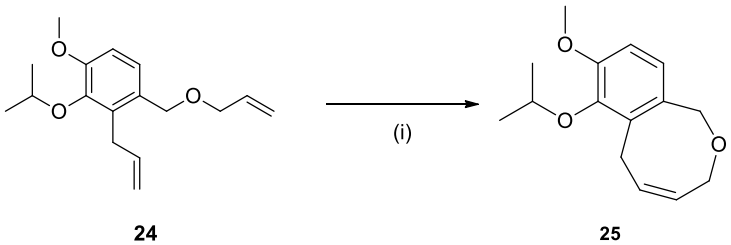

Scheme 45: Ring-closing metathesis (i) Grubbs II catalyst (5 mol %), 60 °C, toluene, 2 hours

3.6.3 Flow results for Ring-Closing metathesis

Our team has previously looked at the RCM stage in-house under flow conditions. The flow setup involved the use of a two HPLC pump connected to a stock solution of **24** and Grubbs II catalysts (0.05 equiv.) in toluene. The reaction was performed using a 2 mL mixing chip at a temperature of 60 °C and 30 minutes residence time to afford a 60 % product conversion. It was chosen to evaluate the flow setup using a static mixer and coil heated to 60 °C. Initial test reactions showed lower product conversion utilizing a coil compared to using a glass mixing chip Thus, a glass mixing chip was chosen for flow optimization.

It was decided to perform a DoE on this step to evaluate the screening area and determine the most suitable catalyst and solvent for this reaction. A full-factorial DoE screening was selected with 19 experiments including 3 replicates. The DoE screening parameters as seen in Table 23 included 4 varying factors and one constant factor. Two factors were qualitative which was the catalysts and solvent. The other two factors were quantitative and is the temperature and residence time. The catalysts loading was kept constant at 3 mol % (0.03 equiv.). The flow setup (Scheme 46) consisted of using the Uniqsis Binary pump equipped with 2 mL sample loops that was purged with degassed solvent prior to loading. The two stock solutions were mixed in a 20 mL glass mixing chip and the pressure were kept between 4-5 bar as the mixing chip has a maximum pressure of 10 bar.

Table 23: Ring-closing metathesis screening approach-DoE Design-Full Factorial Screening

Screening approach-DoE Design-Full Factorial Screening					
Name	**Abbreviation**	**Units**	**Type**	**Use**	**Settings**
Solvent	Sol		Qualitative	Controlled	EtOAc; Toluene
Catalyst	Cat		Qualitative	Controlled	GII; HGII
Temperature	Temp	°C	Quantitative	Controlled	60-90
Residence time	Res	min	Quantitative	Controlled	15-45
Catalyst Loading	Cat	mol%	Quantitative	Constant	3

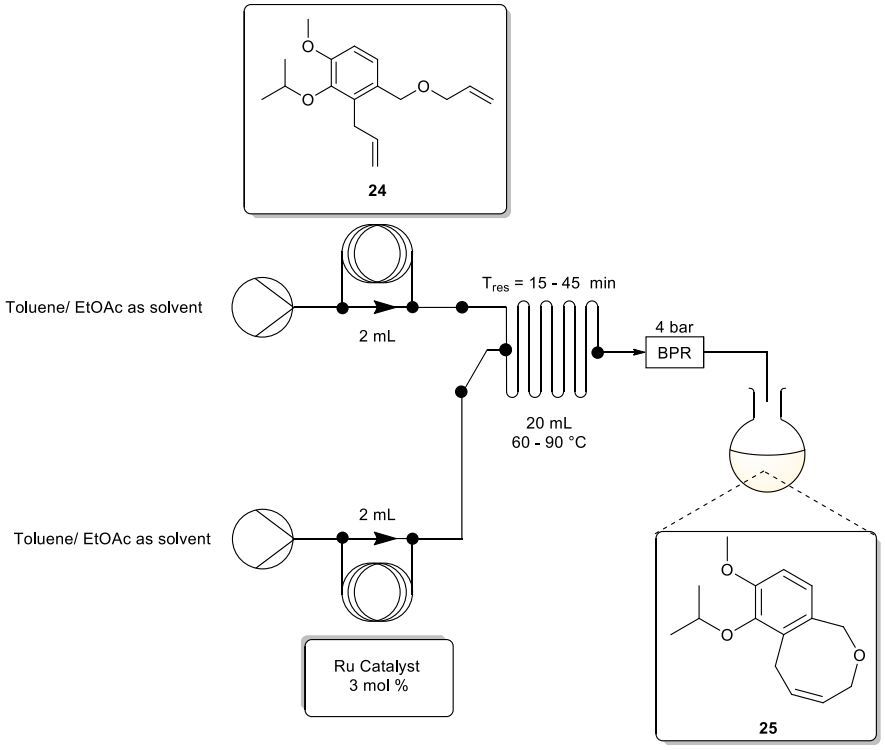

Scheme 46: Flow preparation of the ring closing metathesis of **25**

The DoE screening results are provided in Table 24, and the product conversion was obtained from HPLC analysis using a standard curve. The HPLC sample was prepared by diluting the 20 mL collected product and completing a series of dilutions to obtain a concentration of 20 ppm and 30 ppm. Prior to sample preparation, no workup was done. The conversion form HPLC analysis were captured and analysed on MODDE 13 to illustrate where the optimal conditions might be explored. The product peak obtained from HPLC analysis corresponded to literature for both NMR and HRMS analysis.

Table 24: DoE experiments for ring-closing metathesis of **25**

Entry No	Solvent	Catalyst	Temperature (°C)	Residence time (min)	Catalyst Loading	LC Conversion (%)
1	EtOAc	GII	60	15	3	45.6
2	Toluene	GII	60	15	3	43.3
3	EtOAc	HGII	60	15	3	48.0
4	Toluene	HGII	60	15	3	40.9
5	EtOAc	GII	90	15	3	24.7
6	Toluene	GII	90	15	3	35.9
7	EtOAc	HGII	90	15	3	46.5

8	**Toluene**	**HGII**	**90**	**15**	**3**	**54.8**
9	EtOAc	GII	60	45	3	43.3
10	Toluene	GII	60	45	3	45.4
11	EtOAc	HGII	60	45	3	46.9
12	Toluene	HGII	60	45	3	37.0
13	EtOAc	GII	90	45	3	15.0
14	Toluene	GII	90	45	3	23.4
15	EtOAc	HGII	90	45	3	26.9
16	Toluene	HGII	90	45	3	37.0
17	EtOAc	GII	75	30	3	34.7
18	EtOAc	GII	75	30	3	36.3
19	EtOAc	GII	75	30	3	34.4

The replicate plot depicts the difference between the experimental results achieved and the minimum and maximum value possible, as well as the three replicates reflected in blue are quite near to one another, implying that the results are reproducible (Figure 38). The histogram (Figure 39) depicts a normal distribution indicating a good model estimate. The coefficient plot (Figure 40), displayed the interaction between the elements in the model. The non-significant term removed was the interaction between the solution and residence time as this interaction did not contribute to the model quality. It was noted that there was quite a lot of significant terms and interactions between variables. The coefficient plot revealed that the solvent, catalyst, temperature and residence times affected one another, thus their interactions on each other are significant.

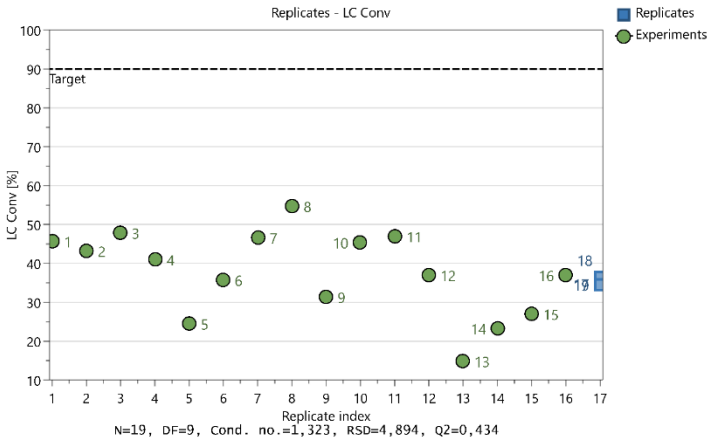

Figure 38: Representation of replicate plot that demonstrates the variation between results within the experimental limit for the RCM step

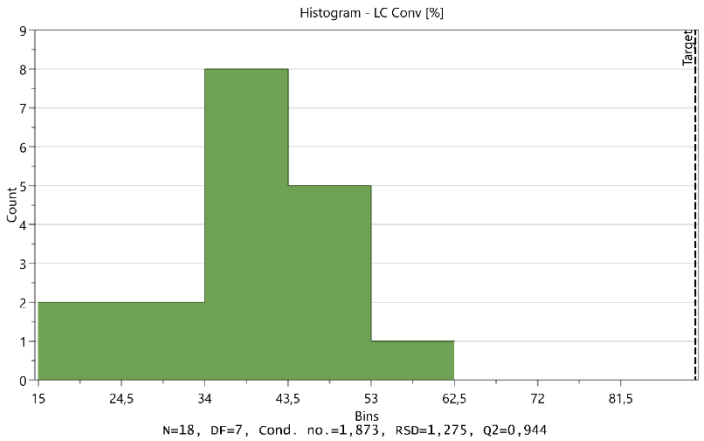

Figure 39: Representation of a histogram that displays a normal distribution curve

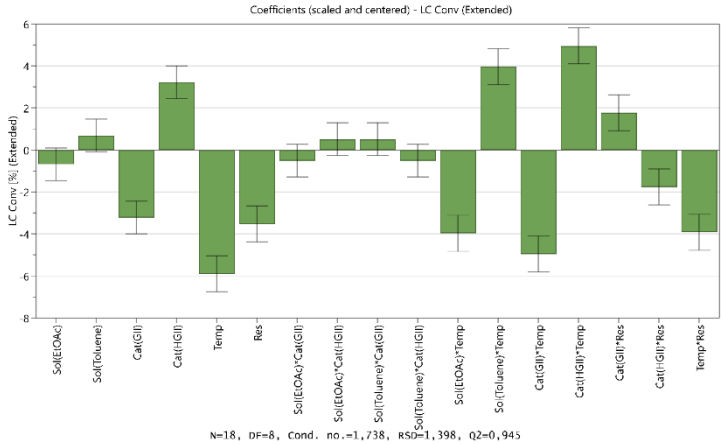

Figure 40: Representation of a coefficient plot illustrating important terms and their interactions for the RCM step

The summary of fit plot (Figure 41) produced revealed the four parameters used to determine the model's quality, with 1 indicating a perfect model and 0 indicating a very poor model. The response has an R2 value of 0.991, indicating that the data fits within the regression model and that the model is significant for its purpose. The Q2 value is 0.945, also indicating a good model. The model validity response was 0.737, indicating a good model and no model flaws were detected. The final parameter is the model's repeatability, which refers to the variation between replicates versus overall variability between outcomes. The value should be greater than 0.50, and the reproducibly in this situation was 0.99, indicating a good model. Overall, the fit plot summarized that the model is quite good and reliable.

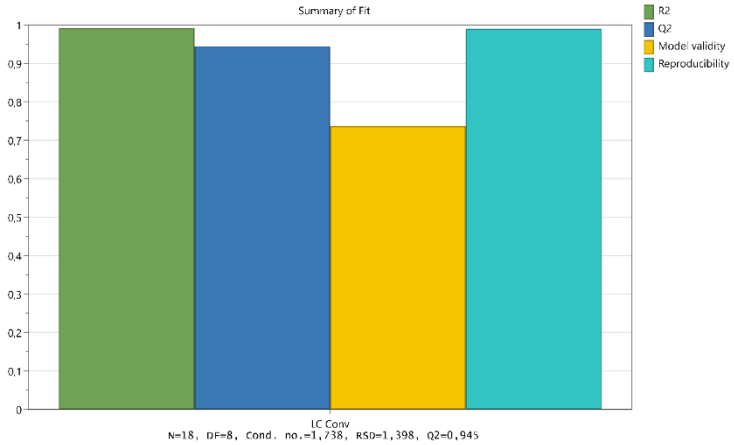

Figure 41: Representation of a summary of fit plot demonstrating the reliability and validity of the model for the RCM step

Finally, the DoE data were transformed into contour plots (Figure 42) with maximum product conversion shown by red zones, which can be used to explore optimal conditions. The outcomes of this DoE process were near to expected values, and the difference between replicates was minor, resulting in a good model with high reliability and reproducibility. The optimized conditions were determined at 90 °C to afford 54.8 % product after 15 minutes residence time in toluene using Hoveyda−Grubbs second-generation catalysts.

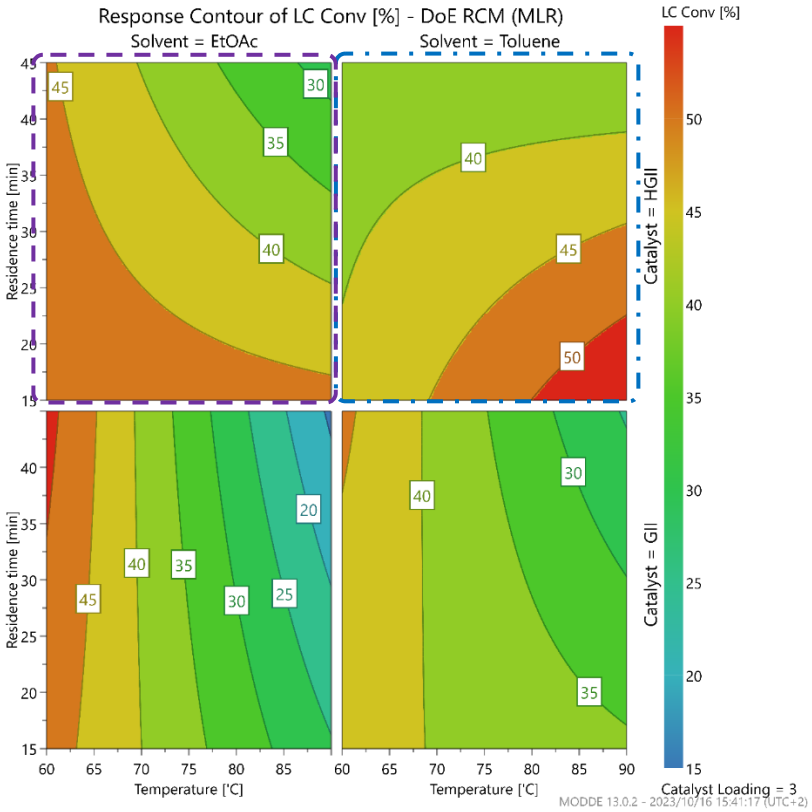

Figure 42: Representation of a 3-D contour plot illustrating the optimal area for achieving high product conversions

After studying the contour plot (Figure 42), a few reactions were conducted using the same flow setup (Scheme 46) and focusing on the area highlighted by the blocks predicted to afford the highest conversions. The first follow-up reactions were conducted using Hoveyda−Grubbs second-generation catalysts in both toluene and ethyl acetate but reducing the residence time to 10 minutes (Table 25, entries 1 and 2). Entry 1 was carried out at 60 °C and entry 2 at 100 °C to afford 53.6 and 35.6 % product conversion. Due to the unexpected low yield at higher temperature in toluene it was decided to replicate the most optimal conditions but changing the equivalents of the catalysts (entries 3-5). It was found that as the equivalents of the catalysts increases, the product conversion decreases. This could be due to the catalysts decomposing (self-poisoning) or due to polymerization and cross-metathesis occurring. The last entry was conducted by increasing the volume of the injection loops to 5 mL (entry 6) to compensate for dispersion. However, a moderate product conversion was obtained. This step will be further optimized as part of future work.

Table 25: Follow-up reaction after DoE analysis for ring-closing metathesis of **25**

Entry No	Solvent	Catalyst	Temperature (°C)	Residence time (min)	Catalyst Loading	LC Conversion (%)
1	EtOAc	HGII	60	10	3	53.6
2	Toluene	HGII	100	10	3	35.6
3	Toluene	HGII	90	15	1	47.5
4	Toluene	HGII	90	15	5	37.7
5	Toluene	HGII	90	15	8	26.6
6[a]	Toluene	HGII	90	15	3	43.0

[a] Larger scale (5 mL injection loops)

3.6.4 Characterisation of RCM

In the stacked ^{1}H NMR spectra (Figure 43), product formation was confirmed by i) the splitting shift of H_9 and H_{16} from 6.01-5.85 ppm to 5.98-5.92 and 5.68-5.61 ppm, ii) the shift downfield of H_{11} from 4.49 ppm to 4.90 ppm, iii) the downfield shift of the CH_2 (H_{15}) from 4.00 ppm to 4.16 ppm, iv) the disappearance of H_{17} and H_{10} in the 5.31-5.16 ppm and 4.98-4.89 ppm region. Additionally, the ^{13}C NMR spectra (Figure 44) also revealed product formation by i) the disappearance of C_{17} and C_{10} at 116.94 and 114.77 ppm, ii) the shift of C_{15} from 70.08 ppm to 66.27 ppm, iii) the shift of C_{16} from 134.97 ppm to 127.91 ppm. The MS spectra (Figure 45) showed a visible $[M+H]^+$ signal at 249.1489 where the product requires a molar mass of 249.14907 $g.mol^{-1}$. The NMR and MS results are comparable to those reported previously by van Otterlo and co-workers.[34]

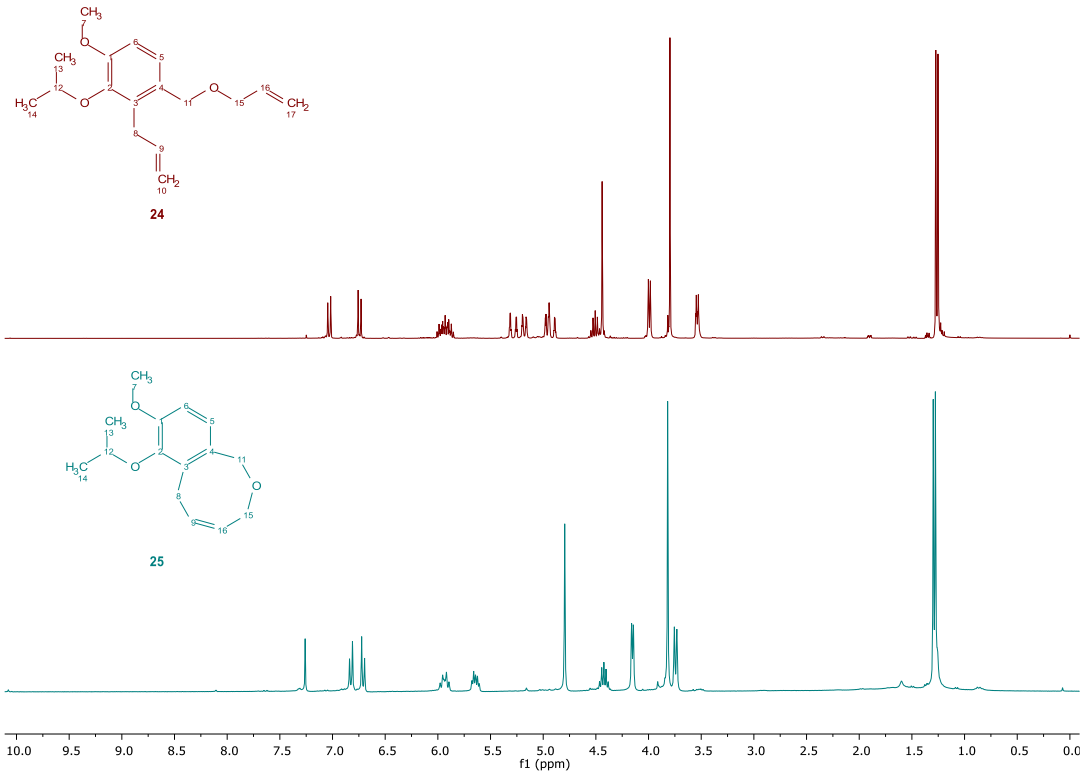

Figure 43: Stacked ^{1}H NMR spectra 2-allyl-1-((allyloxy)methyl)-3-isopropoxy-4-methoxybenzene **24** and (*Z*)-7-isopropoxy-8-methoxy-3,6-dihydro-1*H*-benzo[*c*]oxocine **25**

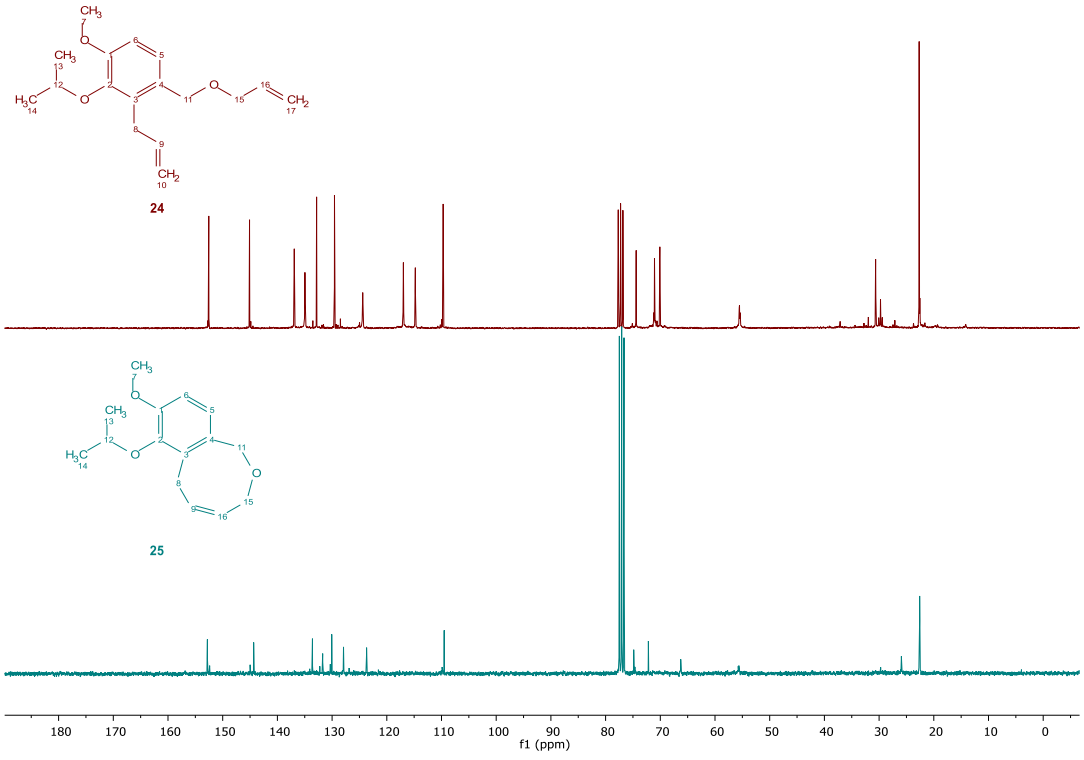

Figure 44: Stacked ^{13}C NMR spectra 2-allyl-1-((allyloxy)methyl)-3-isopropoxy-4-methoxybenzene **24** and (*Z*)-7-isopropoxy-8-methoxy-3,6-dihydro-1*H*-benzo[*c*]oxocine **25**

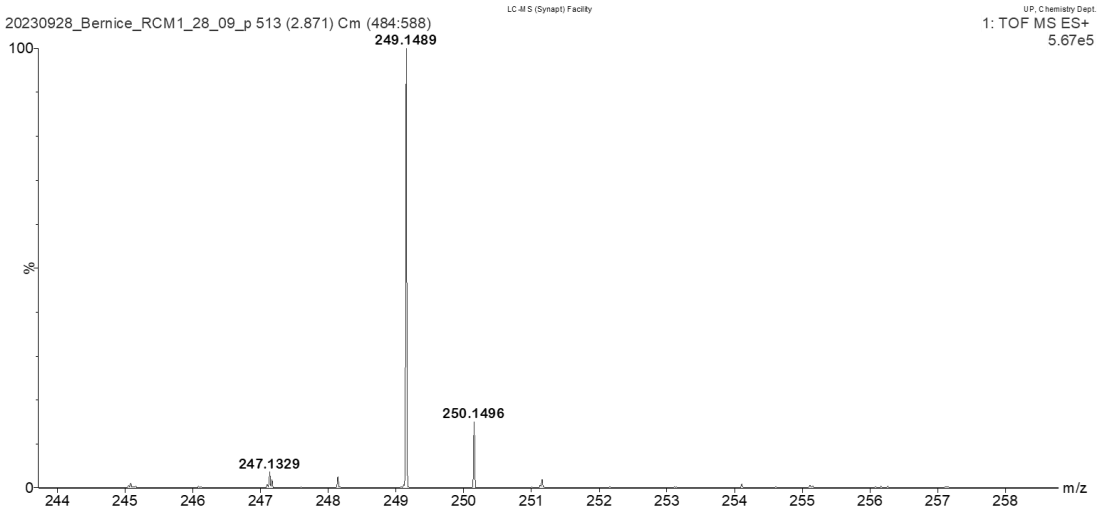

Figure 45: MS spectra of (*Z*)-7-isopropoxy-8-methoxy-3,6-dihydro-1*H*-benzo[*c*]oxocine **25** showing $[M+H]^+$ signal at 249.1489

Chapter 4. Conclusion and future work

This chapter concludes the project and provides an overview of future work that will be conducted.

4.1. Conclusion

In conclusion, the synthesis of (*Z*)-7-isopropoxy-8-methoxy-3,6-dihydro-1*H*-benzo[*c*]oxocine **25** was successfully translated to, and demonstrated under flow conditions. The first stage, the allylation of isovanillin **17** was optimized under flow conditions using two approaches; i) utilizing a packed-bed reactor housing potassium carbonate to afford the desired product **19** in a 92 % yield with a 20 minutes residence time at temperature of 100 ºC using dimethylformamide or by ii) using a coil reactor with a potassium hydroxide solution in methanol to afford **19** in 88 % isolated yield after 15 minutes residence time at temperature of 80 ºC. In comparison, the flow translations showed improved product conversions in reduced time compared to batch approach that required more than 20 hours. This stage also showed the advantage of using different flow approaches and substituting dimethylformamide with greener protic solvents in the form of aqueous methanol or aqueous ethanol.

The Claisen rearrangement was translated under flow using toluene and showed a significant increase in yield (6.9 to 98 %) and time reduction from 72 hours in batch to 15 minutes in flow. This stage also showed the safe use of solvents at temperatures above the solvent's boiling point and performing reactions at elevated pressures. The Claisen rearrangement's optimized conditions involved heating **19** at 240 ºC with a 15 minutes residence time to afford the product **20** in a 98 % isolated yield as a pure product.

The third stage showed improved product conversions (78 to 88 %) with a significant reduction in time from more than 20 hours in batch to 20 minutes in flow using a packed-bed reactor housing potassium carbonate. A further optimisation study is recommended for translating this stage to an approach using a potassium hydroxide solution, see future work section.

The fourth stage involving the reduction of the aldehyde was successfully translated and optimized under flow conditions using two approaches, namely i) the utilization of a packed-bed reactor housing polymer supported sodium borohydride to afford an 87 % product conversion after 45 minutes residence time at room temperature using methanol as the protic solvent source or by ii) using a coil reactor with a sodium borohydride solution at temperature of 30 ºC affording a 93 % isolated yield of product **23** after 30 minutes residence time. In comparison, the flow translations showed improved product conversions in reduced time compared to batch that was conducted for more than 20 hours using Red-Al (60 % in toluene) to afford the product **23** in 76 % yield.

The fifth stage, the second allylation, was successfully translated and optimized under flow conditions using a sodium hydride slurry employing a recycling approach. The DoE results showed that the peristaltic pumps were suitable and compatible for efficiently pumping highly reactive sodium hydride slurries. This stage showed improved product conversions (85 to 92 %) and time reduction from more than 20 hours in batch to 20 minutes under flow conditions.

The final RCM reaction was also successfully translated under flow conditions with an increased yield from 46 % in batch after 2 hours to 55 % under flow within 15 minutes. This stage also made use of DoE and showed that the Hoveyda-Grubbs II catalysts is more suitable for this reaction at higher temperatures and shorter residence times.

The final optimised results are summarised in Table 26, and it can be concluded that the flow approach afforded a higher overall percentage yield of 37.7 % compared to batch 0.77 % in significantly less time of 105 minutes vs.154 hours for the batch approach (Table 26). Overall, there is also an increase in the overall yield obtained under flow when compared to those reported by Van Otterlo and co-workers who obtained an overall percentage yield of 25.6% after 136 hours (Table 27).[34,36]

Table 26: Summary of results obtained for each stage under batch and flow conditions.

Stage: Reaction name	**Batch results**		**Flow results**	
	Time (hours)	**Yield %**	**Time (minutes)**	**Yield %**
1: Allylation (potassium hydroxide solution approach)	20	78	15	93
2: Claisen rearrangement	72	6.9	15	98
3: Alcohol protection	20	78	20	88
4: Aldehyde reduction (sodium borohydride solution approach)	20	47	20	93
5: Second allylation	20	85	20	92
6: RCM	2	46	15	55
Overall % yield	**0.77**		**37.7**	

Table 27: Summary of results obtained for each stage under flow conditions in comparison to literature values obtained from Van Otterlo and co-workers. [34,36]

Stage: Reaction name	**Van Otterlo and co-workers.**[34]		**Flow results**	
	Time (hours)	**Yield %**	**Time (minutes)**	**Yield %**
1: Allylation (potassium hydroxide solution approach)	20	99	15	93
2: Claisen rearrangement	64	/	15	98
3: Alcohol protection	18	75	20	88
4: Aldehyde reduction (sodium borohydride solution approach)	12	86	20	93
5: Second allylation	20	77	20	92
6: RCM	2	52	15	55
Overall % yield	**25.6**		**37.7**	

4.2 Future work

Future work for this project includes i) the optimization of the Claisen rearrangement by reducing the residence time further to perhaps 10 minutes or 5 minutes, ii) performing an optimisation study of the protection stage using potassium hydroxide and swopping dimethylformamide to aqueous methanol or ethanol (Scheme 47). The optimisation study would include residence time, temperature and concentration based on the conditions of stage 1, iii) further optimisation of the RCM stage by using a smaller chip as this may decrease the dispersion and possibly increase the product conversion, also the removal of ethene gas to drive the RCM could be investigated with a tube in tube reactor under vacuum.

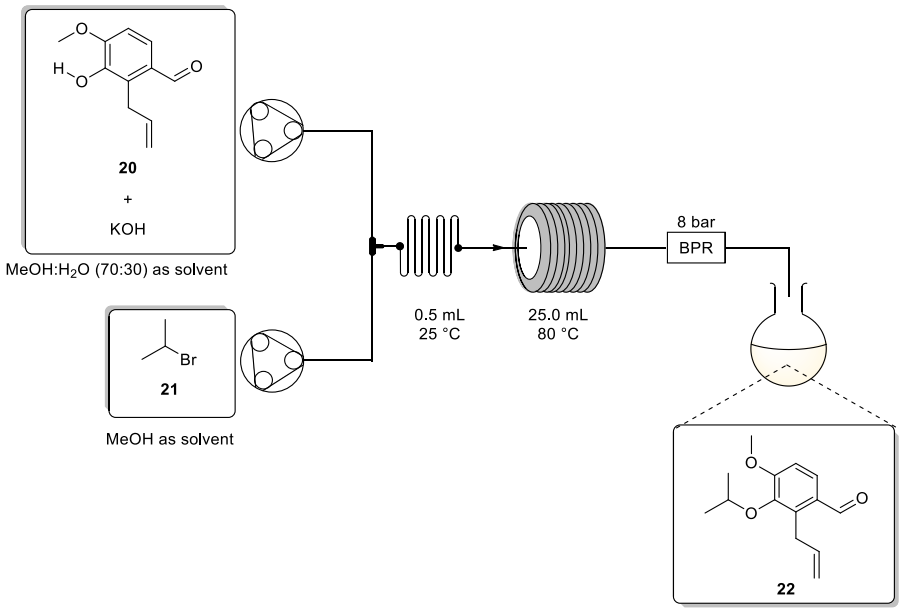

Scheme 47: Proposed alcohol protection flow approach using potassium hydroxide

Telescoping of the flow approach would be investigated (Scheme 48) including:

i. Attempting the Claisen rearrangement in methanol for linking of stage 1 and stage 2 with removal of water with a Syrris Asia FLEXX membrane separator/Zaiput membrane separator,
ii. Linking stage 2 and 3 using methanol as solvent and pumping in 2-bromopropane and potassium hydroxide solution, after which the water will be removed with a Syrris Asia FLEXX membrane separator/ Zaiput membrane separator,
iii. Linking stage 3 and 4 using methanol as solvent and pumping in a sodium borohydride solution, after which the product will be quenched with pumping in

sodium bicarbonate and water followed by concentration and being redissolved in tetrahydrofuran with the addition of sodium hydride and allyl bromide **18,**

iv. Applying a recycling loop will be used for the second allylation followed by the pumping of water after recycling for quenching, after which the product will be concentrated and redissolved in toluene for the final RCM reaction.

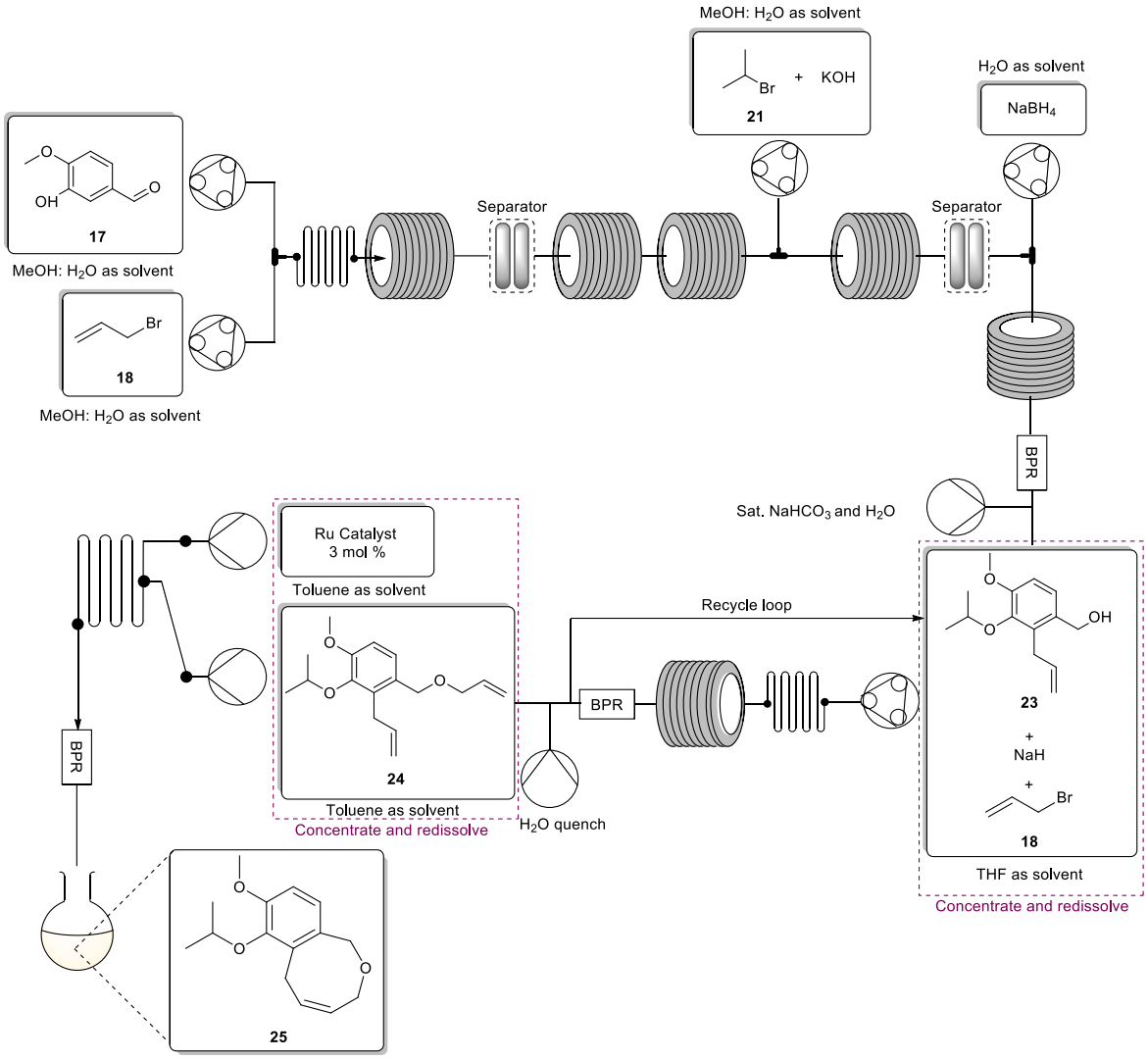

Scheme 48: Proposed telescoped process of **25**

Chapter 5. Experimental

This chapter provides detailed experimental methods for each reaction stage as well as a detailed information about technical aspects, purification methods and flow descriptions.

5.1. Technical aspects

All batch reactions were carried out using traditional chemistry methods, glassware and apparatus found in a standard synthetic laboratory. Prior to use, all glassware was oven- or flame-dried, and specified reactions were carried out under an inert environment using either argon or nitrogen gas. Under an inert environment (nitrogen), certain drying agents were used to distill solvents. Toluene was distilled from sodium, dimethylformamide was distilled using molecular sieves (type 4A molecular sieves), acetonitrile and ethyl acetate were distilled using calcium hydride, and tetrahydrofuran were distilled using sodium with benzophenone added as an indicator.

All starting materials and solvents were purchased from fine chemical vendors and commercial sources and used without purification. The removal of solvent was performed either with the use of evaporation under a flowing stream of compressed air, or by removal under reduced pressure (approximately 20 mmHg) using a standard Heidolph rotary evaporator at temperatures between 40 °C and 90 °C, depending on solvent identity.

5.1.1 Flow reactors and equipment

All flow reactors and specifications are indicated in each experimental description, for convenience a general description is provided below:

1. Flow reactors:
    a. Uniqsis™ Binary Pump Module (BPM) reactor equipped with 10 mL HPLC pump heads
    b. Vapourtec™ E-series easy-Medchem 3-pump peristaltic flow reactor equipped with blue pump tubing compatible with the chosen solvents.
    c. Both reactors were fitted with standard 1/16” outer diameter and 1.0 mm inner diameter or 1/8” outer diameter and 1.5 mm inner diameter PTFE or SS tubing.
2. Coil reactors:
    a. PTFE/PFA coil reactors had a maximum operating temperature of 150 °C and maximum pressure of 362-psi (25 bar) with volumes of 10 or 14 mL (1/16” outer diameter and 1.0 mm inner diameter) and 25 or 52 mL (1/8” outer diameter and 1.5 mm inner diameter).
    b. Stainless-steel coil reactors had a maximum operating temperature of 260 °C and maximum pressure of 1000-psi (70 bar) with volumes of 2 and 20 mL (1/16” outer diameter and 1.0 mm inner diameter).

3. Packed bed reactors:
    a. Omnifit™ glass columns with enhanced PEEK adjustable end fittings and frits were used for packed bed column reactors. The columns had a maximum temperature of 150 °C and maximum pressure of 362-psi (25 bar) for the 10-mm inner diameter column reactor used.
    b. The volume of the columns was determined by packing the column with immobilized reagent and cotton at the ends of the column and sealing it with an end-cap. The column was further packed by flowing through the selected solvent until no air bubbles were observed. The column volume was determined via the difference between the dry and wet weights divided by the density of the solvent.
4. The column and coil reactors were heated using a Uniqsis™ HotCoil flow module that was fitted with the Uniqsis™ HotColumn housing for the columns and has operational temperature ranges from room temperature to 260 °C. A Uniqsis™ Polar Bear PLUS flow module was used for cooling with an operational temperature range of -40 °C to 150 °C.
5. Mixing chips:
    a. A 20 mL Uniqsis™ glass mixing chip was used for the ring-closing metathesis step with a maximum pressure rating of 10 bar
6. Static mixer:
    a. A 0.5 mL Vapourtec™ static mixer was used with maximum pressure rating of 362-psi (25 bar).
7. Cartridge-based back-pressure regulators (BPR) were used with pressures set to 3 bar, 8 bar and 20 barbased on application and they were fitted with chemically resistant perfluoropolymer or Hastelloy components.

5.1.2 Characterisation and purification

2. Purification: Isolated yields were obtained by performing column chromatography using Merck silica gel 60 (0.040–0.063 mm) as the stationary phase. Mobile phase eluents are indicated in in each experimental description.
3. Nuclear Magnetic Radiance (NMR) were performed using a Bruker Ultrashield AVANCE-III spectrometer.
    a. Splitting and multiplicity patterns are reported as singlet (s), doublet (d), doublet of doublet (dd), triplet (t), doublet of triplet (dt), quartet (q), multiplet (m) and broad singlet (bs). Coupling constants, J, were reported in Hertz (Hz). Chemical shifts δ, are reported in parts per million (ppm).

b. ^{1}H NMR were recorded at 300 and 400 MHz and chemical shifts were reported in the following order: chemical shift (δH, ppm); coupling constants (J, Hz); multiplicity; number or protons; proton assignment and all signals are referenced relative to deuterated chloroform ($CDCl_3$) at 7.27 ppm.
c. ^{13}C NMR were recorded at 75MHz and 101 MHz and chemical shifts were reported in the following order: chemical shift (δC, ppm); assignment and all signals are referenced relative to $CDCl_3$ at 77.36 ppm.

4. Thin Layer Chromatography (TLC)
   a. Reaction progress was monitored by TLC or HPLC.
   b. The reported retention factor (R_f) values were obtained from TLC analysis carried out on aluminium sheets pre-coated with silica (Merck Silica Gel 60 F254).
5. Fourier-transform Infrared (FTIR) spectroscopy was performed on a Bruker Alpha Platinum ATR spectrometer instrument.
   a. Functional group signals were reported as wavenumbers (cm^{-1}) in the range of 400 – 3000 cm^{-1}.
6. High-performance liquid chromatography (HPLC) analysis was performed with and Agilent Infinity model and 1260-diode-array dector (DAD, G7115 A).
   a. The injection volume was set to 2.0 µL and the column oven was set to 35 °C and DAD data were reported at wavelengths of 210 and 260 nm. An Agilent Poroshell 120 EC-C18 column (695975-902, 100 × 4.6 mm inner diameter, 2.7-µm particles) was used.
   b. Samples were prepared using analytical grade acetonitrile to approximate concentrations relating to each method.
7. High-resolution mass spectra (HRMS) were recorded on a Waters Synapt G2 Mass Spectrometer at 70 eV and 200 mA.
   a. For analysis, the instrument was operated under the following conditions: a capillary voltage of 2.8 kV (positive mode), a sampling cone (ramped from 20 V – 40 V), an extraction cone of 4 V, a source temperature of 100 °C, a desolvation temperature of 200 °C, cone gas of 100 $L.h^{-1}$, desolvation gas of 500 $L.h^{-1}$, inert gas source: nitrogen.
   b. Samples were prepared in analytical grade acetonitrile to an approximate concentration of 10 $µg.mL^{-1}$.

5.1.3 Nomenclature

1. Compound were named according to IUPAC nomenclature and ChemDraw Ultra 12.0 was used for naming, and numbering was chosen as a matter of convenience
2. NMR spectrums were analyzed using MestreNova 12.0

5.2 Experimental

5.2.1 Isovanillin 17 (Starting material)

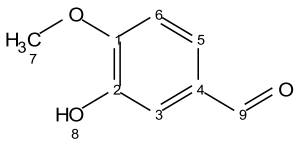

17

Rf = 0.20 (25% ethyl acetate/hexane); **^{1}H NMR (400 MHz, Chloroform-d)** δ 9.82 (s, 1H, H_9), 7.41 (dq, J = 4.1, 2.0 Hz, 2H, H_5,H_3), 6.96 (d, J = 8.7 Hz, 1H, H_6), 5.92 (s, 1H, H_8), 3.97 (s, 3H, H_7), 2.97 ($DMSO_2$, internal standard); **IR V_{max}/cm^{-1}** 3184 (O-H stretch), 2843 (C-H stretch), 1668 (C=O stretch), 1574, 1508, 1243 (C-H bend), 1113 (C-O stretch), 825, 581.

5.2.2 First Allylation: 3-(Allyloxy)-4-methoxybenzaldehyde 19

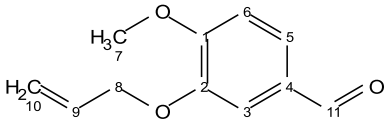

19

5.2.2.1 Batch method using potassium carbonate

Isovanillin **17** (10.05 g, 66.07 mmol, 1.0 equiv.), and allyl bromide **18** (11.45 mL, 132.31 mmol, 2.0 equiv.) were added to a stirring solution of potassium carbonate (22.80 g, 164.94 mmol, 2.5 equiv.) in dimethylformamide (0.50 M, 132.00 mL). The reaction was heated to 60 °C and stirred for 20 hours under argon, then cooled to room temperature and filtered through a celite pad. The residue was then extracted with aqueous sodium hydroxide (3.00 M, 30 mL) and dichloromethane (3 × 30 mL). The organic layers were combined and dried with sodium sulphate, filtered and concentrated *in vacuo* to obtain 3-(allyloxy)-4-methoxybenzaldehyde **19**, as a dark yellow oil (10.43 g, 82 %). **Rf** = 0.53 (25% ethyl acetate/hexane); **^{1}H NMR (300 MHz, Chloroform-d)** δ 9.70 (s, 1H, H_{11}), 7.37 – 7.23 (m, 2H, H_5, H_3), 6.85 (d, J = 8.2 Hz, 1H, H_6), 6.06 – 5.86 (ddt, J = 20.90, 14.22, 14.22 Hz, 1H, H_9), 5.31 (dd, J = 17.3, 1.6 Hz, 1H, H_{10b}), 5.18 (dd, J = 10.5, 1.4 Hz, 1H, H_{10a}), 4.52 (dt, J = 5.4, 1.5 Hz, 2H, H_8), 3.81 (s, 3H, H_7). **^{13}C NMR (101 MHz, Chloroform-d)** δ 190.60 (C=O, C_{11}), 154.59 (C_1), 148.24 (C_2), 132.36 (C_9), 129.72 (C_4), 126.54 (C_5), 118.21 (C_{10}), 110.64 (C_3), 110.52 (C_6), 69.40 (C_8), 55.88 (C_7); **IR V_{max}/cm^{-1}** 2936 (C-H stretch), 2839 (C-H stretch),

1682 (C=O stretch), 1586, 1508, 1433 (C-H bend), 1261, 1127, 1012 (C-O stretch), 806, 636.; **HRMS m/z (ES+)** 193.1040 **[M+H]$^+$** ($C_{11}H_{12}O_3$ requires 192.211 g.mol^{-1})

5.2.2.2 Batch method using potassium hydroxide solution

Potassium hydroxide (0.28 g, 4.99 mmol, 1.5 equiv.) was added to methanol: water (0.40 M, 8.21 mL, 70:30) and allowed to stir for 5 minutes. Isovanillin **17** (0.50 g, 3.23 mmol, 1.0 equiv.) and allyl bromide **18** (0.53 mL, 6.12 mmol,1.85 equiv.) was added to the solution and heated to 70 °C for 20 hours. After 20 hours the reaction was cooled to room temperature the solvent was removed *in vacuo*, and the residue was then extracted with aqueous sodium hydroxide (3.00 M, 30 mL) and dichloromethane (3 × 30 mL). The organic layers were combined and dried with sodium sulphate, filtered and concentrated *in vacuo* to obtain 3-(allyloxy)-4-methoxybenzaldehyde **19** as a dark yellow oil (0.49 g, 78 %).

5.2.2.3 Flow method using potassium carbonate

a. Preparation of stock solution using potassium carbonate

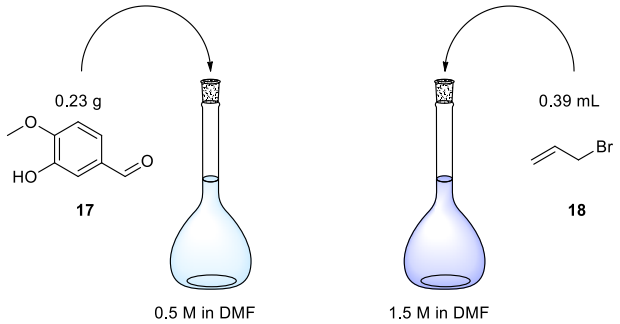

A 0.50 M stock solution of isovanillin **17** was prepared by the dissolution of **17** (0.23 g, 1.50 mmol, 1.0 equiv.) in dimethylformamide to a total volume of 3 mL and a 1.5 M stock solution of allyl bromide **18** was prepared by dissolution of **18** (0.39 mL, 4.50 mmol, 3.0 equiv.) in dimethylformamide to a total volume of 3 mL.

b. Uniqsis^{TM} binary pump reactor setup

Stock solutions were prepared as described above. The Uniqsis^{TM} binary pump reactor was plumbed with two Uniqsis^{TM} 10 mm columns and a 8 bar BPR (Scheme 15). The two columns were packed with crushed potassium carbonate (6.40 g, 46.34 mmol, 3.0 equiv.) and their volumes were determined as 3.20 mL and 3.59 mL respectively. A total flow rate of 0.227 mL.min^{-1} was used to introduce 1.56 mL of each stock from the stock reservoir into the flow system. Dimethylformamide was used as a pushing solvent. The solutions were

combined at the T-piece mixer and pumped through the packed columns held at 100 °C (T_R = 30 min).The solutions was collected, and solvent was removed and processed according to batch method to obtain 3-(allyloxy)-4-methoxybenzaldehyde **19** as a dark yellow oil (92 % from LC conversion).

5.2.2.4 Flow method using potassium hydroxide

a. Preparation of stock solution using potassium hydroxide

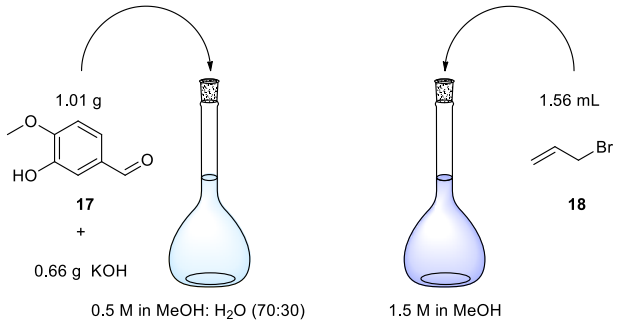

A 0.50 M stock solution of isovanillin **17** was prepared by dissolution of **17**(1.01 g, 6.64 mmol, 1.0 equiv.) and potassium hydroxide (0.66 g, 11.76 mmol, 1.8 equiv.) in methanol:water (13.14 mL of 70:30). A 1.00 M stock solution of allyl bromide **18** was prepared by dissolution of **18** (1.56 mL, 18.03 mmol, 2.0 equiv.) in methanol (16.40 mL).

b. Uniqsis^{TM} binary pump reactor setup and description

Stock solutions were prepared as described above. The Uniqsis^{TM} binary pump reactor was used with a 25.00 mL (1.5 mm inner diameter) coil (Scheme 16). A total flow rate of 1.67 mL.min^{-1} was used to introduce 13.14 mL of each stock from the stock reservoir into the flow system. methanol:water (70:30) was used as a pushing solvent. The solutions were combined at the T-piece mixer and pumped through a static mixer at room temperature and a coil reactor held at 80 °C (T_R = 15 min) with an 8-bar BPR. The solutions was collected, and HPLC analysis was performed before solvent was removed processed according to batch method to obtain 3-(allyloxy)-4-methoxybenzaldehyde **19** as a dark yellow oil (1.12 g, 88%).

5.2.3 Claisen Rearrangement: 2-Allyl-3-hydroxy-4-methoxybenzaldehyde 20

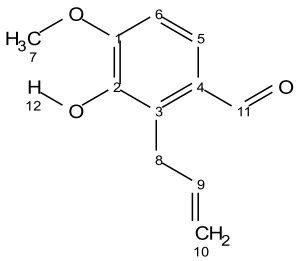

20

5.2.3.1 Batch method

3-(Allyloxy)-4-methoxybenzaldehyde **19** (2.02 g, 10.51 mmol, 1.0 equiv.) was dissolved in toluene (0.25 M, 42.00 mL) and was allowed to reflux for 72 hours at 120 °C. After 72 hours the reaction was cooled to room temperature the solvent was removed *in vacuo* to obtain 2-allyl-3-hydroxy-4-methoxybenzaldehyde **20** as a dark brown oil (6.9 % by qNMR analysis).

5.2.3.2 Flow method

a. Preparation of stock solution

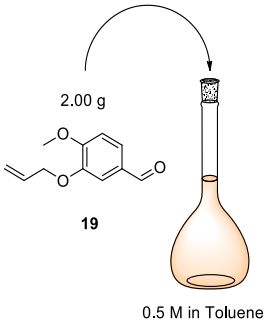

A 1.00 M stock solution of 3-(allyloxy)-4-methoxybenzaldehyde **19** was prepared by dissolution of **19** (2.00 g, 10.04 mmol, 1.0 equiv.) in toluene to a total volume of 10 mL.

b. Uniqsis^{TM} binary pump reactor setup and description

Stock solutions were prepared as described above. The Uniqsis^{TM} binary pump reactor was used with a 20.00 mL (1.0 mm inner diameter) stainless steel coil and a 2.00 mL (1.0 mm inner diameter) stainless steel cooling coil (Scheme 24). A total flow rate of 0.67 mL.min^{-1} was used to introduce 20.0 mL of the stock solution from the stock reservoir into the flow system. Toluene was used as a pushing solvent. The solution was pumped through a

stainless-steel coil reactor held at 240 °C (T_R = 30 min) and a cooling coil held at 0 °C with an 20-bar BPR. The solution was collected, and the solvent was removed *in vacuo* to remove the toluene to obtain 2-allyl-3-hydroxy-4-methoxybenzaldehyde **20** as a dark brown oil (1.99 g, 99 %) **Rf** = 0.44 (25% ethyl acetate/hexane) **^{1}H NMR (300 MHz, Chloroform-d)** δ 10.05 (s, 1H, H_{11}), 7.43 (d, J = 8.5 Hz, 1H, H_5), 6.87 (d, J = 8.5 Hz, 1H, H_6), 6.12 – 5.98 (ddt, J= 17.13, 16.08, 12.07 Hz, 1H, H_9), 5.90 (br s, 1H, H_{12}), 5.01 (dd, *J* = 6.2, 1.7 Hz, 1H, H_{10b}), 5.00 – 4.90 (dd, 1H, H_{10a}), 3.96 (s, 3H, H_7), 3.87 (dt, J = 6.0, 1.7 Hz, 2H, H_8). **^{13}C NMR (101 MHz, Chloroform-d)** δ 191.64 (C=O, C_{11}), 150.94 (C_1), 143.88 (C_2), 136.32 (C_9), 128.21 (C_4), 127.61 (C_3), 125.55 (C_5), 115.37 (C_{10}), 108.19 (C_6), 56.15 (C_7), 28.44 (C_8); **IR V_{max}/cm^{-1}** 3354 (O-H stretch), 2849 (C-H stretch), 1671 (C=O stretch), 1584, 1277(C-H bend), 1241, 1192, 1078 (C-O stretch), 790; **HRMS m/z (ES+)** 193.1040 **[M+H]$^+$** ($C_{11}H_{12}O_3$ requires 192.211 g.mol^{-1}).

5.2.4 Alcohol Protection: 2-Allyl-3-isopropoxy-4-methoxybenzaldehyde 22

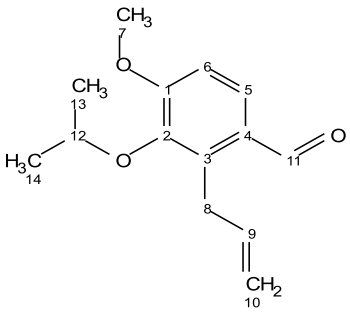

22

5.2.4.1 Batch method

2-Allyl-3-hydroxy-4-methoxybenzaldehyde **20** (9.02 g, 46.94 mmol, 1.0 equiv.) was added to a stirring solution of potassium carbonate (16.21 g, 117.29 mmol, 2.5 equiv.) and 2-bromopropane **21** (11.01 mL, 117.27 mmol, 2.5 equiv.) in dimethylformamide (0.50 M, 94.00 mL). The solution was stirred for 20 hours under argon atmosphere at 60 °C. After 20 hours the reaction was cooled to room temperature was filtered through a celite pad. The solvent was removed under a flow of compressed air, and the residue was then extracted with aqueous sodium hydroxide (3.00 M, 30 mL) and dichloromethane (3 × 30 mL). The organic layers were combined and dried with sodium sulphate, filtered and concentrated *in vacuo* to obtain 2-allyl-3-isopropoxy-4-methoxybenzaldehyde**22**, as a light brown oil (8.59 g, 78 %). **Rf** = 0.67 (25% ethyl acetate/hexane); **^{1}H NMR (300 MHz, Chloroform-d)** δ 10.06 (s, 1H, H_{11}), 7.62 (d, J = 8.6 Hz, 1H, H_5), 6.89 (d, J = 8.6 Hz, 1H, H_6), 5.99 (ddt, J = 17.2, 10.2, 5.7 Hz,

1H, H_9), 5.00 (dd, *J* = 10.2, 1.7 Hz, 1H, H_{10b}), 4.89(dd, J=17.2, 1.8 Hz 1H, H_{10a}), 4.49 (sept, J = 6.2 Hz, 1H, H_{12}), 3.90 (s, 3H, H_7), 3.87 (dt, J = 5.7, 1.9 Hz, 2H, H_8), 1.27 (d, J = 6.2 Hz, 6H, H_{14}, H_{13}).**^{13}C NMR (101 MHz, Chloroform-d)** δ 191.06 (C=O, C_{11}), 157.60 (C_1), 144.94(C_2), 137.14(C_9), 136.36 (C_3), 128.14 (C_4), 128.02 (C_5), 115.57 (C_{10}), 109.67 (C_6), 74.90 (C_{12}), 55.68 (C_7), 29.00 (C_8), 22.53 (C_{14}, C_{13}); **IR V_{max}/cm^{-1}** 2975, 2846, 2723 (C-H stretch), 1684 (C=O stretch), 1581, 1440 (C-H bend), 1275, 1077 (C-O **stretch), 912, 808; HRMS m/z (ES+)** 235.1351 **[M+H]$^+$** ($C_{14}H_{18}O_3$ requires 234.29 g.mol^{-1}).

5.2.4.2 Flow method

a. Preparation of stock solution

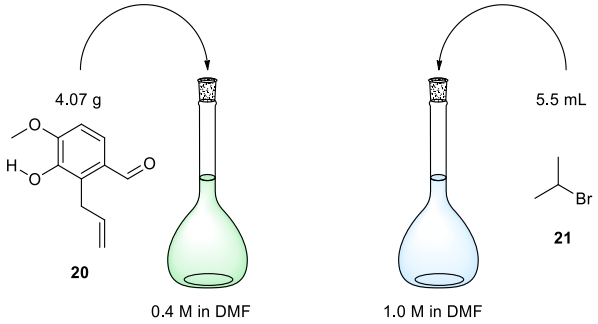

A 0.40 M stock solution of 2-allyl-3-hydroxy-4-methoxybenzaldehyde **20** was prepared by the dissolution of **20** (4.07 g, 21.17 mmol, 1.0 equiv.) in dimethylformamide to a total volume of 50 mL, and a 1.00 M stock solution of 2-bromopropane **21** was prepared by dissolution of **21** (5.50 mL, 58.53 mmol, 2.5 equiv.) in dimethylformamide to a total volume of 50 mL.

b. Uniqsis^{TM} binary pump reactor setup and description

Stock solutions were prepared as described above. The Uniqsis^{TM} binary pump reactor was used with two Uniqsis^{TM} 10 mm columns and an 8 bar BPR (Scheme 27). The two columns were packed with crushed potassium carbonate (8.09 g, 58.52 mmol, 2.5 equiv.) and their total volume was determined to be 8.72 mL. A total flow rate of 0.436 mL.min^{-1} was used to introduce 56.00 mL of each stock from the stock reservoir into the flow system. Dimethylformamide was used as a pushing solvent. The solutions were combined at the T-piece mixer and pumped through the packed columns held at 80 °C (T_R = 20 min).The solutions were collected, and solvent was removed and processed according to batch method to obtain 2-allyl-3-isopropoxy-4-methoxybenzaldehyde**22** as a light brown oil (4.37 g, 88%).

5.2.5 Aldehyde Reduction: (2-Allyl-3-isopropoxy-4-methoxyphenyl)methanol 23

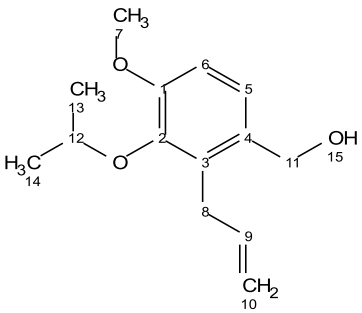

23

5.2.5.1 Batch method using sodium bis(2-methoxyethoxy)aluminum dihydride (Red-Al, 60% in toluene)

Red-Al (60% in toluene, 15.62 mL, 73.85 mmol, 2.5 equiv.) was added dropwise to a stirring solution of 2-allyl-3-isopropoxy-4-methoxybenzaldehyde**22** (4.50 g, 19.21 mmol, 1.0 equiv.) in toluene (0.15 M, 128.00 mL) under argon at 15-20 °C. The solution was left for 20 hours under inert conditions while stirring. The reaction was quenched by adding 10% aqueous sodium hydroxide while stirring for 30 minutes. The solvent was removed *in vacuo*, and the residue was then extracted with water (30 mL) and dichloromethane (3 × 30 mL). The organic layers were combined and dried with magnesium sulphate, filtered and concentrated *in vacuo* to obtain (2-allyl-3-isopropoxy-4-methoxyphenyl)methanol **23** as a dark yellow oil (3.47 g, 76 %). The method was repeated using the same conditions while varying the reducing agent and solvent. **Rf** = 0.46 (25% ethyl acetate/hexane); **^{1}H NMR (300 MHz, Chloroform-d)** δ 7.03 (d, J = 8.4 Hz, 1H, H_5), 6.75 (d, J = 8.4 Hz, 1H, H_6), 5.95 (ddt, J = 17.1, 10.2, 5.8 Hz, 1H, H_9), 5.02 – 4.95 (dd, 1H, H_{10b}), 4.88 (dd, J=1.9 hz, 1H, H_{10a}), 4.55 (br s, 2H, H_{11}), 4.48 (sept, J = 6.2 Hz, 1H, H_{12}), 3.80 (s, 3H, H_7), 3.53 (dt, J = 5.9, 1.8 Hz, 2H, H_8), 2.22 (br s, 1H, H_{15}), 1.25 (d, J = 6.2 Hz, 6H, H_{14} & H_{13}).**^{13}C NMR (75 MHz, Chloroform-d)** δ 152.39 (C_1), 144.96 (C_2), 137.58 (C_9), 132.41 (C_4), 132.12 (C_3), 123.76 (C_5), 114.98 (C_{10}), 109.98 (C_6), 74.61, (C_{12}), 62.91(C_{11}), 55.63, (C_7), 30.54 (C_8),22.64 (C_{14} & C_{13}); **IR V_{max}/cm^{-1}** 3380 (O-H stretch), 2973, 2934 (C-H stretch), 1601, 1485, 1435(C-H bend), 1267, 1081 (C-O stretch), 985, 911, 803; **HRMS m/z (ES+)** 219.1538 **[M-OH]$^+$** ($C_{14}H_{20}O_3$ requires 236.31 g.mol^{-1}).

5.2.5.2 Flow method using polymer supported sodium borohydride

a. Preparation of stock solution

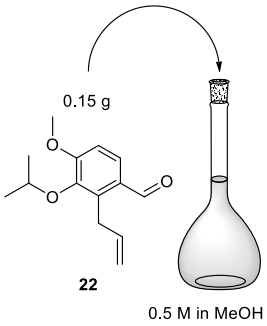

Stock solution of 0.50 M of 2-allyl-3-isopropoxy-4-methoxybenzaldehyde**22** was prepared by dissolution of **22** (0.15 g, 0.63 mmol, 1.0 equiv.) in methanol (1.25 mL).

b. Uniqsis^{TM} binary pump reactor setup and description

Stock solutions were prepared as described above. The Uniqsis^{TM} binary pump reactor was used with one Uniqsis^{TM} 10 mm column and an 8 bar BPR (Scheme 32). The column was packed with polymer supported sodium borohydride and its volumes was determined to be 4.00 mL. A total flow rate of 0.089 mL.min^{-1} was used to introduce 1.28 mL of stock from the stock reservoir into the flow system. Methanol was used as a pushing solvent. The solutions were pumped through the packed column held at room temperature (T_R = 45 min).The solution was collected and HPLC analysis was performed before the solvent was removed *in vacuo* and processed according to batch method to obtain (2-allyl-3-isopropoxy-4-methoxyphenyl)methanol **23** as a dark yellow oil (0.11 g, 68 %).

5.2.5.3 Flow method using sodium borohydride solution

a. Preparation of stock solution

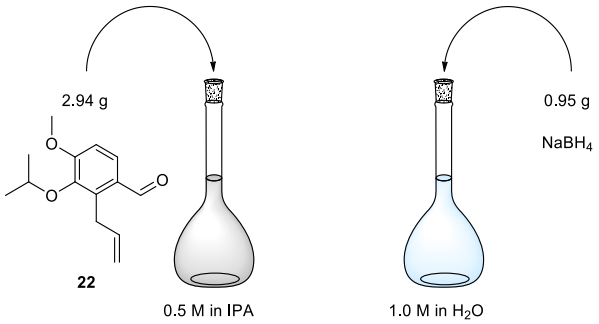

Stock solution of 0.50 M of 2-allyl-3-isopropoxy-4-methoxybenzaldehyde**22** was prepared by dissolution of **22** (2.94 g, 12.53 mmol, 1.0 equiv.) in IPA to a total volume of 25 mL and stock solution of 1.0 M of $NaBH_4$ was prepared by dissolution of $NaBH_4$ (0.95 g, 25.06 mmol, 2.0 equiv.) in water to a total volume of 25 mL.

b. Vapourtec™ peristaltic pump reactor setup and description

Stock solutions were prepared as described above. The Vapourtec™ easy-MedChem E-series peristaltic pump reactor was used with a 3 bar BPR (Scheme 34). A total flow rate of 1.25 mL.min^{-1} was used to introduce 25.00 mL of each stock from the stock reservoir into the flow system. IPA was used as a pushing solvent. The solutions were combined at the T-piece mixer and pumped through a 0.50 mL static mixer at room temperature and a coil reactor held at room temperature (T_R = 20 min).The solution was collected in 5.00 mL saturated $NaHCO_3$ and water and HPLC analysis was performed before solvent was removed *in vacuo* and processed according to batch method to obtain(2-allyl-3-isopropoxy-4-methoxyphenyl)methanol **23** as a dark yellow oil (2.53 g, 85 %).

5.2.6 Second Allylation: 2-Allyl-1-((allyloxy)methyl)-3-isopropoxy-4-methoxybenzene 24

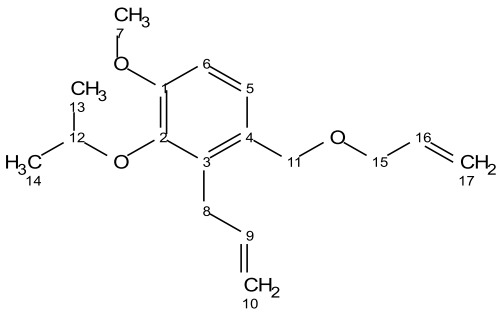

24

5.2.6.1 Batch Procedure

(2-Allyl-3-isopropoxy-4-methoxyphenyl)methanol **23** (1.70 g, 7.21 mol, 1.0 equiv.) was added to a solution of sodium hydride pre-washed with hexane to remove mineral oil (0.72 g, 30.03 mmol, 2.5 equiv., 60% dispersion in mineral oil) and tetrahydrofuran (0.15 M, 50.00 mL) under argon atmosphere. Allyl bromide **18** (1.56 mL, 18.02 mmol, 2.5 equiv.) was added dropwise to the reaction mixture at 15-20 °C and left to reflux for 20 hours while stirring. The reaction was quenched with 10% sodium hydroxide while continuously stirring for 30 minutes. The solvent was removed *in vacuo* and the residue was then extracted with water

(30 mL) and dichloromethane (3 × 30 mL). The organic layers were combined and dried with magnesium sulphate, filtered and concentrated *in vacuo* to obtain 2-allyl-1-((allyloxy)methyl)-3-isopropoxy-4-methoxybenzene **24** as a light yellow oil (1.69 g, 85%). **Rf** = 0.88 (25% ethyl acetate/hexane); **^{1}H NMR (300 MHz, Chloroform-d)** δ 7.03 (d, J = 8.3 Hz, 1H, H_5), 6.74 (d, J = 8.4 Hz, 1H, H_6), 5.94 (ddt, *J* = 12.80, 8.56, 5.86 Hz, 1H, H_9), 5.91 (ddt, J = 9.86, 7.53, 6.30 Hz, 1H, H_{16}), 5.35 – 5.23 (dd, 1H, H_{17b}), 5.28 (dd, *J* = 17.2, 1.7 Hz, 1H, H_{17a}), 5.18 (dd, *J* = 10.2, 1.4 Hz, 1H, H_{10a}), 4.96 (dd, *J* = 9.2 Hz, 1H, H_{10b}), 4.58 – 4.38 (sept, 1H, H_{12}), 4.44 (s, 2H, H_{11}), 3.99 (dt, J = 5.7, 1.4 Hz, 2H, H_{15}), 3.80 (s, 3H, H_7), 3.54 (dt, J = 6.0, 1.8 Hz, 2H, H_8), 1.26 (d, J = 6.2 Hz, 6H, H_{13} & H_{14}).**^{13}C NMR (75 MHz, Chloroform-d)** δ 152.54 (C_1), 145.10 (C_2), 136.91 (C_9), 134.97 (C_{16}), 132.83 (C_3), 129.57 (C_4), 124.42 (C_5), 116.94 (C_{17}), 114.77 (C_{10}), 109.70 (C_6), 74.43 (C_{12}), 71.06 (C_{11}), 70.08 (C_{15}), 55.54 (C_7), 30.63 (C_8), 22.62 (C_{14} & C_{13}); **IR V_{max}/cm^{-1}** 2971 (C-H stretch), 2927, 2855, 1486, 1437 (C-H bend), 1270, 1080 (C-O stretch), 913, 803; **HRMS m/z (ES+)** 276.1749 **[M+H]$^+$** ($C_{17}H_{24}O_3$ requires 276.3739 g.mol^{-1}).

5.2.6.2 Flow method

a. Preparation of stock solution

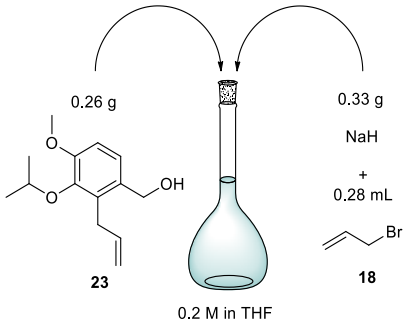

Stock solution of 0.2 M of (2-allyl-3-isopropoxy-4-methoxyphenyl)methanol **23** was prepared by dissolution of **23** (0.26 g, 1.10 mmol, 1.0 equiv.), sodium hydride (0.33 g, 13.57 mmol, 7.5 equiv., 60% dispersion in mineral oil) and allyl bromide **18** (0.28 mL, 3.26 mmol, 3.0 equiv.) in tetrahydrofuran to a total volume of 5.5 mL with continuous stirring under nitrogen atmosphere.

b. Vaportec peristaltic reactor setup and description

Stock solutions were prepared as described above. The Vapourtec™ easy-MedChem E-series peristaltic pump reactor was used with 1.5 mm inner diameter tubing for the sodium hydride slurry and using a 10.00 mL coil reactor. One of the peristaltic pumps was used as a

BPR and the pressure was adjusted to 10 bar (Scheme 41). The reactor was purged with dried tetrahydrofuran. A total flow rate of 0.50 mL.min^{-1} was used to introduce 5.43 mL of stock from the stock reservoir into the flow system. Tetrahydrofuran was used as a pushing solvent. The solutions were mixed at the static mixer at room temperature and was pumped through a coil reactor held at 100 °C (T_R = 20 min).The solution was collected in the reagent reservoir and were allowed to cycle through the reaction path for the required number of cycles before collection into 2.00 mL water. HPLC analysis was performed before solvent was removed *in vacuo* and processed according to batch method to obtain 2-allyl-1-((allyloxy)methyl)-3-isopropoxy-4-methoxybenzene **24** as a light yellow oil (0.21 g, 69%).

5.2.7 RCM: (*Z*)-7-isopropoxy-8-methoxy-3,6-dihydro-1*H*-benzo[*c*]oxocine 25

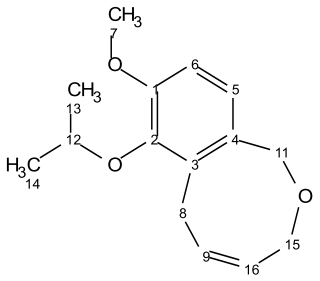

25

5.2.7.1 Batch Procedure

To a solution of 2-allyl-1-((allyloxy)methyl)-3-isopropoxy-4-methoxybenzene **24** (0.28 g, 1.00 mmol, 1.0 equiv.) in degassed toluene (0.012 M, 83.00 mL) was added Grubbs II catalyst (0.042 g, 0.050 mmol, 0.05 equiv.) and the reaction was stirred at 60 °C under an argon atmosphere for 2 hours. The solution was cooled, and the solvent was removed *in vacuo*. The reaction mixture was purified via column chromatography (10 % ethyl acetate/Hexane) to obtain a clear oil of (*Z*)-7-isopropoxy-8-methoxy-3,6-dihydro-1*H*-benzo[*c*]oxocine **25** as a colorless oil (0.012g, 46 %) **Rf** = 0.70 (10% ethyl acetate/hexane); **^{1}H NMR (300 MHz, Chloroform-d)** δ 6.82 (d, J = 8.3 Hz, 1H, H_5), 6.71 (d, J = 8.3 Hz, 1H, H_6), 6.03 – 5.87 (m, 1H, H_9), 5.68 – 5.61 (dt, J = 10.5, 5.1 Hz, 1H, H_{16}), 4.80 (s, 2H, H_{11}), 4.42 (sept, J = 6.2 Hz, 1H, H_{12}), 4.15 (d, J = 5.0 Hz, 2H, H_{15}), 3.82 (s, 3H, H_7), 3.74 (d, J = 7.2 Hz, 2H, H_8), 1.29 (d, J = 6.1 Hz, 6H, H_{13} & H_{14}) ; **^{13}C NMR (75 MHz, Chloroform-d)** δ 152.80 (C_1), 144.34 (C_2), 133.59 (C_4), 131.72 (C_3), 130.07 (C_9), 127.91 (C_{16}), 123.69 (C_5), 109.51 (C_6), 74.81 (C_{12}), 72.18 (C_{11}), 66.27 (C_{15}), 55.75 (C_7), 29.71 (C_8), 22.58 (C_{14} & C_{13}); **HRMS m/z (ES+)** 249.14 **[M+H]$^+$** ($C_{15}H_{20}O_3$ requires 248.14 g.mol^{-1}).

5.2.7.2 Flow procedure

a. Preparation of stock solution

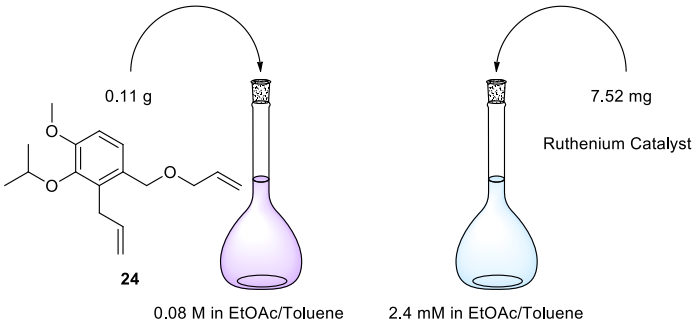

Stock solution of 0.08 M of 2-allyl-1-((allyloxy)methyl)-3-isopropoxy-4-methoxybenzene **24** was prepared by dissolution of **24** (0.11 g, 0.4 mmol, 1.0 equiv.) in toluene/ethyl acetate to a total volume of 5 mL and a 2.4 mM stock solution of catalysts (3 mol %) in toluene/ethyl acetate to a total volume of 5 mL.

b. Uniqsis^{TM} binary pump reactor setup and description

Stock solutions were prepared as described above. The Uniqsis^{TM} binary pump reactor was used with 2.00 mL sample loops. A total flow rate of 0.44 – 1.33 mL.min^{-1} was used to inject 2.00 mL of each stock from the sample loops into the flow system. Toluene/ethyl acetate was used as a pushing solvent. The solutions were pumped through a 20.00 mL glass mixing chip reactor held between 60 - 90 °C (T_R = 15 - 45 min) using a 4 bar BPR (Scheme 46).The solution was collected in the reagent reservoir and HPLC analysis was performed before solvent was removed *in vacuo* and processed according to batch method to obtain (*Z*)-7-isopropoxy-8-methoxy-3,6-dihydro-1*H*-benzo[*c*]oxocine **25** as a colorless oil.

Analysis of compound 19, 20, 22, 23, 24 and 25 corresponded with literature results obtained van Otterlo and co-workers.[34]

References

1 A. M. Sobolewska, *New Generic Synthetic Protocols for Pharmaceutical Intermediates Based on Continuous Flow Multifunctional Platforms*, 2014.

2 Andrew Mansfield, The evolution of flow chemistry and Syrris – which came first, the chicken or the egg?

3 F. Fanelli, G. Parisi, L. Degennaro and R. Luisi, *Beilstein Journal of Organic Chemistry*, 2017, 13, 520–542.

4 E. Riva, *Doctorate School of Chemical Sciences and Technologies Course in Chemical Sciences CHIM 06, XXIII Cycle Flow chemistry applied to the preparation of small molecules potentially useful as therapeutic agents*, 2009.

5 R. Porta, M. Benaglia and A. Puglisi, *Org Process Res Dev*, 2016, 20, 2–25.

6 M. B. Plutschack, B. Pieber, K. Gilmore and P. H. Seeberger, *Chem Rev*, 2017, 117, 11796–11893.

7 M. Guidi, P. H. Seeberger and K. Gilmore, *Chem Soc Rev*, 2020, 49, 8910–8932.

8 M. J. Nieves-Remacha, A. A. Kulkarni and K. F. Jensen, Hydrodynamics of liquid-liquid dispersion in an advanced-flow reactor, *Ind Eng Chem Res*, 2012, **51**, 16251–16262.

9 N. Neyt, J. Jugmohan, W. Bonnet, J. L. Panayides and D. Riley, in *Mechanochemistry and Emerging Technologies for Sustainable Chemical Manufacturing*, CRC Press, 2023, pp. 261–287.

10 L. Malet-Sanz and F. Susanne, *J Med Chem*, 2012, 55, 4062–4098.

11 D. Cortés-Borda, E. Wimmer, B. Gouilleux, E. Barré, N. Oger, L. Goulamaly, L. Peault, B. Charrier, C. Truchet, P. Giraudeau, M. Rodriguez-Zubiri, E. Le Grognec and F. X. Felpin, An Autonomous Self-Optimizing Flow Reactor for the Synthesis of Natural Product Carpanone, *Journal of Organic Chemistry*, 2018, **83**, 14286–14289.

12 S. H. Lau, *Organic Synthesis: Taming Chemistry using Enabling Technologies A dissertation presented by Statement of Length*, 2017.

13 A. R. Bogdan and A. W. Dombrowski, *J Med Chem*, 2019, 62, 6422–6468.

14 S. G. Newman and K. F. Jensen, *Green Chemistry*, 2013, 15, 1456–1472.

15 D. Dallinger and C. O. Kappe, *Curr Opin Green Sustain Chem*, 2017, 7, 6–12.

16 R. J. Ingham, J. College, J. Lane and L. Group, *Control tools for flow chemistry processing and their application to the synthesis of bromodomain inhibitors A thesis presented by*, 2014.

17 P. Bana, R. Örkényi, K. Lövei, Á. Lakó, G. I. Túrós, J. Éles, F. Faigl and I. Greiner, The route from problem to solution in multistep continuous flow synthesis of pharmaceutical compounds, *Bioorg Med Chem*, 2017, **25**, 6180–6189.

18 C. Holtze and R. Boehling, *Curr Opin Chem Eng*, 2022, 36.

19 S. D. Schaber, D. I. Gerogiorgis, R. Ramachandran, J. M. B. Evans, P. I. Barton and B. L. Trout, *Ind Eng Chem Res*, 2011, 50, 10083–10092.

20 N. C. Neyt and D. L. Riley, *React Chem Eng*, 2021, 6, 1295–1326.

21 E. M. Williamson, Z. Sun, L. Mora-Tamez and R. L. Brutchey, Design of Experiments for Nanocrystal Syntheses: A How-To Guide for Proper Implementation, *Chemistry of Materials*, 2022, **34**, 9823–9835.

22 P. M. Murray, F. Bellany, L. Benhamou, D. K. Bučar, A. B. Tabor and T. D. Sheppard, *Org Biomol Chem*, 2016, 14, 2373–2384.

23 S. Weissman, S. A. Weissman and N. G. Anderson, *Design of Experiments (DoE) and Process Optimization. A Review of Recent Publications. Design of Experiments (DoE) and Process Optimization. A Review of Recent Publications*, 2014.

24 R. Carlson and J. E. Carlson, Eds., in *Data Handling in Science and Technology*, Elsevier, 2005, vol. 24, pp. 15–25.

25 S. Weissman, S. A. Weissman and N. G. Anderson, *Design of Experiments (DoE) and Process Optimization. A Review of Recent Publications. Design of Experiments (DoE) and Process Optimization. A Review of Recent Publications*, 2014.

26 R. Carlson, in *Data Handling in Science and Technology*, ed. R. Carlson, Elsevier, 1992, vol. 8, pp. 89–122.

27 N. Holmes, *Self-Optimisation of Automated Continuous Reactors*, 2017.

28 *Other designs for screening experiments 7.1 Redundancy can be expensive*, .

29 H. Venkatachalam, N. Venkatesh and A. Kumar, *The Oxygen-Containing Fused Heterocyclic Compounds*, 200AD.

30 M. Suffness, *Chapter 32. Taxol: From Discovery to Therapeutic Use*, 1993.

31 S. Chen, T. Khusial, D. Patel, S. Singh, T. Yakubova, A. Wang and T. Nguyen, Digoxin use in modern medicine, *U.S. Pharmacist*, 2015, **40**, 44–48.

32 J. M. Henwood, R. C. Heel and P. A. Edwards, *Drug Evaluation Lovastatin A Preliminary Review of its Pharmacodynamic Properties and Therapeutic Use in Hyperlipidaemia*, .

33 L. Gavin Madeley, *Synthesis of benzo-fused heterocycles using isomerization and ring-closing metathesis reactions*, 2010.

34 R. Pathak, J.-L. Panayides, T. D. Jeftic, C. B. De Koning and W. A. L. Van Otterlo, *The Synthesis of 5-, 6-, 7-and 8-Membered Oxygen-containing Benzo-fused Rings using Alkene Isomerization and Ring-closing Metathesis Reactions*, .

35 B. C.-A. Nkeh and D. Njamen, *Anti-inflammatory and analgesic effects of drypemolundein A 27*, 2003.

36 J.-L. Panayides, *Investigations into the use of Ring Closing Metathesis to form 5-, 6-, 7-and 8-membered benzo-fused heterocycles*, 2005.

37 J. Nowicki, Claisen, Cope and Related Rearrangements in the Synthesis of Flavour and Fragrance Compounds, *Molecules*, 2000, **5**, 1033–1050.

38 D. S. Tarbell, *THE CLAISEN REARRANGEMENT*, .

39 J. J. Gajewski, *The Claisen Rearrangement. Response to Solvents and Substituents: The Case for Both Hydrophobic and Hydrogen Bond Acceleration in Water and for a Variable Transition State*, 1997.

40 C. O. Kappe, *Angewandte Chemie - International Edition*, 2004, 43, 6250–6284.

41 H. Egami, S. Tamaoki, M. Abe, N. Ohneda, T. Yoshimura, T. Okamoto, H. Odajima, N. Mase, K. Takeda and Y. Hamashima, Scalable Microwave-Assisted Johnson-Claisen Rearrangement with a Continuous Flow Microwave System, *Org Process Res Dev*, 2018, **22**, 1029–1033.

42 I. R. Baxendale, A. L. Lee and S. V. Ley, A concise synthesis of carpanone using solid-supported reagents and scavengers, *J Chem Soc Perkin 1*, 2002, **2**, 1850–1857.

43 C. P. Casey, *2005 Nobel Prize in Chemistry. Development of the Olefin Metathesis Method in Organic Synthesis*, 2006, vol. 83.

44 R. R. Schrock, *Advanced information on the Nobel Prize in Chemistry: Development of the metathesis method in organic synthesis*, 2005.

45 D. Astruc, *New Journal of Chemistry*, 2005, 29, 42–56.

46 R. H. Grubbs, S. J. Miller, G. C. Fu and M. Beckman, *Ring-Closing Metathesis and Related Processes in Organic Synthesis*, 1995, vol. 28.

47 H. H. Soon, A. G. Wenzel, T. T. Salguero, M. W. Day and R. H. Grubbs, Decomposition of ruthenium olefin metathesis catalysts, *J Am Chem Soc*, 2007, **129**, 7961–7968.

48 A. Michrowska, R. Bujok, S. Harutyunyan, V. Sashuk, G. Dolgonos and K. Grela, Nitro-substituted Hoveyda-Grubbs ruthenium carbenes: Enhancement of catalyst activity through electronic activation, *J Am Chem Soc*, 2004, **126**, 9318–9325.

49 É. De Brito Sá and J. M. E. De Matos, Ring closing metathesis by Hoveyda-Grubbs catalysts: A theoretical approach of some aspects of the initiation mechanism and the influence of solvent, *Inorganica Chim Acta*, 2015, **426**, 20–28.

50 D. Cortés-Borda, E. Wimmer, B. Gouilleux, E. Barré, N. Oger, L. Goulamaly, L. Peault, B. Charrier, C. Truchet, P. Giraudeau, M. Rodriguez-Zubiri, E. Le Grognec and F. X. Felpin, An Autonomous Self-Optimizing Flow Reactor for the Synthesis of Natural Product Carpanone, *Journal of Organic Chemistry*, 2018, **83**, 14286–14289.

51 M. Oltmanns and A. Kirschning, Subsupercritical Water Generated by Inductive Heating Inside Flow Reactors Facilitates the Claisen Rearrangement, *Synlett*, 2020, **31**, 1942–1946.

52 C. J. van der Westhuizen, J. du Toit, N. Neyt, D. Riley and J.-L. Panayides, Use of open-source software platform to develop dashboards for control and automation of flow chemistry equipment, *Digital Discovery*, 2022, **1**, 596–604.

53 M. M. Ramaiah, P. B. Shubha, P. K. Prabhala and N. S. Shivananju, 1,8-Diazabicyclo[5.4.0]undec-7-ene-mediated formation of N-sulfinyl imines, *J Chem Res*, 2020, **44**, 72–79.

54 M. D. Johnson, T. Braden, J. R. Calvin, A. C. Brewer, K. P. Cole, S. Frank, M. Kerr, D. Kjell, M. E. Kopach, J. R. Martinelli, S. A. May, J. Rincón, T. D. White and M. H. Yates, The History of Flow Chemistry at Eli Lilly and Company, *Chimia (Aarau)*, 2023, **77**, 319–326.

55 J. García-Lacuna, G. Domínguez, J. Blanco-Urgoiti and J. Pérez-Castells, Synthesis of treprostinil: Key claisen rearrangement and catalytic pauson-khand reactions in continuous flow, *Org Biomol Chem*, 2019, **17**, 9489–9501.

56 H. Kobayashi, B. Driessen, D. J. G. P. Van Osch, A. Talla, S. Ookawara, T. Noël and V. Hessel, The impact of Novel Process Windows on the Claisen rearrangement, *Tetrahedron*, 2013, **69**, 2885–2890.

57 K. C. Nicolaou, R. (Rudolf) Hanko and W. (Wolfgang) Hartwig, *Handbook of combinatorial chemistry : drugs, catalysts, materials*, Wiley-VCH, 2002.

58 K. Gilmore, S. Vukelić, D. T. McQuade, B. Koksch and P. H. Seeberger, Continuous reductions and reductive aminations using solid NaBH4, *Org Process Res Dev*, 2014, **18**, 1771–1776.

59 D. L. Riley and N. C. Neyt, *Synthesis (Germany)*, 2018, 50, 2707–2720.

60 K. Gilmore, S. Vukelić, D. T. McQuade, B. Koksch and P. H. Seeberger, Continuous reductions and reductive aminations using solid NaBH4, *Org Process Res Dev*, 2014, **18**, 1771–1776.

61 D. Mandala, S. Chada and P. Watts, Semi-continuous multi-step synthesis of lamivudine, *Org Biomol Chem*, 2017, **15**, 3444–3454.

62 *Application Note 53: Sodium Hydride as a Slurry in Continuous Flow*, .

63 J. C. Pastre, P. R. D. Murray, D. L. Browne, G. A. Brancaglion, R. S. Galaverna, R. A. Pilli and S. V. Ley, Integrated Batch and Continuous Flow Process for the Synthesis of Goniothalamin, *ACS Omega*, 2020, **5**, 18472–18483.

64 M. Drop, X. Bantreil, K. Grychowska, G. U. Mahoro, E. Colacino, M. Pawłowski, J. Martinez, G. Subra, P. Zajdel and F. Lamaty, Continuous flow ring-closing metathesis, an environmentally-friendly route to 2,5-dihydro-1H-pyrrole-3-carboxylates, *Green Chemistry*, 2017, **19**, 1647–1652.

65 R. W. Toh, M. Patrzałek, T. Nienałtowski, J. Piątkowski, A. Kajetanowicz, J. Wu and K. Grela, Olefin Metathesis in Continuous Flow Reactor Employing Polar Ruthenium Catalyst and Soluble Metal Scavenger for Instant Purification of Products of Pharmaceutical Interest, *ACS Sustain Chem Eng*, 2021, **9**, 16450–16458.

"For I know the plans I have for you," declares the LORD, "plans to prosper you and not to harm you, plans to give you hope and a future"

- ***Jeremiah 29:11***

Supplementary Information

for the

Synthesis of an 8-membered oxygen-containing benzo-fused heterocycle using flow technologies

Appendix A: Calculations and reactor setup

1. Overall percentage yield and time calculations

Table 28: Calculations of overall percentage yield and total reaction time for batch and flow conditions compared to literature values

Approach	Overall percentage yield	Total reaction time
Batch	(0.78×0.069×0.78×0.47×0.85×0.46)×100 = 0.77 %	(20×4)+72+2 =154 hours
Flow	(0.93×0.98×0.88×0.93×0.92×0.55) ×100 = 37.7 %	(15×3) +(20×3) =105 minutes
Van Otterlo and co-workers	(0.99×0.75×0.86×0.77×0.52)×100 = 25.6 %	20+64+18+12+20+2 =136 hours

2. Reactor setup for each step

Figure 46: First allylation (potassium carbonate approach) setup using Uniqsis Binary Pump

Figure 47: Claisen rearrangement setup using Uniqsis Binary Pump

Figure 48: Protection (potassium carbonate approach) setup using Uniqsis Binary Pump

Figure 49: Reduction (polymer supported sodium borohydride approach) using Uniqsis Binary Pump

Figure 50: Reduction (sodium borohydride solution approach) using Vapourtec peristaltic pumps

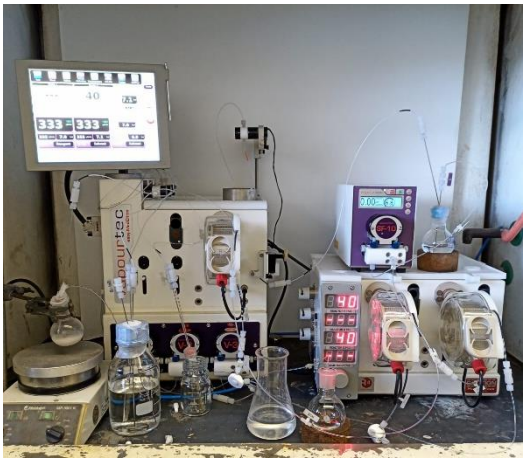

Figure 51: Second allylation (sodium hydride approach using standalone) using Vapourtec peristaltic pumps

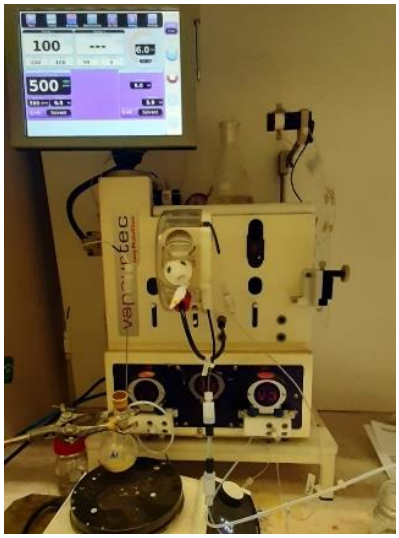

Figure 52: Second allylation (sodium hydride approach using recycling approach) setup using Vapourtec peristaltic pumps

Figure 53: RCM setup using Uniqsis Binary Pump

Appendix B: HPLC Method Information

1. First Allylation HPLC analysis of 3-(allyloxy)-4-methoxybenzaldehyde 19

1.1 General procedure for preparing concentrations for standard curve

Purified 3-(allyloxy)-4-methoxybenzaldehyde **19** (100 mg) was weighed and dissolved in 10mL acetonitrile (10 $mg.mL^{-1}$). From this 2 mL was diluted to 10 mL (2 $mg.mL^{-1}$). A 0.2 $mg.mL^{-1}$ stock was prepared by adding 1mL of the 2 $mg.mL^{-1}$ stock solution and diluting to 10 mL. From these stock solutions several concentrations were prepared in triplicate 10 ppm, 15 ppm, 20 ppm, 25 ppm, 30 ppm, 35 ppm and 40 ppm.

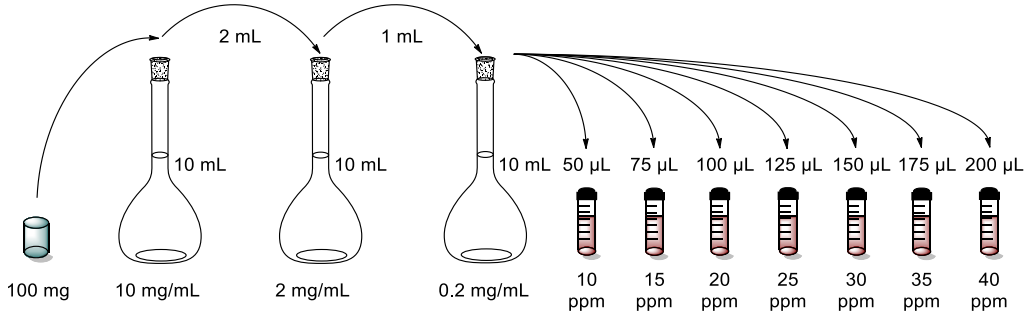

1.2 LC Method details

Table 29: HPLC method information for optimization of 3-(allyloxy)-4-methoxybenzaldehyde **19**

Quat. Pump		
Flow rate	1.00 $mL.min^{-1}$	
Maximum pressure	400 bar	
Stop time	5 minutes	
Oven Temperature	35 °C	
Injection Volume	2.00 uL	
Channel	**Name**	**Percentage (%)**
A	Organic (50 % MeOH/ACN)	60
B	Aqueous 10 mM Phosphate buffer (90 % H_2O/Organic)	40
Signals	**Name**	**Retention time (min)**
260 nm	Isovanillin **17**	1.131
260 nm	3-(allyloxy)-4-methoxybenzaldehyde **19**	1.826
260 nm	Anisole **64** (Internal standard)	2.241

1.3 Raw data for standard curve

Table 30: Raw data for triplicates at each concentration for standard curve for 3-(allyloxy)-4-methoxybenzaldehyde **19**

Isovanillin 17			
PPM	**Retention time**	**Area (mAU*S)**	**Average Area**
10	1.129	63.9542	65.1178
	1.131	66.9859	
	1.129	64.4133	
15	1.128	96.1887	97.2439

	1.129	96.6802	
	1.129	98.8628	
20	1.128	130.27	130.447
	1.131	130.545	
	1.133	130.528	
25	1.13	162.174	157.382
	1.132	160.362	
	1.131	149.609	
30	1.129	194.908	192.485
	1.129	191.528	
	1.13	191.019	
35	1.128	223.121	222.839
	1.13	221.503	
	1.131	223.894	
40	1.13	257.647	258.546
	1.13	254	
	1.159	263.991	
Product: 3-(Allyloxy)-4-methoxybenzaldehyde 19			
PPM	**Retention time**	**Area (mAU*S)**	**Average Area**
10	1.828	34.8695	35.0602
	1.826	34.7801	
	1.815	35.5309	
15	1.821	53.9597	54.0119
	1.822	53.1735	
	1.812	54.9025	
20	1.819	71.2548	72.0068
	1.824	71.6022	
	1.82	73.1634	
25	1.825	87.0507	88.23
	1.826	88.4288	
	1.816	89.2103	
30	1.823	108.553	108.238
	1.82	107.895	
	1.815	108.266	
35	1.818	120.957	124.936
	1.82	128.003	
	1.823	125.848	
40	1.823	143.579	142.37
	1.82	142.599	
	1.92	140.933	
Anisole 64 (Internal Standard)			
PPM	**Retention time**	**Area (mAU*S)**	**Average Area**
10	2.252	31.3119	30.8464

	2.254	31.0402	
	2.213	30.187	
15	2.244	30.3435	30.5361
	2.249	30.4251	
	2.211	30.8397	
20	2.244	31.2041	30.9331
	2.22	30.6329	
	2.22	30.9624	
25	2.249	30.4089	30.3933
	2.258	30.5315	
	2.218	30.2395	
30	2.25	30.6887	30.7177
	2.249	30.8783	
	2.215	30.5861	
35	2.243	30.8532	30.804
	2.215	30.5713	
	2.247	30.9874	
40	2.25	30.766	30.7488
	2.213	31.1933	
	2.349	30.2872	

1.4 Standard Curve

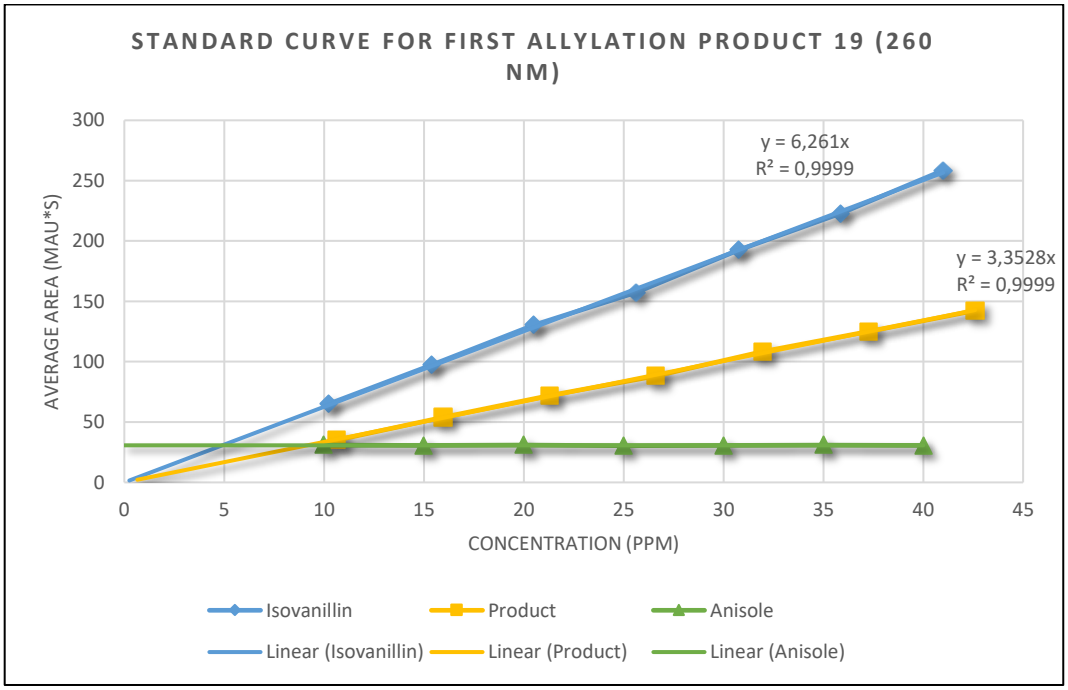

Figure 54: Standard curve for 3-(allyloxy)-4-methoxybenzaldehyde **19** at 260 nm

1.5 HPLC Chromatogram for standard curve

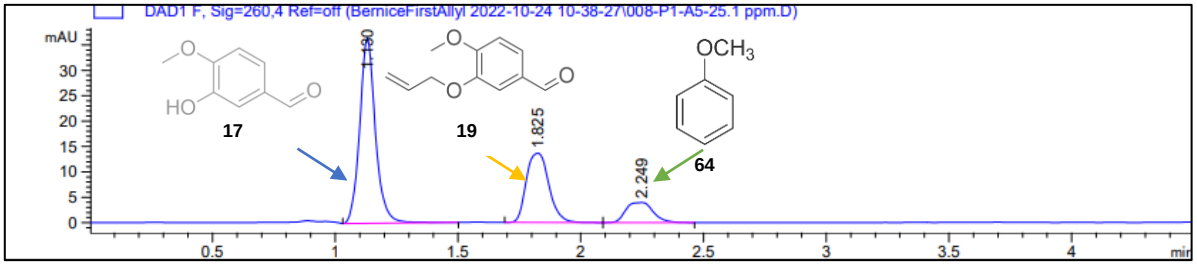

Figure 55: Chromatogram for standard curve at 260 nm at 25 ppm for isovanillin **17** (1.130 min), 3-(allyloxy)-4-methoxybenzaldehyde **19** (1.825 min), and Anisole **64** (2.249 min)

1.6 Experimental data and spreadsheets

Table 31: Descriptions and letters used for calculation of optimization reactions for 3-(allyloxy)-4-methoxybenzaldehyde **19**

Letter	Description
A	Starting material mass (Isovanillin **17**, 95 %)
B	Concentration in 30/40 mL sample
C	Concentration in 10 mL sample
D	Concentration in 1 mL LC vail sample (50 µL)
E	Dilution factor
F	Area of product
G	Area/ Equation of product
H	G × Dilution factor
I	H / 1000
J	I × Collected volume
K	% Conversion

1.6.1 Calculations and spreadsheet using potassium carbonate

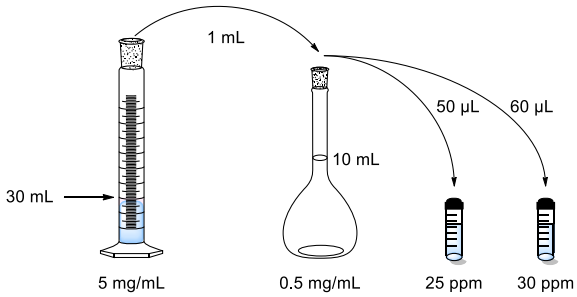

Each reaction was collected and diluted to a volume of 30 mL with acetonitrile, resulting in a concentration of 5 $mg.mL^{-1}$. From here, 1 mL was diluted with acetonitrile to a concentration of 0.5 $mg.mL^{-1}$ in a 10 mL volumetric flask. To obtain 25 ppm, a dilution factor of 200, a 50 µL aliquot of this solution was added to an LC vial and diluted to 1 mL. In addition, a 60 µL aliquot from this solution was added to an LC vial and diluted to 1 mL to give 30 ppm, which equated to a dilution factor of 167 and was used for validation.

Conversions were obtained by dividing the sample's area by the equation deduced from the standard curve- in this case, the allylated product **19**, which was 3.3528. After that, the value was multiplied by the dilution factor, which for 25 ppm was 200. To convert from ppm to mg.Ml^{-1}, this amount was then divided by 1000. The value is then multiplied by the volume of the collection, in this example 30 mL, to obtain the amount obtained in grams. Finally, the conversion is calculated by dividing the number of grams obtained by the number of grams theoretically expected.

Table 32: Calculations for experiments conducted for allylation using potassium carbonate

Exp No	A	B	C	D	E	F	G	H	I	J	K
1	124.8	5.26	0.53	26.28	200	69.26	20.66	4131.26	4.13	123.94	78.61
2	124.8	5.26	0.53	26.28	200	61.75	18.42	3683.23	3.68	110.50	70.09
3	124.9	5.26	0.53	26.30	200	78.50	23.41	4682.81	4.68	140.48	89.03
4	124.7	5.25	0.53	26.26	200	77.35	23.07	4614.26	4.61	138.43	87.87
5	124.7	5.25	0.53	26.26	200	80.79	24.10	4819.06	4.82	144.57	91.77
6	124.9	5.26	0.53	26.30	200	78.63	23.45	4690.58	4.69	140.72	89.18

1.6.2 Calculations and spreadsheet using potassium hydroxide solution

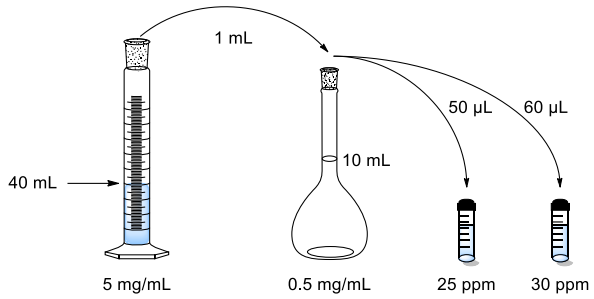

Each reaction was collected and diluted to a volume of 40 mL with acetonitrile, resulting in a concentration of 5 mg.mL^{-1}. From here, 1 mL was diluted with acetonitrile to concentration of 0.5 mg.mL^{-1} in a 10 mL volumetric flask. To obtain 25 ppm, a dilution factor of 200, a 50 µL aliquot of this solution was added to an LC vial and diluted to 1 mL. In addition, a 60 µL aliquot from this solution was added to an LC vial and diluted to 1 mL to give 30 ppm, which equated to a dilution factor of 167.

Conversions were obtained by dividing the sample's area by the equation deduced from the standard curve in this case, the allylated product **19**, which was 3.3528. After that, the value was multiplied by the dilution factor, which for 25 ppm was 200. To convert from ppm to mg.mL^{-1}, this amount was then divided by 1000. The value is then multiplied by the volume of the collection, in this example 40 mL, to obtain the amount obtained in grams. Finally, the conversion is calculated by dividing the number of grams obtained by the number of grams theoretically expected.

Table 33: Calculations for experiments conducted for allylation using potassium hydroxide

Exp No	A	B	C	D	E	F	G	H	I	J	K
1	159.6	5.04	0.50	25.20	200	57.41	17.12	3424.61	3.42	136.98	67.95
2	159.6	5.04	0.50	25.20	200	63.78	19.02	3804.31	3.80	152.17	75.49
3	159.5	5.04	0.50	25.19	200	65.87	19.65	3929.32	3.93	157.17	77.99
4	159.5	5.04	0.50	25.19	200	66.22	19.75	3949.91	3.95	158.00	78.40
5	159.5	5.04	0.50	25.19	200	64.61	19.27	3854.25	3.85	154.17	76.50
6	161.6	5.10	0.51	25.52	200	65.77	19.62	3923.48	3.92	156.94	76.88
7	161.6	5.10	0.51	25.52	200	68.72	20.50	4099.49	4.10	163.98	80.33
8	161.6	5.10	0.51	25.52	200	67.85	20.24	4047.25	4.05	161.89	79.31
9	161.6	5.10	0.51	25.52	200	66.14	19.73	3945.32	3.95	157.81	77.31
10	160.5	5.07	0.51	25.34	200	66.38	19.80	3959.61	3.96	158.38	78.12
11	160.5	5.07	0.51	25.34	200	68.06	20.30	4059.68	4.06	162.39	80.09

1.7 HPLC Chromatogram for experimental calculations

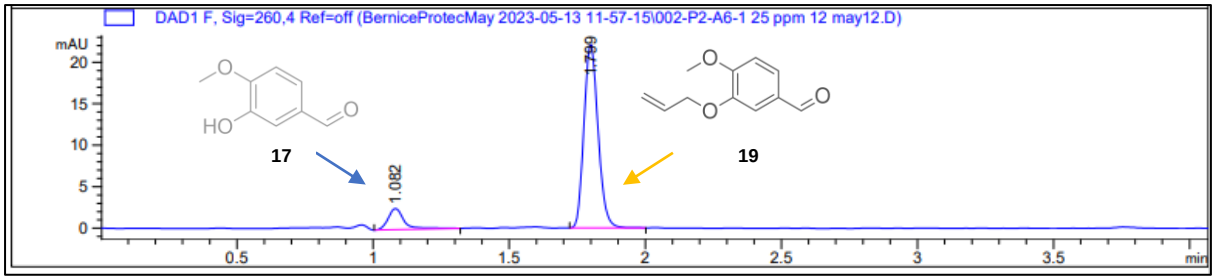

Figure 56: Chromatogram of large-scale allylation reaction using potassium hydroxide at 25 ppm

2. Reduction HPLC analysis of (2-allyl-3-isopropoxy-4-methoxyphenyl)methanol 23

2.1 General procedure for preparing concentrations for standard curve

Purified of (2-allyl-3-isopropoxy-4-methoxyphenyl)methanol **23** (100 mg) was weighed and dissolved in 10 mL acetonitrile (10 mg.mL^{-1}). From this 2 mL was diluted to 10 mL (2 mg.mL^{-1}). A 0.2 mg.mL^{-1} stock was prepared by adding 1 mL of the 2 mg.mL^{-1} stock solution and diluting to 10 mL. From these stock solutions several concentrations were prepared in triplicate 8 ppm, 12 ppm, 16 ppm, 20 ppm, 24 ppm, 28 ppm, 32 ppm, 36 ppm and 40 ppm.

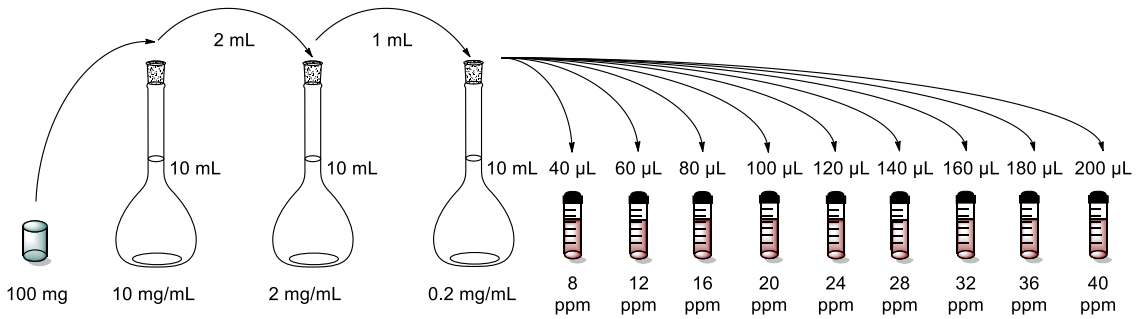

2.2 LC Method details

Table 34: HPLC method information for optimization of (2-allyl-3-isopropoxy-4-methoxyphenyl)methanol **23**

Quat. Pump		
Flow rate	1.00 mL.min^{-1}	
Maximum pressure	400 bar	
Stop time	7 minutes	
Oven Temperature	35 °C	
Injection Volume	2.00 uL	
Channel	**Name**	**Percentage (%)**
A	Organic (50 % MeOH/ACN)	60
B	Aqueous 10 mM Phosphate buffer (90 % H_2O/Organic)	40
Signals	**Name**	**Retention time (min)**
210 nm	2-allyl-3-isopropoxy-4-methoxybenzaldehyde **22**	4.454
210 nm	(2-allyl-3-isopropoxy-4-methoxyphenyl)methanol **23**	2.794
210 nm	Anisole **64** (Internal standard)	2.302

2.3 Raw data for standard curve

Table 35: Raw data for triplicates at each concentration for standard curve for (2-allyl-3-isopropoxy-4-methoxyphenyl)methanol **23**

	(2-allyl-3-isopropoxy-4-methoxyphenyl)methanol 23			**Anisole 64 (Internal standard)**		
PPM	**Retention time**	**Area (mAU*S)**	**Average Area**	**Retention time**	**Area (mAU*S)**	**Average Area**
8	2.822	118.062	117.7746	2.299	195.744	191.73
	2.826	111.586		2.302	189.702	
	2.832	127.538		2.305	195.774	
	2.835	113.912		2.306	185.699	
12	2.843	172.908	172.703	2.311	191.802	193.446
	2.878	170.603		2.33	191.496	
	2.83	179.118		2.306	198.772	
	2.823	168.183		2.3	191.712	
16	2.829	229.446	230.5423	2.304	192.057	193.357
	2.842	227.327		2.312	191.403	
	2.826	228.725		2.301	192.919	
	2.834	236.672		2.309	197.048	
20	2.84	289.051	289.4722	2.311	194.098	194.054
	2.848	288.881		2.316	194.485	

	2.819	288.1		2.298	190.899	
	2.83	291.857		2.305	196.733	
24	2.832	355.547	349.9926	2.304	192.497	194.63
	2.827	346.697		2.303	192.944	
	2.838	347.143		2.309	195.284	
	2.835	350.584		2.308	197.794	
28	2.818	402.65	402.2017	2.297	194.774	197.717
	2.812	403.336		2.294	202.473	
	2.833	401.947		2.304	194.95	
	2.815	400.873		2.295	198.672	
32	2.832	458.862	462.5346	2.307	194.602	196.914
	2.827	462.118		2.302	196.909	
	2.83	466.624		2.307	199.232	
36	2.833	523.034	520.9403	2.309	195.356	197.17
	2.826	518.316		2.303	197.018	
	2.83	520.916		2.306	196.264	
	2.825	521.495		2.301	200.043	
40	2.833	574.388	577.4676	2.308	199.295	195.59
	2.834	574.03		2.307	192.807	
	2.833	583.572		2.307	195.194	
	2.837	577.881		2.309	195.064	

2.4 Standard Curve

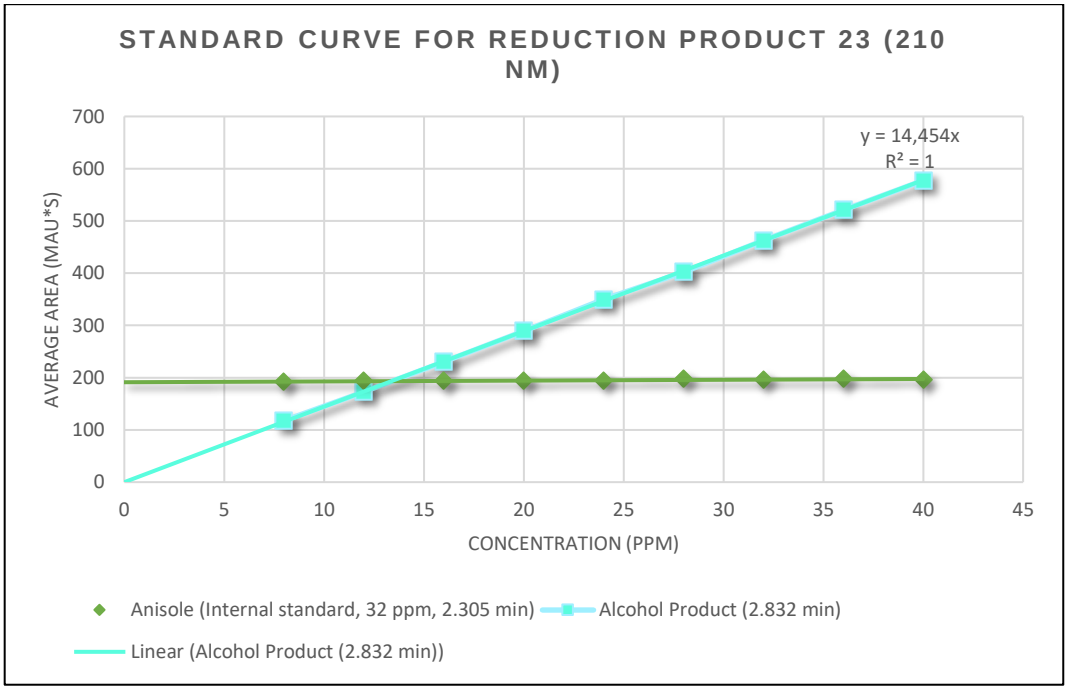

Figure 57: Standard curve for (2-allyl-3-isopropoxy-4-methoxyphenyl)methanol **23** at 210 nm

2.5 HPLC Chromatogram for standard curve

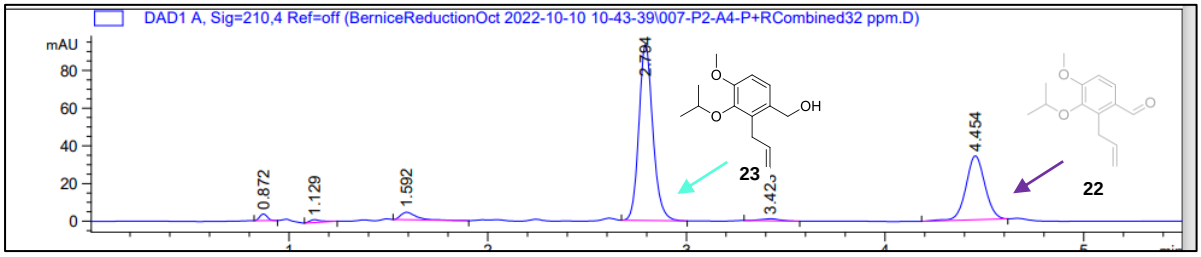

Figure 58: Chromatogram for standard curve at 210 nm at 32 ppm for (2-allyl-3-isopropoxy-4-methoxyphenyl)methanol **23** (2.794 min) and 2-allyl-3-isopropoxy-4-methoxybenzaldehyde **22** (4.454 min)

2.6 Experimental data and spreadsheets

Table 36: Descriptions and letters used for calculation of optimization reactions for (2-allyl-3-isopropoxy-4-methoxyphenyl)methanol **23**

Letter	Description
A	Starting material **22** mass
B	Concentration in 30 mL sample
C	Concentration in 10 mL sample
D	Concentration in 1 mL LC vail sample (50 µL)
E	Dilution factor
F	Area of product
G	Area/ Equation of product
H	G × Dilution factor
I	H / 1000
J	I × Collected volume
K	% Conversion

2.6.1 Calculations and spreadsheet using polymer-supported sodium borohydride

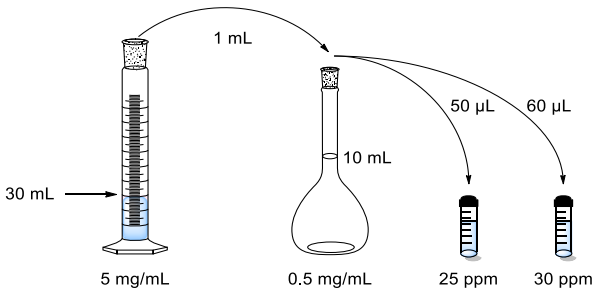

Each reaction was collected and diluted to a volume of 30 mL with acetonitrile, resulting in a concentration of 5 $mg.mL^{-1}$. From here, 1 mL was diluted with acetonitrile to concentration of 0.5 $mg.mL^{-1}$ in a 10 mL volumetric flask. To obtain 25 ppm, a dilution factor of 200, a 50 µL aliquot of this solution was added to an LC vial and diluted to 1 mL. In addition, a 60 µL aliquot from this solution was added to an LC vial and diluted to 1 mL to give 30 ppm, which equated to a dilution factor of 167 and was used for validation.

Conversions were obtained by dividing the sample's area by the equation deduced from the standard curve- in this case, (2-allyl-3-isopropoxy-4-methoxyphenyl)methanol **23**, which was 14.454. After that, the value was multiplied by the dilution factor, which for 25 ppm was 200. To convert from ppm to $mg.mL^{-1}$, this amount was then divided by 1000. The value is then multiplied by the volume of the collection, in this example 30 mL, to obtain the amount obtained in grams. Finally, the conversion is calculated by dividing the number of grams obtained by the number of grams theoretically expected.

Table 37: Calculations for experiments conducted for reduction using polymer supported sodium borohydride

Exp No	A	B	C	D	E	F	G	H	I	J	K
1	148.6	5.00	0.50	24.98	200	213.95	14.80	2960.49	2.96	88.81	59.77
2	148.3	4.99	0.50	24.93	200	248.18	17.17	3434.12	3.43	103.02	69.47
3	148.4	4.99	0.50	24.95	200	160.66	11.12	2223.08	2.22	66.69	44.94
4	148.6	5.00	0.50	24.98	200	243.51	16.85	3369.39	3.37	101.08	68.02
5	148.7	5.00	0.50	25.00	200	227.05	15.71	3141.68	3.14	94.25	63.38
6	148.2	4.98	0.50	24.91	200	287.05	19.86	3971.91	3.97	119.16	80.40
7	148.3	4.99	0.50	24.93	200	311.70	21.56	4312.94	4.31	129.39	87.25

2.6.2 Calculations and spreadsheet using sodium borohydride solution

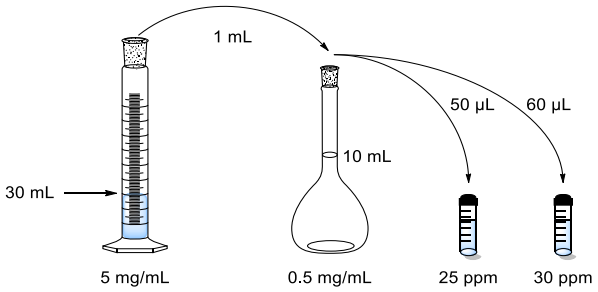

Each reaction was collected and diluted to a volume of 30 mL with acetonitrile, resulting in a concentration of 5 $mg.mL^{-1}$. From here, 1 mL was diluted with acetonitrile to a concentration of 0.5 $mg.mL^{-1}$ in a 10 mL volumetric flask. To obtain 25 ppm, a dilution factor of 200, a 50 µL aliquot of this solution was added to an LC vial and diluted to 1 mL. In addition, a 60 µL aliquot from this solution was added to an LC vial and diluted to 1 mL to give 30 ppm, which equated to a dilution factor of 167 and was used for validation.

Conversions were obtained by dividing the sample's area by the equation deduced from the standard curve- in this case, (2-allyl-3-isopropoxy-4-methoxyphenyl)methanol **23**, which was 14.454. After that, the value was multiplied by the dilution factor, which for 25 ppm was 200. To convert from ppm to $mg.mL^{-1}$, this amount was then divided by 1000. The value is then multiplied by the volume of the collection, in this example 30 mL, to obtain the amount obtained in grams. Finally, the conversion is calculated by dividing the number of grams obtained by the number of grams theoretically expected.

Table 38: Calculations for experiments conducted for reduction using sodium borohydride solution

Exp No	A	B	C	D	E	F	G	H	I	J	K
1	150.9	5.07	0.51	25.37	203	358.13	24.78	5028.17	5.03	125.70	82.59
2	150.9	5.07	0.51	25.37	203	345.89	23.93	4856.29	4.86	121.41	79.77
3	150.9	5.07	0.51	25.37	203	380.30	26.31	5339.40	5.34	133.48	87.70
4	150.9	5.07	0.51	25.37	203	392.27	27.14	5507.39	5.51	137.68	90.46
5	148.7	5.00	0.50	24.99	200	362.39	25.07	5012.52	5.01	125.31	83.57
6	149.9	5.04	0.50	25.20	202	343.37	23.76	4788.43	4.79	119.71	79.19
7	149.9	5.04	0.50	25.20	202	353.64	24.47	4931.69	4.93	123.29	81.56
8	148.7	5.00	0.50	24.99	200	402.00	27.81	5560.38	5.56	139.01	92.71
9	148.7	5.00	0.50	24.99	200	362.39	25.07	5012.52	5.01	125.31	83.57
10	148.7	4.99	0.50	24.97	200	346.34	23.96	4786.15	4.79	124.44	83.07
11	149.9	5.04	0.50	25.20	202	343.37	23.76	4788.43	4.79	119.71	79.19

2.7 HPLC Chromatogram for experimental calculations

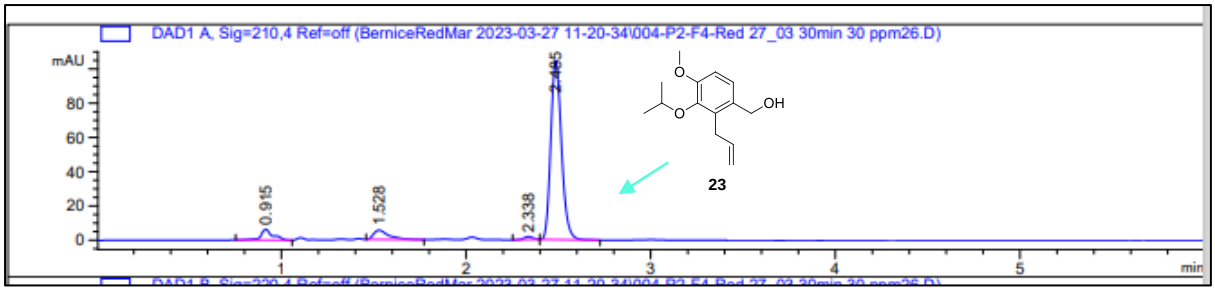

Figure 59: Chromatogram reduction reaction (entry 10) using sodium borohydride solution at 30 ppm

3. Second Allylation HPLC analysis of 2-allyl-1-((allyloxy)methyl)-3-isopropoxy-4-methoxybenzene 24

3.1 General procedure for preparing concentrations for standard curve

Purified 2-allyl-1-((allyloxy)methyl)-3-isopropoxy-4-methoxybenzene **24** (100 mg) was weighed and dissolved in 10 mL acetonitrile (10 mg.mL^{-1}). From this 2 mL was diluted to 10 mL (2 mg.mL^{-1}). A 0.2 mg.mL^{-1} stock was prepared by adding 1 mL of the 2 mg.mL^{-1} stock solution and diluting to 10 mL. From these stock solutions several concentrations were prepared in triplicate 8 ppm, 12 ppm, 16 ppm, 20 ppm, 24 ppm, 28 ppm, 32 ppm, 36 ppm and 40 ppm.

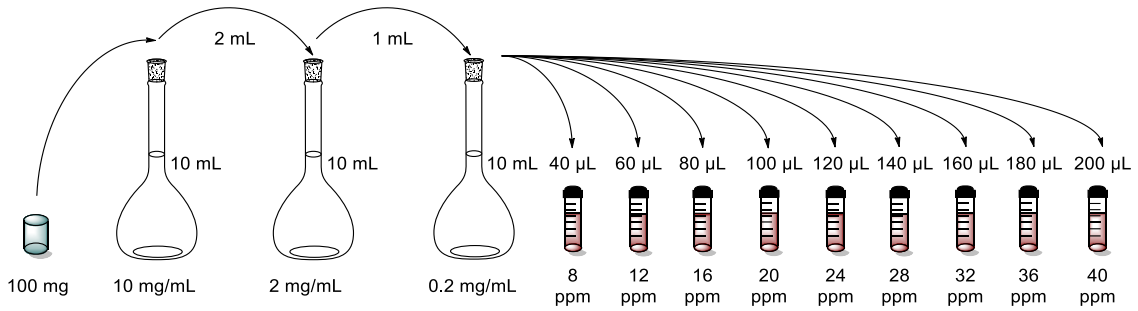

3.2 LC Method details

Table 39: HPLC method information for optimization of 2-allyl-1-((allyloxy)methyl)-3-isopropoxy-4-methoxybenzene **24**

Quat. Pump		
Flow rate	1.00 mL.min^{-1}	
Maximum pressure	400 bar	
Stop time	15 minutes	
Oven Temperature	35 °C	
Injection Volume	2.00 uL	
Channel	**Name**	**Percentage (%)**
A	Organic (50 % MeOH/ACN)	60
B	Aqueous 10 mM Phosphate buffer (90 % H_2O/Organic)	40
Signals	**Name**	**Retention time (min)**
210 nm	2-allyl-3-isopropoxy-4-methoxyphenyl)methanol **23**	2.842
210 nm	2-allyl-1-((allyloxy)methyl)-3-isopropoxy-4-methoxybenzene **24**	12.635
210 nm	Anisole **64** (Internal standard)	2.312

3.3 Raw data for standard curve

Table 40: Raw data for triplicates at each concentration for standard curve for 2-allyl-1-((allyloxy)methyl)-3-isopropoxy-4-methoxybenzene **24**

	2-allyl-1-((allyloxy)methyl)-3-isopropoxy-4-methoxybenzene 24			**Anisole 64 (Internal standard)**		
PPM	**Retention time**	**Area (mAU*S)**	**Average Area**	**Retention time**	**Area (mAU*S)**	**Average Area**
8	12.498	108.301	112.633	2.299	195.744	191.73
	12.529	113.333		2.302	189.702	
	12.543	116.618		2.305	195.774	
	12.516	112.281		2.306	185.699	
12	12.564	170.909	160.798	2.311	191.802	193.446
	12.887	156.423		2.33	191.496	

	12.528	170.925		2.306	198.772	
	12.501	144.934		2.3	191.712	
16	12.488	214.966	209.593	2.304	192.057	193.357
	12.635	186.987		2.312	191.403	
	12.464	203.858		2.301	192.919	
	12.527	232.56		2.309	197.048	
20	12.54	256.135	268.122	2.311	194.098	194.054
	12.631	284.768		2.316	194.485	
	12.475	267.461		2.298	190.899	
	12.531	264.125		2.305	196.733	
24	12.514	305.583	308.535	2.304	192.497	194.63
	12.601	316.829		2.303	192.944	
	12.537	312.303		2.309	195.284	
	12.524	299.424		2.308	197.794	
28	12.51	357.065	360.322	2.297	194.774	197.717
	12.548	370.957		2.294	202.473	
	12.384	359.945		2.304	194.95	
	12.502	353.322		2.295	198.672	
32	12.531	412.432	413.423	2.307	194.602	196.914
	12.467	410.094		2.302	196.909	
	12.54	417.744		2.307	199.232	
36	12.58	464.48	475.525	2.309	195.356	197.17
	12.468	472.772		2.303	197.018	
	12.48	472.633		2.306	196.264	
	12.513	492.213		2.301	200.043	
40	12.478	514.906	525.35	2.308	199.295	195.59
	12.531	538.272		2.307	192.807	
	12.504	509.217		2.307	195.194	
	12.476	539.004		2.309	195.064	

3.4 Standard Curve

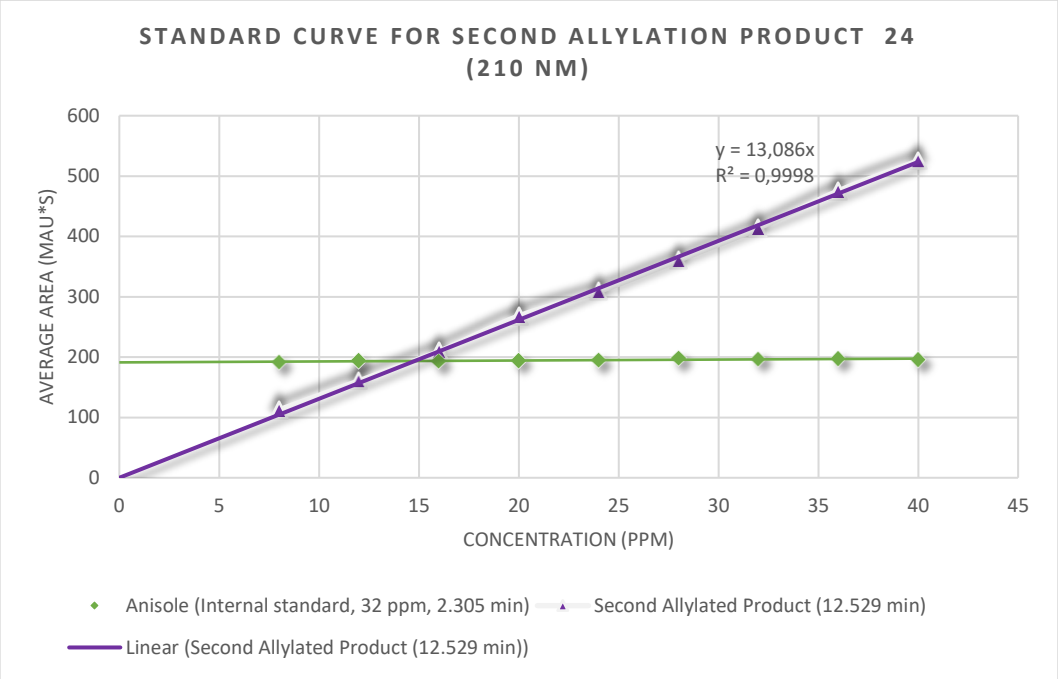

Figure 60: Standard curve for 2-allyl-1-((allyloxy)methyl)-3-isopropoxy-4-methoxybenzene **24** at 210 nm

3.5 HPLC Chromatogram for standard curve

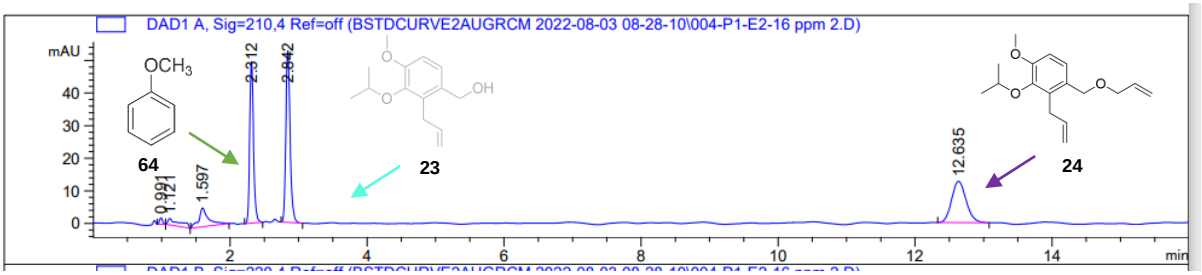

Figure 61: Chromatogram for standard curve at 210 nm at 16 ppm for 2-allyl-3-isopropoxy-4-methoxyphenyl)methanol **23** (2.842 min), 2-allyl-1-((allyloxy)methyl)-3-isopropoxy-4-methoxybenzene **24** (12.365 min), and Anisole **64** (2.312 min)

3.6 Experimental data and spreadsheets

Table 41: Descriptions and letters used for calculation of optimization reactions for 2-allyl-1-((allyloxy)methyl)-3-isopropoxy-4-methoxybenzene **24**

Letter	Description
A	Starting material mass **23**
B	Concentration in 60 mL sample
C	Concentration in 10 mL sample
D	Concentration in 1 mL LC vail sample (50 µL)
E	Dilution factor

F	Area of product
G	Area/ Equation of product
H	G × Dilution factor
I	H / 1000
J	I × Collected volume
K	% Conversion

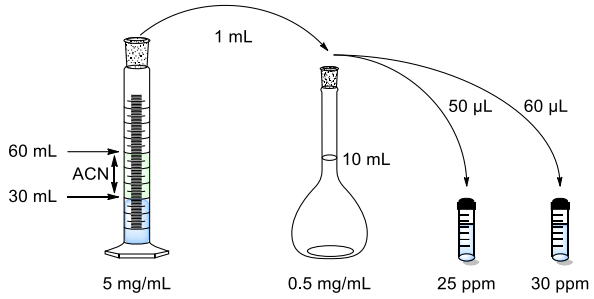

Each reaction was collected and diluted to a volume of 30 mL with acetonitrile, resulting in a concentration of 10 $mg.mL^{-1}$. The measuring cylinder was further diluted with acetonitrile to a volume of 60 mL mark with, resulting in a concentration of 5 $mg.mL^{-1}$. From here, 1 mL was diluted with acetonitrile to concentration of 0.5 $mg.mL^{-1}$ in a 10 mL volumetric flask. To obtain 25 ppm, a dilution factor of 200, a 50 µL aliquot of this solution was added to an LC vial and diluted to 1 mL. In addition, a 60 µL aliquot from this solution was added to an LC vial and diluted to 1 mL to give 30 ppm, which equated to a dilution factor of 167.

Conversions were obtained by dividing the sample's area by the equation deduced from the standard curve- in this case, the allylated product **24**, which was 13.086. After that, the value was multiplied by the dilution factor, which for 25 ppm was 200. To convert from ppm to $mg.mL^{-1}$, this amount was then divided by 1000. The value is then multiplied by the volume of the collection, in this example 60 mL, to obtain the amount obtained in grams. Finally, the conversion is calculated by dividing the number of grams obtained by the number of grams theoretically expected.

Table 42: Calculations for experiments conducted for 2-allyl-1-((allyloxy)methyl)-3-isopropoxy-4-methoxybenzene **24**

Exp No	A	B	C	D	E	F	G	H	I	J	K
1	255.7	4.98	0.50	24.92	200	199.64	15.26	3051.16	3.05	183.07	61.22
2	255.2	4.97	0.50	24.87	200	291.65	22.29	4457.42	4.46	267.45	89.61
3	255.8	4.99	0.50	24.93	200	100.75	7.70	1539.86	1.54	92.39	30.88
4	256.4	5.00	0.50	24.99	200	260.77	19.93	3985.54	3.99	239.13	79.75
5	255	4.97	0.50	24.85	200	205.13	15.68	3135.16	3.14	188.11	63.08
6	256.2	4.99	0.50	24.97	200	293.93	22.46	4492.29	4.49	269.54	89.96
7	255.7	4.98	0.50	24.92	200	123.25	9.42	1883.72	1.88	113.02	37.79
8	255.1	4.97	0.50	24.86	200	280.30	21.42	4283.91	4.28	257.03	86.15
9	255.9	4.99	0.50	24.94	200	149.27	11.41	2281.35	2.28	136.88	45.74
10	255.1	4.97	0.50	24.86	200	260.30	19.89	3978.32	3.98	238.70	80.01
11	256.3	5.00	0.50	24.98	200	129.19	9.87	1974.44	1.97	118.47	39.52

12	256.7	5.00	0.50	25.02	200	269.12	20.57	4113.11	4.11	246.79	82.20
13	255.7	4.98	0.50	24.92	200	192.98	14.75	2949.39	2.95	176.96	59.18
14	255.6	4.98	0.50	24.91	200	274.72	20.99	4198.65	4.20	251.92	84.27
15	255.6	4.98	0.50	24.91	200	99.39	7.59	1518.97	1.52	91.14	30.49
16	256.2	4.99	0.50	24.97	200	301.08	23.01	4601.50	4.60	276.09	92.14
17	256.5	4.98	0.50	24.89	200	234.54	17.92	3584.58	3.58	215.07	72.00
18	255.4	4.98	0.50	24.89	200	215.53	16.47	3294.08	3.29	197.64	66.17

3.7 HPLC Chromatogram for experimental calculations

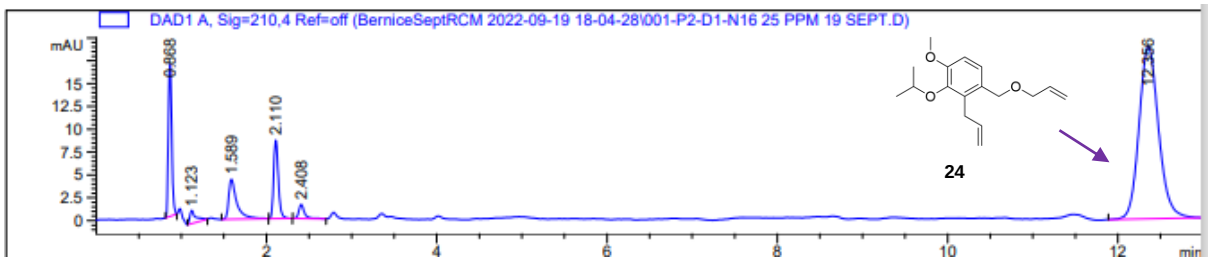

Figure 62: Chromatogram of 2-allyl-1-((allyloxy)methyl)-3-isopropoxy-4-methoxybenzene **24** (entry 16) at 25 ppm

4. RCM HPLC analysis of (*Z*)-7-isopropoxy-8-methoxy-3,6-dihydro-1*H*-benzo[*c*]oxocine 25

4.1 General procedure for preparing concentrations for standard curve

Purified of (*Z*)-7-isopropoxy-8-methoxy-3,6-dihydro-1*H*-benzo[*c*]oxocine **25** (10 mg) was weighed and dissolved in 10 mL acetonitrile (2 mg.mL^{-1}). From this 1 mL was diluted to 10 mL (0.2 mg.mL^{-1}). From these stock solutions several concentrations were prepared in triplicate 8 ppm, 12 ppm, 16 ppm, 20 ppm, 24 ppm, 28 ppm, 32 ppm, 36 ppm and 40 ppm.

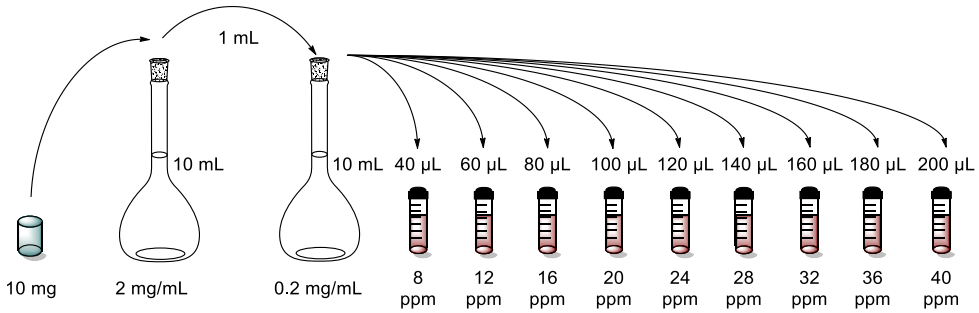

4.2 LC Method details

Table 43: HPLC method information for optimization of (*Z*)-7-isopropoxy-8-methoxy-3,6-dihydro-1*H*-benzo[*c*]oxocine **25**

Quat. Pump	
Flow rate	1.00 mL.min^{-1}
Maximum pressure	400 bar
Stop time	15 minutes
Oven Temperature	35 °C

Injection Volume	2.00 uL	
Channel	**Name**	**Percentage (%)**
A	Organic (50 % MeOH/ACN)	60
B	Aqueous 10 mM Phosphate buffer (90 % H_2O/Organic)	40
Signals	**Name**	**Retention time (min)**
210 nm	2-allyl-1-((allyloxy)methyl)-3-isopropoxy-4-methoxybenzene **24**	11.407
210 nm	(*Z*)-7-isopropoxy-8-methoxy-3,6-dihydro-1*H*-benzo[*c*]oxocine **25**	4.408
210 nm	Anisole **64** (Internal standard)	2.158

4.3 Raw data for standard curve

Table 44: Raw data for triplicates at each concentration for standard curve for (*Z*)-7-isopropoxy-8-methoxy-3,6-dihydro-1*H*-benzo[*c*]oxocine **25**

	RCM Product 25			Anisole 64 (Internal standard)		
PPM	Retention time	Area (mAU*S)	Average Area	Retention time	Area (mAU*S)	Average Area
8	4.472	76.00193	76.56762	2.183	243.965	245.689
	4.451	75.96502		2.175	247.224	
	4.466	77.7359		2.18	245.878	
12	4.457	117.3149	115.0638	2.175	248.04	248.023
	4.408	112.7567		2.158	247.604	
	4.409	115.1197		2.159	248.426	
16	4.488	151.5451	152.9026	2.181	247.708	247.674
	4.49	153.7041		2.188	247.149	
	4.493	153.4585		2.19	248.167	
20	4.427	185.8389	188.6931	2.165	250.686	246.954
	4.362	191.0564		2.15	245.378	
	4.36	189.1839		2.15	244.798	
24	4.372	222.6228	227.1958	2.155	250.405	249.683
	4.487	230.6926		2.185	247.385	
	4.473	228.272		2.183	251.26	
28	4.364	264.0697	263.6516	2.154	247.846	247.52
	4.369	261.9721		2.148	244.727	
	4.394	264.913		2.154	249.987	
32	4.398	306.9771	306.9647	2.163	246.263	245.851
	4.389	304.1098		2.158	248.801	
	4.554	309.8073		2.227	242.488	
36	4.401	341.0914	342.8133	2.172	246.392	246.198
	4.378	341.9056		2.153	245.791	
	4.392	345.443		2.161	246.411	

40	4.9	382.4654	382.5757	2.153	246.858	246.397
	4.376	381.9564		2.159	245.278	
	4.376	383.3054		2.159	247.056	

4.4 Standard Curve

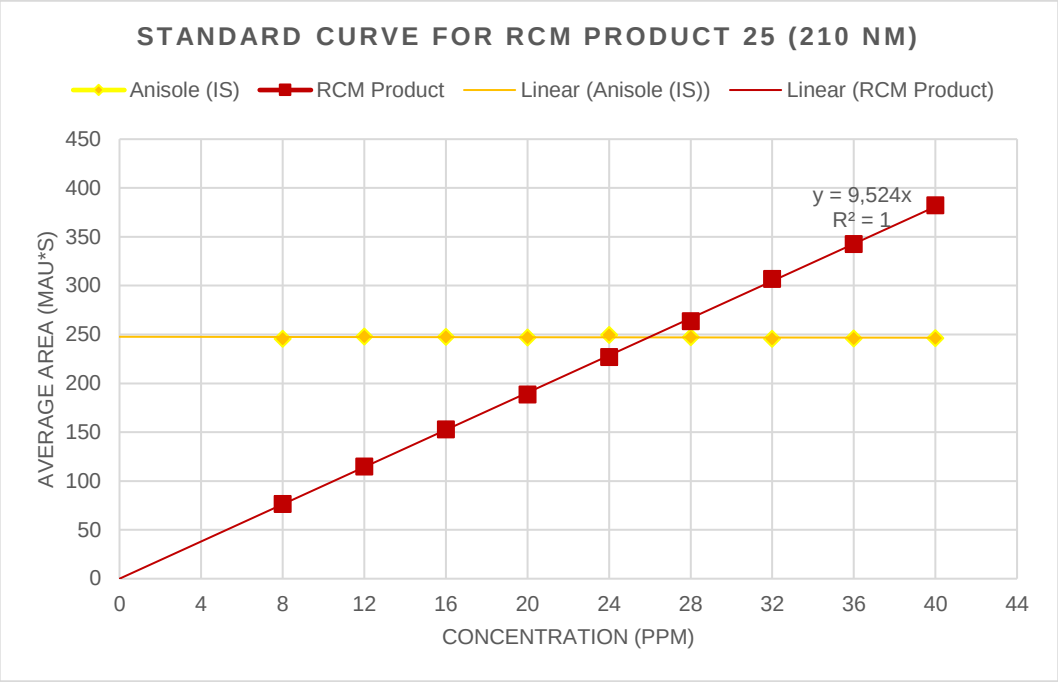

Figure 63: Standard curve for (*Z*)-7-isopropoxy-8-methoxy-3,6-dihydro-1*H*-benzo[*c*]oxocine **25** at 210 nm

4.5 HPLC Chromatogram for standard curve

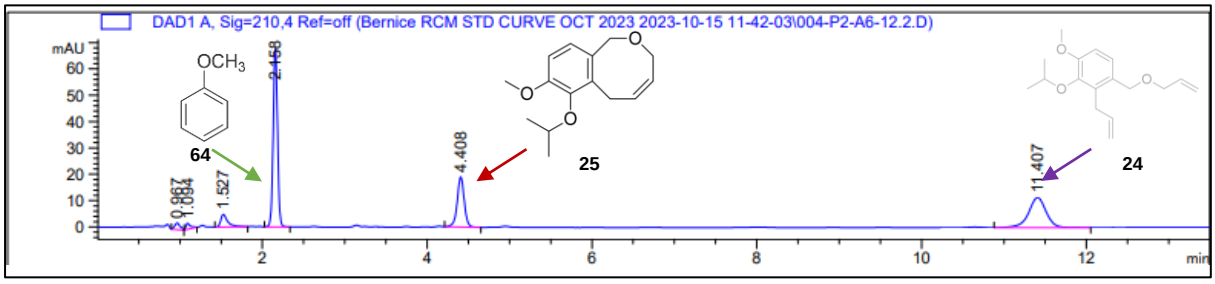

Figure 64: Chromatogram for standard curve at 210 nm at 25 ppm for -allyl-1-((allyloxy)methyl)-3-isopropoxy-4-methoxybenzene **24** (11.407 min), (*Z*)-7-isopropoxy-8-methoxy-3,6-dihydro-1*H*-benzo[*c*]oxocine **25** (4.408 min), and Anisole **64** (2.158 min)

4.6 Experimental data and spreadsheets

Table 45: Descriptions and letters used for calculation of optimization reactions for (*Z*)-7-isopropoxy-8-methoxy-3,6-dihydro-1*H*-benzo[*c*]oxocine **25**

Letter	Description
A	Starting material mass **24**
B	Concentration in 20 mL sample
C	Concentration in 10 mL sample
D	Concentration in 1 mL LC vail sample (100 µL)
E	Dilution factor
F	Area of product
G	Area/ Equation of product
H	G × Dilution factor
I	H / 1000
J	I × Collected volume
K	% Conversion

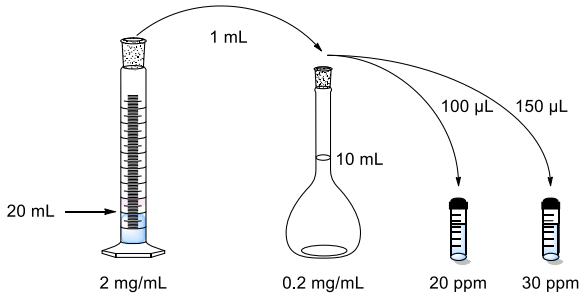

Each reaction was collected and diluted to a volume of 20 mL with acetonitrile, resulting in a concentration of 2 mg.mL^{-1}. From here, 1 mL was diluted with acetonitrile to a concentration of 0.2 mg.mL^{-1} in a 10 mL volumetric flask. To obtain 20 ppm, a dilution factor of 100, a 100 µL aliquot of this solution was added to an LC vial and diluted to 1 mL. In addition, a 150 µL aliquot from this solution was added to an LC vial and diluted to 1 mL to give 30 ppm, which equated to a dilution factor of 67 and was used for validation.

Conversions were obtained by dividing the sample's area by the equation deduced from the standard curve- in this case, the RCM product **25**, which was 9.524. After that, the value was multiplied by the dilution factor, which for 20 ppm was 100. To convert from ppm to mg.mL^{-1}, this amount was then divided by 1000. The value is then multiplied by the volume of the collection, in this example 20 mL, to obtain the amount obtained in grams. Finally, the conversion is calculated by dividing the number of grams obtained by the number of grams theoretically expected.

Table 46: Calculations for experiments conducted for (*Z*)-7-isopropoxy-8-methoxy-3,6-dihydro-1*H*-benzo[*c*]oxocine **25**

Exp No	A	B	C	D	E	F	G	H	I	J	K
1	111.2	2.00	0.20	19.98	100	86.69	9.10	910.21	0.91	18.20	45.55

2	110.5	1.99	0.20	19.86	100	81.83	8.59	859.17	0.86	17.18	43.27
3	110.8	1.99	0.20	19.91	100	91.02	9.56	955.72	0.96	19.11	48.00
4	110.3	1.98	0.20	19.82	100	77.15	8.10	810.11	0.81	16.20	40.87
5	111.5	2.00	0.20	20.04	100	47.14	4.95	494.96	0.49	9.90	24.70
6	110.8	1.99	0.20	19.91	100	67.98	7.14	713.80	0.71	14.28	35.85
7	110.7	1.99	0.20	19.89	100	88.08	9.25	924.80	0.92	18.50	46.49
8	111.2	2.00	0.20	19.98	100	104.19	10.94	1093.99	1.09	21.88	54.75
9	111.2	2.00	0.20	19.98	100	59.45	6.24	624.22	0.62	12.48	43.28
10	110.5	1.99	0.20	19.86	100	85.80	9.01	900.89	0.90	18.02	45.37
11	110.8	1.99	0.20	19.91	100	54.15	5.69	568.56	0.57	11.37	28.56
12	110.3	1.98	0.20	19.82	100	69.81	7.33	732.96	0.73	14.66	36.98
13	111.5	2.00	0.20	20.04	100	28.66	3.01	300.93	0.30	6.02	15.02
14	110.8	1.99	0.20	19.91	100	44.40	4.66	466.22	0.47	9.32	23.42
15	110.7	1.99	0.20	19.89	100	50.98	5.35	535.33	0.54	10.71	26.91
16	111.2	2.00	0.20	19.98	100	70.44	7.40	739.58	0.74	14.79	37.01
17	111.4	2.00	0.20	20.02	100	66.09	6.94	693.91	0.69	13.88	34.66
18	111.4	2.00	0.20	20.02	100	69.15	7.26	726.10	0.73	14.52	36.27
19	111.4	2.00	0.20	20.02	100	65.49	6.88	687.63	0.69	13.75	34.35

4.7 HPLC Chromatogram for experimental calculations

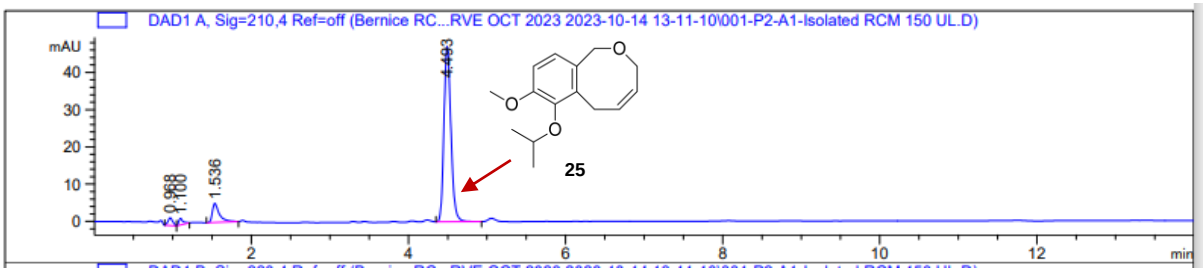

Figure 65: Chromatogram of (*Z*)-7-isopropoxy-8-methoxy-3,6-dihydro-1*H*-benzo[*c*]oxocine **25** (Batch isolated)

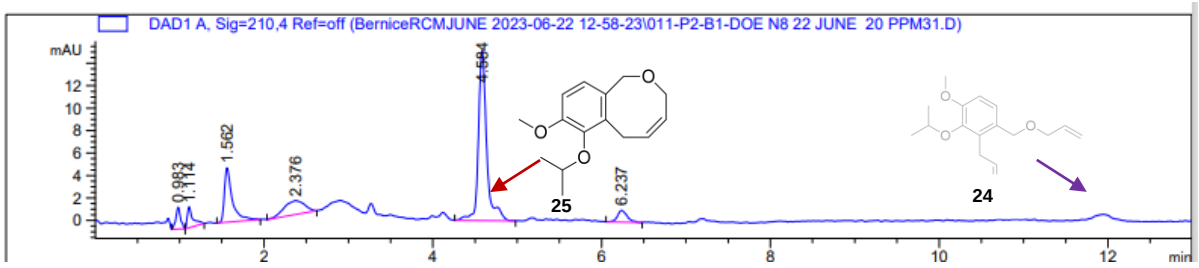

Figure 66: Chromatogram of (*Z*)-7-isopropoxy-8-methoxy-3,6-dihydro-1*H*-benzo[*c*]oxocine **25** (entry 8)

Appendix C: Nuclear magnetic resonance spectrums

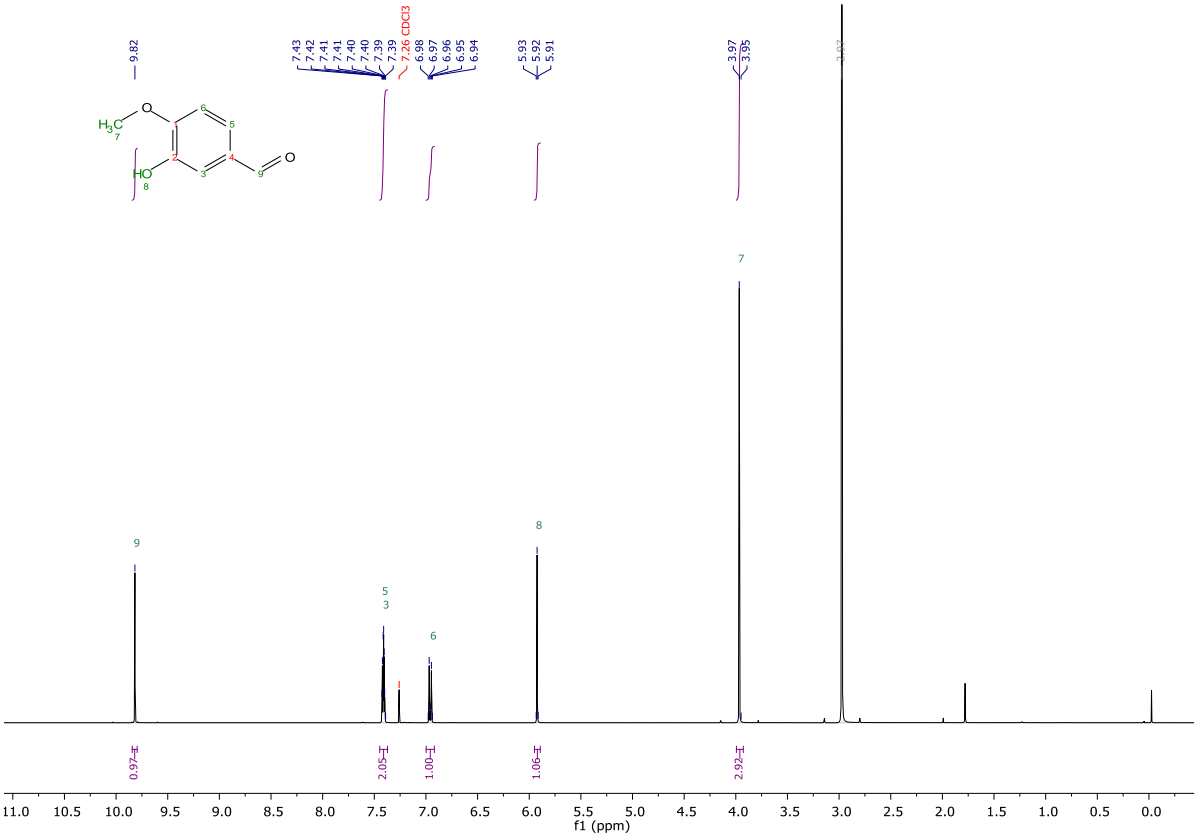

NMR 1: ^{1}H spectrum for Isovanillin **17** using internal standard $DMSO_2$

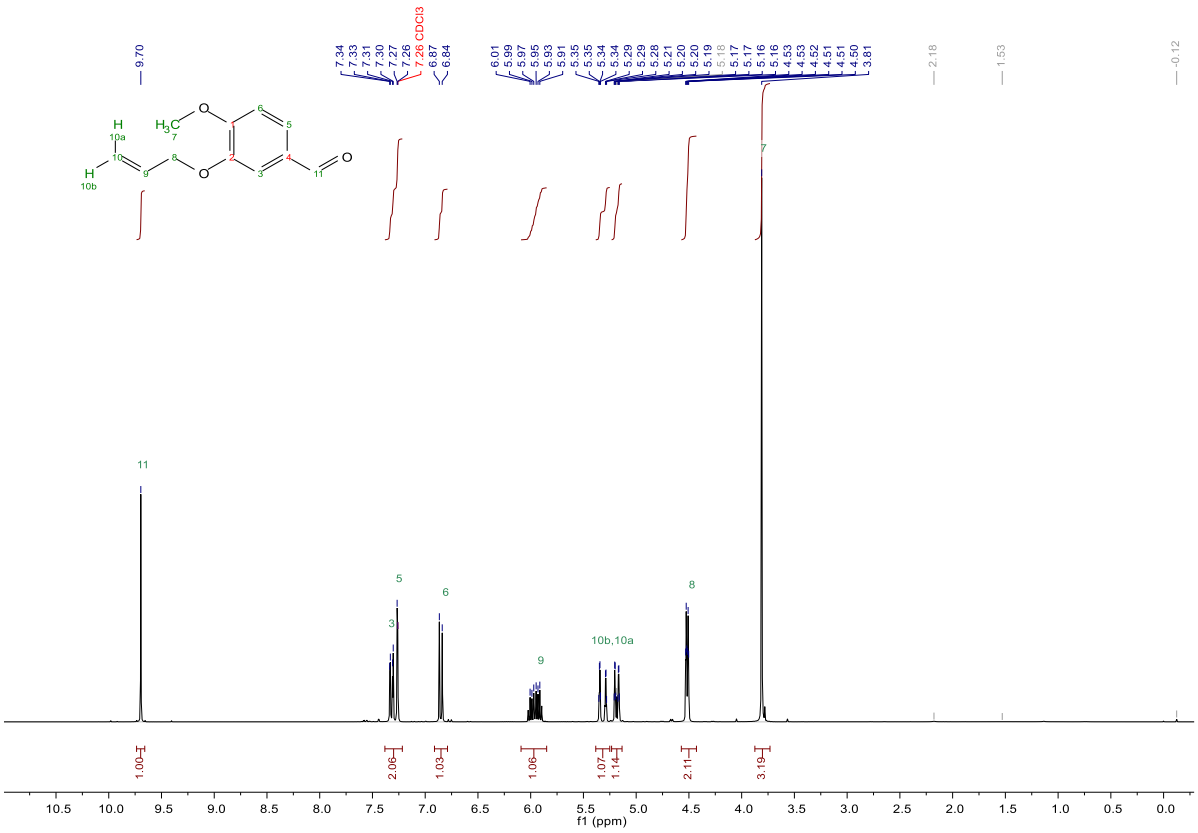

NMR 2: ^{1}H spectrum for 3-(allyloxy)-4-methoxybenzaldehyde **19**

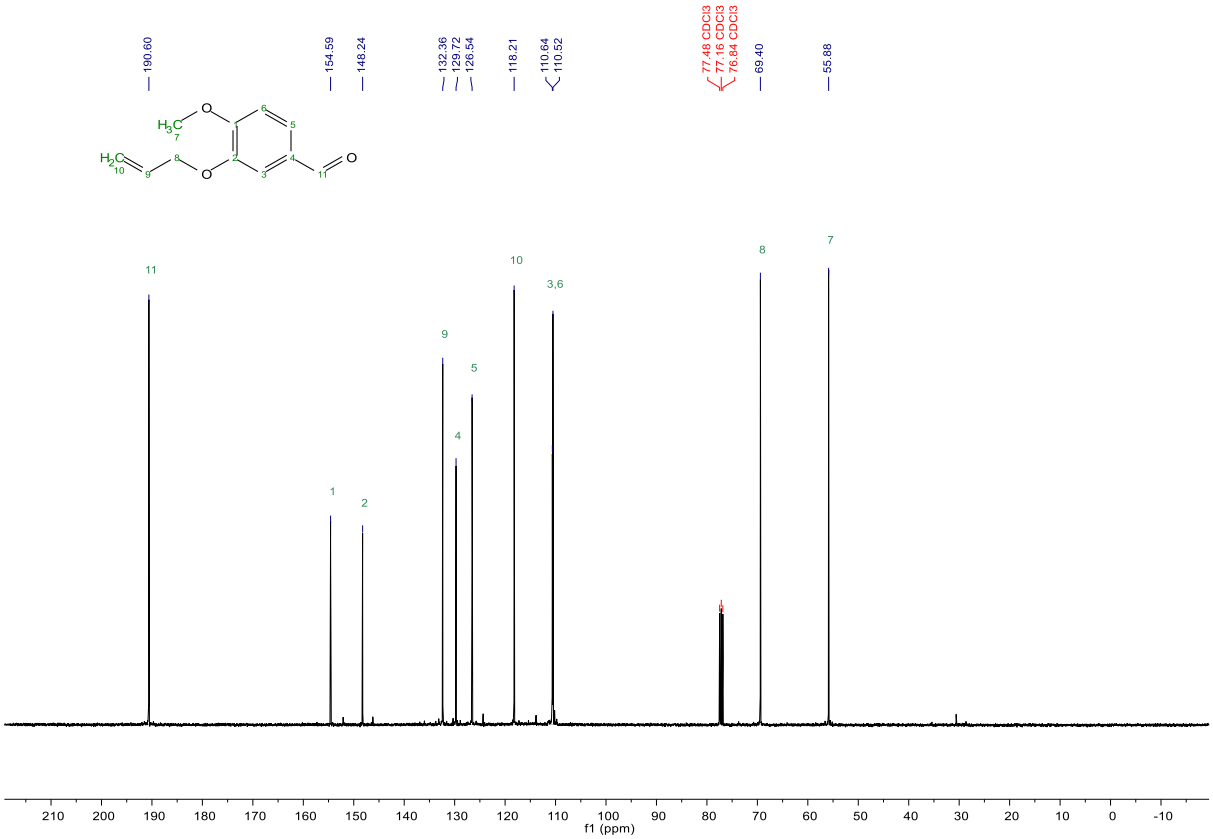

NMR 3: ^{13}C spectrum for 3-(allyloxy)-4-methoxybenzaldehyde **19**

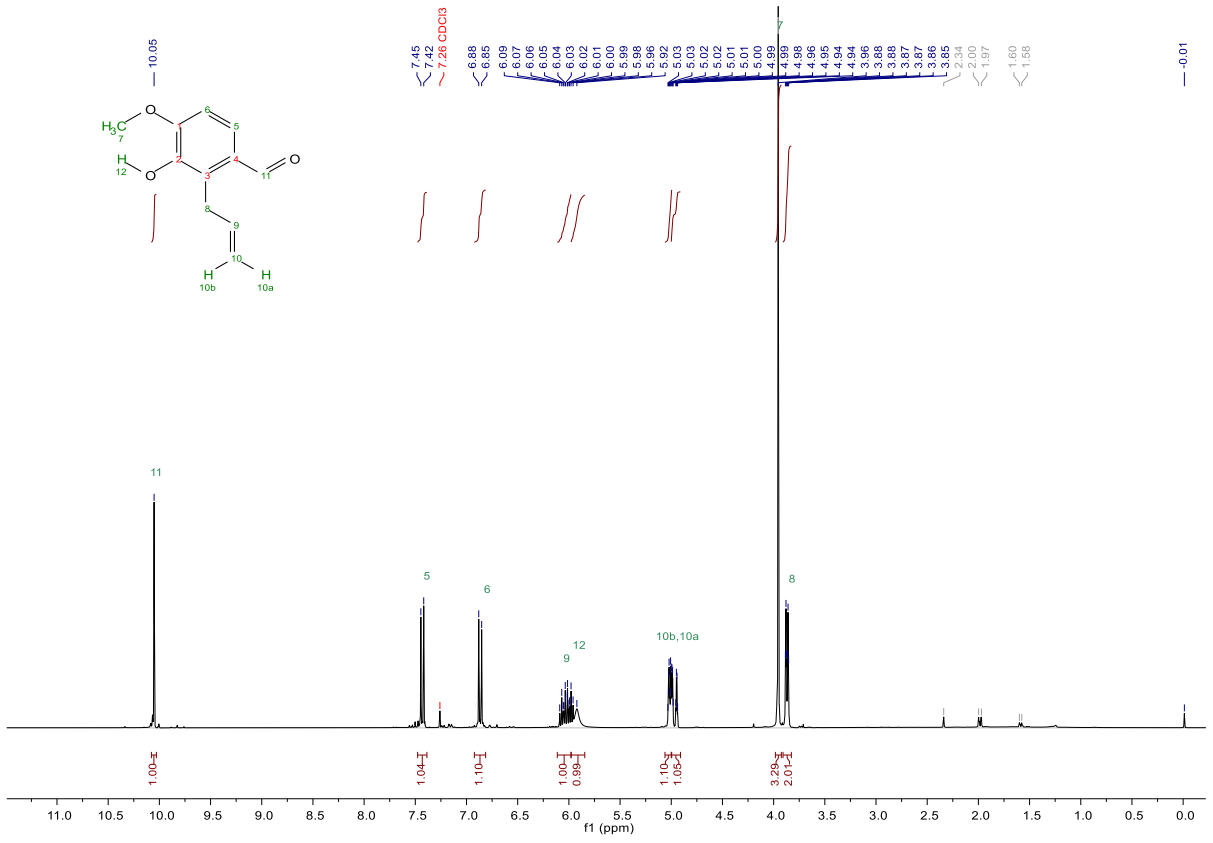

NMR 4: ^{1}H spectrum for 2-allyl-3-hydroxy-4-methoxybenzaldehyde **20**

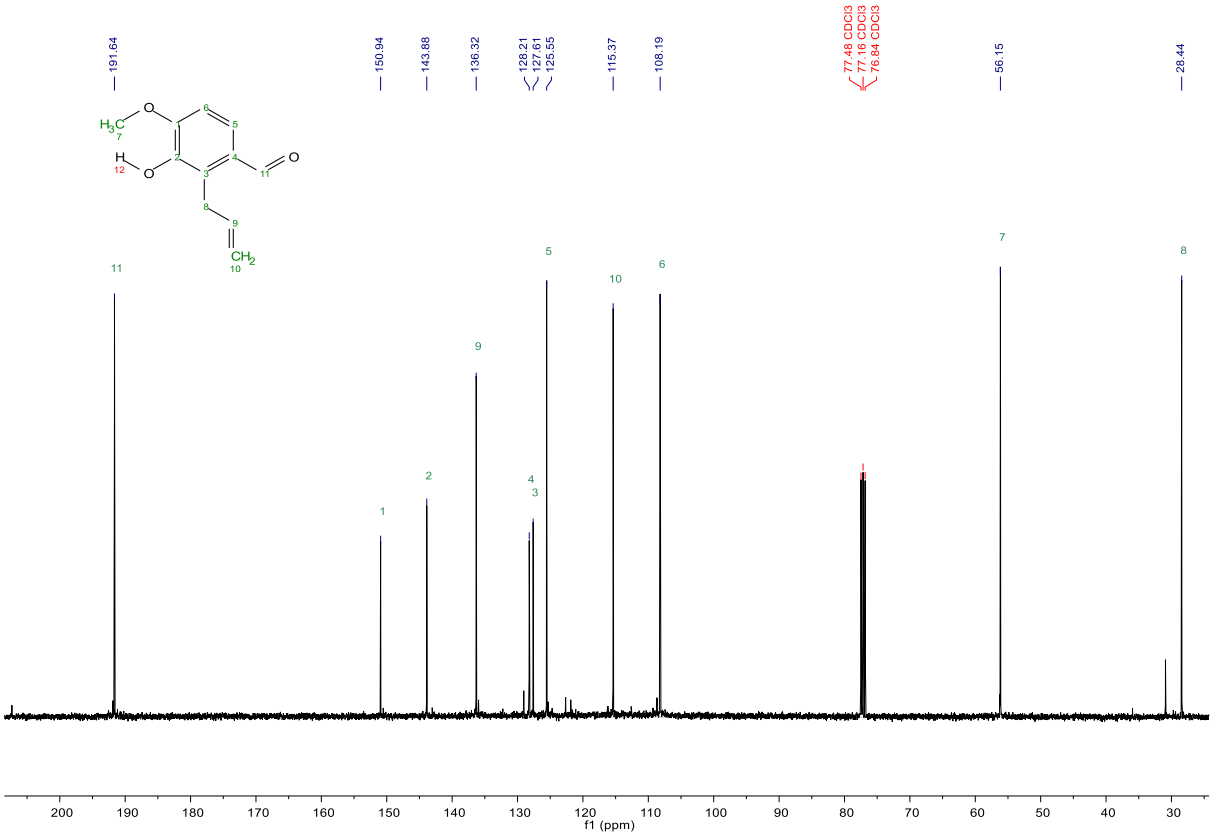

NMR 5: ^{13}C spectrum for 2-allyl-3-hydroxy-4-methoxybenzaldehyde **20**

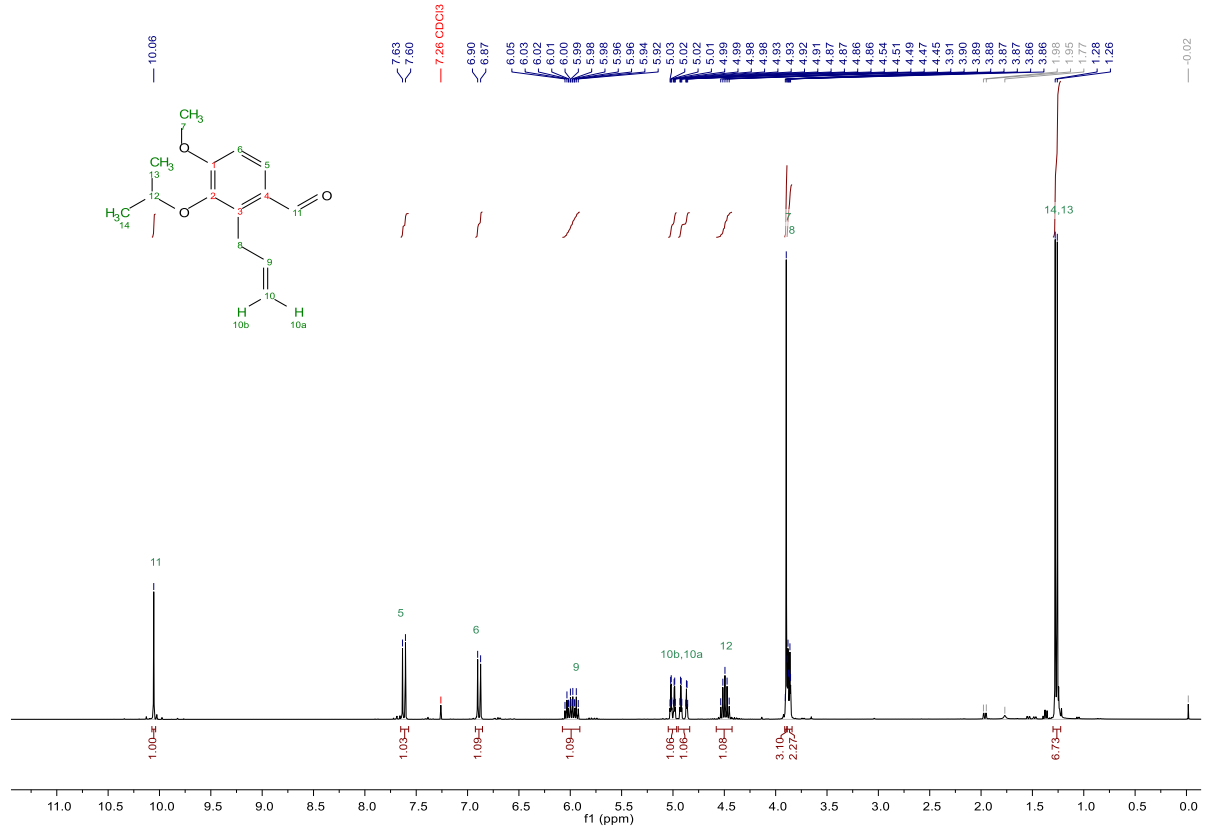

NMR 6: ^{1}H spectrum for 2-allyl-3-isopropoxy-4-methoxybenzaldehyde **22**

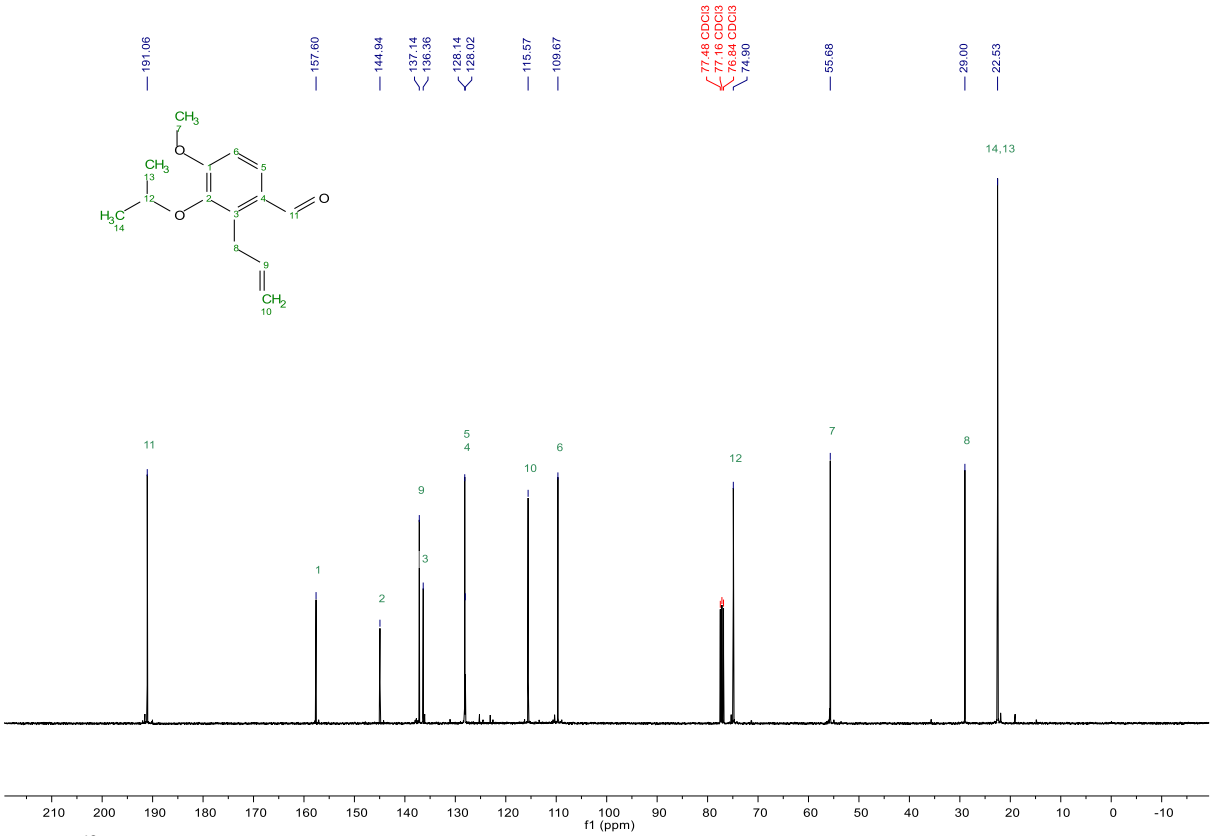

NMR 7: ^{13}C spectrum for 2-allyl-3-isopropoxy-4-methoxybenzaldehyde **22**

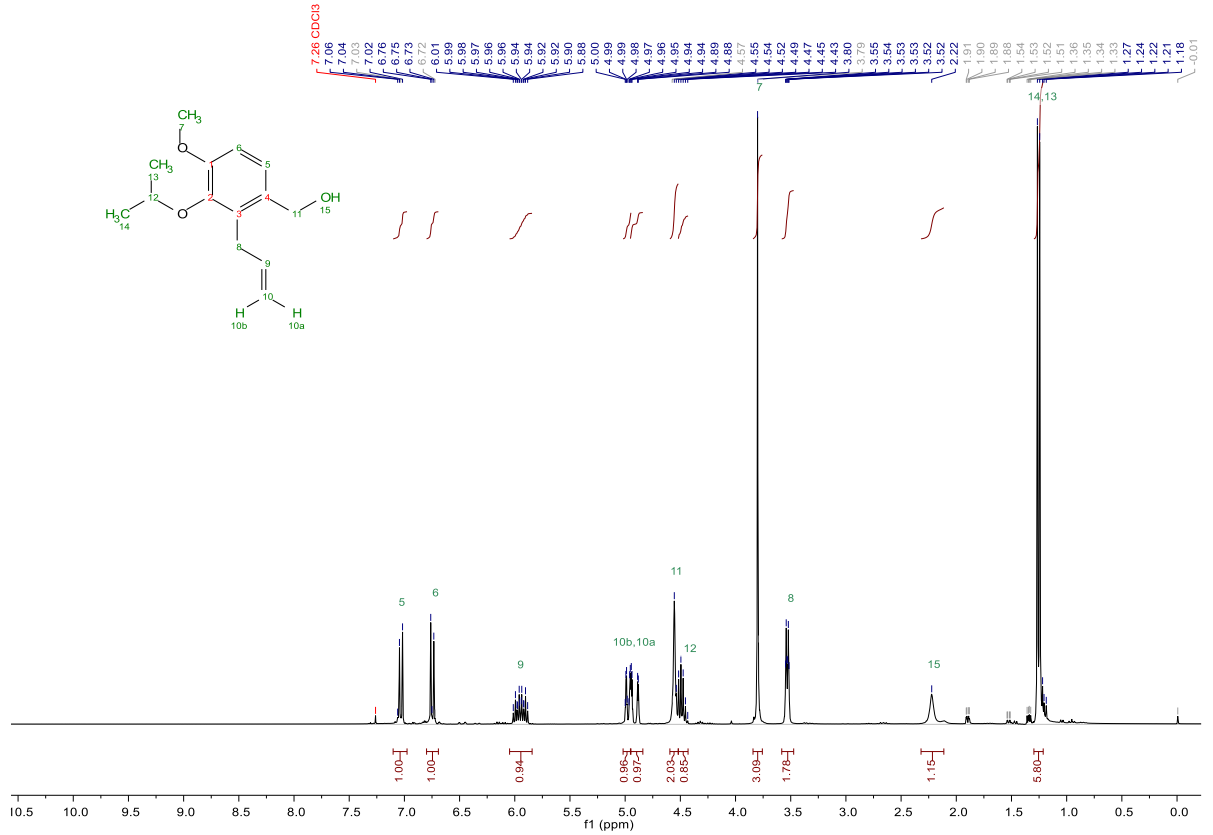

NMR 8: ^{1}H spectrum for (2-allyl-3-isopropoxy-4-methoxyphenyl)methanol **23**

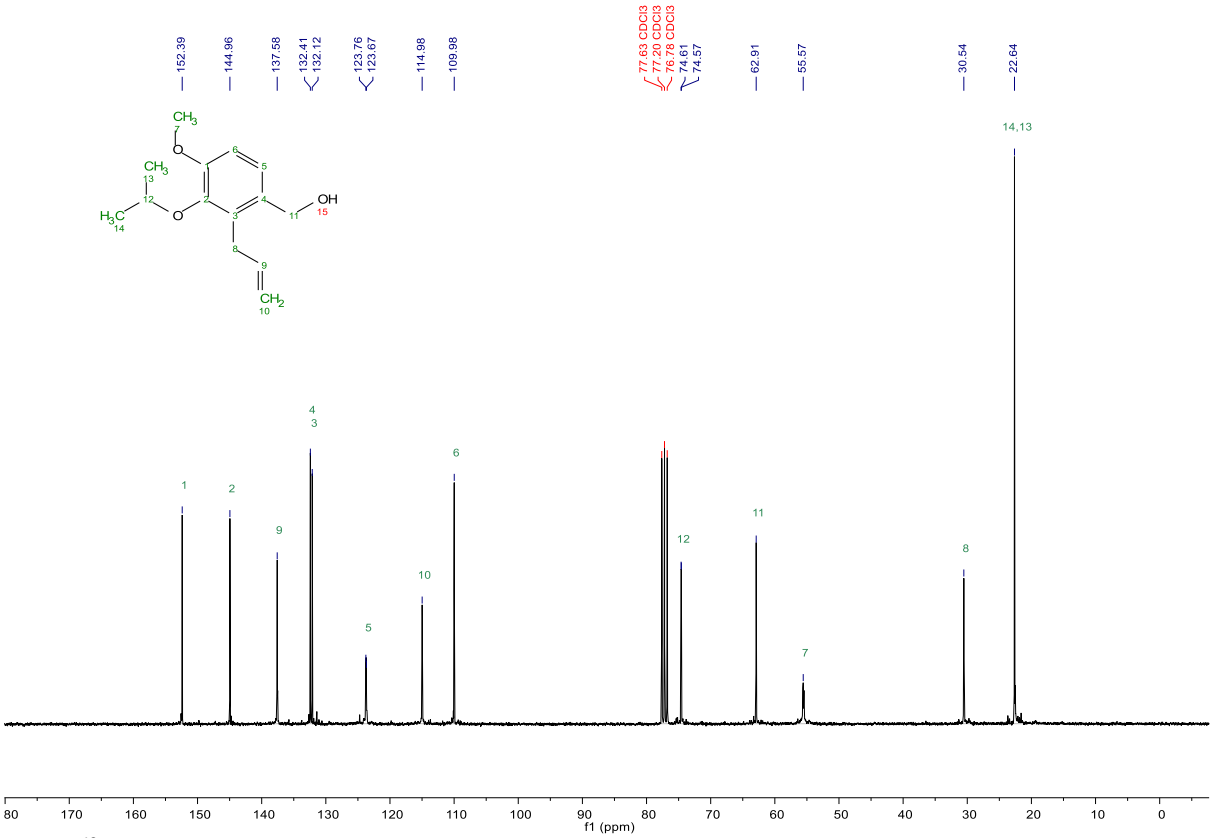

NMR 9: ^{13}C spectrum for (2-allyl-3-isopropoxy-4-methoxyphenyl)methanol **23**

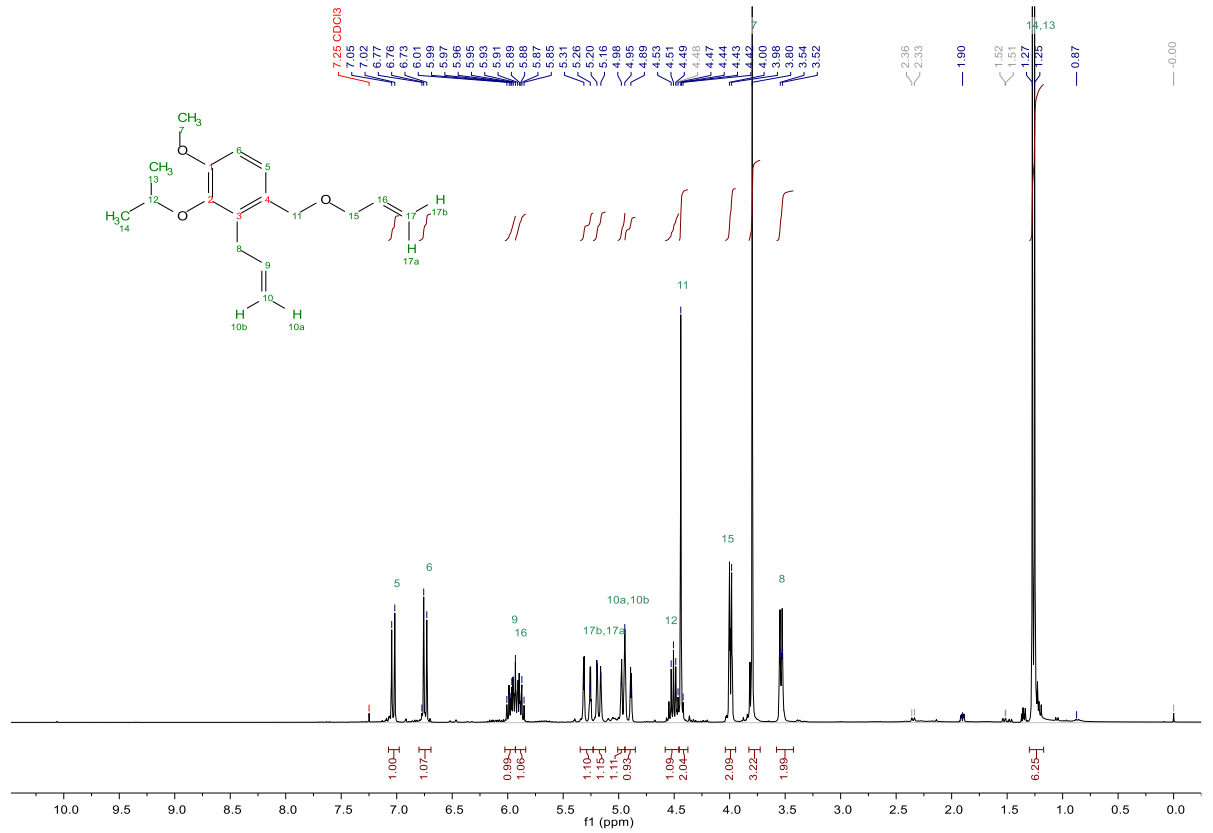

NMR 10: ^{1}H spectrum for 2-allyl-1-((allyloxy)methyl)-3-isopropoxy-4-methoxybenzene **24**

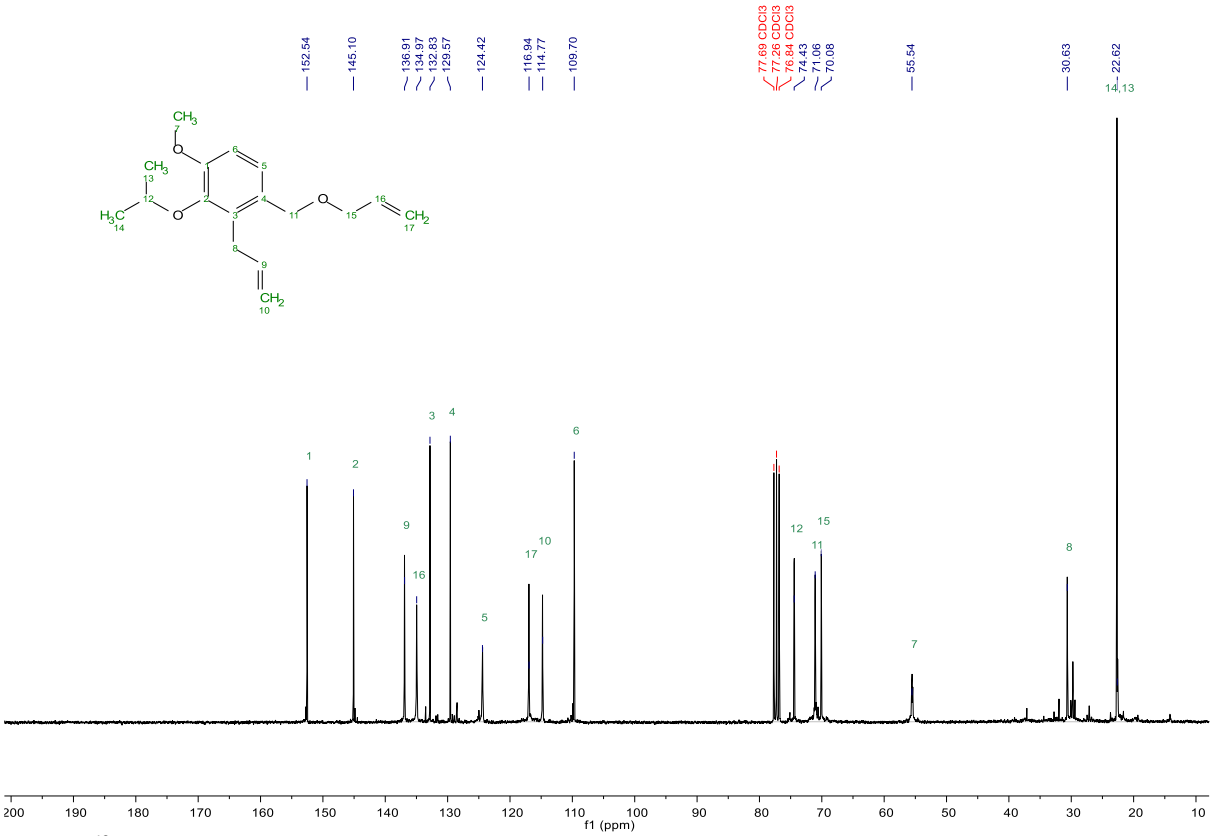

NMR 11: ^{13}C spectrum for 2-allyl-1-((allyloxy)methyl)-3-isopropoxy-4-methoxybenzene **24**

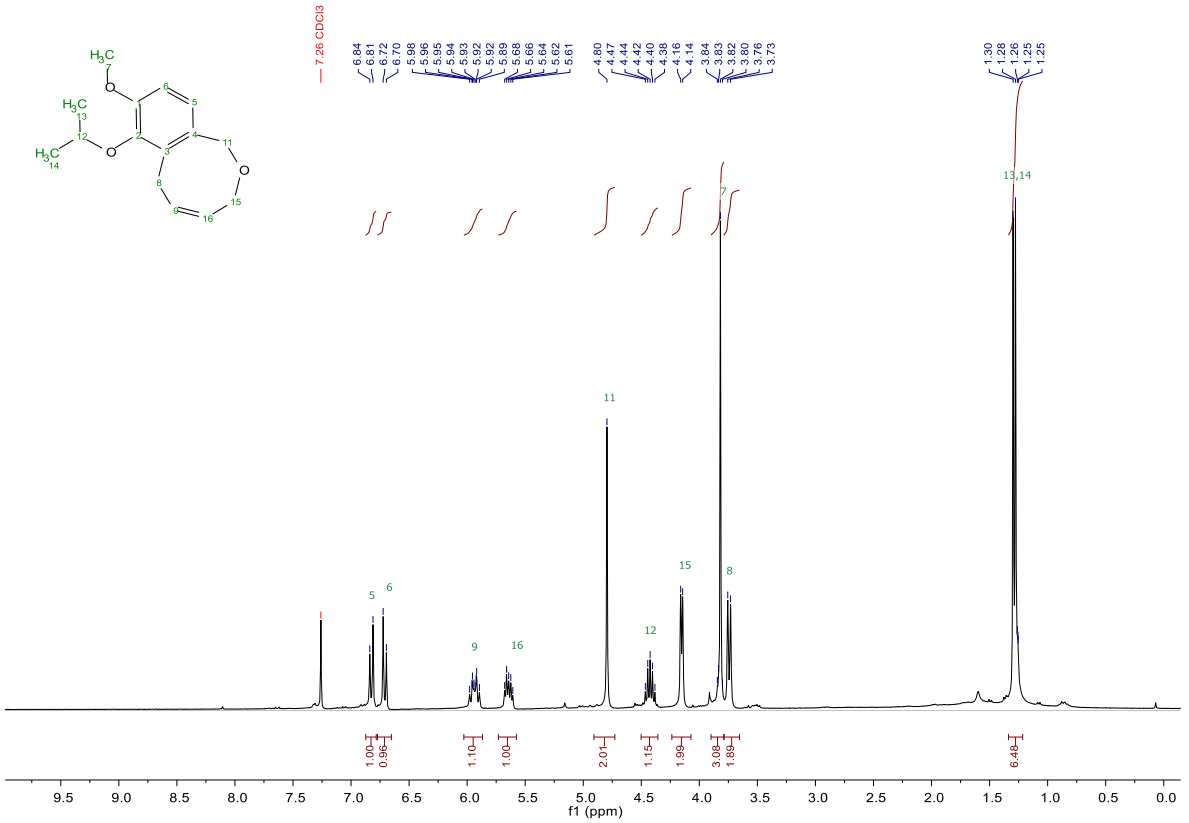

NMR 12: ^{1}H spectrum for (*Z*)-7-isopropoxy-8-methoxy-3,6-dihydro-1*H*-benzo[*c*]oxocine **25**

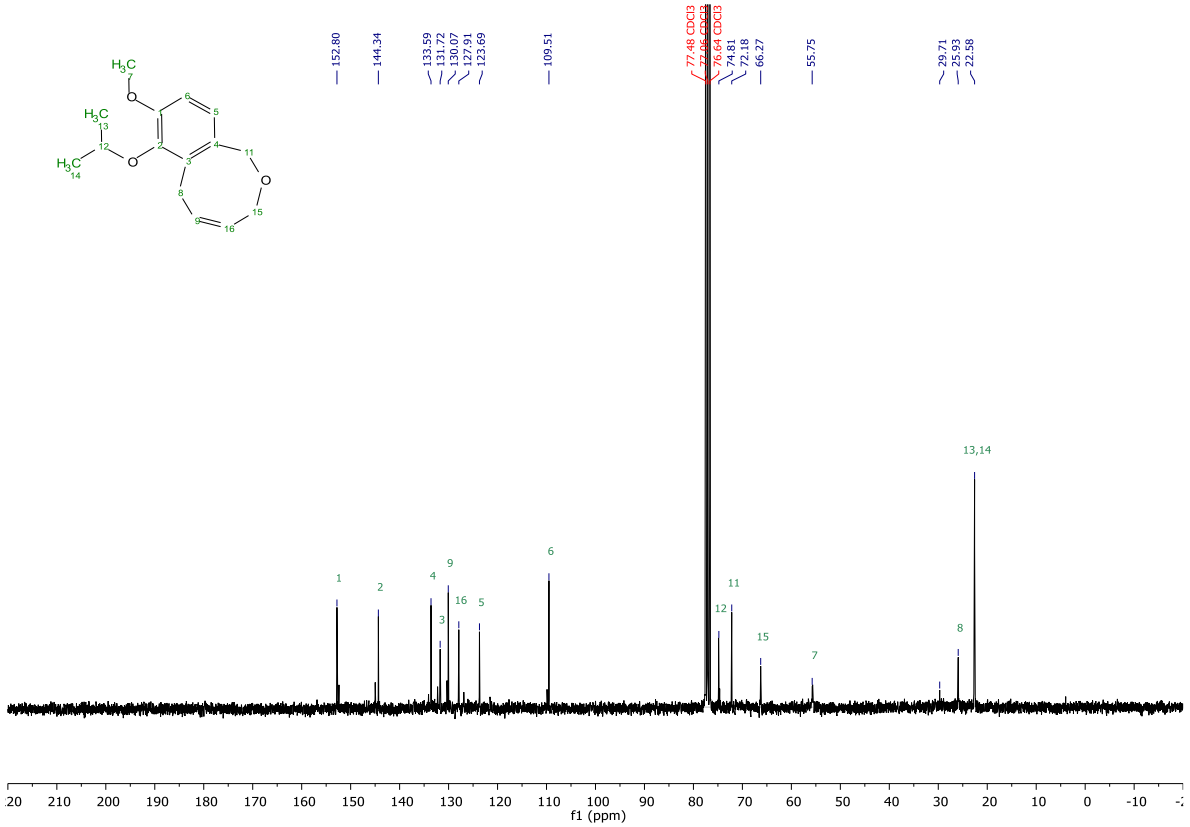

NMR 13: ^{13}C spectrum for (*Z*)-7-isopropoxy-8-methoxy-3,6-dihydro-1*H*-benzo[*c*]oxocine **25**

Appendix D: Fourier transform infrared spectrums

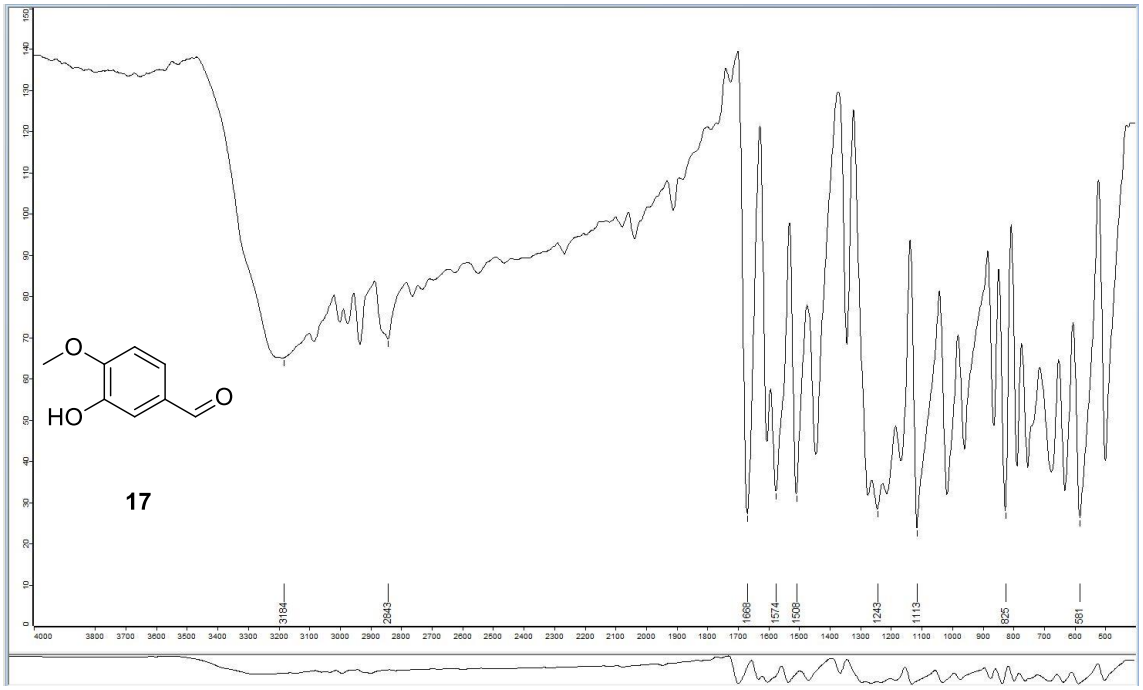

IR spectrum 1: Isovanillin **17**

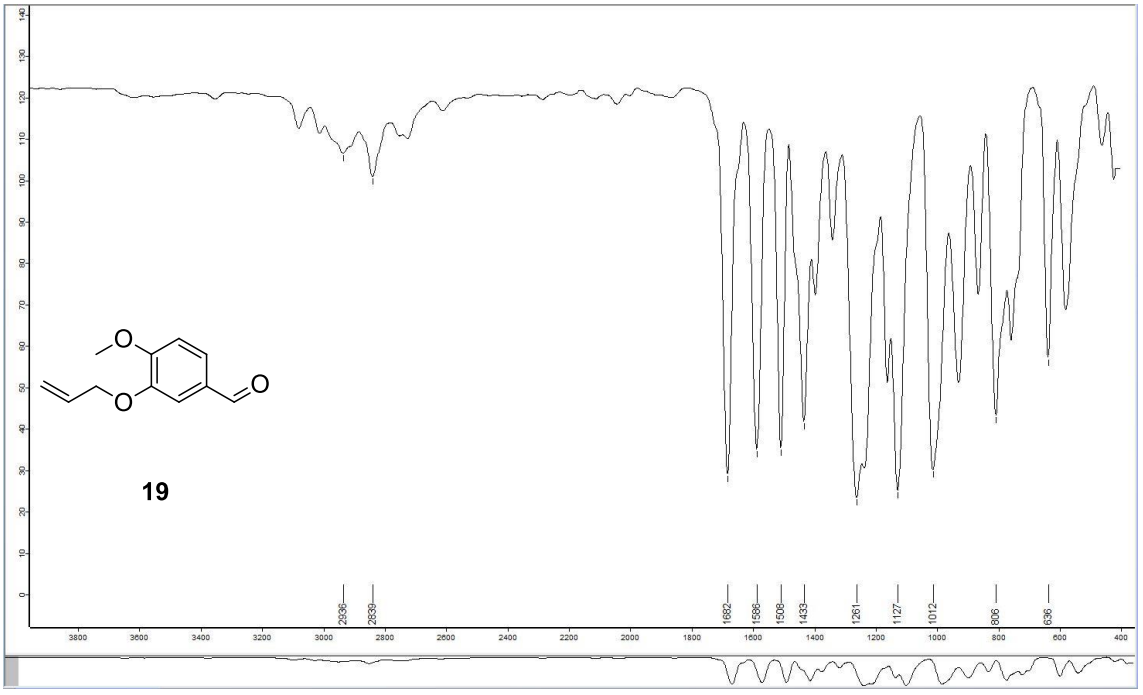

IR spectrum 2: 3-(allyloxy)-4-methoxybenzaldehyde **19**

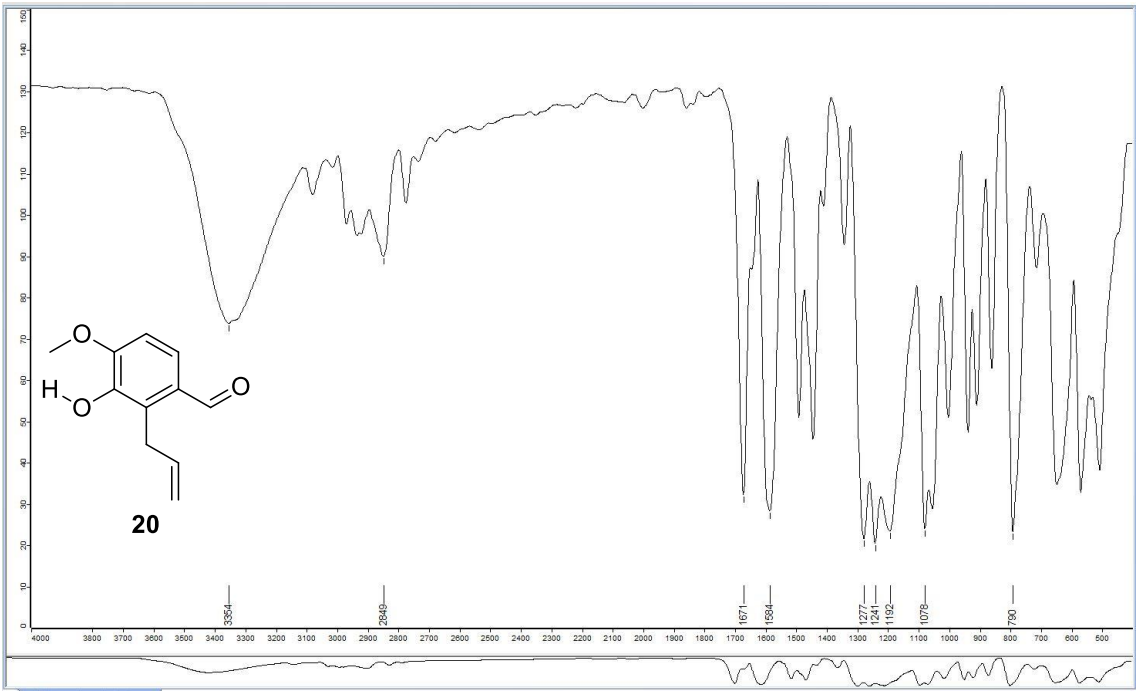

IR spectrum 3: 2-allyl-3-hydroxy-4-methoxybenzaldehyde **20**

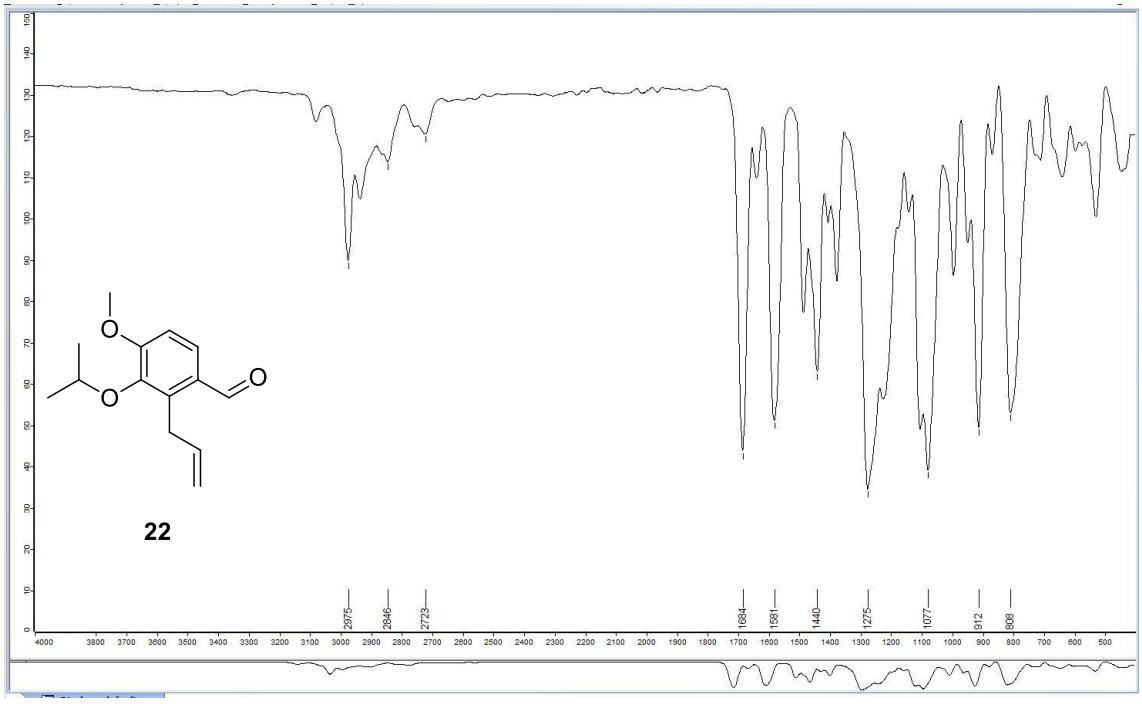

IR spectrum 4: 2-allyl-3-isopropoxy-4-methoxybenzaldehyde**22**

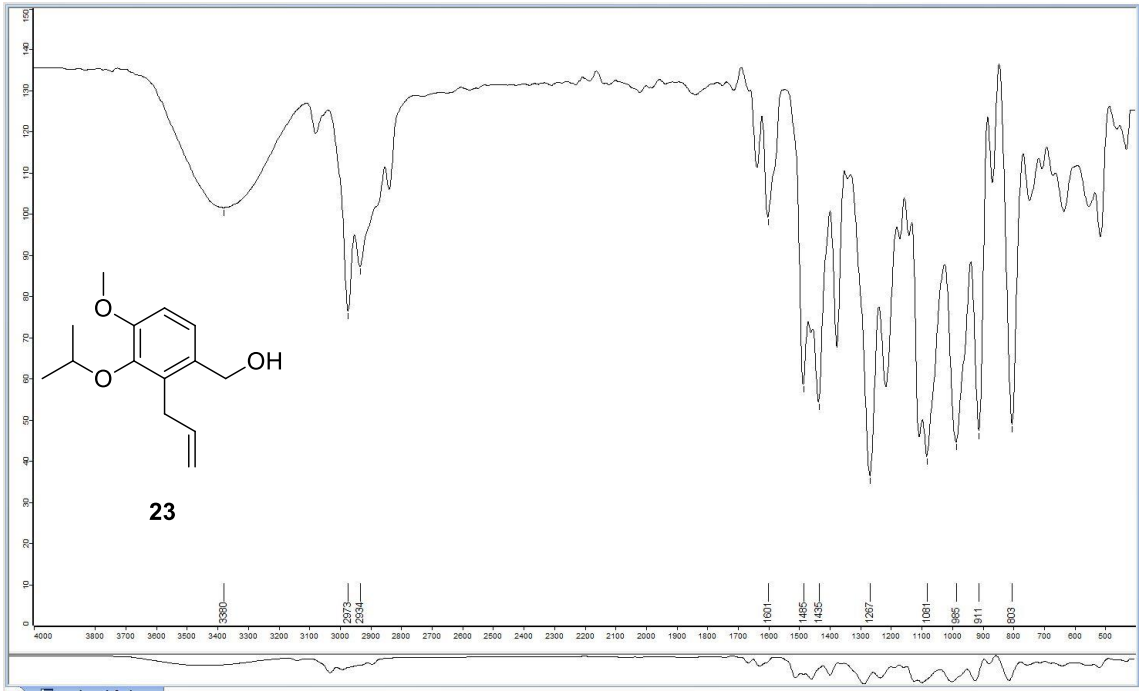

IR spectrum 5: (2-allyl-3-isopropoxy-4-methoxyphenyl)methanol **23**

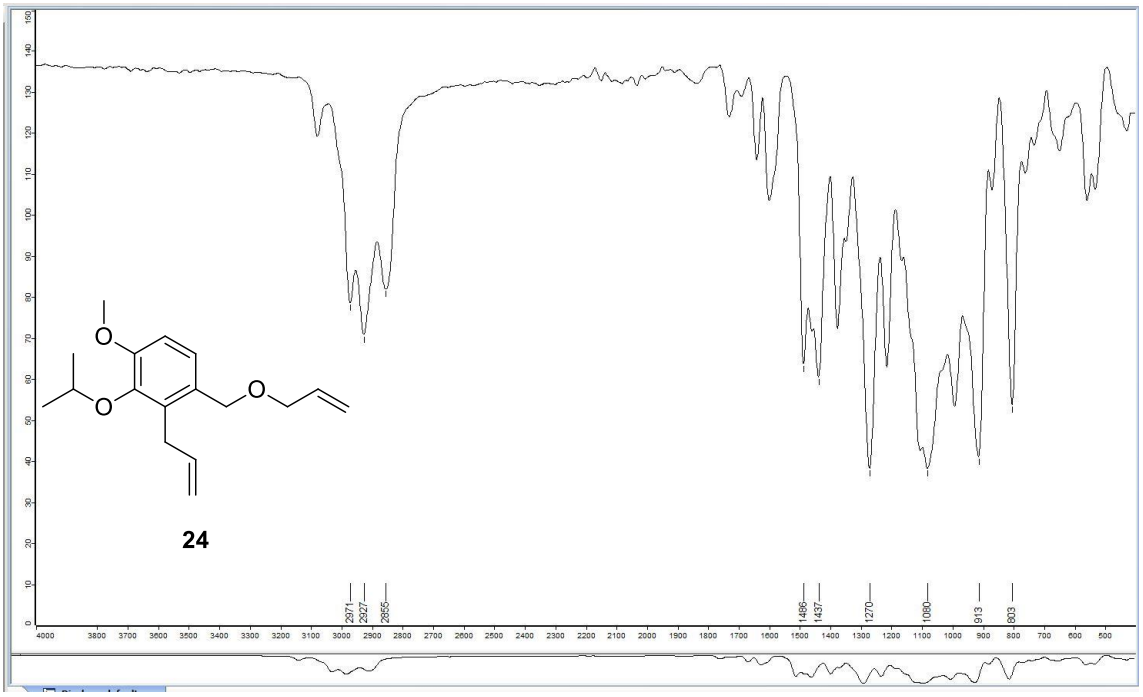

IR spectrum 6: 2-allyl-1-((allyloxy)methyl)-3-isopropoxy-4-methoxybenzene **24**

Appendix E: Mass spectrometry spectrums

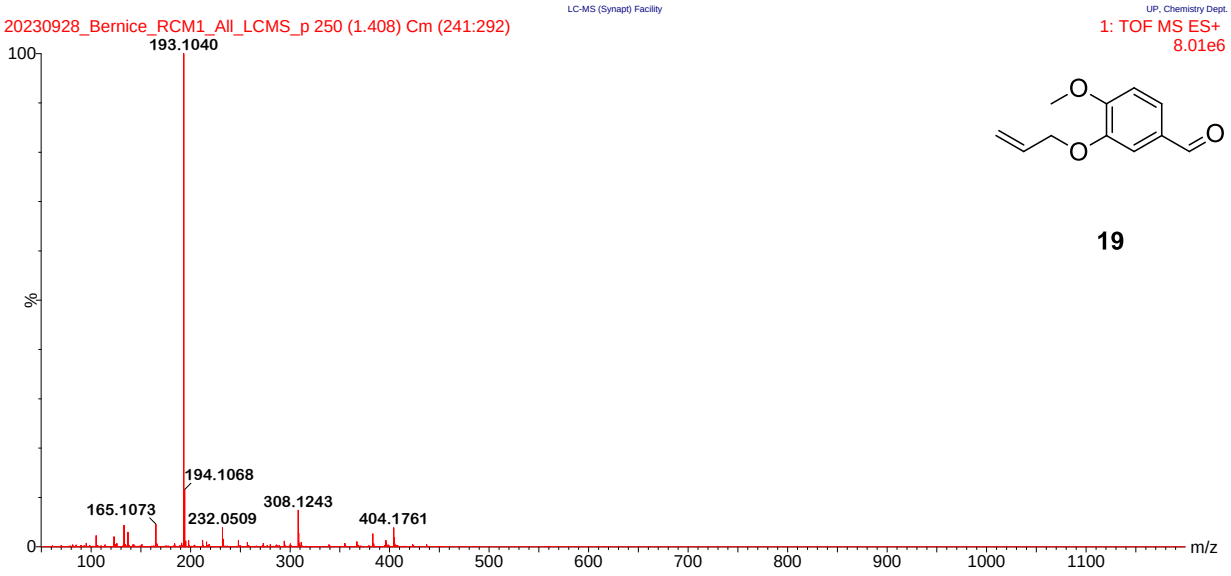

Mass spectrum 1: 3-(allyloxy)-4-methoxybenzaldehyde **19**

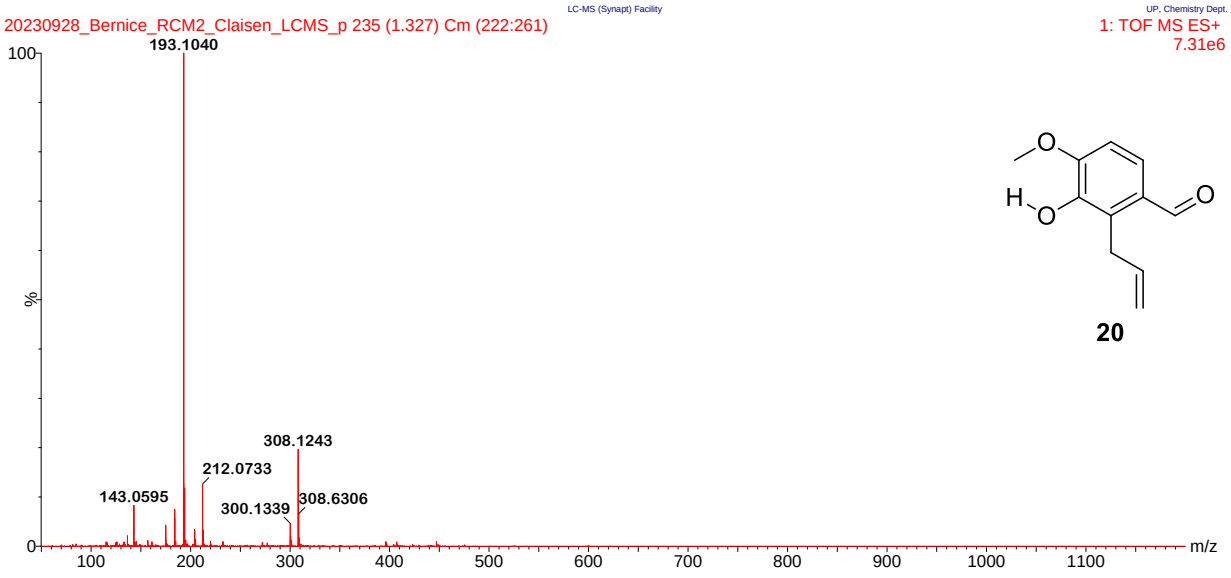

Mass spectrum 2: 2-allyl-3-hydroxy-4-methoxybenzaldehyde **20**

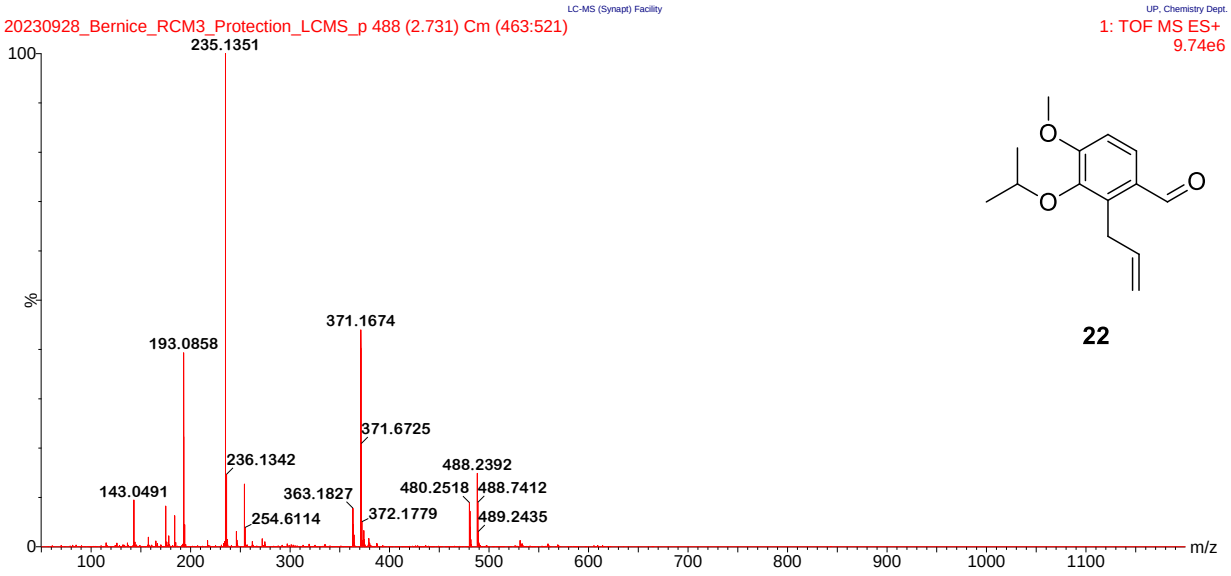

Mass spectrum 3:2-allyl-3-isopropoxy-4-methoxybenzaldehyde**22**

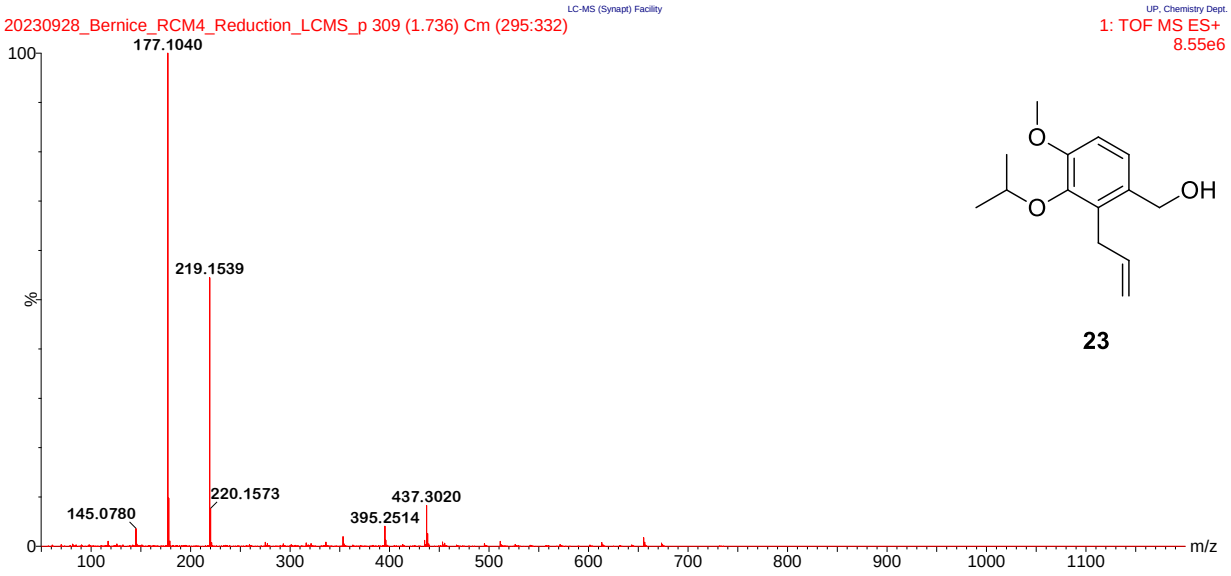

Mass spectrum 4: (2-allyl-3-isopropoxy-4-methoxyphenyl)methanol **23**

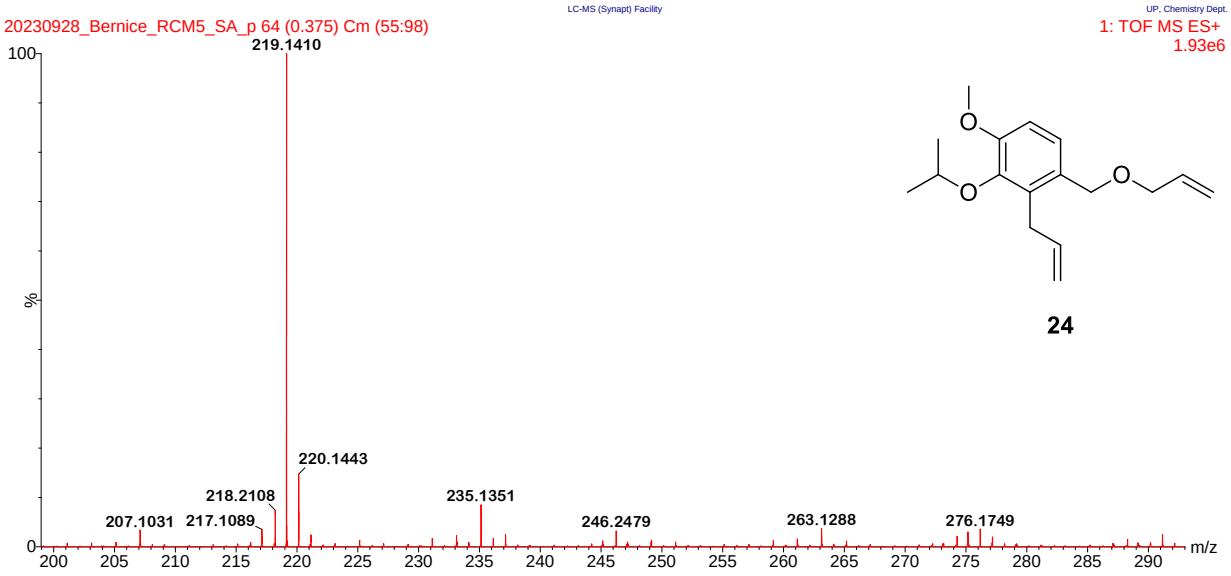

Mass spectrum 5: 2-allyl-1-((allyloxy)methyl)-3-isopropoxy-4-methoxybenzene **24**

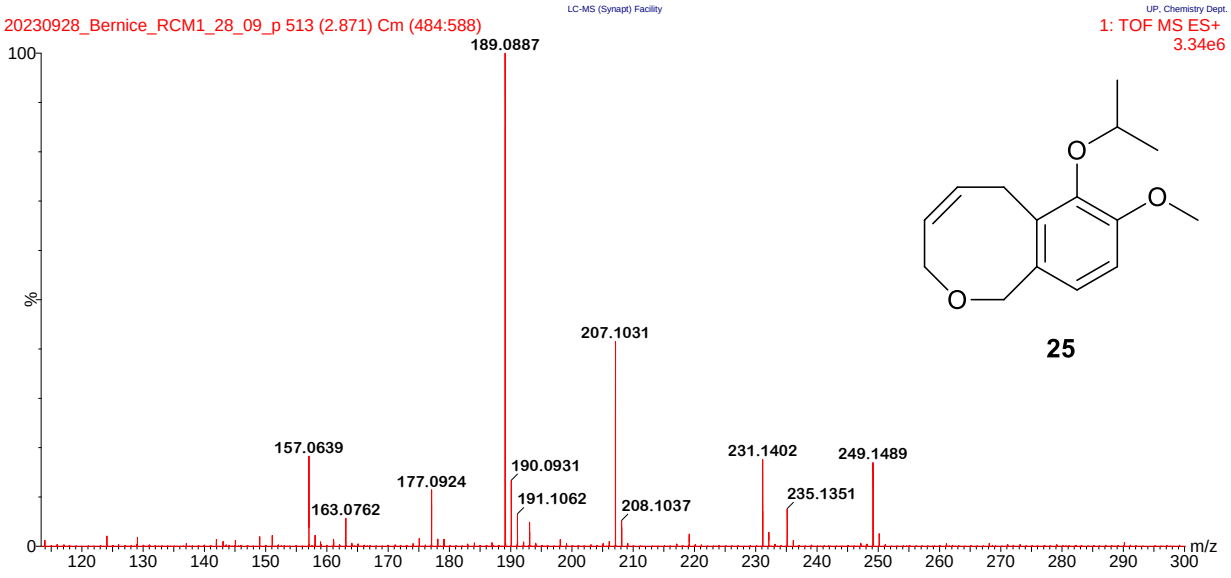

Mass spectrum 6: (*Z*)-7-isopropoxy-8-methoxy-3,6-dihydro-1*H*-benzo[*c*]oxocine **25**

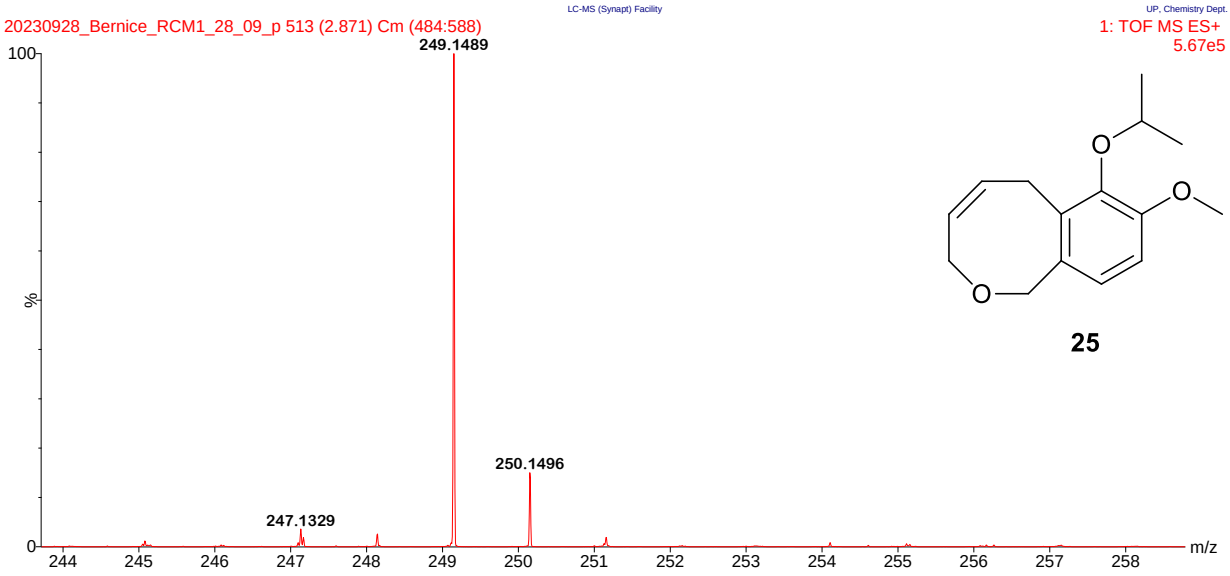

Mass spectrum 7: (*Z*)-7-isopropoxy-8-methoxy-3,6-dihydro-1*H*-benzo[*c*]oxocine **25**

Appendix F: Hazard Analysis

A. SUMMARY OF HAZARDS

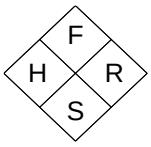	F: Flammability H: Health R: Reactivity S: Special	0: None 1: Low 2: Medium 3: High 4: Extreme

SOLVENTS

Chemical name	Potential Hazard	Severity	Preventative control measure
Toluene	• Highly flammable liquid and vapor (H225) • May be fatal if swallowed (H304) • Causes skin irritation (H315) • May cause drowsiness or dizziness (H336) • May cause damage to organs (central nervous system) through prolonged or repeated exposure (H373) • Harmful to aquatic life with long lasting effects (H412) • UEL: 7.1 % v/v • LEL: 1.2 % v/v • Flash point 4.0 °C		• Wear PPE (safety glasses, gloves, lab coat) • Conduct work in fume-cupboard • Keep away from heat, other ignition sources • Use carbon dioxide foam dry powder extinguisher in case of fire • If inhaled, remove from exposure and seek medical attention • If swallowed, rinse mouth and seek medical attention • Do NOT induce vomiting • In case of skin contact, wash with water remove contaminated clothing • In case of eye contact, flush with water
Chemical name	**Potential Hazard**	**Severity**	**Preventative control measure**
Methanol	• Highly flammable liquid and vapor (H225) • Toxic if swallowed(H301), in contact with skin (H311) or if inhaled (H331) • Causes damage to organs (eyes, central nervous system) (H370) • UEL: 44 % v/v • LEL: 5.5 % v/v • Flash point 9.7 °C – closed cup		• Wear PPE (safety glasses, gloves, lab coat) • Conduct work in fume-cupboard • Keep away from heat, hot surfaces, other ignition sources • If inhaled, remove from exposure and seek medical attention • If swallowed, immediately seek medical attention • In case of skin contact, wash with water remove contaminated clothing

Chemical name	Potential Hazard	Severity	Preventative control measure
Dimethylformamide (DMF)	• Flammable liquid and vapor (H226) • Harmful in contact with skin(H312) or if inhaled (H332) • Causes serious eye irritation (H319) • UEL: 16 % v/v • LEL: 2.2 % v/v • Flash point 57.5 °C – closed cup		• Wear PPE (safety glasses, gloves, lab coat) • Conduct work in fume-cupboard • Keep away from heat, other ignition sources • Use carbon dioxide foam dry powder extinguisher in case of fire • If inhaled, remove from exposure to fresh air and seek medical attention if needed • If swallowed, rinse mouth and seek medical attention • In case of skin contact, rinse skin with water and remove contaminated clothing • In case of eye contact, flush eyes with water for several minutes
Chemical name	**Potential Hazard**	**Severity**	**Preventative control measure**
Dichloromethane (DCM)	• Causes skin irritation (H315) • Causes serious eye irritation (H319) • May cause drowsiness or dizziness (H336) • Suspected of causing cancer (H351) • UEL: 22 % v/v • LEL: 13 % v/v		• Wear PPE (safety glasses, gloves, lab coat) • Conduct work in fume-cupboard • Keep away from heat, other ignition sources • Use water foam carbon dioxide dry powder extinguisher in case of fire • If inhaled, remove from exposure to fresh air and seek medical attention if needed • If swallowed, rinse mouth and seek medical attention • In case of skin contact, wash skin thoroughly after handling • In case of eye contact, flush eyes with water for several minutes
Chemical name	**Potential Hazard**	**Severity**	**Preventative control measure**
Tetrahydrofuran (THF)	• Highly flammable liquid and vapor (H225) • Harmful if swallowed (H302) • Causes serious eye irritation (H319) • May cause respiratory irritation (H335) • May cause drowsiness or dizziness (H336) • Suspected of causing cancer (H351)		• Wear PPE (safety glasses, gloves, lab coat) • Conduct work in fume-cupboard • Keep away from heat, other ignition sources • Use carbon dioxide foam dry powder extinguisher in case of fire • If inhaled, remove from exposure to fresh air and seek medical attention if needed • If swallowed, rinse mouth and seek

	• UEL: 11.8 % v/v • LEL: 1.8 % v/v • Flash point -21.2 °C – closed cup- DIN 51755 (part 1)		medical attention • In case of skin contact, wash skin thoroughly after handling • In case of eye contact, flush eyes with water for several minutes
Chemical name	**Potential Hazard**	**Severity**	**Preventative control measure**
Acetonitrile (ACN)	• Highly flammable liquid and vapor (H225) • Harmful if swallowed (H302) or in contact with skin (H312) or if inhaled(H332) • Causes serious eye irritation (H319) • UEL: 16 % v/v • LEL: 4.4 % v/v • Flash point 2.0. °C – closed cup		• Wear PPE (safety glasses, gloves, lab coat) • Conduct work in fume-cupboard • Keep away from heat, other ignition sources • Use carbon dioxide foam dry powder extinguisher in case of fire • If inhaled, remove from exposure to fresh air and seek medical attention if needed • If swallowed, rinse mouth and seek medical attention • In case of skin contact, wash skin thoroughly after handling • In case of eye contact, flush eyes with water for several minutes

REAGENTS

Chemical name	**Potential Hazard**	**Severity**	**Preventative control measure**
Potassium Carbonate	• Causes skin irritation (H315) • Causes serious eye irritation (H319) • May cause respiratory irritation (H335)	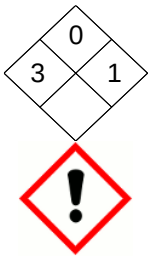	• Wear PPE (safety glasses, gloves, lab coat) • Conduct work in fume-cupboard • If swallowed, rinse mouth and seek medical attention • In case of skin contact, wash skin thoroughly after handling • In case of eye contact, flush eyes with water for several minutes
Chemical name	**Potential Hazard**	**Severity**	**Preventative control measure**
(Red-Al ≥60 wt. % in toluene)	• Highly flammable liquid and vapor (H225) • In contact with water releases flammable gases which may ignite spontaneously (H260) • May be fatal if swallowed and enters airways (H304) • Causes severe skin burns and eye damage (H314)		• Wear PPE (safety glasses, gloves, lab coat) • Conduct work in fume-cupboard • Keep away from heat, other ignition sources • Handle and store contents under inert gas. Protect from moisture • Use dry powder extinguisher and dry sand in case of fire

	• May cause drowsiness or dizziness(H336) • Suspected of damaging the unborn child (H361d) • May cause damage to organs (central nervous system) through prolonged or repeated exposure (H373) • Harmful to aquatic life with long lasting effects (H412) • UEL: 7 % v/v • LEL: 1.27 % v/v • Flash point 4 °C – closed cup		• Do NOT use water jet • If inhaled, remove from exposure to fresh air and seek medical attention • If swallowed, rinse mouth and seek medical attention • Do NOT induce vomiting • In case of skin contact, wash skin thoroughly after handling • In case of eye contact, flush eyes with water for several minutes • **Supplemental Hazard information (EU) EUH014 Reacts violently with water**
Chemical name	**Potential Hazard**	**Severity**	**Preventative control measure**
Sodium Hydride (60 % dispersion in mineral oil)	• Flammable solid (H228) • In contact with water releases flammable gases which may ignite spontaneously (H260) • May be corrosive to metals (H290) • Causes severe skin burns and eye damage (H314) •		• Wear PPE (safety glasses, gloves, lab coat) • Conduct work in fume-cupboard • Keep away from heat, other ignition sources • Handle and store contents under inert gas. Protect from moisture • Use carbon dioxide foam dry powder extinguisher in case of fire • Do NOT use water foam • If inhaled, seek medical attention • If swallowed, seek medical attention • In case of skin contact, wash skin thoroughly after handling • In case of eye contact, seek medical attention • **Supplemental Hazard information (EU) EUH014 Reacts violently with water**
Chemical name	**Potential Hazard**	**Severity**	**Preventative control measure**
Sodium borohydride	• Substances and mixtures which in contact with water emit flammable gases (H260) • Acute toxicity, (H301) • Skin corrosion (H314) • Serious eye damage (H318) • Reproductive toxicity (H360FD) • LEL: 3.02 % v/v • Flash point 69 °C – closed cup		• Wear PPE (safety glasses, gloves, lab coat) • Conduct work in fume-cupboard • Keep away from heat, other ignition sources • Handle and store contents under inert gas. Protect from moisture • Use Sand Dry powder Cement in case of fire • Do NOT use water carbon dioxide foam extinguisher • If inhaled, remove from exposure to

			fresh air and seek medical attention if needed • If swallowed, rinse mouth and seek medical attention • In case of skin contact, wash skin thoroughly after handling • In case of eye contact, flush eyes with water for several minutes
Chemical name	**Potential Hazard**	**Severity**	**Preventative control measure**
Grubbs Catalyst® (M204) and Hoveyda-Grubbs Catalyst	• Flammable solid (H228)		• Wear PPE (safety glasses, gloves, lab coat) • Conduct work in fume-cupboard • Keep away from heat, other ignition sources • Use water spray, alcohol-resistant foam, dry chemical or carbon dioxide extinguishers in case of fire • If inhaled, remove from exposure and give artificial respirator • If swallowed, Do NOT induce vomiting Never give anything by mouth to an unconscious person. Rinse mouth with water Consult a physician. • In case of skin contact, wash skin thoroughly with soap and water after handling • In case of eye contact, flush eyes with water for several minutes
Chemical name	**Potential Hazard**	**Severity**	**Preventative control measure**
Isovanillin	• Not a hazardous substance or mixture according to Regulation (EC) No. 1272/2008 •	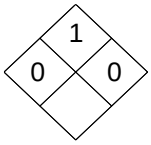	• Wear PPE (safety glasses, gloves, lab coat) • Conduct work in fume-cupboard • If inhaled, remove from exposure. • In case of skin contact, wash skin thoroughly with soap and water after handling • In case of eye contact, flush eyes with water for several minutes
Chemical name	**Potential Hazard**	**Severity**	**Preventative control measure**
Allyl Bromide	• Highly flammable liquid and vapor (H225) • Toxic if swallowed(H301) or if inhaled (H331) • Causes severe skin burns and eye	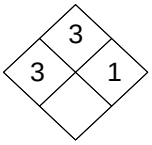	• Wear PPE (safety glasses, gloves, lab coat) • Conduct work in fume-cupboard • Keep away from heat, other ignition sources

	damage (H314) • May cause genetic defects (H340) • May cause cancer (H350) • Very toxic to aquatic life (H400) • UEL: 7.3 % v/v • LEL: 4.4 % v/v Flash point -1 °C – closed cup		• Use carbon dioxide foam dry powder extinguisher in case of fire • If inhaled, remove from exposure. If not breathing, give artificial respiration, if necessary, also give oxygen. • If swallowed, seek medical advice • In case of skin contact, wash skin thoroughly with soap and water after handling In case of eye contact, flush eyes with water for several minutes
Chemical name	**Potential Hazard**	**Severity**	**Preventative control measure**
2-Bromopropane	• Flammable liquids (H225) • Reproductive toxicity (H360F) • Specific target organ toxicity - repeated exposure (H373) Flash point 19 °C – closed cup		• Wear PPE (safety glasses, gloves, lab coat) • Conduct work in fume-cupboard • Keep away from heat, other ignition sources • Use dry powder or dry sand extinguisher in case of fire • Do NOT use water jet • If inhaled, remove from exposure. • If swallowed, seek medical advice • In case of skin contact, wash skin thoroughly with soap and water after handling • In case of eye contact, flush eyes with water for several minutes **Supplemental Hazard information (EU)EUH066 Repeated exposure may cause skin dryness or cracking.**
Chemical name	**Potential Hazard**	**Severity**	**Preventative control measure**
Potassium hydroxide	• Corrosive to metals (H290) • Harmful if swallowed (H302) • Causes severe skin burns and eye damage (H314)	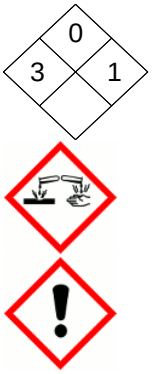	• Wear PPE (safety glasses, gloves, lab coat) • Conduct work in fume-cupboard • Keep away from heat, other ignition sources • If swallowed, seek medical advice • In case of skin contact, wash skin thoroughly with soap and water after handling In case of eye contact, flush eyes with water for several minutes

B. PRELIMINARY RISK ANALYSIS

Chemical: Toluene

Toxicity Oral (LD_{50}, mg/kg)	(Extremely toxic) ≤5		(Highly toxic) 5-50	X	(Toxic or unknown) 50-500		(Non-toxic) >500	
Sensitisation	Extreme		Moderate - Severe		Unknown, Mild	X	Non-sensitising	
irritation/Corrosion			Corrosive, Severely irritation		Unknown, Moderately irritation		Non- or Mildly irritation	X
Carcinogenicity	A1 or 2		A3		A4		A5	X
Hazard Classification	**Extreme Hazard**		**High Hazard**		**Medium Hazard**	X	**Non-Hazardous**	

Acute toxicity: LD50 Oral - Rat - male - 5.580 mg/kg (Directive 92/69/EEC.)
LC50 Inhalation - Rat - male and female - 4 h - 25,7 mg/l (OECD Test Guideline 403)
LD50 Dermal - Rabbit - > 5.000 mg/kg
Carcinogenicity: No data available
Ecotoxicity: Aquatic vertebrated: LC50 - Oncorhynchus kisutch (coho salmon) - 5,5 mg/l – 96(**ECHA**)
Daphnia and other aquatic invertebrates EC50 - Ceriodaphnia dubia (water flea) - 3,78 mg/l –48 h (US-EPA)
Bacteria static test EC50 - Bacteria - 84 mg/l - 24 h (ECHA)
Biodegradability: 86% - Readily biodegradable
Bioconcentration Factor: 90
Control Measures and PPE:

Lab coat	X	Nitrile gloves	X	Safety glasses	X	Safety shoes	X	Face shield	
Overall		4 H gloves		Safety goggles		Respirator		Apron	
Other (specify)	Do not breathe vapours or let vapours accumulate, use adequate ventilation or fume cupboard. Keep away from all sources or ignition. Avoid skin and eye contact								

Storage

Toxic		Harmful		Non-harmful		Flammable	X
Acid		Bases		Oxidant		Reductant	
Incompatibilities	Avoid rubber and various plastics. Store container in a dry and well-ventilated place away from heat sources and direct sunlight.						

Disposal

Acid		General organic	X	Halogenated		Toxic		Solid	
Comments	Dispose of as hazardous general organic waste								

Spill/Leak

Evacuate area		Add sand		Add Absorbent	X	Neutralise with		Sweep up	X
Comments	In the case of a spill, carefully take up with liquid-absorbent and dispose of properly. Clean up affected area. Prevent disposal into drains or rivers. Do not release vapours into environment. Clean up affected area.								

Chemical: Methanol

Toxicity Oral (LD_{50}, mg/kg)	(Extremely toxic) ≤5		(Highly toxic) 5-50		(Toxic or unknown) 50-500	X	(Non-toxic) >500	
Sensitisation	Extreme		Moderate - Severe		Unknown, Mild		Non-sensitising	X
irritation/Corrosion			Corrosive, Severely irritation		Unknown, Moderately irritation		Non- or Mildly irritation	X
Carcinogenicity	A1 or 2		A3		A4	X	A5	
Hazard Classification	**Extreme Hazard**		**High Hazard**		**Medium Hazard**	X	**Non-Hazardous**	

Acute toxicity: Acute toxicity estimate Oral - 100,1 mg/kg
Carcinogenicity: No data available
Ecotoxicity: Aquatic vertebrated: LC50 - Lepomis macrochorus (Bluegill) - 15.400,0 mg/l - 96 h (US-EPA)
Daphnia and other aquatic invertebrates EC50 - Daphnia magna (Water flea) - 18.260 mg/l - 96 h (OECD Test Guideline 202)
Bacteria static test IC50 - activated sludge - > 1.000 mg/l - 3 h (OECD Test Guideline 209)
Biodegradability: 99%- Readily biodegradable
Bioconcentration Factor: 1.0
Control Measures and PPE:

Lab coat	X	Nitrile gloves	X	Safety glasses	X	Safety shoes	X	Face shield	
Overall		4 H gloves		Safety goggles		Respirator		Apron	
Other (specify)	Do not breathe vapours or let vapours accumulate, use adequate ventilation. Keep away from all sources or ignition. Avoid skin and eye contact								

Storage

Toxic		Harmful		Non-harmful		Flammable	X
Acid		Bases		Oxidant		Reductant	
Incompatibilities	Avoid magnesium, zinc alloys and various plastics. Store container in a dry and well-ventilated place away from heat sources and direct sunlight.						

Disposal

Acid		General organic	X	Halogenated		Toxic		Solid	
Comments	Dispose of as hazardous general organic waste								

Spill/Leak

Evacuate area		Add sand		Add Absorbent		Neutralise with		Sweep up	X
Comments	In the case of a spill, carefully clean up affected area. Prevent disposal into drains or rivers. Do not release vapours into environment. Hydrolyzes readily with water								

Chemical: Dimethylformamide (DMF)

Toxicity Oral (LD_{50}, mg/kg)	(Extremely toxic) ≤5	X	(Highly toxic) 5-50		(Toxic or unknown) 50-500		(Non-toxic) >500	
Sensitisation	Extreme		Moderate - Severe		Unknown, Mild	X	Non-sensitising	
irritation/Corrosion			Corrosive, Severely irritation		Unknown, Moderately irritation		Non- or Mildly irritation	X
Carcinogenicity	A1 or 2		A3		A4	X	A5	
Hazard Classification	**Extreme Hazard**		**High Hazard**		**Medium Hazard**	X	**Non-Hazardous**	

Acute toxicity: LD50 Oral - Rat - male and female - 3.010 mg/kg (OECD Test Guideline 401)
Carcinogenicity: No data available
Ecotoxicity: Aquatic vertebrated: LC50 - Lepomis macrochirus (Bluegill sunfish) - 7.100 mg/l - 96 h (US-EPA)
Daphnia and other aquatic invertebrates static test EC50 - Daphnia magna (Water flea) - 13.100 mg/l - 48 h (OECD Test Guideline 202)
Bacteria static test EC50 - Vibrio fischeri - 12.300 - 17.500 mg/l - 5 min Remarks: (ECHA)
Biodegradability: 100%-Readily biodegradable
Bioconcentration Factor: 0.3-1.2 (OECD Test Guideline 305C)
Control Measures and PPE:

Lab coat	X	Nitrile gloves	X	Safety glasses	X	Safety shoes	X	Face shield	
Overall		4 H gloves		Safety goggles		Respirator		Apron	
Other (specify)	Work in fumehood, do not breathe vapours or let vapours accumulate, use adequate ventilation. Keep away from all sources or ignition. Avoid skin and eye contact								

Storage

Toxic		Harmful	X	Non-harmful		Flammable	
Acid		Bases		Oxidant		Reductant	
Incompatibilities	Avoid Tin, Coper and various plastics. Store container in a dry and well-ventilated place away from heat sources and direct sunlight.						

Disposal

Acid		General organic	X	Halogenated		Toxic		Solid	
Comments	Dispose of as hazardous general organic waste								

Spill/Leak

Evacuate area		Add sand		Add Absorbent	X	Neutralise with		Sweep up	X
Comments	In the case of a spill, carefully take up with liquid-absorbent and dispose of properly. Clean up affected area. Prevent disposal into drains or rivers. Do not release vapours into environment.								

Chemical: Dichloromethane (DCM)

Toxicity Oral (LD_{50}, mg/kg)	(Extremely toxic) ≤5	X	(Highly toxic) 5-50		(Toxic or unknown) 50-500		(Non-toxic) >500	
Sensitisation	Extreme		Moderate - Severe		Unknown, Mild	X	Non-sensitising	
irritation/Corrosion			Corrosive, Severely irritation		Unknown, Moderately irritation	X	Non- or Mildly irritation	
Carcinogenicity	A1 or 2		A3	X	A4		A5	
Hazard Classification	**Extreme Hazard**		**High Hazard**		**Medium Hazard**	X	**Non-Hazardous**	

Acute toxicity: LD50 Oral - Rat - male and female - > 2.000 mg/kg (OECD Test Guideline 401)
Carcinogenicity: Suspected human carcinogens
Ecotoxicity: Aquatic vertebrated: LC50 - Pimephales promelas (fathead minnow) - 193,00 mg/l - 96 h Remarks: (ECHA)
Daphnia and other aquatic LC50 - Daphnia magna (Water flea) - 27 mg/l - 48 h (US-EPA)
Bacteria static test EC50 - activated sludge - 2.590 mg/l - 40 min (OECD Test Guideline 209)
Biodegradability: 68 % - Readily biodegradable.
Bioconcentration Factor: 2-5.4
Control Measures and PPE:

Lab coat	X	Nitrile gloves	X	Safety glasses	X	Safety shoes	X	Face shield	
Overall		4 H gloves		Safety goggles		Respirator		Apron	
Other (specify)	Do not breathe vapours or let vapours accumulate, use adequate ventilation or fume cupboard. Keep away from all sources or ignition. Avoid substance contact with skin and eyes.								

Storage

Toxic		Harmful	X	Non-harmful		Flammable	
Acid		Bases		Oxidant		Reductant	
Incompatibilities	Avoid rubber and various plastics. Store container in a dry and well-ventilated place away from heat sources and direct sunlight.						

Disposal

Acid		General organic	X	Halogenated		Toxic		Solid	
Comments	Dispose of as hazardous general organic waste								

Spill/Leak

Evacuate area		Add sand		Add Absorbent	X	Neutralise with		Sweep up	X
Comments	In the case of a spill, carefully take up with liquid-absorbent and dispose of properly. Clean up affected area. Prevent disposal into drains or rivers. Do not release vapours into environment.								

Chemical: Tetrahydrofuran (THF)

Toxicity Oral (LD_{50}, mg/kg)	(Extremely toxic) ≤5	X	(Highly toxic) 5-50		(Toxic or unknown) 50-500		(Non-toxic) >500	
Sensitisation	Extreme		Moderate - Severe		Unknown, Mild	X	Non-sensitising	
irritation/Corrosion			Corrosive, Severely irritation		Unknown, Moderately irritation	X	Non- or Mildly irritation	
Carcinogenicity	A1 or 2		A3		A4	X	A5	
Hazard Classification	**Extreme Hazard**		**High Hazard**		**Medium Hazard**	X	**Non-Hazardous**	

Acute toxicity: LD50 Oral - Rat - male and female - 1.650 mg/kg Remarks: (ECHA)
Carcinogenicity: No data available
Ecotoxicity: Aquatic vertebrated: flow-through test LC50 - Pimephales promelas (fathead minnow) - 2.160 mg/l - 96 h (OECD Test Guideline 203)
Daphnia and other aquatic EC50 - Daphnia magna (Water flea) - 3.485 mg/l - 48 h (OECD Test Guideline 202)
Bacteria static test EC20 - activated sludge - ca. 800 mg/l - 0,5 h (OECD Test Guideline 209)
Biodegradability: 39 % - Not readily biodegradable.

Control Measures and PPE:

Lab coat	X	Nitrile gloves	X	Safety glasses	X	Safety shoes	X	Face shield	
Overall		4 H gloves		Safety goggles		Respirator	X	Apron	
Other (specify)	Do not breathe vapours or let vapours accumulate, use adequate ventilation or fume cupboard. Keep away from all sources or ignition. Avoid skin and eye contact. Use respirator (Filter A, for organic compounds)								

Storage

Toxic		Harmful		Non-harmful		Flammable	X
Acid		Bases		Oxidant		Reductant	
Incompatibilities	Avoid Tin, rubber and various plastics. Store container in a dry and well-ventilated place away from heat sources and direct sunlight. Avoid moisture conditions						

Disposal

Acid		General organic	X	Halogenated		Toxic		Solid	
Comments	Dispose of as hazardous general organic waste								

Spill/Leak

Evacuate area		Add sand		Add Absorbent	X	Neutralise with		Sweep up	X
Comments	In the case of a spill, carefully take up with liquid-absorbent and dispose of properly. Clean up affected area. Prevent disposal into drains or rivers. Do not release vapours into environment.								

Chemical: Acetonitrile (ACN)

Toxicity Oral (LD_{50}, mg/kg)	(Extremely toxic) ≤5		(Highly toxic) 5-50		(Toxic or unknown) 50-500		(Non-toxic) >500	X
Sensitisation	Extreme		Moderate - Severe		Unknown, Mild	X	Non-sensitising	
irritation/Corrosion			Corrosive, Severely irritation		Unknown, Moderately irritation		Non- or Mildly irritation	X
Carcinogenicity	A1 or 2		A3		A4		A5	X
Hazard Classification	**Extreme Hazard**		**High Hazard**		**Medium Hazard**	X	**Non-Hazardous**	

Acute toxicity: LD50 Oral - Mouse - male and female - 617 mg/kg (OECD Test Guideline 401)
Carcinogenicity: No data available
Ecotoxicity: Aquatic vertebrated: LC50 - Pimephales promelas (fathead minnow) - 1.640 mg/l - 96 h Remarks: (ECHA)
Biodegradability: 70% - Readily biodegradable
Control Measures and PPE:

Lab coat	X	Nitrile gloves	X	Safety glasses	X	Safety shoes	X	Face shield	
Overall		4 H gloves		Safety goggles		Respirator		Apron	
Other (specify)	Do not breathe vapours or let vapours accumulate, use adequate ventilation or fume cupboard. Keep away from all sources or ignition. Avoid skin and eye contact								

Storage

Toxic		Harmful		Non-harmful		Flammable	X
Acid		Bases		Oxidant		Reductant	
Incompatibilities	Store container in a dry and well-ventilated place away from heat sources and direct sunlight.						

Disposal

Acid		General organic	X	Halogenated		Toxic		Solid	
Comments	Dispose of as hazardous general organic waste								

Spill/Leak

Evacuate area		Add sand		Add Absorbent		Neutralise with		Sweep up	X
Comments	In the case of a spill, carefully clean up affected area. Prevent disposal into drains or rivers. Do not release vapours into environment.								

Chemical: Potassium Carbonate

Toxicity Oral (LD_{50}, mg/kg)	(Extremely toxic) ≤5	X	(Highly toxic) 5-50		(Toxic or unknown) 50-500		(Non-toxic) >500	
Sensitisation	Extreme		Moderate - Severe		Unknown, Mild		Non-sensitising	X
irritation/Corrosion			Corrosive, Severely irritation		Unknown, Moderately irritation	X	Non- or Mildly irritation	
Carcinogenicity	A1 or 2		A3		A4	X	A5	
Hazard Classification	**Extreme Hazard**		**High Hazard**		**Medium Hazard**	X	**Non-Hazardous**	

Acute toxicity: LD50 Oral - Rat - male and female - > 2.000 mg/kg (OECD Test Guideline 401)
Carcinogenicity: No data available
Ecotoxicity: Aquatic vertebrated: flow-through test LC50 - Oncorhynchus mykiss (rainbow trout) - 68 mg/l - 96 h Remarks: (ECHA)
Daphnia and other aquatic EC50 - EC50 - Daphnia pulex (Water flea) - 200 mg/l - 48 h Remarks: (ECHA)

Control Measures and PPE:

Lab coat	X	Nitrile gloves	X	Safety glasses	X	Safety shoes	X	Face shield	
Overall		4 H gloves		Safety goggles		Respirator		Apron	
Other (specify)	Do not breathe dust or let dust accumulate, use adequate ventilation or fume cupboard. Keep away from all sources or ignition. Avoid skin and eye contact. Avoid exposure to moisture								

Storage

Toxic		Harmful	X	Non-harmful		Flammable	
Acid		Bases		Oxidant		Reductant	
Incompatibilities	Avoid acids. Store container in a dry and well-ventilated place away from heat sources and direct sunlight. Avoid exposure to moisture						

Disposal

Acid		General organic	X	Halogenated		Toxic		Solid	
Comments	Dispose of as hazardous general organic waste								

Spill/Leak

Evacuate area		Add sand		Add Absorbent		Neutralise with		Sweep up	X
Comments	In the case of a spill, carefully take up and dispose of properly. Clean up affected area. Prevent disposal into drains or rivers. Do not release vapours into environment.								

Chemical: Sodium bis(2-methoxyethoxy)aluminum hydride solution (Red-Al ≥60 wt. % in toluene)

Toxicity Oral (LD_{50}, mg/kg)	(Extremely toxic) ≤5	X	(Highly toxic) 5-50		(Toxic or unknown) 50-500		(Non-toxic) >500	
Sensitisation	Extreme	X	Moderate - Severe		Unknown, Mild		Non-sensitising	
irritation/Corrosion			Corrosive, Severely irritation	X	Unknown, Moderately irritation		Non- or Mildly irritation	
Carcinogenicity	A1 or 2		A3	X	A4		A5	
Hazard Classification	**Extreme Hazard**	X	**High Hazard**		**Medium Hazard**		**Non-Hazardous**	

Control Measures and PPE:

Lab coat	X	Nitrile gloves	X	Safety glasses	X	Safety shoes	X	Face shield	X
Overall		4 H gloves		Safety goggles		Respirator		Apron	
Other (specify)	Do not breathe vapours or let vapours accumulate, use adequate ventilation or fume cupboard. Keep away from all sources or ignition. Avoid skin and eye contact. Avoid exposure to moisture								

Storage

Toxic	X	Harmful		Non-harmful		Flammable	X
Acid		Bases		Oxidant		Reductant	
Incompatibilities	Avoid water, oxidizing agents and combustible material. Store container in a dry and well-ventilated place away from heat sources and direct sunlight. Keep away from moisture and store as hazardous materials, which set free flammable gases upon contact with water Air and moisture sensitive. Store under inert gas.						

Disposal

Acid		General organic	X	Halogenated		Toxic	X	Solid	
Comments	Dispose of as hazardous, flammable organic waste								

Spill/Leak

Evacuate area		Add sand	X	Add Absorbent		Neutralise with		Sweep up	X
Comments	In the case of a spill, carefully take up with non-combustible absorbent material dispose of in labelled container. Do NOT flush with water. Clean up affected area. Prevent disposal into drains or rivers. Do not release vapours into environment.								

Chemical: Sodium Hydride (60 % dispersion in mineral oil)

Toxicity Oral (LD_{50}, mg/kg)	(Extremely toxic) ≤5	X	(Highly toxic) 5-50		(Toxic or unknown) 50-500		(Non-toxic) >500	
Sensitisation	Extreme		Moderate - Severe		Unknown, Mild	X	Non-sensitising	
irritation/Corrosion			Corrosive, Severely irritation	X	Unknown, Moderately irritation		Non- or Mildly irritation	
Carcinogenicity	A1 or 2		A3	X	A4		A5	
Hazard Classification	**Extreme Hazard**	X	**High Hazard**		**Medium Hazard**		**Non-Hazardous**	

Carcinogenicity: No data available

Control Measures and PPE:

Lab coat	X	Nitrile gloves	X	Safety glasses	X	Safety shoes	X	Face shield	
Overall		4 H gloves		Safety goggles		Respirator	X	Apron	
Other (specify)	Do not breathe dust or let dust accumulate, use adequate ventilation or fume cupboard. Keep away from all sources or ignition. Avoid skin and eye contact. Avoid exposure to **moisture**								

Storage

Toxic		Harmful	X	Non-harmful		Flammable	X
Acid		Bases		Oxidant		Reductant	
Incompatibilities	Avoid metals and moisture Store container in a dry and well-ventilated place away from heat sources and direct sunlight. Air and moisture sensitive. Store under inert gas.						

Disposal

Acid		General organic	X	Halogenated		Toxic	X	Solid
Comments	Dispose of as hazardous general organic waste							

Spill/Leak

Evacuate area		Add sand		Add Absorbent		Neutralise with		Sweep up	X
Comments	In the case of a spill dispose of properly. Clean up affected area. Prevent disposal into drains or rivers. Do not release vapours into environment. Avoid accumulation of dusts							

Chemical: Sodium borohydride

Toxicity Oral (LD_{50}, mg/kg)	(Extremely toxic) ≤5		(Highly toxic) 5-50		(Toxic or unknown) 50-500	X	(Non-toxic) >500	
Sensitisation	Extreme		Moderate - Severe		Unknown, Mild	X	Non-sensitising	
irritation/Corrosion			Corrosive, Severely irritation	X	Unknown, Moderately irritation		Non- or Mildly irritation	
Carcinogenicity	A1 or 2		A3	X	A4		A5	
Hazard Classification	**Extreme Hazard**		**High Hazard**	X	**Medium Hazard**		**Non-Hazardous**	

Acute toxicity: Acute toxicity estimate Oral - 162 mg/kg (Calculation method)
Carcinogenicity: No data available
Ecotoxicity: Aquatic vertebrated: LC50 - Danio rerio (zebra fish) - > 100 mg/l - 96 h Remarks: (External MSDS)

Control Measures and PPE:

Lab coat	X	Nitrile gloves	X	Safety glasses	X	Safety shoes	X	Face shield	
Overall		4 H gloves		Safety goggles		Respirator		Apron	
Other (specify)	Do not breathe dust or let dust accumulate, use adequate ventilation or fume cupboard. Keep away from all sources or ignition. Avoid skin and eye contact. Avoid exposure to moisture								

Storage

Toxic		Harmful	X	Non-harmful		Flammable	X
Acid		Bases		Oxidant		Reductant	
Incompatibilities	Store container in a dry and well-ventilated place away from heat sources and direct sunlight. Air and moisture sensitive. Store under inert gas.						

Disposal

Acid		General organic	X	Halogenated		Toxic		Solid	
Comments	Dispose of as hazardous general organic waste								

Spill/Leak

Evacuate area		Add sand		Add Absorbent		Neutralise with		Sweep up	X
Comments	In the case of a spill, carefully take up carefully and dispose of properly. Clean up affected area. Prevent disposal into drains or rivers. Do not release vapours into environment.								

Chemical: Grubbs Catalyst M204 and Hoveyda Grubbs catalyst

Toxicity Oral (LD_{50}, mg/kg)	(Extremely toxic) ≤5		(Highly toxic) 5-50		(Toxic or unknown) 50-500	X	(Non-toxic) >500	
Sensitisation	Extreme		Moderate - Severe		Unknown, Mild	X	Non-sensitising	
irritation/Corrosion			Corrosive, Severely irritation		Unknown, Moderately irritation	X	Non- or Mildly irritation	
Carcinogenicity	A1 or 2		A3		A4	X	A5	
Hazard Classification	**Extreme Hazard**		**High Hazard**		**Medium Hazard**	X	**Non-Hazardous**	

Carcinogenicity: No data available

Control Measures and PPE:

Lab coat	X	Nitrile gloves	X	Safety glasses	X	Safety shoes	X	Face shield	X
Overall		4 H gloves		Safety goggles		Respirator		Apron	
Other (specify)	Do not breathe dust or let dust accumulate, use adequate ventilation or fume cupboard. Keep away from all sources or ignition. Avoid skin and eye contact. Avoid exposure to moisture								

Storage

Toxic		Harmful	X	Non-harmful		Flammable	X
Acid		Bases		Oxidant		Reductant	
Incompatibilities	Avoid strong oxidizing agents and exposure to air. Store container fridge. Handle and store under inert gas. Prevent exposure to light and air						

Disposal

Acid		General organic	X	Halogenated		Toxic		Solid	
Comments	Dispose of as hazardous general organic waste								

Spill/Leak

Evacuate area		Add sand		Add Absorbent		Neutralise with		Sweep up	X
Comments	In the case of a spill, carefully contain spillage and collect with collect with an electrically protected vacuum cleaner or by wet-brushing and place in container and dispose of properly. Clean up affected area. Prevent disposal into drains or rivers. Do not release vapours into environment.								

Chemical: Isovanillin

Toxicity Oral (LD_{50}, mg/kg)	(Extremely toxic) ≤5		(Highly toxic) 5-50		(Toxic or unknown) 50-500		(Non-toxic) >500	X
Sensitisation	Extreme		Moderate - Severe		Unknown, Mild		Non-sensitising	X
irritation/Corrosion			Corrosive, Severely irritation		Unknown, Moderately irritation		Non- or Mildly irritation	X
Carcinogenicity	A1 or 2		A3		A4		A5	X
Hazard Classification	**Extreme Hazard**		**High Hazard**		**Medium Hazard**		**Non-Hazardous**	X

Carcinogenicity: No data available

Control Measures and PPE:

Lab coat	X	Nitrile gloves	X	Safety glasses	X	Safety shoes	X	Face shield	
Overall		4 H gloves		Safety goggles		Respirator		Apron	
Other (specify)	Do not swallow, use adequate ventilation or fume cupboard. Keep away from all sources or ignition. Avoid skin and eye contact								

Storage

Toxic		Harmful		Non-harmful	X	Flammable	
Acid		Bases		Oxidant		Reductant	
Incompatibilities	Avoid strong oxidizing agents and strong bases. Store container in a dry and well-ventilated place away from heat sources and direct sunlight.						

Disposal

Acid		General organic	X	Halogenated		Toxic		Solid	
Comments	Dispose of as hazardous general organic waste								

Spill/Leak

Evacuate area		Add sand		Add Absorbent		Neutralise with		Sweep up	X
Comments	In the case of a spill, carefully clean up affected area. Prevent disposal into drains or rivers. Do not release vapours into environment.								

Chemical: Allyl Bromide

Toxicity Oral (LD_{50}, mg/kg)	(Extremely toxic) ≤5		(Highly toxic) 5-50		(Toxic or unknown) 50-500	X	(Non-toxic) >500	
Sensitisation	Extreme		Moderate - Severe		Unknown, Mild	X	Non-sensitising	
irritation/Corrosion			Corrosive, Severely irritation	X	Unknown, Moderately irritation		Non- or Mildly irritation	
Carcinogenicity	A1 or 2		A3	X	A4		A5	
Hazard Classification	**Extreme Hazard**		**High Hazard**		**Medium Hazard**	X	**Non-Hazardous**	

Acute toxicity: Acute toxicity estimate Oral - 200 mg/kg (Calculation method)
Carcinogenicity: No data available
Ecotoxicity: Aquatic vertebrated: LC50 - Carassius auratus (goldfish) - 0,8 mg/l - 24 h Remarks: (ECHA)
Biodegradability: Readily biodegradable
Control Measures and PPE:

Lab coat	X	Nitrile gloves	X	Safety glasses	X	Safety shoes	X	Face shield	
Overall		4 H gloves		Safety goggles		Respirator	X	Apron	
Other (specify)	Do not breathe vapours or let vapours accumulate, use adequate ventilation or fume cupboard. Keep away from all sources or ignition. Avoid skin and eye contact. Wear respirator (Filter A for organic vapours)								

Storage

Toxic		Harmful	X	Non-harmful		Flammable	X
Acid		Bases		Oxidant		Reductant	
Incompatibilities	Avoid rubber and various plastics. Store container fridge. Prevent exposure to light and air						

Disposal

Acid		General organic	X	Halogenated		Toxic		Solid	
Comments	Dispose of as hazardous general organic waste								

Spill/Leak

Evacuate area		Add sand		Add Absorbent		Neutralise with		Sweep up	X
Comments	In the case of a spill, carefully take up with liquid-absorbent and dispose of properly. Clean up affected area. Prevent disposal into drains or rivers. Do not release vapours into environment. Clean up affected area.								

Chemical: 2-Bromopropane

Toxicity Oral (LD_{50}, mg/kg)	(Extremely toxic) ≤5		(Highly toxic) 5-50		(Toxic or unknown) 50-500	X	(Non-toxic) >500	
Sensitisation	Extreme		Moderate - Severe		Unknown, Mild	X	Non-sensitising	
irritation/Corrosion			Corrosive, Severely irritation		Unknown, Moderately irritation	X	Non- or Mildly irritation	
Carcinogenicity	A1 or 2		A3		A4	X	A5	
Hazard Classification	**Extreme Hazard**		**High Hazard**		**Medium Hazard**	X	**Non-Hazardous**	

Carcinogenicity: No data available
Ecotoxicity: Aquatic vertebrated: LC50 - Carassius auratus (goldfish) - 150 mg/l - 24 h
Control Measures and PPE:

Lab coat	X	Nitrile gloves	X	Safety glasses	X	Safety shoes	X	Face shield	
Overall		4 H gloves		Safety goggles		Respirator		Apron	
Other (specify)	Do not breathe vapours or let vapours accumulate, use adequate ventilation or fume cupboard. Keep away from all sources or ignition. Avoid skin and eye contact								

Storage

Toxic		Harmful	X	Non-harmful		Flammable	X
Acid		Bases		Oxidant		Reductant	
Incompatibilities	Avoid rubber and various plastics. Store container in cool place away from heat sources and direct sunlight.						

Disposal

Acid		General organic	X	Halogenated		Toxic		Solid	
Comments	Dispose of as hazardous general organic waste								

Spill/Leak

Evacuate area		Add sand		Add Absorbent		Neutralise with		Sweep up	X
Comments	In the case of a spill cleanup affected area. Prevent disposal into drains or rivers. Do not release vapours into environment.								

Chemical: Potassium hydroxide

Toxicity Oral (LD_{50}, mg/kg)	(Extremely toxic) ≤5		(Highly toxic) 5-50		(Toxic or unknown) 50-500	X	(Non-toxic) >500	
Sensitisation	Extreme		Moderate - Severe		Unknown, Mild	X	Non-sensitising	
irritation/Corrosion			Corrosive, Severely irritation		Unknown, Moderately irritation	X	Non- or Mildly irritation	
Carcinogenicity	A1 or 2		A3		A4	X	A5	
Hazard Classification	**Extreme Hazard**		**High Hazard**		**Medium Hazard**	X	**Non-Hazardous**	

Carcinogenicity: No data available
Ecotoxicity: LC50 - Gambusia affinis (Mosquito fish) - 80 mg/l - 96 h (ECOTOX Database)
Control Measures and PPE:

Lab coat	X	Nitrile gloves	X	Safety glasses	X	Safety shoes	X	Face shield	
Overall		4 H gloves		Safety goggles		Respirator		Apron	
Other (specify)	Do not breathe dust or let dust accumulate, use adequate ventilation or fume cupboard. Keep away from all sources or ignition. Avoid skin and eye contact. Avoid exposure to moisture								

Storage

Toxic		Harmful	X	Non-harmful		Flammable	X
Acid		Bases		Oxidant		Reductant	
Incompatibilities	Avoid rubber and various plastics. Store container in cool place away from heat sources and direct sunlight.						

Disposal

Acid		General organic		Halogenated		Toxic		Solid	X
Comments	Dispose of as hazardous, corrosive, combustible general organic waste								

Spill/Leak

Evacuate area		Add sand		Add Absorbent		Neutralise with		Sweep up	X
Comments	In the case of a spill cleanup affected area. Prevent disposal into drains or rivers. Do not release dust into environment.								

C. CHEMICAL INTERACTION DATA

Legend: **d = desired reaction**

K = known reaction

- = no hazards

x = chemicals will not be used in the same reaction

	Chemicals	A	B	C	D	E	F	G	H	I
A	Isovanillin		d	d	d	-	-	-	-	d
B	Allyl Bromide			d	d	-	-	-	-	d
C	Potassium carbonate				d	x	x	x	-	-
D	2- Bromopropane					d	-	-	-	d
E	Sodium bis(2-methoxyethoxy)aluminum hydride solution (Red-Al ≥60 wt. % in toluene						k	-	-	x
F	Sodium borohydride							k	-	x
G	Sodium Hydride (60 % dispersion in mineral oil)								k	x
H	Grubbs Catalyst and Hoveyda Grubbs catalyst									x
I	Potassium hydroxide									

D. MATERIAL COMPATIBILITIES

Chemicals	A	B	C	D	E	F	G	H	I
Materials of construction									
Glass	Y	Y	Y	Y	Y	Y	Y	Y	Y
316 SS	Y	Y	Y	Y	N	Y	N	N	N

E. EFFLUENT SPECIFICATIONS

The process under normal conditions consists of single filtration steps (inorganic salts of potassium carbonate and potassium hydroxide salts). The residue is to be disposed of as solid organic waste. The filtrate will be concentrated and the solvents will be recycled. The process also involves the quenching with water or methanol for Sodium bis(2-methoxyethoxy)aluminium hydride solution (Red-Al ≥60 wt. % in toluene), Sodium borohydride and Sodium Hydride (60 % dispersion in mineral oil). It also involves DCM and water extractions and filtration of any inorganic products. The residue is to be disposed of as toxic solid organic waste. Any side-products formed is isolated by extraction and filtration. Process amounts is unknown at the current time.

Appendix G: Draft Article

ARTICLE

ROYAL SOCIETY OF CHEMISTRY

Received 00th January 20xx,
Accepted 00th January 20xx
DOI: 10.1039/x0xx00000x

Synthesis of an 8-membered oxygen-containing benzo-fused heterocycle using flow technologies

Bernice M. Currie *[a] Darren L. Riley [b] and Jenny-Lee Panayides [c]

Flow chemistry has become an appealing alternative globally over the last few decades finding application in both academic and industrial laboratories. Flow is driven largely by the fact that it commonly provides higher selectivity, yield and purity compared to batch chemistry that has become time-consuming, ineffective, and challenging to scale up. This article described the application and development of a flow process towards the synthesis of an 8-membered oxygen-containing benzo-fused heterocycle. The synthesis consisted of six stages that included two allylation steps, a claisen rearrangement, an alcohol protection, an aldehyde reduction and a ring-closing metathesis step. The target molecule, (Z)-7-Isopropoxy-8-methoxy-3,6-dihydro-1H-benzo[c]oxocine **10,** was selected as a flow synthesis for the 8-membered ring has not yet been reported. In summary, all six steps were successfully translated into flow and improved yields were shown with the use of greener solvents and operating at unconventionally high temperature and pressures especially when considering the Claisen rearrangement step. Design of experiment was also used in the last two stages which included i) the second allylation which required a strong base such as sodium hydride and was used as a slurry pumping through peristaltic pumps, and ii) the final ring closing metathesis stage in which two ruthenium-based catalysts were investigated with the use of a greener solvent. It was found that the flow approach yielded an overall percentage yield of 37.7 % in 105 minutes, compared to the batch approach that yielded an overall percentage yield of 0.77 % in 154 hours.

Introduction

Benzo fused heterocycles are a class of compounds consisting of benzene rings fused with heterocyclic rings containing at least one atom of nitrogen, oxygen, or sulfur. Due to their natural abundance and biological activities, oxygen-containing heterocycles have historically provided a substantial contribution to drug discovery and synthetic applications.[1] Examples of 5-,6-,7- and 8-membered oxygen-containing heterocycles containing the oxygen atom in the one-position are commonly reported in literature as these heterocycles are frequently used as antibiotics and antimicrobial agents in pharmaceutical applications.[2] However, compounds with the oxygen atom in the two-position are more uncommon since these compounds mostly occur in higher oxidized forms.[3] These compounds are also beneficial as pharmaceutical templates. For instance, Drypemolundein A **1**, which was isolated from the stem bark of the plant *Drypetes molunduana*, has demonstrated anti-inflammatory and analgesic properties. [4]

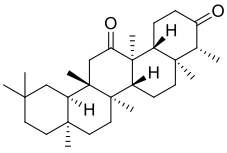

1

Figure 67: Drypemolundein A chemical structure

It was noted that ring-closing metathesis (RCM) was a common step often employed in the synthesis processes of benzo-fused heterocycles. Van Otterlo and co-workers employed ruthenium-mediated metathesis with second-generation Grubbs II catalyst, focusing on RCM and alkene isomerization for the synthesis of 5,6-, 7- and 8-membered oxygen-containing heterocycles. [3]The overarching aim of this article was to evaluate the use of flow technologies for the optimization and synthesis of the target 8-membered oxygen-containing benzo-fused heterocycle. The target molecule, (Z)-7-isopropoxy-8-methoxy-3,6-dihydro-1h-benzo[c]oxocine **10** was selected as we were interested in developing an improved approach to accessing the scaffold for future structure-activity relationship screening and to demonstrate that modern process technologies like flow can also be used routinely to perform fundamental research in a more sustainable and responsible manner. A batch synthetic route to this pharmaceutical template has been investigated and published by van Otterlo and co-workers,[3] however, the flow synthesis for the 8-membered ring has not yet been translated to flow conditions.

Flow technology has emerged as a disruptive/leapfrogging technology in academia and the pharmaceutical manufacturing sector as it provides several key advantages over batch-mode synthesis such as i) large surface area-to-volume ratio,[5,6] ii) control over reaction parameters,[7] iii) operating at pressures and temperatures above the boiling point of solvents,[6,8] iv) simple control of hazardous reagents or unstable intermediates,[8] v)

[a] *Department Chemistry, University of Pretoria, Pretoria, 0028, South Africa;*
[b] *Pharmaceutical Technologies, Chemicals cluster, CSIR, Pretoria campus, Pretoria, 0001, South Africa;*
[c] *Correspondence: Darren.riley@up.ac.za; Tel.: +2712-420-3097*
Electronic Supplementary Information (ESI) available: See DOI: 10.1039/x0xx00000x

simple scaling up,[5] vi) telescoping,[9] vii) in-line monitoring and purification,[9,10] and viii) chemical sustainability, as it provides sustainable synthesis by implementing the twelve principles of green chemistry and green engineering by i) maximizing efficiency, ii) minimizing excess, iii) designing processes that are more environmentally sustainable, and iv) recycling of catalysts and solvents.[11]

Although flow chemistry represents a very adaptable and practical method for conducting chemical reactions, there are a few drawbacks to consider such as i) solvent choice when telescoping as it should solubilize the starting reagents, products and by-products that are formed while simplifying or eliminating workup, enhancing purification, recycling of solvent, and reducing solvent consumption and the need for energetically unfavorable evaporations and solvent swopping is avoided,[10] and ii) clogging and fouling in the presence due to the small dimensions of flow components,[12] but can be managed by using ultrasonication, piezoelectricity or with the inclusion of a solubilizing stream, but this of course adds complexity to the process.[6,13] That being said, the technology is essentially directly scalable and the use of appropriate dimensional scaling techniques in conjunction with numbering up (if required) still offers distinct advantage over dimensional upscaling under batch mode. Finally, the process of developing a flow method can be time consuming, which could pose a constraint when adhering to deadlines, however, once a general method is developed it can often be routinely and rapidly adapted.[6] Thus, the focus of this article was to evaluate and improve the synthesis of the target benzo-fused heterocycle under batch and flow conditions in the context of yields, environmental impact and greenness of reagents and solvents.

Results and Discussion

Stage 1: First allylation

Batch results

The standard batch allylation conditions outlined by van Otterlo and co-workers were employed using allyl bromide **3** and potassium carbonate as a base in dimethylformamide (0.50 M).[14] The reaction was heated at 60 °C over 20 hours under an argon atmosphere to afford 82 % of the desired product **2**. The use of dimethylformamide was deemed undesirable from an environmental and safety point-of-view as it is flagged as being a red solvent, in addition, its high boiling point means that its removal is time consuming and energetically unfavourable. We considered using toluene as a replacement, as the reaction did not actually require access to temperatures more than that afforded by toluene.

Unfortunately, toluene proved to be less effective affording a poor yield of 2.1 % after 20 hours reaction time. As dimethylformamide is a polar aprotic solvent, and toluene is a non-polar solvent we though that there may be solvent effects at play. As such we next elected to screen acetonitrile as an alternative as it is a polar aprotic solvent but it is more easily removed due to a lower boiling point. In addition, acetonitrile is better from a greenness point-of-view being designated as an amber solvent and afforded 66 % yield after 20 hours and 88 % yield after 32 hours. It was also decided to investigate the use of a basic solution of potassium hydroxide as recommended by Cortés-Borda and co-workers.[15] The reaction was carried out at a temperature of 70 °C using two different protic solvent systems (70% methanol/water and 70% ethanol/water) to solubilized the formation of potassium bromide. In both instances good, comparable yields of 78 and 83 % respectively were obtained.

Flow results

Initial screening experiments were performed using acetonitrile as the solvent of choice as it is ecologically friendlier than dimethylformamide. Initially, the use of acetonitrile as a solvent in conjunction with a packed-bed reactor housing potassium carbonate was attempted. Unfortunately, the reaction aborted due to precipitation in the PTFE tubing after the column which appears to have been brought on by potassium carbonate leaching from the column. Since Riley and co-workers had previously performed the allylation using potassium carbonate as base and dimethylformamide as solvent, we chose to follow that route.[16] Optimal conditions were determined using stock solutions of isovanillin **2** (0.50 M) and allyl bromide **3** (1.50 M) both in dimethylformamide at 100 °C with a 20 minute residence time to afforded the desired product **4** in a 92 % (by HPLC analysis) and 85 % isolated yield. Although, the use of a packed bed reactor is efficient, it is not ideal as it requires manual intervention to change the base and as such will create automation challenges and complicate reaction scale-up. As a result, it was decided to replace a packed bed reactor with a coil and use a basic solution of potassium.[15]

As the reaction produced moderate yields in batch without precipitation, it was decided to translate this step into flow using a similar setup to the one reported by Cortés-Borda and co-workers.[15] The flow setup (Scheme 49) was compromised of two peristaltic pumps connected downstream to stock solutions of isovanillin **2** (0.50 M) with potassium hydroxide in methanol: water and allyl bromide **3** in methanol only. As allyl bromide and water are not miscible it is important to use only methanol for the second stock solution to ensure that a consistent concentration of the allyl bromide is introduced into the reactor. The two stock solutions were then combined at a T-piece mixer followed by a 0.5 mL static mixer for facilitating rapid mixing of the resulting biphasic matrix. This was followed by a 25 mL PTFE coil with an internal diameter of 1.5 mm that was mounted on a standalone Uniqsis heating block. It was chosen to employ the bigger diameter coil, instead of the normal 1.0 mm inner-diameter coil, to achieve faster flow rates and better mixing as initial test reactions showed no significant difference in conversion from using a smaller diameter coil.

Initial reactions were performed using similar conditions to those reported by Cortés-Borda and co-workers using 1.80 equivalents of allyl bromide and 1.50 equivalents of potassium hydroxide with residence time of 15 minutes[15] Under these conditions, a modest conversion of 68.0 % was realised (Table 47, entry 1). Thereafter, increasing the residence time to 22.5 minutes and the temperature to 85 °C afforded an increase in conversion to 75.5 % (entry 2). It was then decided to increase the equivalents of allyl bromide to 2.0 and a similar conversion of 78.0 % was observed at 80 °C for both 15 minutes and 10 minutes residence time (entries 3 and 4). Additionally, it was found that increasing the temperature to 100 °C, had little effect on the observed conversion rate (entry 5).

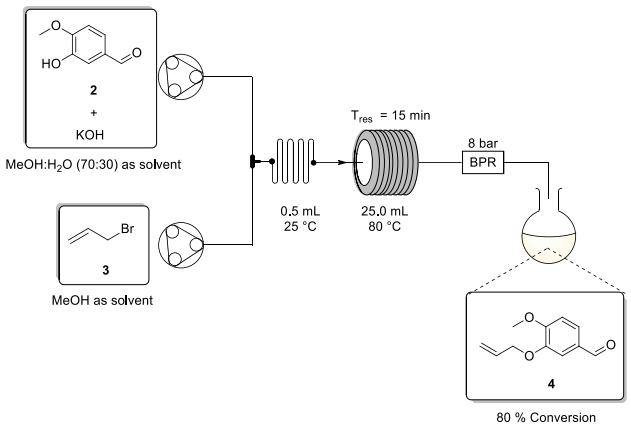

Scheme 49: Flow synthesis for the allylation of isovanillin **2** using potassium hydroxide solution

Table 47: Flow experiments for the allylation of isovanillin **2** using potassium hydroxide solution in aqueous methanol

Exp No	KOH (equiv.)	3 (equiv.)	Temp. (°C)	T_{res} (min)	LC Conv. (%)
1	1.50	1.8	75	15	68.0
2	1.50	1.8	85	22.50	75.5
3	1.50	2.0	80	15	78.0
4	1.50	2.0	80	10	78.4
5	1.50	2.0	100	10	76.5
6	1.80	2.0	75	15	76.9
7	**1.80**	**2.0**	**80**	**15**	**80.3**
8	1.80	2.0	85	15	79.3
9	1.80	2.0	90	15	77.3
10	1.85	2.0	80	15	78.1
11	1.85	2.1	80	15	80.1
12	**1.80**	**2.0**	**80**	**15**	**92.9** [a]

[a] 88 % Isolated yield. Reaction carried out on 1.0-gram scale

Overall, the reaction performed best with temperatures ranging between 80-85 °C coupled with a shorter residence time of 15 minutes The shorter residence time is likely benefiting the reaction as the flow rate is higher, resulting in better mixing and mass transfer. Several additional screens led to the identification of optimal conditions employing the use of 1.80 equivalents potassium hydroxide and 2.00 equivalents allyl bromide at 80 °C with a 15 minutes residence time when using the 70:30 of methanol: water solvent mix (entries 6-11). On a 1.00-gram scale, a conversion of 92.9 % was observed which translated to an isolated yield of 88 % (entry 12).

In conclusion, the allylation stage was successfully translated and optimized under flow conditions in one of two ways: either by utilizing a packed-bed reactor housing potassium carbonate yielding 92 % of desired product at optimized flow conditions of 20 minutes residence time at a temperature of 100 °C, or by using a coil reactor with a potassium hydroxide solution yielding the desired product in an 88% isolated yield when using a 15-minute residence time at 80 °C. The first approach suffered from limitations, including, i) the use of a hazardous solvent (dimethylformamide), ii) challenges with automation and up-scaling linked to dispersion issues in the packed-bed reactor and iii) the need for manual intervention linked to repacking and replacing the packed-bed reactor when the base was spent. As a result, the reaction was modified by substituting dimethylformamide with greener protic solvents in the form of aqueous methanol or aqueous ethanol and replacing a packed bed reactor with a potassium hydroxide solution.

Stage 2: Claisen rearrangement

Batch results

This step was attempted in-house using dimethylformamide as a solvent, refluxing for 64 hours at 150-160 °C to obtain **5** in a low yield of 27 %. Critically, in dimethylformamide some decomposition and precipitation were observed visually after the 24 hours mark. Toluene was chosen as an alternative solvent despite having a lower boiling point, as its use afforded a simpler workup, and it is a greener solvent choice. Toluene's removal *in vacuo* also offers the possibility for solvent recycling, which is less challenging and energy intensive than when trying to recover and recycle dimethylformamide. In addition, dimethylformamide is carcinogenic and teratogenic, hence it should ideally not be released into the environment. A batch reaction was carried out in a round-bottom flask on a 2.00-gram scale. The reaction was refluxed for 72 hours at temperature of 110-120 °C in toluene at a concentration of 0.25 M, resulting in a disappointing 6.9 % conversion. (Conversion was determined by q-NMR analysis using dimethyl sulfone as an internal standard). Despite this disappointing result, the reaction matrix was homogeneous and deemed suitable for flow translation.

Flow results

The Claisen rearrangement was evaluated in-house under flow using dimethylformamide as a solvent. It was noted that decomposition and precipitation occurred at longer residence times and higher temperatures (>220 °C), resulting in reactor blockage and fouling. In-house results showed that high product conversions could be achieved at residence times ranging from 45 to 60 minutes at a temperature of 240 °C. As noted earlier, it was decided to replace dimethylformamide with toluene, and test reactions were carried out using previously described conditions.

The flow setup as seen in Scheme 50 was constructed using a Uniqsis Binary pump reactor system which is compatible with higher temperatures. A single HPLC pump was connected upstream to a stock solution of **4** in toluene and thereafter downstream to a heated 20 mL stainless steel coil, followed by a 2 mL stainless steel cooling coil at 0 °C. The latter ensured that the reaction mixture was rapidly cooled prior to passage through a 20 bar BPR and collection Furthermore, it was essential to include the cooling coil to i) ensure that the reaction stopped rapidly on exiting the heating coil, this prevented additional conversion from occurring in the collection flask which would lead to inaccuracies in the conversions observed and ii) as a safety measure it prevented rapid uncontrolled gassing out upon exiting the reactor.

Flow experiments were carried out using a stock solution of 4 in toluene at various concentrations (Table 48). Immediately we observed near quantitative conversions (entries 1-4), regardless

of the concentration, indicating the reaction is concentration independent. This was however not surprising as the process is a unimolecular rearrangement, but the experiments served to confirm that we could work up to 1.00 M concentration without any deleterious precipitation events. Furthermore, when the reaction was performed on a larger scale at concentration of 1.00 M, there was again no substantial variation in product yield (entries 5).

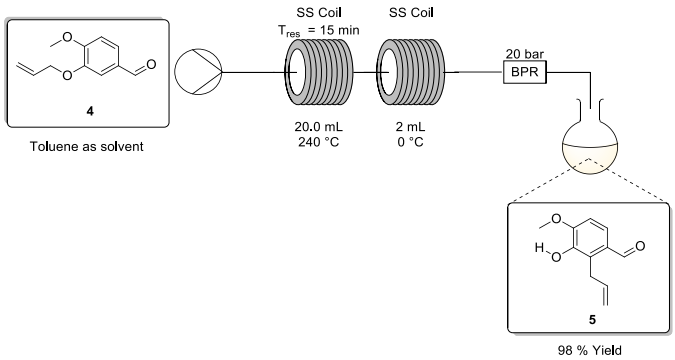

Scheme 50: Flow preparation for the Claisen rearrangement **5** using toluene

Additional optimization experiments were conducted at a 30-minute residence time using a 0.50 M solution, yielding the desired product **5** in 99 % product (entry 8). The residence time was also reduced while maintaining the temperature at 240 °C (entries 8-10). Based on entry 10, the ideal conditions for the Claisen rearrangement are attained after 15 minutes residence time with a temperature of 240 °C using a 20-bar BPR (entry 10). As a result of the shorter residence time, these conditions afforded a higher productivity and used less energy in comparison to when performed with a 45-minute residence time. As a result, the reaction may run for longer periods of time with less energy and solvent required, thus lowering the cost and carbon footprint related to the process.

Table 48: Optimisation flow experiments for the Claisen rearrangement of **4**

Exp No	Reaction scale (g)	Conc. [M]	T_{res} (min)	Flow rate (mL.min-1)	Yield (%)
1	2.00	0.25	45	0.44	96
2	2.00	0.50	45	0.44	98
3	2.00	0.75	45	0.44	95
4	2.00	1.00	45	0.44	94
5	10.00	1.00	45	0.44	99
6	2.00	0.50	30	0.67	99
7	0.38	1.00	45	0.44	93
8	0.38	1.00	30	0.67	96
9	0.38	1.00	20	1.00	100
10	0.38	1.00	15	1.33	98

Stage 3: Alcohol protection

Batch results

The batch procedure was based on reaction conditions by van Otterlo and co-workers using 2-bromopropane **6** and potassium carbonate.[14] The reaction was initially performed in dimethylformamide (0.50 M) for over 20 hours under an argon atmosphere at temperature of 60 °C affording the desired product in 78 % yield. Additional screens were carried out to test reagent/product solubilities in different solvents for flow translation. Initially tetrahydrofuran was screened as it can be used to link the protection stage to the next allylation stage, unfortunately, a disappointingly low yield of 3.1 % was observed. Alternatively, toluene was also evaluated as this would allow us to easily link the previous Claisen stage directly into the protection. Once again, we were left disappointed with a low yield of only 2.8 % observed. As a result, dimethyl formamide at a 0.50 M concentration was selected for flow translation.

Flow results

This step was investigated previously in-house, looking at various residence times and concentrations. Based upon these studies, preliminary reaction conditions involved performing the reaction at a concentration of 0.13 M in dimethylformamide using a packed-bed reactor housing potassium carbonate, with a 20-minute residence time at 80 °C to afford the product in 92 % yield. The flow configuration was comprised of two HPLC pumps connected downstream to stock solutions of **5** and 2-bromopropane **6** both in dimethyl formamide (Scheme 51). The solution was then mixed at a T-piece connector before passing through an Omnifit™ glass column packed bed reactor housing crushed potassium carbonate followed by an 8-bar BPR and finally product collection.

The effect of concentration and the equivalents of 2-bromopropane **6** was studied while maintaining the temperature at 80 °C and residence time at 20 minutes When performed at 0.40 M in dimethyl formamide using 2.5 equivalents of 2-bromopropane the desired product was formed in high isolated yields of 86-88% (Table 49, entries 1 and 2). Interestingly, as noted in entry 3, as the concentration was increased slightly, the product yield decreased to 77% (entries 1 and 2 vs. 3). Furthermore, decreasing the equivalents of 2-bromopropane also resulted in a sharp drop-off in yield (entries 3-6).

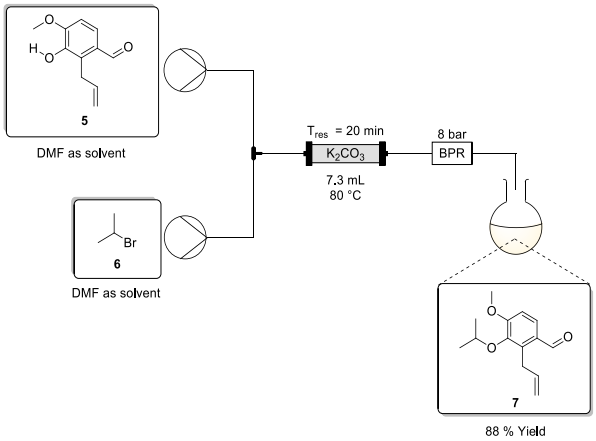

Scheme 51 Flow synthesis of the protection of **5** using potassium carbonate

Although counterintuitive, increasing the concentration while retaining the residence time at 20 minutes may have negatively impacted the overall mass transfer occurring in the packed-bed reactor. We hypothesise that at lower concentrations the mass transfer is more efficient as there is less competition at the liquid-solid interface arising from the liquid phase reaction components. As the concentration of these components increases a saturation point is reached resulting in the mass transfer plateauing. Possible solutions to working at higher concentrations if required would be to work at lower flow rates (i.e. longer residence times), or alternatively to simply increase the volume of the packed-bed reactor while maintaining the flowrate.

Table 49: Flow experiments of the alcohol protection using potassium carbonate and different equivalents of 2-bromopropane **6**

Exp No	Reaction scale (g)	Conc. [M]	6 (equiv.)	T_{res} (min)	Yield (%)
1	4.34	0.40	2.5	20	86.0
2	4.07	0.40	2.5	20	88.0
3	0.25	0.50	2.5	20	77.0
4	0.25	0.50	2.0	20	68.0
5	0.25	0.50	1.5	20	64.0
6	0.25	0.50	1.0	20	60.0

As a result, the ideal conditions of this stage was determined to be a concentration of 0.40 M in dimethylformamide at temperature of 80 °C, 20 minutes residence time, using 2.5 equivalents of 2-bromopropane **6** to obtain the product **7** in 88 % yield after isolation.

Stage 4: Aldehyde reduction

Batch results

Previously, van Otterlo and co-workers performed the reduction step in tetrahydrofuran for 12 hours using lithium aluminium hydride at 0 °C to afford the product **8** in an isolated yield of 86 %.[14] This reaction was also investigated in-house using Red-Al (65 % toluene) in dichloromethane at a temperature of 15 – 20 °C affording a 93 % isolated yield. We elected to use toluene instead of a halogenated solvent in an effort to improve the safety and greenness of the reaction. The reaction was performed in a round-bottom flask under argon atmosphere for over 20 hours using distilled toluene (0.15 M) at 0-20 °C to obtain **8** in 76 % yield (Table 50, entries 1 and 2). Although the use of Red-Al afforded the product in good yield additional reactions were screened using alternative reducing agents as Red-Al is not ideal for flow translation, primarily due to its high viscosity. Sodium borohydride and sodium acetoxyborohydrde was screened producing the desired product **8** in 62 and 59% yields under comparable reaction conditions (entries 3 and 4). Critically, some precipitation was observed and it was therefore decided to test the approach by Watts and co-workers, using sodium borohydride in aqueous methanol.[17] After 20 hours, the product was isolated in a 47 % yield. Although lower yielding, we elected to translate this approach to flow as it did not suffer from the viscosity issues associated with Red-Al.

Table 50: Batch experiments of aldehyde reduction using various bases in different solvents

Exp No	Reaction scale (g)	Reducing agent	Solvent	Yield (%)
1	3.38	Red-Al (60 %)	Toluene	75.0
2	4.50	Red-Al (60 %)	Toluene	76.0
3	0.50	$NaBH_4$	EtOH	62.0
4	0.50	$NaBH(OAc)_3$	EtOH	59.0
5	0.50	$NaBH_4$	MeOH:H_2O	47.0

Flow results

Initial test reactions were investigated using a packed-bed reactor housing polymer supported sodium borohydride. A full-factorial DoE screening was chosen to test whether the result from utilizing a packed column is effective and reproducible. DoE screening reactions were carried out while maintaining the column temperature at room temperature and altering the concentration and residence time while using methanol as the pushing solvent. Two replicates were conducted at 45 minutes and 0.50 M concentration. The column's consistency was attempted to be maintained by packing the same mass of borohydride each time to a specified line marked on the column. Based on the screen, the reaction achieved maximum conversion of 87.2 % after 45 minutes and concentration of 0.50 M. Unfortunately, the screening data indicated a poor and irreproducible model because its replicates were not within close enough proximity to one another. It did however provide us with an expected optimal area to be further explored. The optimal area can be explored at lower concentrations, however additional reactions would be required to determine the ideal residence time. Although, polymer supported reagent offers the advantage of no additional workup and possible recycling, it also has limitations such as high costs, lower reactivity, non-reproducible results, and dispersion. As a result, we elected to not pursue this approach further instead opting to adapt the method reported by Watts and co-workers. [17]

An initial test reaction was carried out by adapting the method reported by Watts and co-workers.[17] Frustratingly, the HPLC pumps struggled to pump the sodium borohydride solution, resulting in a poor yield of only 10.7 %. After this setback, two additional batch reactions were carried out using an isopropanol: water and a methanol: water solvent mix respectively without the addition of sodium hydroxide. The reactions were performed at room temperature over 20 hours. Encouragingly, good yields were obtained in both instances with the aqueous isopropanol solvent mix performing best with an 87 % yield. It was noted that the sodium hydroxide additive suggested by Watts and co-worker had little effect on the overall yield with comparable yields being obtained with and without it. Moving forward, we elected to continue development using aqueous isopropanol as it afforded a higher overall yield and from a safety perspective did not suffer from the toxicity issues associated with methanol.

In translating to flow we elected to use two peristaltic pumps connected downstream of a stock solution of **7** in isopropyl alcohol, and an aqueous suspension of sodium borohydride. The peristaltic pumps were selected as they are capable of pumping fine suspensions/slurries. As seen in Scheme 52, a static mixer was used, along with a 25 mL PTFE coil (1.5 mm internal diameter) for heating and a 3 bar BPR. Before performing HPLC

analysis, the product was quenched with saturated sodium bicarbonate and water An initial reaction was carried out at concentration of 1.00 M, however the solution remained viscous, and only 83 % product conversion was achieved after 30 minutes residence time at 60 °C. This was already an improvement over the batch results obtained at room temperature for 24 hours.

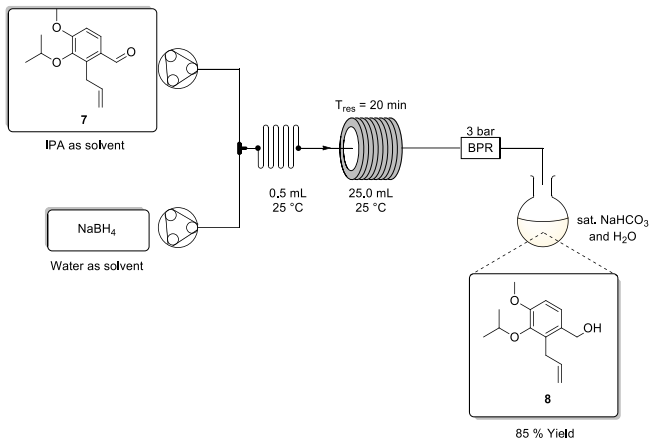

Scheme 52: Flow synthesis of aldehyde reduction using sodium borohydride in water

Further test reactions were carried out at a lower concentration of 0.25 M. Overall, higher product conversions were achieved with longer residence times, with a maximum conversion of 93 % obtained with a 20-minute residence time at 30 °C (Table 51, entry 4). Additionally, increasing the concentration to 0.50 M, reduced product conversion (entries 5-8), and increasing the temperature to 60 °C when performed at 0.5 M did not show any additional improvement (entry 7). Thus, the optimal conditions for the reduction step were identified as a temperature of 25 °C with a 20-minute residence time. At the determined optimal conditions, a larger scale reaction of about 3 grams was performed (entry 8), and 88 % product conversion was achieved with an isolated yield of 85 %.

Table 51: Flow experiments for aldehyde reduction using sodium borohydride in water and isopropyl alcohol

Exp No	Reaction scale (g)	Conc. [M]	T_{res} (min)	Temp. (°C)	LC Conv (%)
1[a]	0.15	1.00	30	60	83.0
2	0.15	0.25	5	30	79.0
3	0.15	0.25	10	30	82.0
4	0.15	0.25	20	30	93.0
5	0.15	0.50	20	30	84.0
6	0.15	0.50	30	30	83.0
7	0.15	0.50	20	60	79.0
8[b]	2.94	0.50	20	25	88.0

[a] Viscous sodium borohydride solution, [b] Isolated yield after workup 85 %.

Stage 5: Second allylation

Batch results

Reaction conditions outlined by van Otterlo and co-workers were followed using allyl bromide **3**.[14] Initially, we investigated the possibility of using potassium carbonate because it was successful the first allylation step. However, no product was formed (Table 52, entry 1). This is not unexpected as the proton of the phenolic hydrogen in the first allylation was more acidic due to charge stabilization resulting from being directly bonded to the aromatic ring. This is not the case for the benzylic hydrogen, it is less reactive as it is a primary alcohol and thus requires a stronger base. As a result, various reactions were carried out as detailed in Table 52 with the incorporation of different bases and solvents for testing flow compatibility and product conversion.

Unfortunately, no product conversion was achieved after 20 hours utilizing triethylamine, sodium methoxy, potassium tert-butoxide, lithium diisopropylamide, DBU, and DMAP. Interestingly, there was some product conversion at 80 °C using DMAP in both acetonitrile and DMSO as solvents. As expected, high product conversion was achieved at both room temperature and 60 °C using sodium hydride in tetrahydrofuran (0.20 M). A maximum product conversion of 85 % was achieved by washing the sodium hydride to remove the mineral oil. As the mineral oil is employed as a protective layer, washing the sodium hydride with a hydrocarbon solvent such as hexane makes it more reactive by improving mass transfer, resulting in higher conversions.

Table 52: Batch experiments for the second allylation using different bases in selected solvents

Exp No	Solvent	Base	Base pka	Base equiv.	Product conv.
1	DMF	K_2CO_3	10.3	5.0	No
2	DMSO	TEA	10.8	3.0	No
3[1]	ACN	TEA	10.8	3.0	No
4	MeOH	$NaOCH_3$	15-16	10.0	No
5	THF	KtBu	17.0	5.0	No
6	ACN	DBU	24.0	3.0	No
7	THF	LDA	35.7	5.0	No
8	ACN	DMAP	28.1	1.2	No
9[1]	ACN	DMAP	28.1	2.5	Yes (8.0 %)
10[1]	DMSO	DMAP	28.1	2.5	Yes (27.0 %)
11	THF	NaH[a]	35.0	5.0	Yes (41.0 %)
12	THF	NaH[b]	35.0	5.0	Yes (80.0 %)
13[2]	THF	NaH[b]	35.0	2.5	Yes (85.0 %)

[1]Refluxed at 80 °C, [2] Heated to 60 °C, [a] Unwashed NaH (containing mineral oil) was used, [b] Washed NaH with hexane prior reaction

Flow results

The second allylation was previously attempted in-house using triethylamine under flow conditions, but no product was produced. DMAP or sodium hydride were initially planned to be used for flow translation since they produced moderate yields in batch. Initially, the use of a column packed with polymer supported DMAP dispersed on celite was screened at 80 °C, but

no product was obtained after monitoring the reaction for a few reaction cycles, each with a 20-minute residence time. Secondly, a column packed with washed sodium hydride was attempted but was terminated because the sodium hydride produced a significant amount hydrogen gassing out in the BPR preventing the solvent and reagent from pumping through at a consistent residence time. As a result, it was decided to employ the method detailed in the Vapourtec application note, which uses a sodium hydride slurry, as it represented a safer and more time efficient approach.

To facilitate the pumping of the slurry we employed the use of peristaltic pumps as the pumping units, in addition a peristaltic pump was also used in place of a cartridge based BPR to regulate the system pressure. This was accomplished by manually setting the pressure to 7 bar. Mechanically, this works by pumping in the opposite direction at a specified flow rate to generate the appropriate back pressure. The system was kept inert by purging with nitrogen gas using the reactor gas manifold, as well as employing the use of distilled tetrahydrofuran which was also kept inert.

After various test reactions and different flow setups, it was decided to combine all the reagents into a single stock reservoir. This was deemed feasible as it was monitored that they do not react within the reservoir at ambient temperature. To improve the product conversion, we recycled the reaction solution prior to product collection. The flow setup for the DoE screening consisted of using a two-pump peristaltic system with one peristatic pump employed to pump the slurry and a second peristatic pump acting as the BPR (Scheme 53). The flow stream was passed through a 0.5 mL static mixer connected in series to a 10 mL coil reactor (1.0 mm inner diameter).

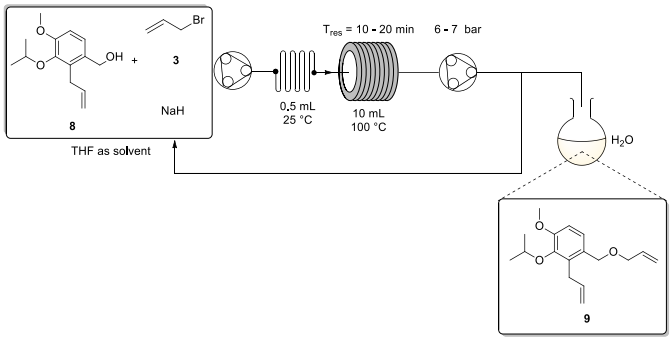

Scheme 53: Flow synthesis for recycling of the second allylation using one peristaltic pump and a static mixer with sodium hydride slurry

A full-factorial screen was chosen with 2 replicates and 18 experiments. While maintaining the concentration of the starting material and the temperature at 100 °C, a sodium hydride stoichiometric excess range of 2.5 to 7.5 equivalents and an allyl bromide stoichiometric excess range of 1.5 to 3.0 equivalents was selected. This was primarily driven by chemical intuition and our previous experience with the system. The residence time range employed was 10 to 20 minutes and the recycling range was from 3 to 9 recycles. The DoE screening results are summarised in Table 53. The conversion from HPLC analysis was captured and analysed using the MODDE 13 software package to determine where, under the ranges selected, the reaction optimum lies.

Table 53: DoE experiments for the recycling of second allylation

Exp No	NaH (eq)	3 Eq	T_{res} (min)	Cycles	LC Conv. (%)
1	2.5	1.5	10	3	61.0
2	7.5	1.5	10	3	89.2
3	2.5	1.5	20	3	30.8
4	7.5	1.5	20	3	79.7
5	2.5	1.5	10	9	62.7
6	7.5	1.5	10	9	89.9
7	2.5	1.5	20	9	37.7
8	7.5	1.5	20	9	85.7
9	2.5	3.0	10	3	45.7
10	7.5	3.0	10	3	79.6
11[a]	2.5	3.0	20	3	39.5
12	7.5	3.0	20	3	82.3
13	2.5	3.0	10	9	59.0
14	7.5	3.0	10	9	84.0
15	2.5	3.0	20	9	30.4
16[b]	7.5	3.0	20	9	92.0
17	5.0	2.3	15	6	71.7
18	5.0	2.3	15	6	65.9

[a] q-NMR revealed 49.66 % product conversion, [b] q-NMR revealed 99.09 % product conversion, 69 % Isolated Product

From the DOE results, the flow conditions with the highest conversions were identified to be at 20 minutes residence time, and 3 cycles using 7.5 equivalents of sodium hydride and 1.5 equivalents of allyl bromide. It is worth noting that all reactions that used 7.5 equivalents of sodium hydride had the highest conversion when compared to reactions that used 2.5 equivalents of sodium hydride under the same conditions. Table 21, entry 16 had a maximum conversion at 92 %, while entry 15 had the lowest conversion. It can be inferred that the peristaltic pumps were suitable and compatible for efficiently pumping highly reactive sodium hydride slurries. Repeatable results were obtained, and more research into the red region is required to identify the optimal conditions. DoE provided an indicator of reproducibility, precision, and selectivity. The outcomes of this DoE process were near to expected values, and the difference between replicates was minor, resulting in a good model with high reliability and reproducibility.

Stage 6: RCM

Batch results

The final stage was reported by van Otterlo and co-workers employing the Grubbs II catalyst (5 mol %) in toluene at 60 °C for 2 hours under inert conditions to obtain 52% of product.[14] It was discovered that this step had challenges as long reaction times were required while affording low yields and some catalyst decomposition. This reaction was performed in batch employing the Grubbs II catalyst (5 mol %) in toluene at 60 °C for 2 hours under inert conditions to obtain 46 % of product.

Flow results

It was chosen to investigate this step by comparing the yields obtained by a static mixer and coil heated to 60 °C and a 20 mL glass mixing chip. Initial test reactions showed lower product conversion utilizing a coil compared to using a glass mixing chip Thus, a glass mixing chip was chosen for flow optimization. It was decided to perform a DoE to evaluate the screening area and determine the most suitable catalyst and solvent for this reaction. A full-factorial DoE screening was selected with 19 experiments including 3 replicated. The DoE screening parameters included 4 varying factors and one constant factor. Two factors were qualitative which was the catalysts and solvent. The other two factors were quantitative and is the temperature and residence time. The catalysts loading was kept constant at 3 mol % (0.03 equiv.).

The flow setup (Scheme 54) consisted of using the Uniqsis Binary pump equipped with 2 mL sample loops that was purged with degassed solvent prior to loading. The two stock solutions were mixed in a 20 mL glass mixing chip and the pressure were kept between 4-5 bar as the mixing chip has a maximum pressure of 10 bar. The DoE screening results are provided in

Table 54 and the product conversion form HPLC analysis were captured and analysed on MODDE 13 to illustrate where the optimal conditions might be explored. The product signal obtained from HPLC analysis corresponded to literature for both NMR and HRMS analysis.

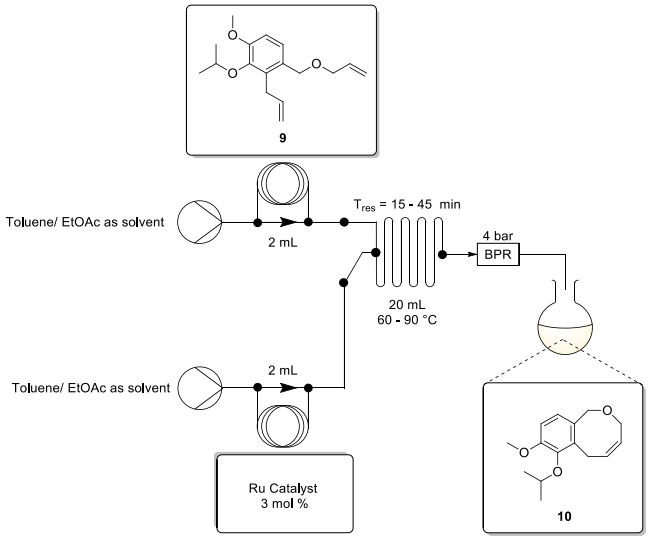

Scheme 54: Flow preparation of the ring closing metathesis of **10**

Table 54: DoE experiments for ring-closing metathesis of **10**

Exp No	Solvent	Catalyst	Temp. (°C)	T_{res} (min)	LC Conv. (%)
1	EtOAc	GII	60	15	45.6
2	Toluene	GII	60	15	43.3
3	EtOAc	HGII	60	15	48.0
4	Toluene	HGII	60	15	40.9
5	EtOAc	GII	90	15	24.7
6	Toluene	GII	90	15	35.9
7	EtOAc	HGII	90	15	46.5
8	Toluene	HGII	90	15	54.8
9	EtOAc	GII	60	45	43.3
10	Toluene	GII	60	45	45.4
11	EtOAc	HGII	60	45	46.9
12	Toluene	HGII	60	45	37.0
13	EtOAc	GII	90	45	15.0
14	Toluene	GII	90	45	23.4
15	EtOAc	HGII	90	45	26.9
16	Toluene	HGII	90	45	37.0
17	EtOAc	GII	75	30	34.7
18	EtOAc	GII	75	30	36.3
19	EtOAc	GII	75	30	34.4

After studying the DoE results, a few reactions were conducted using the same flow setup and focusing on the areas predicted where higher conversions can be achieved. The first follow-up reactions were conducted using Hoveyda−Grubbs second-generation catalysts in both toluene and ethyl acetate but reducing the residence time to 10 minutes (Table 55, entries 1 and 2). Entry 1 was carried out at 60 °C and entry 2 at 100 °C to afford 53.6 and 35.6 % product conversion. Due to the unexpected low yield at higher temperature in toluene it was decided to replicate the most optimal conditions but changing the equivalents of the catalysts (entries 3-5). It was found that as the equivalents of the catalysts increases, the product conversion decreases. This could be due to the catalysts decomposing or due to polymerization and cross-metathesis occurring. The last entry was conducted by increasing the volume of the injection loops to 5 ml (entry 6) to compensate for dispersion. However, a moderate product conversion was obtained. This step would be further optimized as part of future work.

Table 55: Follow-up reaction after DoE analysis for ring-closing metathesis of **10**

Exp No	Solvent	Cat.	Temp. (ºC)	T_{res} (min)	Catalyst (mol %)	LC Conv. (%)
1	EtOAc	HGII	60	10	3	53.6
2	Toluene	HGII	100	10	3	35.6
3	Toluene	HGII	90	15	1	47.5
4	Toluene	HGII	90	15	5	37.7
5	Toluene	HGII	90	15	8	26.6
6[a]	Toluene	HGII	90	15	3	43.0

[a] Larger scale (5 mL injection loops)

Conclusions

In conclusion, the synthesis of (Z)-7-Isopropoxy-8-methoxy-3,6-dihydro-1H-benzo[c]oxocine **10** was successfully translated under flow conditions. The first stage, the allylation of isovanillin **2** was optimized under flow conditions using two approaches; i) utilizing a packed-bed reactor housing potassium carbonate to afford the desired product **4** in a 92 % yield with a 20 minute

residence time at temperature of 100 ºC using dimethylformamide or by ii) using a coil reactor with a potassium hydroxide solution in methanol to afford **4** in 88 % isolated yield after 15 minutes residence time at temperature of 80 ºC. In comparison, the flow translations showed improved product conversions in reduced time compared to batch approach that required more than 20 hours The Claisen rearrangement was translated under flow using toluene and showed a significant increase in yield (6.9 to 98 %) and time reduction from 72 hours in batch to 15 minutes in flow. This stage also showed the safe use of solvents at temperatures above the solvent's boiling point and performing reactions at elevated pressures. The Claisen rearrangement was optimized at 240 ºC using 15 minutes residence time to afford the product **5** in a 98 % isolated yield as a pure product. The third stage showed improved product conversions (78 to 88 %) with a significant reduction in time from more than 20 hours in batch to 20 minutes in flow using a packed-bed reactor housing potassium carbonate. A further optimisation study is recommended for translating this stage to an approach using a potassium hydroxide solution, see future work section.

The fourth stage involving the reduction of the aldehyde was successfully translated and optimized under flow conditions using two approaches by the i) utilization of a packed-bed reactor housing polymer supported sodium borohydride to afford 87 % product conversion after 45 minutes residence time at room temperature using methanol as the protic solvent source or by ii) using a coil reactor with a sodium borohydride solution at temperature of 30 ºC affording 93 % of product **8** after 30 minutes residence time. In comparison, the flow translations showed improved product conversions in reduced time compared to batch that was conducted for more than 20 hours using Red-Al (60 % in toluene) to afford 76 % product.

The fifth stage, the second allylation was successfully translated and optimized under flow conditions using a sodium hydride slurry employing a recycling approach. The DoE results showed that the peristaltic pumps were suitable and compatible for efficiently pumping highly reactive sodium hydride slurries. This stage showed improved product conversions (85 to 92 %) and time reduction from more than 20 hours in batch to 20 minutes under flow conditions. The final RCM reaction was also successfully translated under flow conditions with an increased yield from 46 % in batch after 2 hours to 55 % under flow within 15 minutes This stage also made use of DoE and showed that the Hoveyda-Grubbs II catalysts is more suitable for this reaction at higher temperatures and shorter residence times. In conclusion the final optimised results are shown in Table 56, and it can be concluded that the flow approach afforded a higher overall percentage yield of 37.7 % compared to batch 0.77 % in less time of 105 minutes vs. 154 hours for the batch approach (Table 56). Overall, there is also an increase in the overall yield for the last three stages affording 47.1 % product when compared to Van Otterlo and co-workers that obtained an overall percentage yield of 34.4% after 34 hours.[14]

Table 56: Summary of results obtained for each stage under batch and flow conditions.

Stage: Reaction name	**Batch results**		**Flow results**	
	Time (hours)	**Yield %**	**Time (minutes)**	**Yield %**
1: Allylation (KOH solution approach)	20	78	15	93
2: Claisen rearrangement	72	6.9	15	98
3:Alcohol protection	20	78	20	88
4: Aldehyde reduction ($NaBH_4$ solution approach)	20	47	20	93
5: Second allylation	20	85	20	92
6: RCM	2	46	15	55
Overall % yield	**0.77**		**37.7**	

Conflicts of interest

There are no conflicts to declare

Acknowledgements

This work was supported by the Council for Scientific and Industrial Research (CSIR) and the University of Pretoria (University, Science Faculty Research Councils and Research and Development Program). The authors would like to gratefully acknowledge Mamoalosi Selepe for NMR spectroscopy services, Madelien Wooding for mass spectroscopy services, Uniqsis Ltd and Vapourtec Ltd for flow equipment.

References

1 H. Venkatachalam, N. Venkatesh and A. Kumar, *The Oxygen-Containing Fused Heterocyclic Compounds*, 200AD.

2 L. Gavin Madeley, *Synthesis of benzo-fused heterocycles using isomerization and ring-closing metathesis reactions*, 2010.

3 R. Pathak, J.-L. Panayides, T. D. Jeftic, C. B. De Koning and W. A. L. Van Otterlo, *The Synthesis of 5-, 6-, 7-and 8-Membered Oxygen-containing Benzo-fused Rings using Alkene Isomerization and Ring-closing Metathesis Reactions*, .

4 B. C.-A. Nkeh and D. Njamen, *Anti-inflammatory and analgesic effects of drypemolundein A 27*, 2003.

5 S. G. Newman and K. F. Jensen, *Green Chemistry*, 2013, 15, 1456–1472.

6 S. H. Lau, *Organic Synthesis: Taming Chemistry using Enabling Technologies A dissertation presented by Statement of Length*, 2017.

7 R. J. Ingham, J. College, J. Lane and L. Group, *Control tools for flow chemistry processing and their application to the synthesis of bromodomain inhibitors A thesis presented by*, 2014.

8 A. R. Bogdan and A. W. Dombrowski, *J Med Chem*, 2019, 62, 6422–6468.

9 L. Malet-Sanz and F. Susanne, *J Med Chem*, 2012, 55, 4062–4098.

10 P. Bana, R. Örkényi, K. Lövei, Á. Lakó, G. I. Túrós, J. Éles, F. Faigl and I. Greiner, The route from problem to solution in multistep continuous flow synthesis of pharmaceutical compounds, *Bioorg Med Chem*, 2017, **25**, 6180–6189.

11 D. Dallinger and C. O. Kappe, *Curr Opin Green Sustain Chem*, 2017, 7, 6–12.

12 M. Guidi, P. H. Seeberger and K. Gilmore, *Chem Soc Rev*, 2020, 49, 8910–8932.

13 M. B. Plutschack, B. Pieber, K. Gilmore and P. H. Seeberger, *Chem Rev*, 2017, 117, 11796–11893.

14 R. Pathak, J.-L. Panayides, T. D. Jeftic, C. B. De Koning and W. A. L. Van Otterlo, *The Synthesis of 5-, 6-, 7-and 8-Membered Oxygen-containing Benzo-fused Rings using Alkene Isomerization and Ring-closing Metathesis Reactions*, .

15 D. Cortés-Borda, E. Wimmer, B. Gouilleux, E. Barré, N. Oger, L. Goulamaly, L. Peault, B. Charrier, C. Truchet, P. Giraudeau, M. Rodriguez-Zubiri, E. Le Grognec and F. X. Felpin, An Autonomous Self-Optimizing Flow Reactor for the Synthesis of Natural Product Carpanone, *Journal of Organic Chemistry*, 2018, **83**, 14286–14289.

16 C. J. van der Westhuizen, J. du Toit, N. Neyt, D. Riley and J.-L. Panayides, Use of open-source software platform to develop dashboards for control and automation of flow chemistry equipment, *Digital Discovery*, 2022, **1**, 596–604.

17 D. Mandala, S. Chada and P. Watts, Semi-continuous multi-step synthesis of lamivudine, *Org Biomol Chem*, 2017, **15**, 3444–3454.

It's been a journey but all thanks and gratitude to the Lord.

For "I will thank you Lord, among all the people, I will sing your praises"
(Ps 57:4), for you gave me strength and knowledge.

And I will "Give thanks to the Lord, for He is good. His faithful love endures forever"
(Ps 107:1).